2013

OXIDATIVE DAMAGE TO DNA IN ALZHEIMER'S DISEASE

Sony Soman
University of Kentucky, sso223@uky.edu

STUDENT AGREEMENT:

I represent that my thesis or dissertation and abstract are my original work. Proper attribution has been given to all outside sources. I understand that I am solely responsible for obtaining any needed copyright permissions. I have obtained and attached hereto needed written permission statements(s) from the owner(s) of each third-party copyrighted matter to be included in my work, allowing electronic distribution (if such use is not permitted by the fair use doctrine).

I hereby grant to The University of Kentucky and its agents the non-exclusive license to archive and make accessible my work in whole or in part in all forms of media, now or hereafter known. I agree that the document mentioned above may be made available immediately for worldwide access unless a preapproved embargo applies.

I retain all other ownership rights to the copyright of my work. I also retain the right to use in future works (such as articles or books) all or part of my work. I understand that I am free to register the copyright to my work.

REVIEW, APPROVAL AND ACCEPTANCE

The document mentioned above has been reviewed and accepted by the student's advisor, on behalf of the advisory committee, and by the Director of Graduate Studies (DGS), on behalf of the program; we verify that this is the final, approved version of the student's dissertation including all changes required by the advisory committee. The undersigned agree to abide by the statements above.

Sony Soman, Student

Dr. Mark A. Lovell, Major Professor

Dr. Dong-Sheng Yang, Director of Graduate Studies

OXIDATIVE DAMAGE TO DNA IN ALZHEIMERS DISEASE

ABSTRACT OF DISSERTATION

A dissertation submitted in partial fulfillment of the
requirements for the degree of Doctor of Philosophy in the
College of Arts and Sciences
at the University of Kentucky

By

Sony Soman

Lexington, Kentucky

Director: Dr. Mark A. Lovell, Professor of Chemistry

Lexington, Kentucky

2013

ABSTRACT OF DISSERTATION

OXIDATIVE DAMAGE TO DNA IN ALZHEIMERS DISEASE

Previous studies from our laboratory and others show a significant increase in levels of both nuclear and mitochondrial DNA and RNA oxidation in vulnerable brain regions in the progression of Alzheimer's disease (AD). Although total DNA oxidation is increased in AD it remains unclear whether oxidative damage is widespread throughout the genome or is concentrated to specific genes. To test the ***hypothesis*** that specific genes are more highly oxidized in the progression of AD, we propose to quantify the percent oxidative damage in genes coding for proteins shown to be altered in the progression of AD using quantitative/real-time polymerase chain reaction (qPCR/ RT-PCR). To further test the ***hypothesis*** that diminished DNA repair capacity in the progression of AD contributes to increased DNA oxidation we will use custom PCR arrays and qPCR, Western blot analysis and activity assays to quantify changes in enzymes involved in base excision repair (BER).

In order to carry out these studies tissue specimens from superior and middle temporal gyri (SMTG) and inferior parietal lobe (IP), as well as, a non-vulnerable region, the cerebellum (CER) will be analyzed from normal control (NC) subjects and subjects throughout the progression of AD including those with preclinical AD (PCAD), mild cognitive impairment (MCI), and late stage AD (LAD). We will also analyze specimens from diseased control subjects (DC; Frontotemporal dementia (FTD) and dementia with Lewy bodies (DLB)) to determine if the changes we observe in AD are specific.

KEYWORDS: Alzheimer’s disease (AD), oxidative stress, base excision repair, DNA oxidation

OXIDATIVE DAMAGE TO DNA IN ALZHEIMERS DISEASE

By

Sony Soman

Dr. Mark A. Lovell
Director of Dissertation

Dr. Dong-Sheng Yang
Director of Graduate Study

October 8, 2013

ACKNOWLEDGMENTS

I must start my acknowledgements by thanking Dr. Lovell for being the best advisor, a graduate student could ask for and for creating a wonderful learning environment in the lab. “Boss”, you’ve taught me an incredible amount; self-reliance in research, encouragement to pursue ideas that piqued my interest and most of all to just keep moving on even when you are completely discouraged. I’ve always appreciated your indefatigable determination and the freedoms allowed to me while in your group. You have inspired me for a lifetime. I would not have been able to even start my research without the help of my wonderful colleagues, Shuling Xiong-Fister, Melissa Bradley and Ganna Lyubartseva. Without their help in training on various instruments and techniques and their constructive critiques of experimental methods and results, my research efforts would not even have taken off the ground in the first place. Shuling and Melissa, I appreciate your constant encouragement and friendship during my stay within the group. I have never felt the absence of my family here because of these two truly awesome friends and their families.

I would also like to thank my doctoral committee for their support during this process. Dr. Lynn, it has been a pleasure sparring with you in my committee meetings. Your comments got me thinking about my research from a different perspective many times. Dr. Levine, I appreciate your support, your professionalism and your kind words of encouragement whenever we talked about my research. Dr. Wei, thank you for your support and guidance throughout this process. I must extend thanks to Dr. Peter Nelson, Dr. Donna Wilcock and their lab members for their help and support. I am also grateful for the funding that supported my research including my RCTF fellowship, the

University of Kentucky Graduate College, and the University of Kentucky Chemistry department.

Last but not the least I must thank my husband Partha for being my pillar of strength through so many difficult times. I would like to express my love and gratitude to my parents C.G. Soman Pillai and Thankam S. Pillai and and my sister Swapna Soman for all the love and encouragement that they have given me all my life. I would also like to mention here the love of my life, my son Rishi Soman Jana who has made my life so beautiful. A special thanks to my friends from the Sanders Brown Center on Aging for making my stay in UK so agreeable.

TABLE OF CONTENTS

LIST OF TABLES

LIST OF FIGURES

CHAPTER 1: INTRODUCTION AND BACKGROUND

1.1. Alzheimer's Disease (AD)

1.1.1. Discovery and Incidence

Alzheimer' disease (AD) is a progressive neurodegenerative disorder, first described by Alois Alzheimer in 1906 at the 37th meeting of South-West German Psychiatrists in Tubingen. Alzheimer's lecture at Tubingen described the symptomatology, progression and course of disease over a period of about five years as well as the histological and morphological features of the brain after the death of a patient, Auguste Deter. The clinical characteristics of Auguste D. included sleep disorders, memory loss, aggressiveness, aphasia and progressive confusion. Histopathologically, Alzheimer reported the presence of intracellular and extracellular aggregates in the brain of Auguste D after autopsy. Intracellular aggregates composed of hyperphosphorylated microtubule associated tau protein (neurofibrillary tangles) and extracellular aggregates of β-amyloid peptide (senile plaques) are now recognized as two of the main pathological markers of AD (Hippius and Neundorfer, 2003). Despite discovery a century ago, it is only during the last few decades that research into the symptoms, causes and treatment of AD has gained momentum as the number of people affected by this disease increased dramatically.

At present, AD affects 5.2 million Americans with an estimated cost of ~200 billion dollars annually. One in 8 Americans age 65 and over suffers from AD, and at present there is no way to prevent, cure or even slow the progression of the disease (Burns and Iliffe, 2009; Hebert et al., 2013). Death of patients with AD increased by 68% between 2000 and 2010 whereas death by other major diseases including breast cancer, prostate

cancer, heart disease, stroke and HIV decreased (Thies and Bleiler, 2013). After diagnosis, most people with AD survive 4-8 years, on average, with some surviving as long as 20 years. On average, 40% of this time is spent in the most severe stage of the disease when a patient is completely incapable of taking care of themselves. Although AD is the sixth leading cause of mortality in the United States, death is generally due to secondary illness/infection Unless medical breakthroughs identify ways to prevent or more effectively treat the disease, the number of AD patients in the US is expected to triple by the year 2050, with annual costs that may singlehandedly create a massive health care crisis (Burns and Iliffe, 2009; Thies and Bleiler, 2011, 2013).

1.1.2. Clinical Characteristics

The major difficulty in the diagnosis of AD is the lack of laboratory tests to confirm AD in a patient antemortem. Clinical diagnosis of AD is based on medical history and clinical examination, coupled with laboratory tests and brain imaging (computed tomography or magnetic resonance imaging) to exclude other forms of dementia. The criteria set by the Diagnostic and Statistical Manual of Mental Disorders, Fourth Edition (DSM-IV), and the National Institute of Neurological and Communicative Disorders and Stroke and the Alzheimer's disease and Related Disorders Association (NINCDS-ADRDA) are the two most common clinical criteria used for the diagnosis of AD. These criteria state that the leading diagnostic element for AD is the steady onset and progression of dementia in a patient with no other known cause of dementia. Eventually, this steady decline across multiple cognitive domains leads to late stage dementia where the patient is almost totally dependent on caregivers for even the most basic functions (Brookmeyer et al., 2002; Burns and Iliffe, 2009; Yaari and Corey-Bloom, 2007).

The DSM-IV criteria require an insidious onset along with cognitive function decline, memory impairment and a second cognitive deficit such as aphasia, apraxia, agnosia or impairment of executive functioning. DSM-IV criteria require that other psychiatric, neurological, metabolic or systemic diseases be excluded as a reason for impairments in social or occupational functioning before the confirmation of a diagnosis for AD. In comparison, the NINCDS-ADRDA guidelines are more comprehensive and provide a disease progression sequence for AD classified as probable, possible and definite AD. Probable and possible AD diagnosis can be made antemoretem whereas definite AD can only be identified postmortem. Probable AD is characterized by deficits in two or more cognitive domains, progressive memory deterioration, preserved consciousness and onset between ages 40-90 in the absence of alternative reasons for the symptoms. “Possible AD” patients display atypical onset of dementia along with the presence of additional signs of dementia. Definite AD can only be diagnosed postmortem by a combination of clinical diagnosis and neuropathological evaluation of the brain after autopsy. The average time from onset of AD to death varies from 4 to 10 years depending on the age of the patient at onset (Dubois et al., 2007; Khachaturian and Radebaugh, 1996; McKhann et al., 1984; Yaari and Corey-Bloom, 2007).

1.1.3. Pathological Features

Pathologically, a gross visual inspection of an AD brain displays the presence of marked cerebral cortical atrophy epitomized by widening of the sulci and shrinkage of the gyri (Figure 1.1). Several microscopic changes distinctive of AD include loss of neuronal and synaptic densities in the hippocampus, amygdala, entorhinal cortex, neocortex, and nucleus basalis of Meynert. Neuropathologically, the AD brain is

characterized principally by the presence of two distinctive hallmarks: senile plaques (SP) and neurofibrillary tangles (NFT) (Khachaturian and Radebaugh, 1996; Yaari and Corey-Bloom, 2007). Neither of the neuropathological hallmarks is unique to AD and are also seen in cognitively normal individuals although AD subjects show considerably higher densities. NFTs are also observed in patients with other neurodegenerative diseases including frontotemporal dementia (Braak and Braak, 1991; Graff-Radford and Woodruff, 2007; Grossman, 2002).

Two different types of senile plaques can be observed in the AD brain: neuritic and diffuse. Neuritic plaques contain tendrils or dense cores of fibrillar amyloid surrounded by dystrophic neurites, reactive astrocytes and activated microglia. Diffuse plaques on the other hand are amorphous in appearance, have no abnormal neurites and contain little or no fibrillar amyloid. Senile plaques (SP) are principally composed of insoluble amyloid beta (Aβ) peptides specifically a mixture of $A\beta_{1\text{-}42/43}$ (> 95%) and small amounts of $A\beta_{1\text{-}40}$ (reviewed in (Markesbery and Lovell, 2006)). Amyloid β is a ~4 kDa peptide containing 11-15 amino acids from the transmembrane domain and 28 amino acids from the extracellular domain of the amyloid precursor protein (APP). On average, 90% of the larger APP protein is cleaved by α-secretase generating a large secreted derivative sAPPα and an 83 amino acid fragment CTFα. CTFα subsequently gets cleaved by γ-secretase producing the benign p3 fragment and a cytosolic element, APP intracellular domain (AICD). The remaining 10% of APP is cleaved first by β-secretase to produce a large secreted derivative sAPPβ and a membrane bound 99 amino acid fragment CTFβ. γ-secretase cleaves the CTFβ fragment further to generate AICD and Aβ40 (~80-90%) or Aβ42 (~5-10%). Rapid nucleation of $A\beta_{1\text{-}42/43}$ into amyloid fibrils is considered to be the

seed for aggregation and consequent deposition of Aβ in SPs. Although studies have shown evidence of Aβ's involvement in synaptic dysfunction, disruption of neural connectivity and neuronal death, only weak correlations have been observed between the extent and distribution of Aβ deposition and the clinical manifestation of AD (Khachaturian and Radebaugh, 1996; reviewed in Murphy and LeVine, 2010; Selkoe, 2001).

NFTs are composed of paired helical filaments (PHFs) and 15 nm straight filaments. PHFs which can also be present in neutrophil threads and dystrophic neurites principally contain abnormally hyperphosphorylated isoforms of tau, a protein associated with microtubules. Customarily, tau binds to microtubules supporting their formation and stabilization. Hyperphosphorylated tau is unable to bind microtubules making them unstable leading to their disintegration. Unbound tau then bundles together to form neurofibrillary tangles. Tau pathology has also been observed in patients with Parkinson's disease (PD), progressive supranuclear palsy and frontotemporal dementia (Khachaturian and Radebaugh, 1996). Unlike SPs, there is a strong correlation between number of NFTs and cognitive deficits and neuronal loss in an AD patient's brain. NFTs exhibit a characteristic distribution in the brain allowing differentiation into six stages described by the Braak staging scheme (Braak and Braak, 1991). The presence of NFT's primarily in the transentorhinal region of the brain indicates Braak stages I and II (cognitively normal subjects) whereas stages III and IV indicate progression of tangles into limbic regions such as the hippocampus, and V and VI when there's extensive tangle formation in neocortical regions (late AD patients) (Braak and Braak, 1991; Grundke-Iqbal et al., 1986; Khachaturian and Radebaugh, 1996).

It has been suggested that progressive inflammation and oxidative stress may be major factors leading to synaptic dysfunction and the loss of neuronal integrity which usually pave the way for the appearance of amyloid plaques and neurofibrillary tangles in the brains of AD patients (Jicha and Markesbery, 2010; Khachaturian and Radebaugh, 1996). The neuropathological hallmarks of AD can be evaluated by several diagnostic criteria including the National Institute of Neurological and Communicative Disorders and Stroke and the Alzheimer's disease and Related Disorders Association (NINCDS-ADRDA) criteria (McKhann et al., 1984), the Consortium to Establish a Registry for Alzheimer's disease (CERAD) criteria (Mirra, 1997) and the National Institute of Aging-Reagan Institute (NIA-RI) consensus criteria (NIA-Reagan-Institute, 1997). The NINCDS-ADRDA criteria require a certain number of SP in an age-dependent manner in the neocortex. In this criteria, the type of SP is not identified, changes in the entorhinal cortex, hippocampus or amygdala are not considered and presence of NFTs is only considered for patients under the age of 50 (Markesbery, 1997a; McKhann et al., 1984). The CERAD criteria is based on the semiquantification of neuritic plaques (NPs) as sparse, moderate or frequent in three brain regions: middle frontal gyrus, superior and middle temporal gyri and inferior parietal lobule in individuals in three different age categories: less than 50, 50 to 75 and over 75. The criteria also require correlation of the pathological characteristics with a clinical diagnosis of dementia. The CERAD criteria fail to consider the presence of NFTs and the changes in the hippocampus, entorhinal cortex and amygdala for AD diagnosis(Markesbery, 1997a; Mirra, 1997). The NIA-RI consensus criteria consider the correlation of both SPs and NFTs with AD. This criteria is based on the semiquantification of NPs (CERAD criteria), determination of extent of

NFTs in hippocampus and neocortex (Braak score) and clinical diagnosis of dementia (Geddes et al., 1997; NIA-Reagan-Institute, 1997).

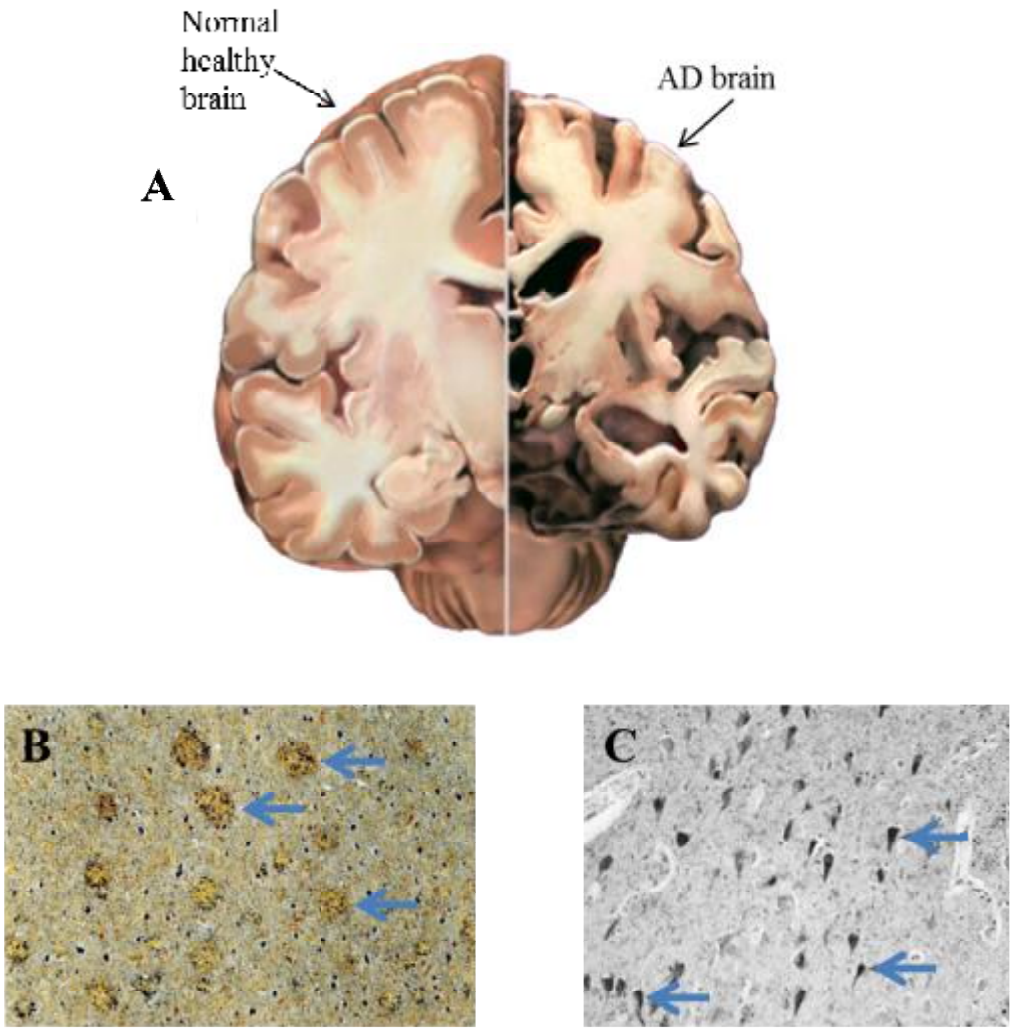

Figure 1.1. Macroscopic and microscopic changes in the human brain associated with Alzheimers disease including (A) widened sulci and shrunken gyri in the coronal sectioned AD brain (right) compared to the age matched normal control subject (left), (B) staining of senile plaques (SPs) and (C) staining of neurofibrillary tangles (NFTs) (Adapted from (Lovell et al., 1993; Lovell et al., 1998)).

1.1.4. Risk Factors

Several factors contribute to the probability of a person developing AD including age, genetic predisposition and head trauma. Aging is considered the primary risk factor for AD (Evans et al., 1989) and the risk of developing the disease dramatically increases with age. After age 65 the possibility of developing AD doubles every five years and reaches 50% in people aged 85 and over (Kawas et al., 2000). Family history is the next important risk factor in the incidence of AD (Henderson, 1986). There is a ~ 10-14% higher risk of AD in people who have close relatives (parent, brother, sister or child) suffering from the disease compared to unrelated individuals (Burns and Iliffe, 2009). The expression of Apolipoprotein E (ApoE), a protein involved in cholesterol transport in the bloodstream, has also been linked with the incidence of late-onset AD. There are three isoforms of ApoE: ε2, ε3 (most common) and ε4. Expression of the ε4 isoform of ApoE is associated with increased risk of AD. Studies show the existence of one or two copies of the ApoE- ε4 gene in 40-65% of people diagnosed with AD (Farrer et al., 1997; Hollingworth et al., 2011; Saunders et al., 1993). On the other hand, factors such as high educational and occupational attainment, high levels of social and cognitive engagement, postmenopausal estrogen replacement therapy, and long-term use of anti- inflammatory drugs have been implicated in decreasing the risk of AD (Khachaturian and Radebaugh, 1996; Mortimer et al., 2003; Prasad et al., 2002; reviewed in Murphy and LeVine, 2010; Zhang et al., 1990). Additionally, traumatic brain injury, smoking and obesity have been implicated in increasing the risk of AD (Gustafson et al., 2003; Merchant et al., 1999; Mortimer et al., 1985; Mortimer et al., 1991; Ott et al., 1998). Less than 1% of AD patients are affected by Familial Alzheimer's disease (FAD) or early-onset Alzheimer's,

an inherited, rare form of the disease which can occur as early as age 35. Mutations in APP (located on chromosome 21) or presenelin-1 (PS-1) (located on chromosome 14) or presenelin-2 (PS-2) (located on chromosome 1) have been shown to be the cause of FAD (Hollingworth et al., 2011; Xie and Tanzi, 2006). Individuals with Down's syndrome have an extra copy of the APP gene which could be a factor in the development of AD-associated pathology in them as early as age 40 (Mann et al., 1990; Thies and Bleiler, 2013).

1.1.5. Early Stages

Increasing evidence suggests that in an Alzheimer's patient, pathological changes in the brain may begin decades before the appearance of clinical symptoms (Fagan et al., 2005; Lange et al., 2002). In a neuropathological study conducted in 1997, Braak and Braak reported the presence of NFTs in subjects as young as 40 years old (Braak and Braak, 1997). Thus there has been considerable interest in the diagnosis and characterization of the preliminary phases of AD. Identification of the early phases of AD may help in the identification of the pathogenesis of AD thus expediting enhancement/discovery of early pharmacological intervention and possible reversal of the disease. Based on both pathological and/or clinical diagnosis, AD can be broadly classified into the following stages:

Amnestic Mild Cognitive Impairment (MCI):

MCI is the phase between normal aging and early dementia characterized as the earliest detectable clinical phase of AD. Petersen et al. define amnestic MCI patients as individuals with symptoms which include: (a) memory impairment observed over time corrected for age and education (b) normal general cognitive function (c) intact activities

of daily living and (d) the subject not meeting criteria for dementia (DeCarli, 2003; Maynard et al., 2010). Thus, patients with MCI exhibit characteristics of both clinically normal individuals as well as AD patients. MCI subjects go on to develop AD with a conversion rate of ~ 15% per year. Histopathologically, MCI subjects show a significant increase in neuritic plaques in neocortical regions and a significant increase in neurofibrillary tangles in the hippocampus, entorhinal cortex and amygdala, compared to NC subjects. Braak staging scores for MCI subjects are usually in the range of III-IV (DeCarli, 2003; Petersen et al., 2009; Wang et al., 2005).

Preclinical AD (PCAD):

The criteria for identifying PCAD subjects are not well-defined. Schmitt et al. define subjects with PCAD as individuals who show normal antemortem psychometric test scores adjusted for age and education, but at autopsy demonstrate distinct AD pathology that meets NIA-RI intermediate or high-likelihood criteria for the histopathological diagnosis of AD. PCAD subjects demonstrate Braak staging scores of III or higher, moderate or frequent neuritic plaque scores, neuronal hypertrophy, increased synaptic plasticity and alterations in zinc transporters (Bradley et al., 2010; Schmitt et al., 2000). Preclinical AD (PCAD) subjects are diagnosed based on the tentative criteria set by the UK-ADC which includes (a) pronounced AD pathology with Braak scores of III-V and (b) antemortem psychometric tests in the normal range when corrected for age and education (Schmitt et al., 2000).

1.1.6. Etiology

The etiology and pathogenesis of AD are unknown at present. In order to explain the pathology of the disease, several hypotheses have been advanced, including genetic

abnormalities, slow or latent virus disorder, deficits in energy metabolism, glutamate excitotoxicity, defects in mitochondria, the amyloid cascade, tau abnormality, acetylcholine deficiency, trace element neurotoxicity or oxidative stress. Currently, none of these hypotheses alone can adequately explain the clinical and pathological aspects of AD. It is probable that AD is a multifactorial disease and a combination of multiple hypotheses may more adequately explain the pathogenesis of the disease. Multiple studies have shown presence of oxidative stress in AD patients, even though the exact role of oxidative stress in the pathogenesis of AD is not known (Khachaturian and Radebaugh, 1996; Markesbery, 1997b; Thies and Bleiler, 2011). The oxidative stress hypothesis is described below as the work in this thesis examines the oxidative damage caused to biomolecules when they undergo oxidative stress.

1.2. Oxidative Stress and AD

1.2.1 Reactive Oxygen Species (ROS)

A free radical is an atom or molecule containing one or more unpaired electrons in its outer shell. Free radicals are produced both exogenously and endogenously in the human body. Oxygen free radicals (the most common free radicals present in the human body) including superoxide ($O_2^{\bullet -}$), hydroxyl ($^{\bullet}OH$), peroxyl ($RO_2^{\bullet -}$) and alkoxyl ($^{\bullet}OR$) radicals along with non-radicals such as hypochlorous acid (HOCl), ozone (O_3), peroxynitrite ($ONOO^-$), singlet oxygen ($^1O_2$) and H_2O_2 that can be easily converted to radicals, are collectively labeled as “reactive oxygen species” (ROS) (Apel and Hirt, 2004; Murphy, 2009). Reactive oxygen species (ROS) such as $^{\bullet}OH$, and $O_2^{\bullet -}$ are predominantly produced during normal cellular metabolism like oxidative phosphorylation during normal cellular respiration. In a normally functioning cell,

approximately 2% of oxygen consumed during oxidative phosphorylation is converted to ROS (reviewed in (Murphy, 2009)). In a normal biological system, excess ROS are scavenged by enzymes such as superoxide dismutase, glutathione peroxidase and catalase among others, making them less detrimental. Superoxide radicals are converted to hydrogen peroxide by antioxidant enzymes, superoxide dismutases. Hydrogen peroxide thus produced can be rendered harmless either by conversion to water and molecular oxygen by glutathione peroxidase/ catalase or can diffuse into the cytoplasm and react with Fe (Fenton's reaction) or Cu (Haber-Weiss reaction) present to generate hydroxyl radicals which cause oxidative damage (Figure 1.2) (Markesbery, 1997b; Wiseman and Halliwell, 1996). ROS can also be produced by ionizing or ultraviolet radiation, smoking, air pollution and other biological processes such as inflammation (Cooke et al., 2003; Markesbery, 1997b; Markesbery and Lovell, 2006; Wiseman and Halliwell, 1996). As a result of its high oxygen consumption (1/5 of consumed oxygen) , substantial lipid content, relatively high levels of redox active metals, and the comparative inadequacy of antioxidant enzymes, the brain is especially susceptible to damage by free radicals (Markesbery, 1997b).

1.2.2. Oxidative Stress

A discrepancy between the production of ROS and the biological system's ability to eliminate these reactive intermediates results in oxidative stress and subsequently mitochondrial dysfunction and neuronal damage. Oxidative stress has been linked to aging and various age-associated neurodegenerative diseases including AD, Parkinson's disease and amyotrophic lateral sclerosis (Bowling et al., 1993; Harman, 1956; Jenner, 2003; Markesbery, 1997b). Studies have suggested that the late life onset and slow

progression of these conditions could thus be accounted for by cumulative and irreversible oxidative damage over time. Oxidative stress can cause damage to most biomolecules in the body. Some biomarkers of oxidative damage are 8-hydroxyguanosine (oxidative damage of nucleic acids), protein carbonyls, 3-nitrotyrosine (oxidative damage of proteins) and 4-hydroxynonenal and malondialdehyde (oxidative damage of lipids). Several of the above markers have been detected in multiple vulnerable regions of the brains of LAD and MCI patients, leading to the theory that oxidative stress has a prominent role in the early pathogenesis of AD (Cooke et al., 2003; Markesbery, 1997b; Markesbery and Lovell, 2006).

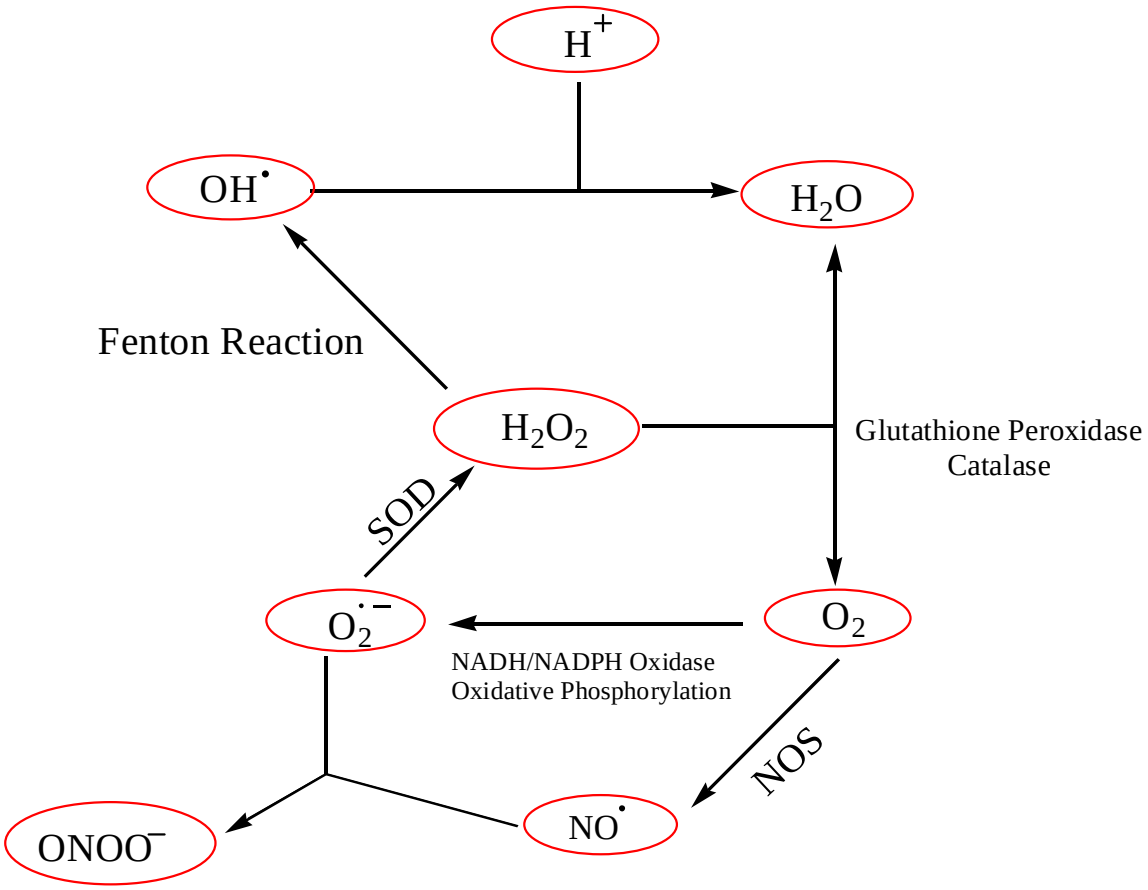

Fenton Reaction: $Fe^{2+} + H2O_2 \longrightarrow Fe^{3+} + OH^{\bullet -} + OH^-$

Figure 1.2. Formation of free radicals in human body (adapted from (Wu et al., 2009)

1.2.3. Lipid Peroxidation and Protein Oxidation

Biological membranes are composed of 30-80% lipids by mass and are vitally important for the preservation of cellular homeostasis. Elevated levels of both lipid and protein oxidation have been reported in several neurodegenerative diseases such as AD and Parkinson's disease (Bradley et al., 2010; Jenner, 2003; Markesbery, 1997b; Markesbery and Carney, 1999; Williams et al., 2006; Zhou et al., 2008). Measurements of thiobarbituric acid reactive substances (TBARS), changes in polyunsaturated fatty acids (PUFA) and breakdown products of PUFA (aldehydes and isoprostanes) are indicators of lipid peroxidation in a biological system. Peroxidation of lipids produces multiple aldehydic by-products including malonialdehyde, C_3-C_{10} straight chain aldehydes and α,β-unsaturated aldehydes such as 4-hydroxynonenal (HNE) and acrolein. HNE and acrolein are neurotoxic, can form adducts with DNA/protein thus affecting their function and are frequently used as markers of lipid oxidation. Levels of HNE and acrolein have been shown to be elevated in AD brain and CSF (Bradley et al., 2010; Bruce-Keller et al., 1998a; Bruce-Keller et al., 1998b; Montine et al., 1998; Williams et al., 2006). Previous studies show that isoprostanes, produced by free-radical peroxidation of arachidonic acid are also elevated in the CSF of AD subjects as compared to control subjects (Milne et al., 2005; Montine et al., 1998).

Oxidative damage to proteins causes a decrease in protein activity; probably due to elevation in protein carbonylation levels, side chain oxidation and protein crosslinking (Poon et al., 2004; Soskic et al., 2008). Protein oxidative damage is principally analyzed by the hydrazide reactive protein carbonyl analysis (Smith et al., 1991). Previous studies show the presence of nitrotyrosine in NFT's and an elevation in protein carbonyl levels in

the hippocampus and the frontal and parietal lobes in the brain of AD patients compared to control subjects (Hensley et al., 1995; Smith et al., 1991; Smith et al., 1997).

1.2.4. Nucleic Acid Oxidation

The attack of ROS on DNA can generate more than 20 kinds of oxidized base adducts including 8-hydroxyguanine (8-OHG), 2,6-diamino-4-hydroxy-5-formamidopyrimidine (fapy guanine), 8-hydroxyadenine (8-OHA), 4,6-diamino-5-formamidopyrimidine (fapy adenine) 5-hydroxycytosine (5-OHC) and 5-hydroxyuracil (5-OHU) (Figure 1.3A) (Cooke et al., 2003; Gabbita et al., 1998; Markesbery and Carney, 1999). ROS such as hydroxyl radical reacts with the double bonds in both purines and pyrimidines leading to the formation of purine-OH (at positions C4, C5 or C8) or pyrimidine-OH (at position C5 or C6) adducts. 8-hydroxyguanine (-OHG) /8-hydroxyadenine (8-OHA) are produced by oxidation of the C8-hydroxyl radical formed by the reaction of $^{\bullet}$OH radical with the C8-N9 double bond of purines. In the absence of oxygen however, 2,6-diamino-4-hydroxy-5-formamidopyrimidine (fapyguanine; fapyG) and 4,6-diamino-5-foramidopyrimidine (fapyadenine; fapyA) are formed due to imidazole ring opening at the C8-N9 site (Figure 1.3B and 1.3C). 5-hydroxycytosine (5-OHC) is formed by dehydration of cytosine glycol and 5-hydroxyuracil (5-OHU) is produced by deamination of cytosine glycol. Cytosine glycol is in turn produced by reduction of the pyrimidine-OH adduct with water (Figure 1.3D) (Cooke et al., 2003; Steenken, 1989a, b). Bulky exocyclic adducts are formed when DNA base modifications are caused by lipid peroxidation products including 4-hydroxynonenal and acrolein. These modifications in DNA bases could cause mispairing during DNA replication

eventually leading to altered protein synthesis (Markesbery and Carney, 1999; Wang et al., 2005).

As a result of its high electron density and low oxidation potential, guanine (G) is the most vulnerable to oxidation among the five DNA bases (Bhattacharya and Barton, 2001; Candeias and Steenken, 1989; Steenken and Jovanovic, 1997). Oxidation of guanine leads to the formation of 8-OHG under elevated oxygen levels and fapyguanine under hypoxic conditions (Steenken and Jovanovic, 1997). The predominant biomarker for oxidative damage of DNA is the major oxidation product of guanine, 8-OHG. 8-hydroxyguanine production can lead to its mispairing with adenine and even misreading of adjacent bases during replication (Cheng et al., 1992). Previous studies have shown an increase in levels of 8-OHG and 8-OHA in nDNA from various regions of the brain including the temporal, parietal and frontal lobes of AD patients even in the earlier stages of the disease as compared to normal control subjects (Gabbita et al., 1998; Wang et al., 2008).

Increased oxidation of nuclear and mitochondrial DNA, and RNA by ROS especially the hydroxyl radical ($^{\bullet}OH$), have been implicated in multiple neurodegenerative diseases including AD, PD and DLB (Bowling et al., 1993; Gabbita et al., 1998; Lyras et al., 1998; Wang et al., 2005; Zhang et al., 1999; Zhou et al., 2008). Although oxidation in both nuclear and mitochondrial DNA in AD subjects has been extensively studied, there are few studies that focus on RNA oxidation in AD. Shan et al. showed an elevation of 8-OHG in mRNA and a corresponding decrease in protein expression in LAD subjects compared to NC subjects (Shan et al., 2007; Shan and Lin, 2006). Messenger RNA oxidation may result in premature translation termination and reduction in activity of

translated mRNAs (Shan et al., 2007; Shan et al., 2003). Due to the lack of protective histones, lack of rich antioxidant system, diminished DNA repair capability and the proximity to the site of generation of ROS, mitochondrial DNA (mtDNA) appears to be more vulnerable to oxidative damage compared to nuclear DNA. Previous studies have found ~ 2-10 fold higher levels of oxidized bases in mtDNA compared to nDNA (Mecocci et al., 1993; Wang et al., 2005). Oxidative damage to DNA by ROS can result in base alterations, single and double strand breaks, DNA-DNA/DNA-protein crosslinks, sister-chromatid exchange and translocation. These changes in the DNA can lead to altered protein expression which in turn may cause apoptosis.

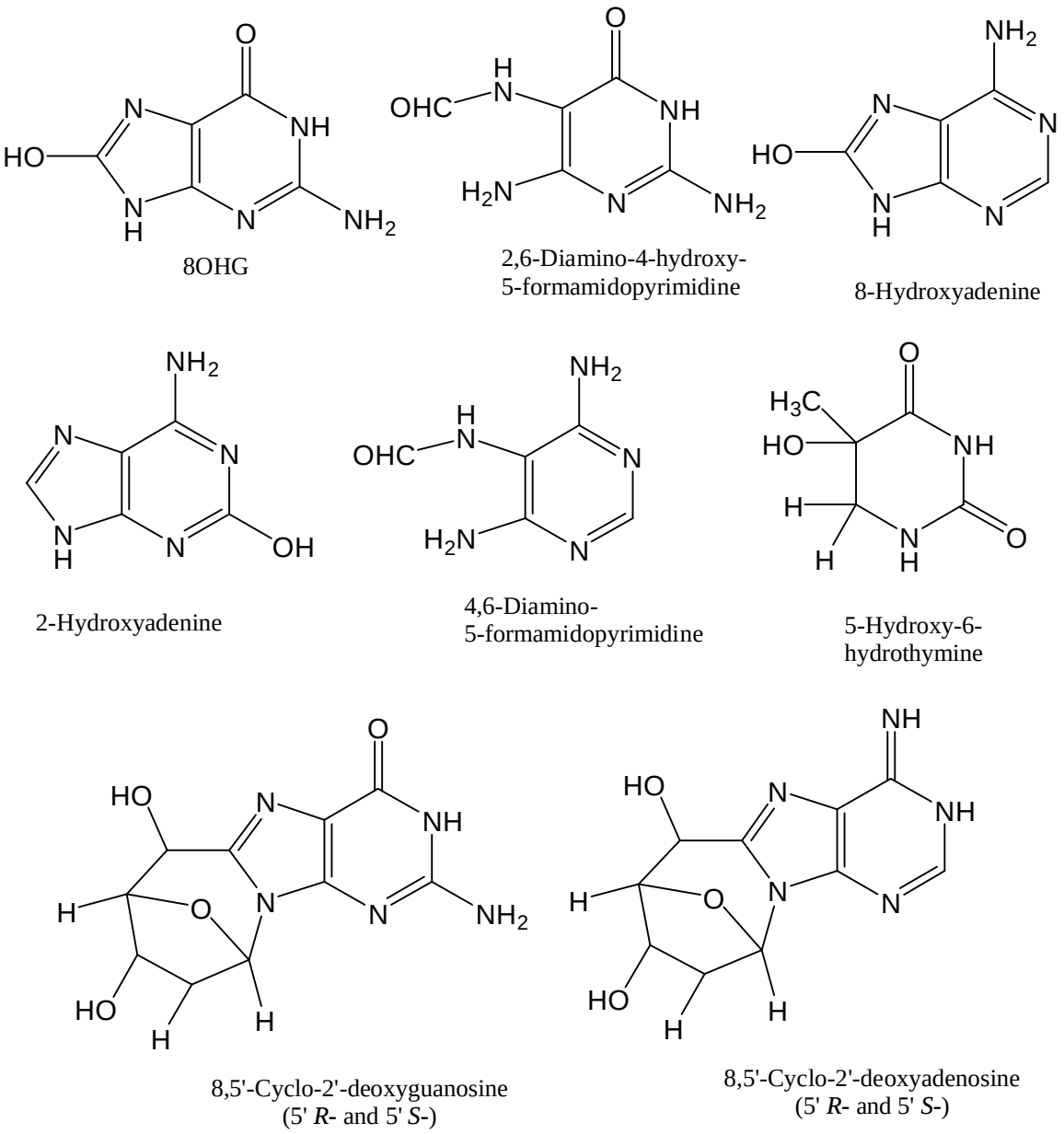

Figure 1.3A. Structure of some representative oxidized DNA bases

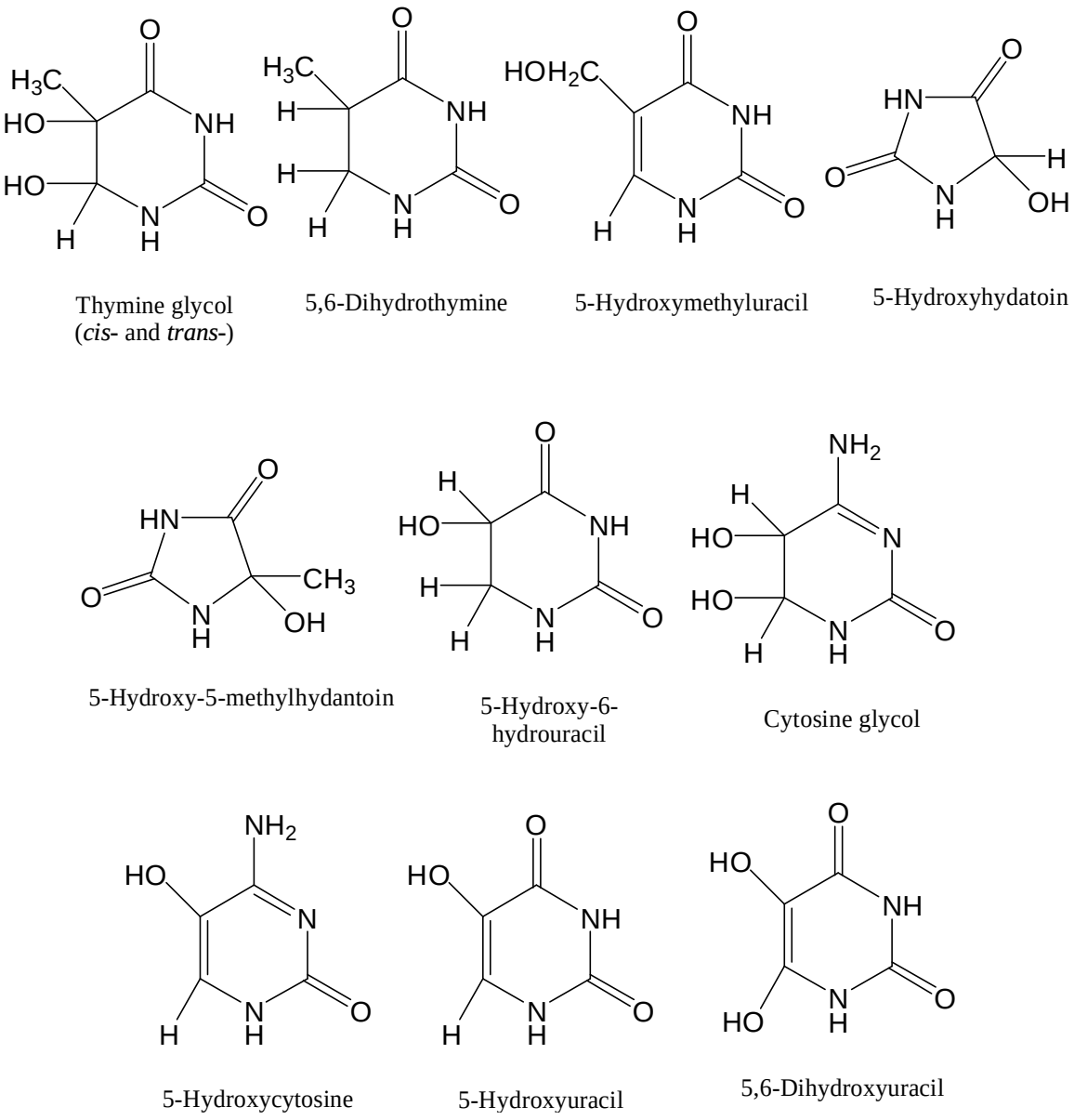

Figure 1.3A Contd. Structure of some representative oxidized DNA bases

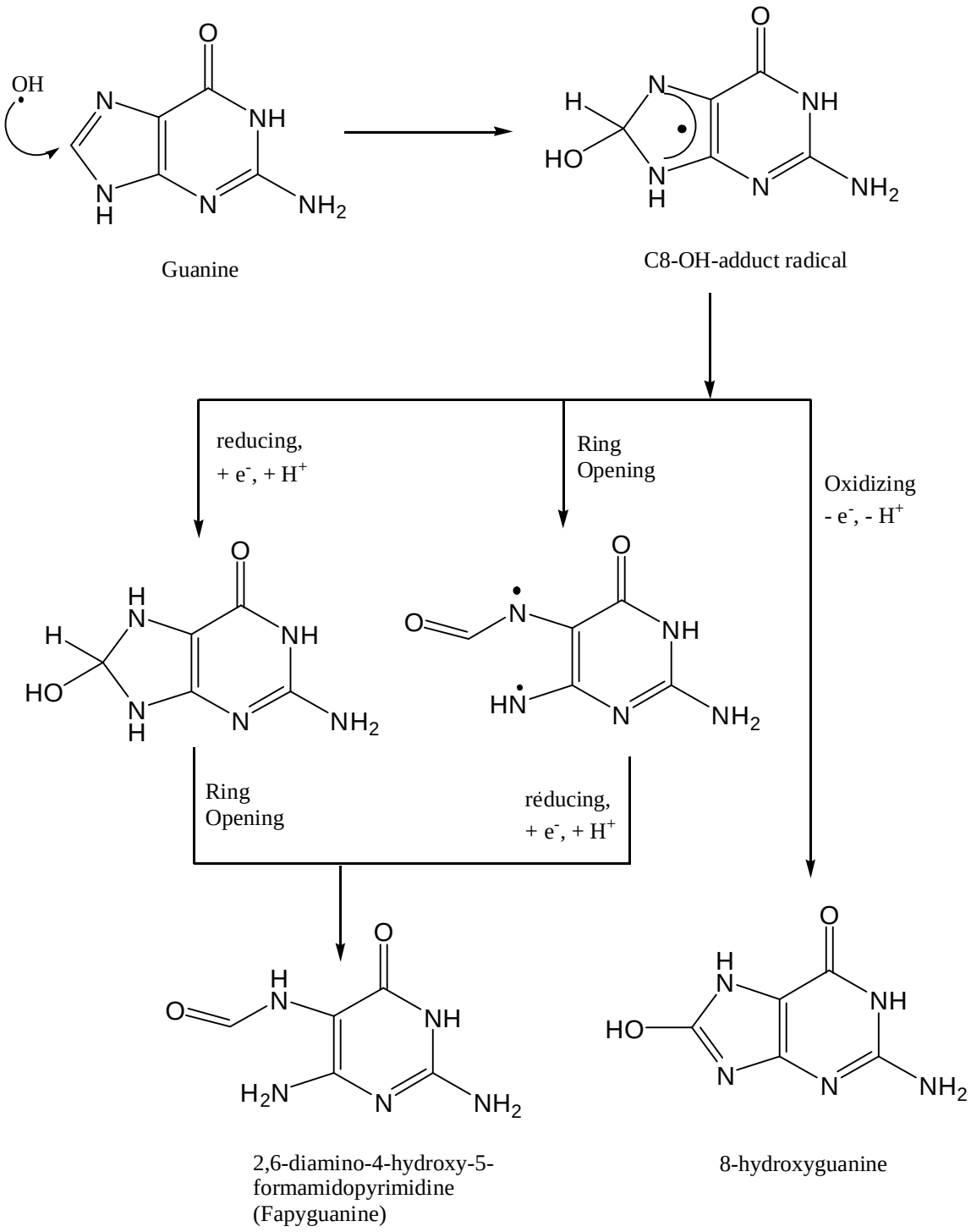

Figure 1.3B. Reaction scheme for oxidation of guanine

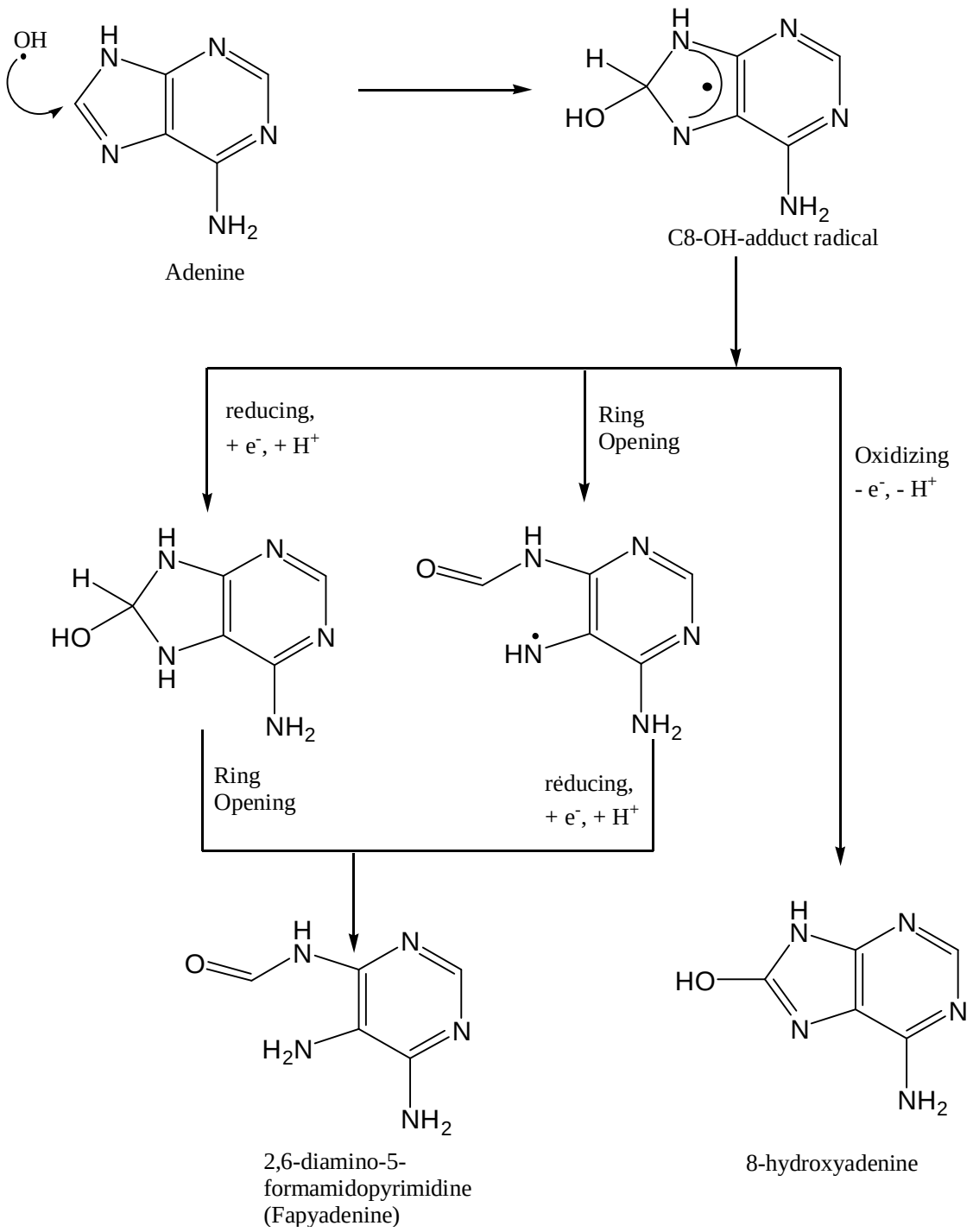

Figure 1.3C. Reaction scheme for oxidation of adenine

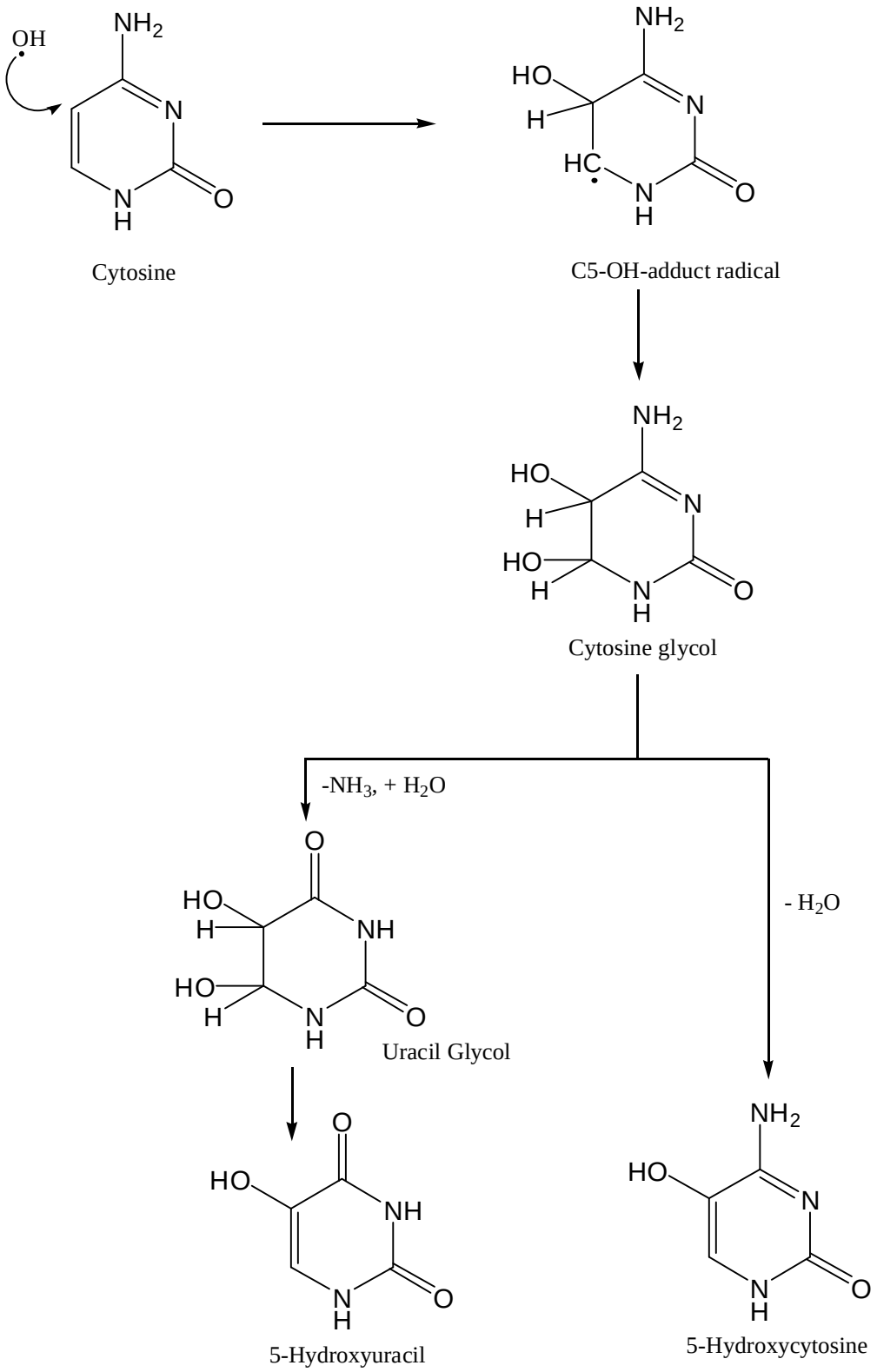

Figure 1.3D. Reaction scheme for oxidation of cytosine

1.3. DNA Repair Pathways

In healthy individuals, damaged DNA is repaired via multiple DNA repair pathways including base excision repair (BER), nucleotide excision repair (NER), double strand break repair (DSB) and mismatch repair (MMR). A brief description of these repair pathways is given below.

1.3.1. Base Excision Repair (BER) Pathway

The primary pathway for DNA repair of small base modifications such as alkylation, deamination and oxidation is the BER pathway. The BER pathway proceeds via removal of damaged DNA bases by substrate specific glycosylases including oxoguanine DNA glycosylase (OGG1) and uracil DNA glycosylase (UNG), incision of the apurinic/apyrimidinic site by endonucleases such as AP endonuclease (APE1), followed by incorporation of the correct nucleotide(s) by DNA polymerase and strand ligation by DNA ligase (Figure 1.4). The BER pathway is further divided into two sub-pathways: short-patch BER (single nucleotide excision) and long-patch BER (repair patch size of 2-8 nucleotides). It is postulated that in age-related neurodegenerative diseases like AD, the DNA repair system loses its capacity leading to accumulated oxidative DNA damage (Lovell et al., 2000; Markesbery and Lovell, 2006; Moreira et al., 2008; Weissman et al., 2007).

Proteins implicated in aging/AD from the base excision repair (BER) pathways including 8-oxoguanine DNA glycosylase (OGG1), Uracil-DNA glycosylase (UNG), APE nuclease1 (APE1), Polymerase (DNA directed), beta (POLB), Flap structure-specific endonuclease 1 (FEN1), Poly (ADP-ribose) polymerase 1 (PARP1) and X-ray repair complementing defective repair in Chinese hamster cells 1 (XRCC1) were

investigated in this study. Previous studies have shown that 8-hydroxyguanine or its isomeric form 7,8-dihydro-8-oxoguanine is the major DNA lesion resulting from nuclear/mitochondrial DNA oxidation (Cooke et al., 2003; Loft et al., 2008; Moreira et al., 2008). Unrepaired 8-hydroxyguanine induces G:C → A:T transversion mutations during replication or in the case of postmitotic cells like neurons, it may lead to diminished cellular activity and death. 8-oxoguanine DNA glycosylase (OGG1) is the principal enzyme for excision of 8-oxoguanine in the initiation step of the BER pathway for both nuclear and mitochondrial DNA lesions. Previous studies show a decrease in gene expression, protein levels and incision activity of nuclear OGG1 in vulnerable brain regions of patients suffering from AD (Dorjsuren et al., 2011; Lovell and Markesbery, 2007b; Weissman et al., 2007). Mao et al. showed that there was complete loss of 8-oxo-guanine glycosylase activity *in vitro* with a single base deletion (C796) observed in a subset of AD subjects whereas, two different single base substitutions resulted in reduced glycosylase activity *in vitro* (Mao et al., 2007). Another common lesion observed in DNA is the introduction of uracil into genomic DNA by deamination of cytosine. Unrepaired uracil in DNA leads to a C→T transition mutations during replication. Uracil-DNA glycosylase (UNG) initiates the BER pathway in cases of misincorporation of uracil into DNA and is the primary enzyme for removal of uracil from DNA. UNG protein levels and protein activity are lower in AD subjects compared to clinically normal subjects (Hegde et al., 2008; Kruman et al., 2004; Weissman et al., 2007). Both OGG1 and UNG lead to the creation of an apurinic/apyrimidinic (AP) site after excision of the damaged base. APE nuclease1 (APE1), a multifunctional DNA repair enzyme, primarily functions as a nuclease in the second and rate limiting step in the BER pathway. APE1 removes the

AP site by cleaving the DNA strand 5□ to the AP site leaving a gap in the DNA strand with a 3□ OH and a 5□ deoxyribose phosphate terminus (Hegde et al., 2008; Weissman et al., 2007). Studies have shown an increase in the expression of ***APE1*** but no significant changes in AP-site incision activity or APE1 protein levels in the brain of AD patients compared to normal control subjects (Burns and Iliffe, 2009; Davydov et al., 2003; Weissman et al., 2007).

Polymerase (DNA directed), beta (POLB) is implicated occasionally in ***de novo*** DNA synthesis. Recent studies indicate POLB may be involved early in the pathogenesis of AD. An increase in expression of POLB was observed in neurons with minor AD-related neuropathology but the protein expression reduced with severity of pathology (Copani et al., 2006; Weissman et al., 2007). X-ray repair complementing defective repair in Chinese hamster cells 1 (XRCC1) facilitates the repair and rejoining of DNA strand breaks and repairs gaps left during BER. Doğru-Abbasoğlu et al. found that the Trp allele of the functional ***XRCC1*** Arg194Trp genetic polymorphism occurs more frequently in AD patients than in clinically normal individuals (Dogru-Abbasoglu et al., 2007; Woodhouse and Dianov, 2008). Poly (ADP-ribose) polymerase 1 (PARP1) is activated when oxidative damage leads to single strand or double strand breaks of DNA. PARP1 acts as a catalyst in two processes: (a) cleavage of NAD^+ into adenosine 5'-diphosphoribose (ADP-ribose) and nicotinamide and (b) the covalent attachment of ADP-ribose polymers to nuclear proteins such as histones. An increase in gene expression of PARP1 in AD patients, leading to massive NAD^+ depletion and subsequent cell death, has been reported (Reddy P.V., 2006). Flap endonuclease 1 (FEN1) acts as an 5'-exonuclease and gap endonuclease in DNA replication and long patch BER respectively.

FEN1 helps remove the flap segment formed during long-patch BER by addition of nucleotides around the damaged base by POLB. DNA ligase then seals the gap that remains after repair (Podlutsky et al., 2001a; Zheng et al., 2011).

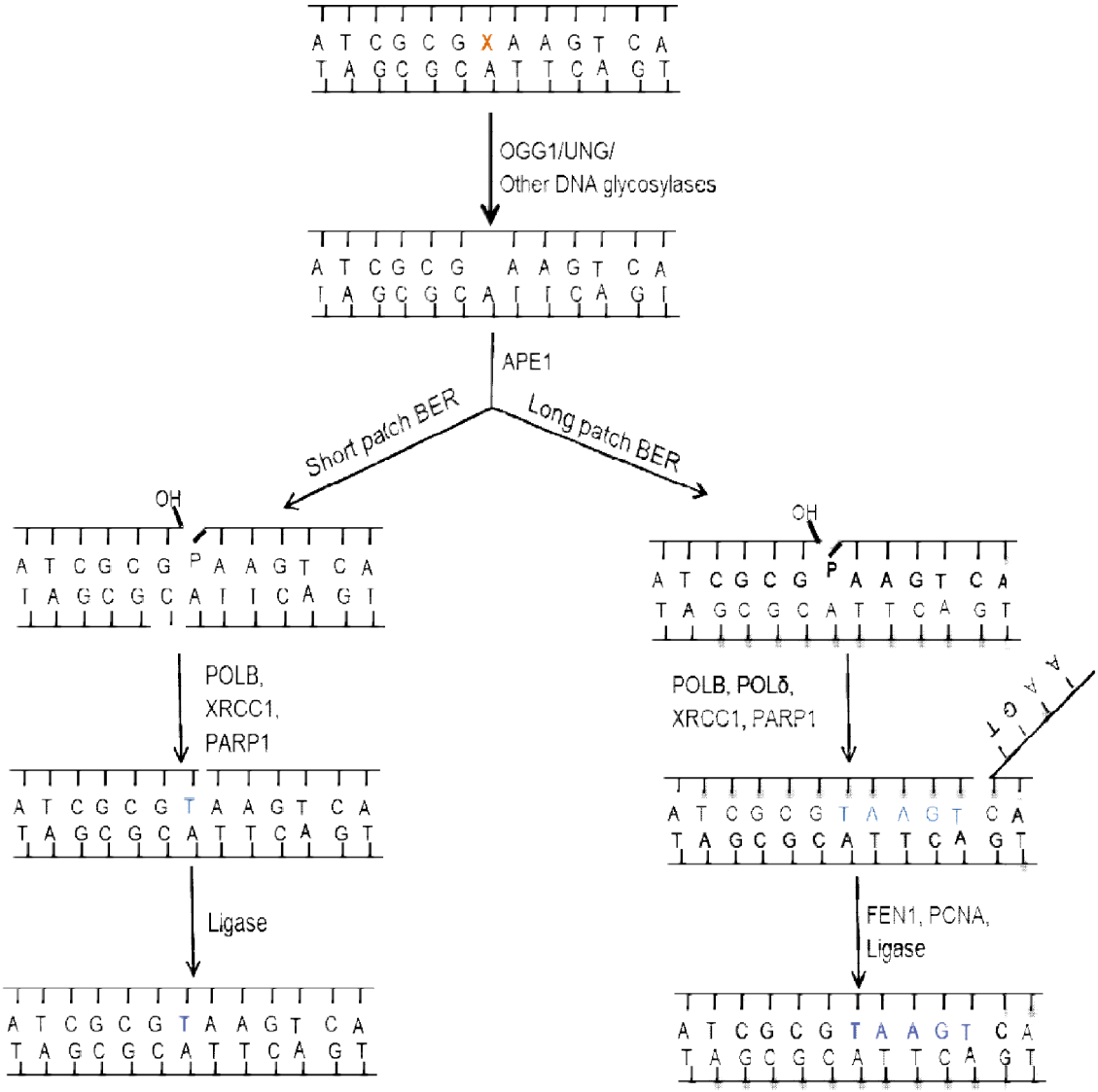

Figure 1.4. Base Excision Repair (BER) Pathway

1.3.2 Nucleotide Excision Repair (NER) Pathway

The NER pathway is the principal repair mechanism for removal of bulky helix distortions such as lesions made by UV-induced pyrimidine dimers, intra-strand crosslinks, protein DNA crosslinks, and bulky chemical adducts. Multiple enzymes including xeroderma pigmentosum, EF-hand protein, replication protein A (RPA) and the UV-damaged DNA-binding protein (UV-DDB) are functional in the NER pathway. In humans, multiple inherited disorders caused by mutations in NER enzymes have been diagnosed. Studies show that in non-replicating cells such as neurons, NER is highly diminished. (von Kobbe et al., 2003). Xeroderma pigmentosum complementation group A (XPA), an enzyme in the nucleotide excision repair (NER) pathway, has also been implicated in aging. Subjects with XP, a rare autosomal recessive disease characterized by hypersensitivity of skin to sunlight and an increased risk of skin cancer of sun-exposed parts of the body, show a defect in the early step of nucleotide-excision repair. Xeroderma pigmentosum consists of eight different complementation groups (groups A–G, and a variant). Of all the complementation groups, Group A (XPA) is the most severe clinical form (Bennett et al., 1997).

1.3.3. Double Strand Break (DSB) Repair Pathway

The DSB repair pathway is involved in the repair of potentially lethal DNA double-strand break lesions formed by broken strands of the DNA duplex. DSBs can be caused by both exogenous agents such as ionizing radiation and cellular processes such as DNA replication (Chapman et al., 2012). Flap structure-specific endonuclease 1 (FEN1), Meiotic recombination 11 homolog A (MRE11A) and RAD50 homolog (RAD50) are enzymes that function in the DSB repair pathway. FEN1 is a nuclease protein in the BER

pathway and helps in the Polγ-catalyzed DNA synthesis process. Polymerase γ is necessary for replication and repair as it is the only currently identified mitochondrial DNA polymerase (Podlutsky et al., 2001a). MRE11A is a part of the Mre11 protein complex which also includes Rad50 and Nbs1 proteins. The Mre11 protein complex has multiple functions including initiation of cell cycle checkpoints and recognition and repair of damaged DNA. Studies have shown a reduction in the expression of the Mre11 complex proteins in neurons of AD cortex compared to age-matched controls (Jacobsen et al., 2004).

1.3.4. Mismatch Repair (MMR) Pathway

The MMR pathway repairs base-base and insertion/deletion mismatches that escape proof-reading by DNA polymerase during replication and recombination. If left unrepaired these mismatches can lead to mutations in DNA in subsequent replication cycles which in turn can lead to phenotype changes and consequent dysfunction and disease (Henneke et al., 2003; Hsieh and Yamane, 2008; Yamaguchi et al., 1989). EXO1 is an essential enzyme in the mismatch repair pathway and is involved in 5'-3' exonuclease activity on dsDNA, 5' flap endonuclease activity and weak RNaseH activity (Balusu et al., 2007).

1.3.5. Other Genes Involved in DNA Repair

Other genes related to DNA repair studied in this project include Ataxia telangiectasia mutated (ATM). ATM helps in regulation of the activity of molecules that manage cell-cycle arrest and repair by initiating signal transduction pathways. ATM deficiency may lead to radiation sensitivity, germ cell degeneration, mild

immunodeficiency, and an extreme sensitivity to developing T cell lymphomas (Strom et al., 2011).

1.4. Additional Neurodegenerative Diseases

Besides AD, several other types of dementia leading to neurodegeneration exist including vascular dementia, dementia with lewy bodies, frontotemporal dementia, Creutzfeldt-Jakob disease, Parkinson's disease, normal pressure hydrocephalus, Huntington's disease and Wernicke-Korsakoff syndrome. In order to determine if the changes seen in this study were AD-specific or were a common phenomenon of dementia, tissue specimens were studied from diseased control subjects suffering from dementia with lewy bodies (DLB) and frontotemporal dementia (FTD).

1.4.1. Dementia with Lewy Bodies

Dementia with Lewy bodies accounts for 10-25% of dementia cases making it the second most common form of dementia in elderly populations after AD (Zaccai et al., 2005). Clinically, DLB is difficult to diagnose as it shares clinical, neuropsychological and pathological hallmarks with AD, vascular dementia and Parkinson's disease. DLB patients suffer from visual hallucinations, delusions, significant memory loss, impairment in thinking and reasoning, REM sleep disorder and Parkisonian symptoms such as hunched posture, rigid muscles and shuffled gait. The neuropathological hallmark for DLB is the presence of spherical intracellular microscopic inclusions called Lewy bodies in the midbrain and cerebral cortex. The primary structural component of Lewy bodies is a protein called α-synuclein (Henchcliffe et al., 2011; Zaccai et al., 2005). Currently, the clinical diagnosis for DLB are based on criteria described by the Consortium on DLB criteria and includes the semi-quantitative evaluation of lesion density in the brainstem,

basal forebrain/limbic regions and neocortical regions, alpha-synuclein immunohistochemistry, REM sleep behavior disorder, severe neuroleptic sensitivity, and decreased activity of striatal dopamine transporter (McKeith et al., 2005).

1.4.2. Frontotemporal Dementia (FTD)

Frontotemporal dementia is defined as a group of multiple neurodegenerative diseases caused by progressive neurodegeneration in the frontal and temporal lobes. FTD accounts for approximately 4-20% of all dementia cases with average age of onset being in the 50's or early 60's. Patients with FTD can survive from 2-20 years with most subjects surviving an average of 6-8 years. Occurrence of FTD is more common in men than women at a ratio of 14:3 (Grossman, 2002; Ratnavalli et al., 2002). Symptoms of FTD can be categorized into three different groups:

1.4.2.1. Behavioral Variant Frontotemporal Dementia (bvFTD)

Patients with bvFTD primarily show changes in personality and behavior. Clinically, bvFTD patients suffer from disinhibition, apathy, loss of sympathy, compulsive behaviors, hyperorality and a dysexecutive neuropsychological profile (Rascovsky et al., 2011).

1.4.2.2. Primary Progressive Aphasia (PPA)

In PPA, language is impaired in the early stage of the disease followed by changes in behavior in advanced stages. The two primary forms of PPA are semantic dementia and progressive nonfluent aphasia (PNFA). Semantic dementia patients are characterized by increasing decline of naming and word comprehension but retention of fluency in syntax and phonology. People with PNFA suffer from impairments in speech articulation and

reading and writing ability but preserve speech comprehension abilities (2010; Lambon Ralph et al., 1999; Sobol et al., 1996).

1.4.2.3. FTD Movement Disorders (FTDMD)

Impairments in language, behavior and involuntary, automatic muscle functions are characteristic of FTD movement disorders. Most prevalent forms of FTDMD include corticobasal degeneration (CBD) and progressive supranuclear palsy (PSP). CBD is characterized by shakiness, lack of coordination, muscle rigidity and spasms whereas PSP patients show eye movement, walking and balance problems; neck and upper body muscle stiffness and frequent falls (Keith-Rokosh and Ang, 2008; Mahapatra et al., 2004; Scaravilli et al., 2005).

Clinical diagnosis of FTD is based on observation of behavioral changes, brain imaging and neuropsychological tests. MRI images can help detect frontal/temporal atrophy characteristic of FTD in the later stages. The similarity of symptoms between AD and FTD makes the clinical diagnosis of FTD difficult. Pathologically FTD diagnosis is based on immunohistochemical evaluation for Tau epitopes, PHF1 (PHD finger protein 1) and AT8 (paired helical filament tau), ubiquitin and α-synuclein in the middle frontal gyrus (MFG), superior temporal gyri (SMG), parietal lobe (PL), hippocampus/parahippocampal gyri (HPG), and the cingulated gyrus (CG) (Hutton et al., 1998; Neumann et al., 2007; Rosen et al., 2002; Talbot et al., 1998).

1.5. Statements of Research Projects

1.5.1. Oxidative DNA Damage in Genes of Proteins Modified During AD

Although multiple studies demonstrate increased oxidative DNA damage in the progression of AD (Gabbita et al., 1998; Lovell et al., 1999; Lovell and Markesbery,

2007b; Markesbery and Lovell, 2006), the exact site of the oxidation in the human genome remains unclear. We hypothesized that DNA oxidative damage is not an arbitrary process but may be distinctively localized to specific genes. We further hypothesize that the most highly oxidized genes are those coding for proteins whose expression has shown to be altered in the brain of AD subjects. In order to test this hypothesis, nDNA from NC, MCI, PCAD and LAD specimens were treated with formamidopyrimidine glycosylase (fpg), a DNA repair enzyme that recognizes and removes damaged bases including 8-oxoguanine, 8-oxoadenine, fapy-guanine, methy-fapy-guanine, fapy-adenine, aflatoxin B_1-fapy-guanine, 5-hydroxy-cytosine and 5-hydroxy-uracil. Formamidopyrimidine glycosylase has both N-glycosylase (release of damaged purines from dsDNA creating an apurinic (AP) site) and AP-lyase (cleavage of AP site) activities leading to a single-nucleotide gap flanked by phosphate termini in damaged DNA (Du et al., 2009). The percent oxidative damage in different amplicons of genes coding for proteins shown to be altered in the progression of AD were then quantified using quantitative/real-time polymerase chain reaction (qPCR/ RT-PCR). To understand the utilization of qPCR in this study, both traditional PCR and qPCR are discussed in the following section. Table 1.1 lists several genes for which alterations in proteins are observed in AD. This study focused on the three isoforms of the voltage dependent anion channel proteins, VDAC1, 2 and 3. VDACs were the ideal candidate for this study as the three forms differ in abundance, size and activity, and are altered differentially in the AD brain. Lovell et al. found a significant elevation of VDAC1 levels, no significant change in VDAC2 levels and a trend towards significant increase of VDAC3 levels in Aβ-treated primary rat cortical neuron cultures (Lovell et al., 2005). To

test the assumption oxidation of the coding sequence of a protein leads to differential protein levels and activity, we designed an experiment using the protein IGF2 (insulin like growth factor-II). IGF2 was selected for this experiment because it has one of the smallest coding sequences (only 202 bp in length) and well characterized activity assays. Progressively increasing amounts of 8-oxoguanine were incorporated into the IGF2 coding sequence and the DNA thus obtained subjected to *in vitro* transcription and translation using a cell free system to produce the IGF2 protein. The protein levels and activity in these samples was quantified and compared to a positive control sample containing no oxo-guanine.

1.5.1.1. Polymerase Chain Reaction

Polymerase chain reaction (PCR) is a biochemical technique conceived by Kary Mullis and colleagues in 1985 for exponentially amplifying short DNA segments (100-600 bases). Automation of PCR following the discovery and isolation of thermo-stable DNA polymerase (Taq polymerase) from the bacterium *Thermus aquaticus* has led to its application in multiple facets of biology and chemistry. The reaction components of a traditional PCR reaction include target DNA, forward and reverse primers, DNA polymerase, deoxynucleotide triphosphates (dNTPs), $MgCl_2$, PCR reaction buffer and water. The PCR reaction buffer provides an optimal pH and monovalent salt environment and water acts as an interaction medium for the other reaction components of the PCR reaction. Magnesium cations required as cofactors for the DNA polymerase enzymes are provided by $MgCl_2$. Individual DNA bases are supplied by the dNTPs to DNA polymerases for formation of new DNA strands during a PCR reaction. The β and γ phosphates of the dNTPs also fulfill the energy requirements of the PCR reaction. Target

DNA provides the template for amplification by DNA polymerases. Ideally, template DNA should be uncontaminated by any other DNA/RNA source. Specific thermostable DNA polymerases including Taq polymerase (source: ***Thermus aquaticus)*** , Tth polymerase (source: ***Thermus thermophilus***), Tfl polymerase (source: ***Thermus flavus***), Pfu polymerase (source: ***Pyrococcus furiosus***) Tli polymerase (source: ***Thermus litoralis***) and ***Pyrococcus species*** GB-D may be used in PCR reactions dependent on specific application. The DNA polymerase enzyme for a PCR reaction is selected based on three factors, (1) processivity (rate at which the polymerase produces a complementary copy of the template), fidelity (accuracy of complementary copy formation) and persistence (stability of enzyme at high temperature). Taq polymerase, the most commonly used enzyme in PCR, has a procesivity of 50-60 nucleotides per second at 72 C, an error rate of 285 x 10^{-6} errors per template nucleotide and a half-life of 1.5 hours at 95 C. Taq polymerases have 5'→3' nuclease activity but lack 3'→5' proof reading ability leading to the incorporation of a single 3' adenosine nucleotide on both strands of every amplicon. Primers are short oligonucleotide sequences designed to be complementary to the target DNA necessary for new DNA strand synthesis and are usually added in excess amounts in a PCR reaction. For maximum efficiency of a PCR reaction, primers should be at least 20 nucleotides in length with PCR reaction compatible melting temperatures and the forward and reverse primers should not form primer-dimer bands. In conventional PCR, PCR products are visualized using ethidium bromide on an agarose gel and analyzed using radio-imaging or other densitometric methods.

Typically a PCR reaction is characterized by three steps shown in Figure 1.5:

a) Denaturation in which the double stranded target DNA is denatured by heating to 94-95 ^{o}C to produce single stranded DNA strands that act as templates for new DNA strand synthesis.

b) Annealing in which DNA primers anneal to the complementary single stranded DNA in preparation for DNA synthesis by DNA polymerases. This annealing process requires cooling to the primer annealing temperature which is determined by the melting temperatures of the primers. The temperature at which 50% of a DNA duplex dissociates to become single stranded DNA is called its melting temperature (T_m). T_m's are dependent on pH, ionic strength and base composition of DNA. Primer annealing temperatures are typically 2 ^{o}C lower than the lowest primer T_m.

c) Elongation in which new DNA is synthesized by addition of dNTPs onto the primers by DNA polymerase in the 5'→ 3' direction from the primer. The release of pyrophosphate on addition of dNTPs to the growing DNA strand provides the energy needed for the polymerase to appropriate and add the next complementary base. Polymerization usually occurs at a temperature of 72 ^{o}C, the optimal temperature for Taq polymerase but the polymerization temperature used can vary based on length of product, number of cycles and usage of other DNA polymerases for polymerization.

These three steps are repeated for a defined number of cycles depending on the output required. A PCR reaction with 25-40 cycles is the usual norm.

A PCR reaction theoretically doubles the amount of target DNA after each reaction cycle. For example, a PCR reaction with 25 cycles should produce 2^{25} or more than 33 million copies of the amplicon for each double stranded target DNA molecule present. This can be represented by the exponential curve shown in Figure 1.6a. Experimentallly

PCR amplification typically resembles Figure 1.6b and is composed of three separate sequential phases:

a) Exponential phase: In the initial exponential phase DNA polymerase works at near optimum capacity leading to almost exact doubling in the amount of product after each cycle. This phase closely resembles the theoretical expectation of PCR amplicon production and has high specificity and precision.

b) Linear phase: After a time, reaction components are consumed at different rates, the amplicon production slows down and the PCR reaction enters a quasi-linear phase. Amplification of the target is highly variable in this phase.

c) Plateau phase: This is the final phase of the PCR reaction which is traditionally detected by gels (end-point detection). In this phase, amplicon production is negligible. Consumption of reaction components, reduction in DNA polymerase activity due to heat, limited concentrations and increasing pyrophosphate concentration, reannealing of products at higher concentrations and risk of degradation of products over time due to Taq polymerase 5'-3' exonuclease activity are some of the factors contributing to the plateau phase in later PCR cycles (Garrett and Grisham, 2010; Kainz, 2000; Lehninger et al., 2005; Peake, 1989; Rose, 1991; Saiki et al., 1985)

Figure 1.7 shows the PCR amplification of three replicate samples with the same amount of DNA at the start of the reaction. After PCR, these samples show different quantities instead of identical quantities at the plateau phase. On the other hand, the replicate samples have identical graphs in the exponential phase. Figure 1.8 shows the PCR amplification curve for a 7-fold dilution series. Although the exponential phase distinctively shows a difference between the samples, the difference in DNA quantities is

not very perceptible in the plateau phase. Hence, it seems more accurate to measure the amount of DNA in the exponential phase rather in the plateau phase as has been done traditionally.

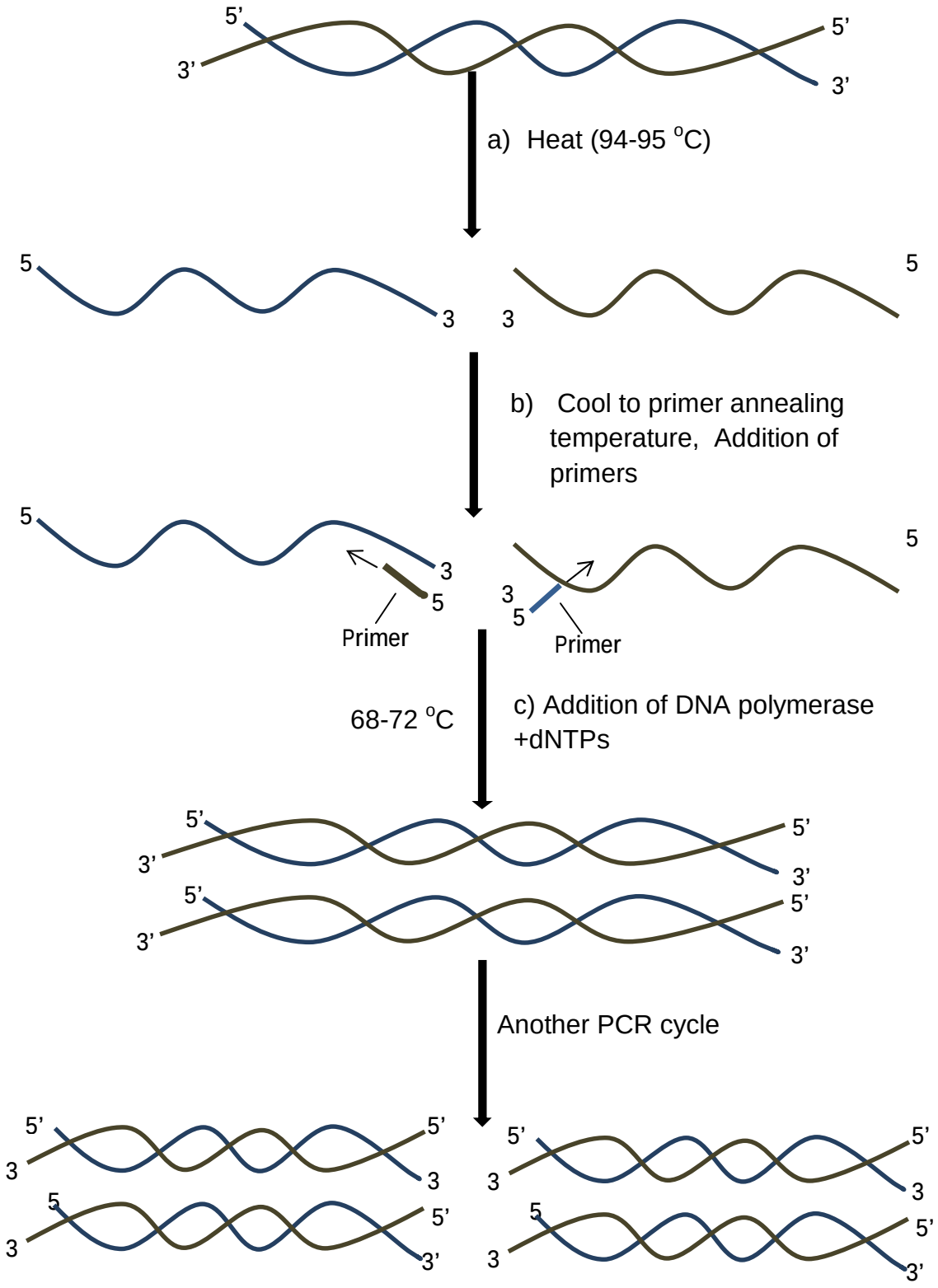

Figure 1.5 DNA amplification by PCR

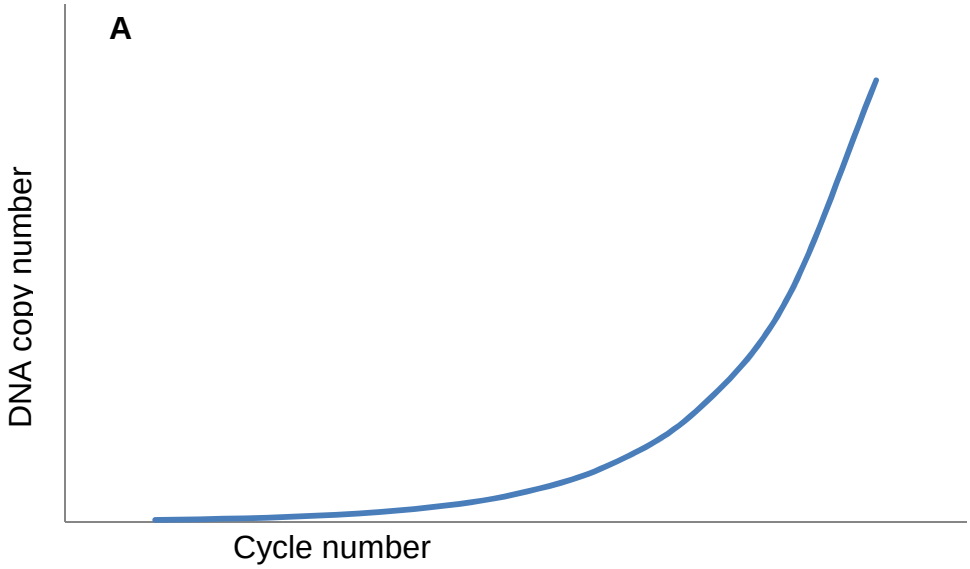

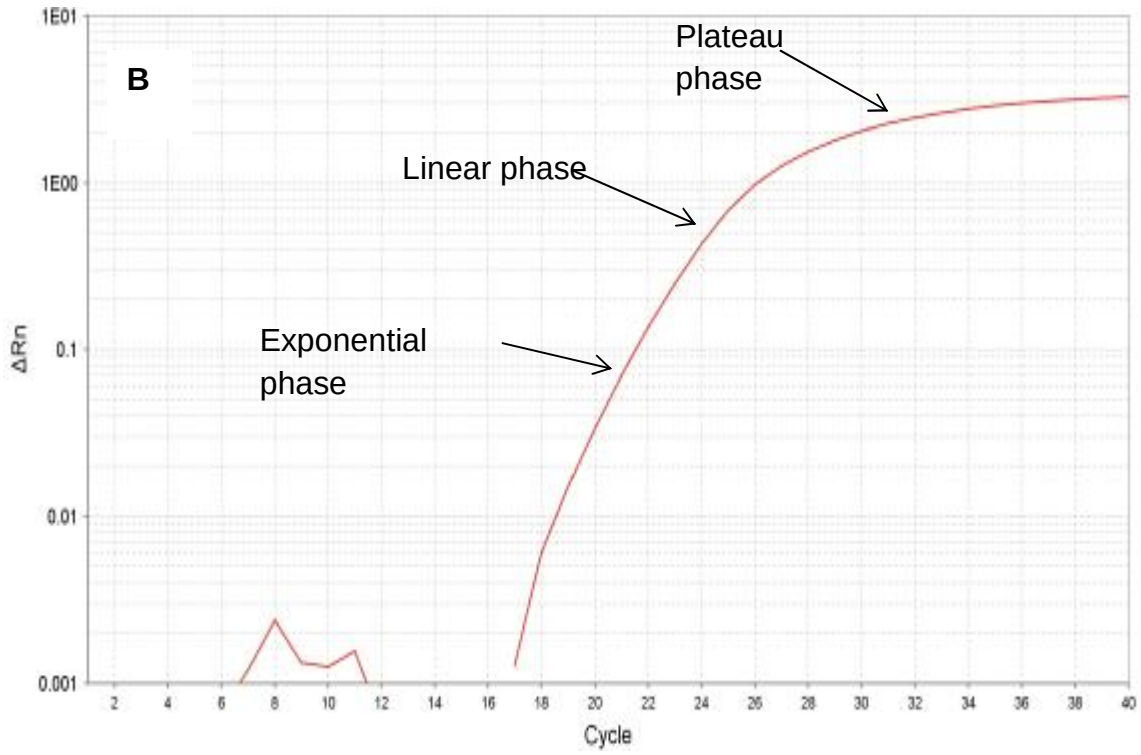

Figure 1.6: PCR amplification (A) theoretical and (B) experimental

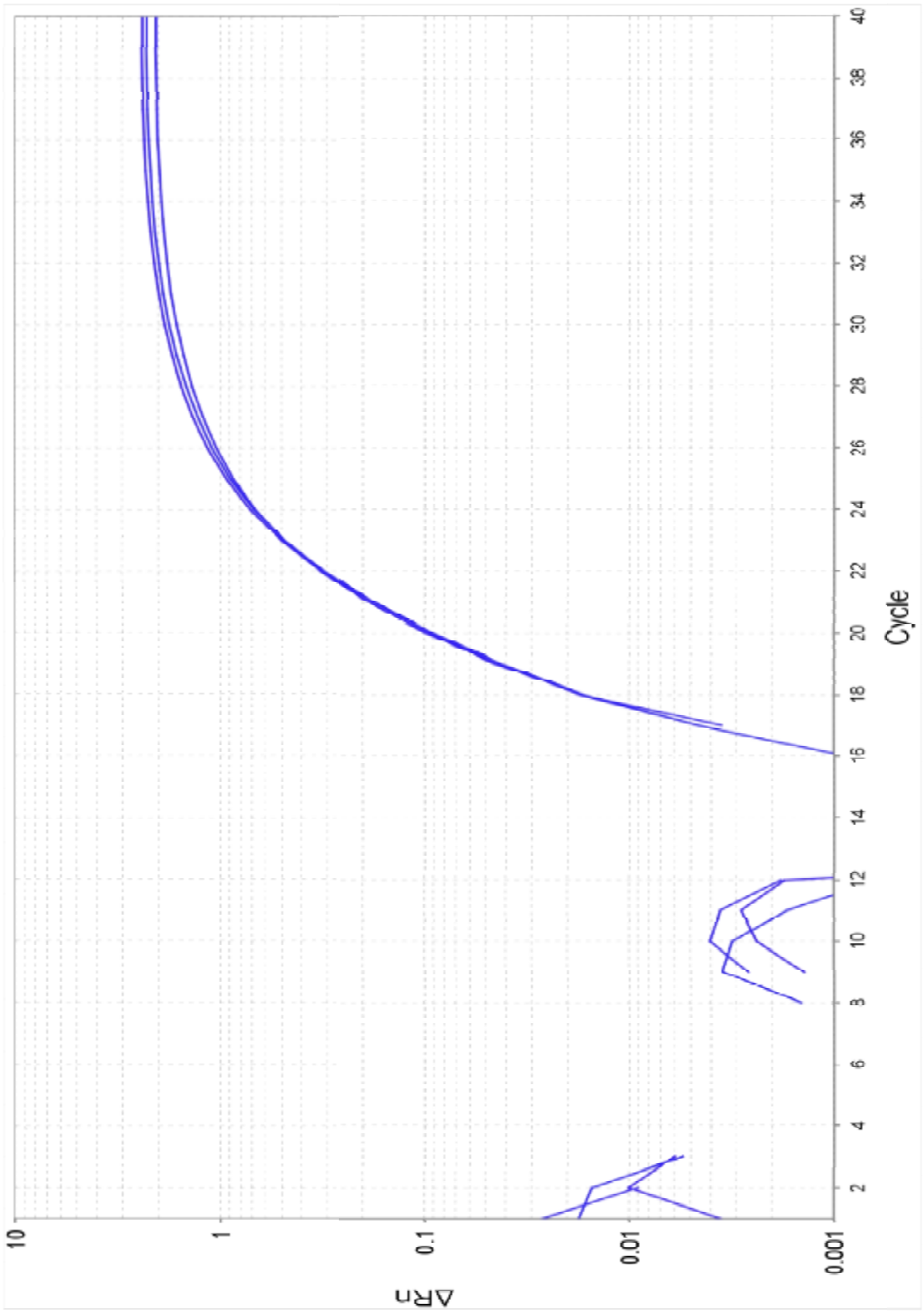

Figure 1.7: PCR amplification of 3 replicate samples

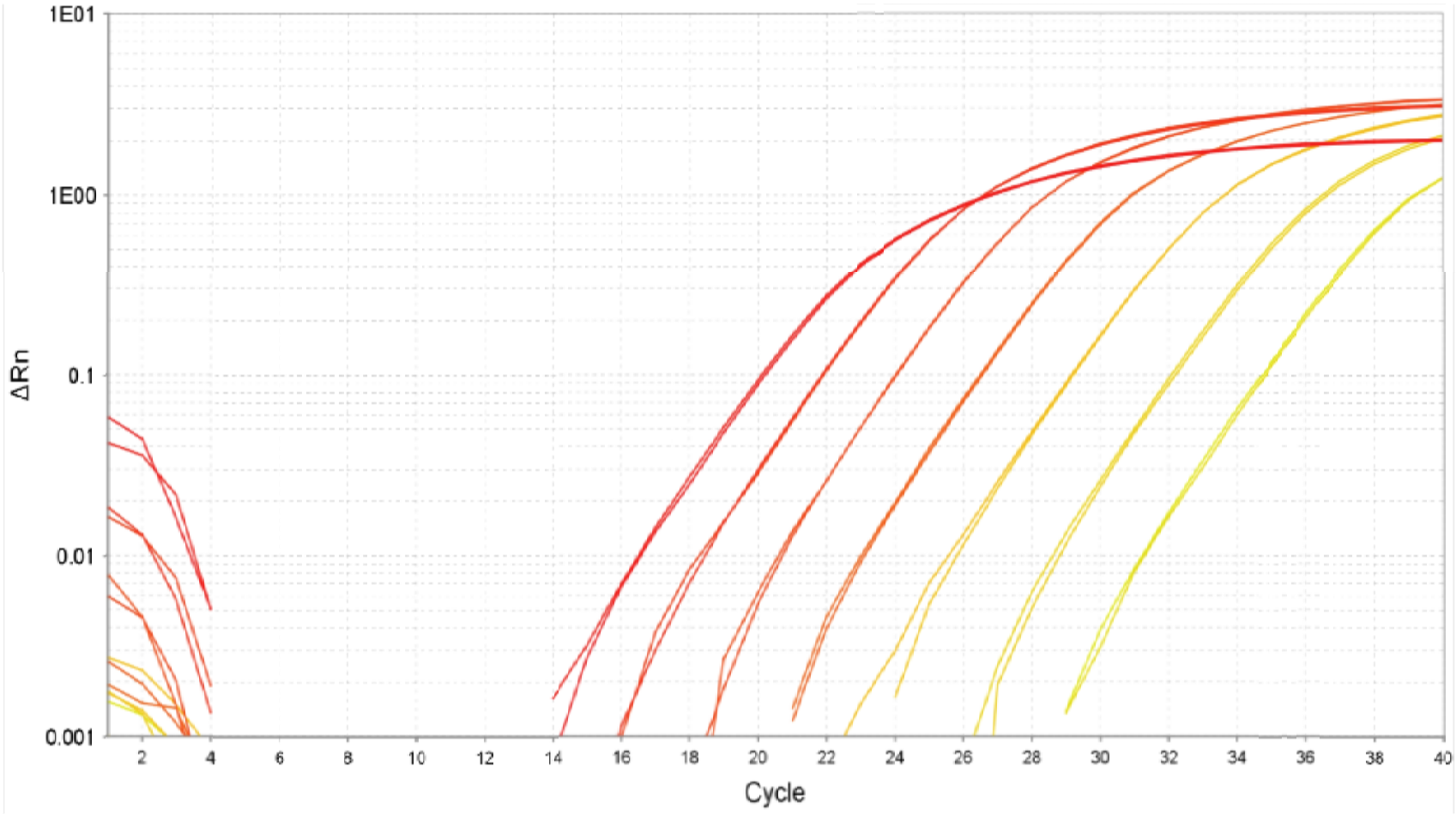

Figure 1.8 : PCR amplification of a 7-fold dilution series

1.5.1.2. Real Time Quantitative PCR (qPCR)

Due to the limitations of end-point detection in traditional PCR, the amount of product obtained is not always fully comparable to the amount of input DNA. Thus this method can at best be characterized as semi-quantitative/qualitative. Traditional PCR also has the disadvantages of low sensitivity and resolution, non-quantitative staining by ethidium bromide, additional post PCR processing steps and a narrow dynamic range (< 2 logs). In contrast, real time quantitative PCR quantifies amplification in the exponential phase of the PCR reaction thus eliminating the inconsistency associated with end-point detection in traditional PCR and therefore providing the accurate amount of starting target sample. Real time quantitative PCR (qPCR) can detect upto a two-fold change in concentration compared to agarose gel analysis which can only detect a 10-fold change in concentration. qPCR also uses highly sensitive fluorescent dyes such as SYBR green for detection instead of a low fluorescence dye like ethidium bromide. qPCR also has the advantages of wide dynamic range (> 10^7 fold) and an absence of post PCR processing.

Since the first reported qPCR procedure by Higuchi et al in 1993 (Higuchi et al., 1993), qPCR has found use in multiple biochemical applications including gene expression studies, quantification of DNA copy number in genomic or viral DNA, quantitation of cytokine levels, microarrays and allelic discrimination assays. 5' nuclease assays using Taqman probes, molecular beacons and SYBR Green fluorescent dyes are the most common chemistries used in qPCR (Bustin et al., 2005; Espy et al., 2006; Mackay et al., 2002; VanGuilder et al., 2008) .

1.5.1.3. qPCR Data Analysis

The increase in fluorescence during a PCR reaction is detected in real time using any of the different probe chemistries used in qPCR. Some of the important terms used in data analysis are briefly described below (Figure 1.9) (Arya et al., 2005):

a) Baseline: The baseline for a qPCR reaction is usually between cycles 1 and 15 and is defined as the number of qPCR cycles that lead to a fluorescence signal below the limits of detection of the qPCR instrument.

b) ΔR_n: ΔR_n is the difference between the fluorescence signal of the product at each time point and the fluorescence signal of the baseline. Amplification curves in a qPCR reaction are produced by plotting ΔRn vs cycle number.

c) Threshold: An arbitrary threshold, measured as approximately ten times the standard deviation of the average fluorescent signal of the baseline is usually chosen by the qPCR software. The threshold is in the region of exponential amplification and provides a minimal detection level for the qPCR reaction. It can be changed manually to include the amplification curves of multiple reactions.

d) C_t (Threshold cycle): C_t is the PCR cycle number at which a detectable, statistically significant fluorescence signal is observed. The higher the initial concentration of template DNA in the qPCR reaction, the lower the C_t value. The C_t value is always observed in the exponential phase of DNA amplification and is the basis for data analysis methods in qPCR.

The two different methods used for quantification and analysis of data obtained in qPCR: absolute quantification/ standard Curve method and the relative quantification/ comparative C_t method which are briefly described below.

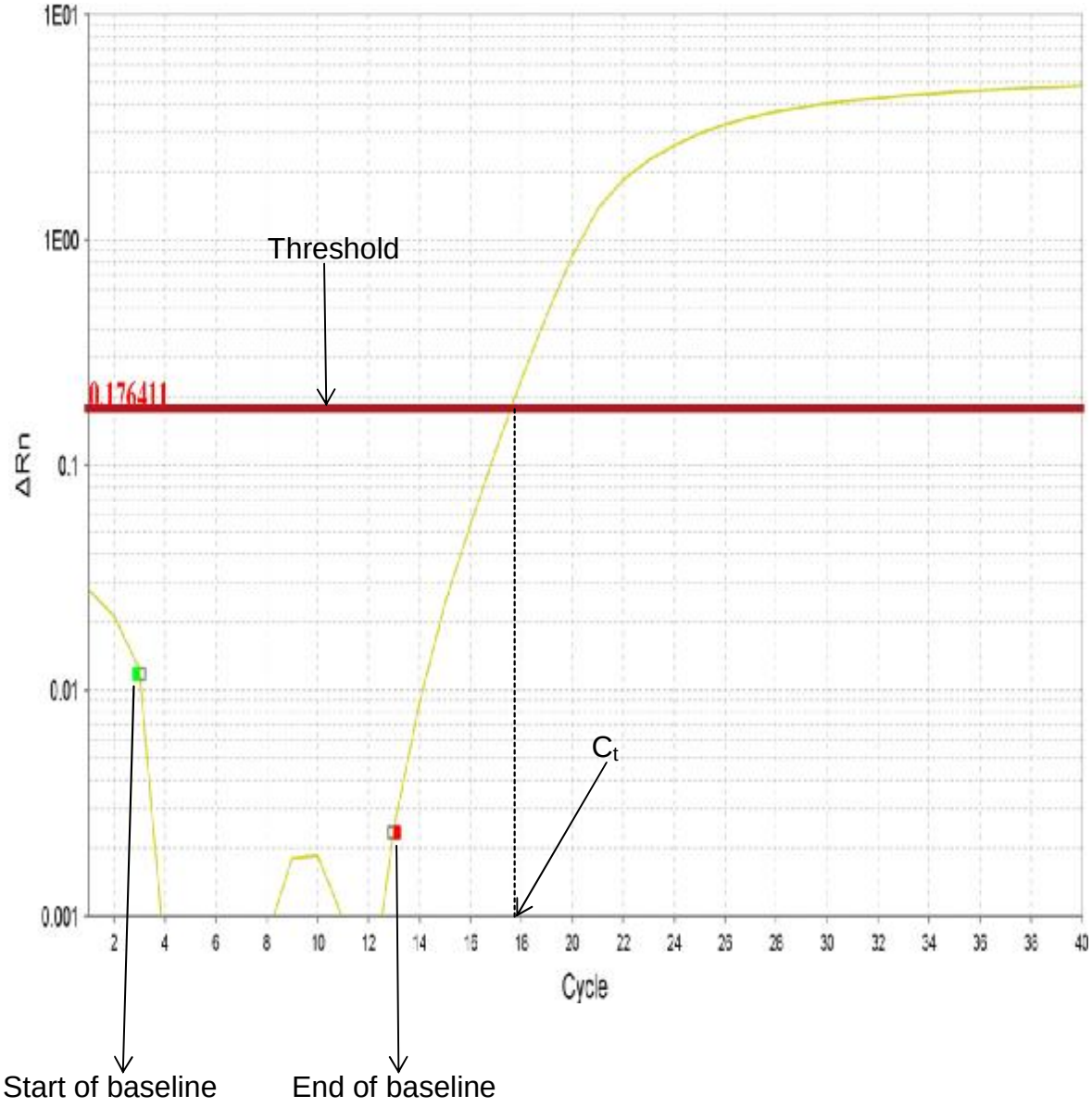

Figure 1.9. Description of terms used in qPCR data analysis

1.5.1.3.1. Absolute Quantification/ Standard Curve Method

In this method, a standard curve is obtained by plotting the log of initial DNA concentration for a set of known standards (five or ten fold dilution series) versus C_t and should be a straight line for an efficient qPCR reaction (Higuchi et al., 1993). The amount of DNA in unknown samples is then determined by measuring their C_t values and comparing these C_t values with the standard curve. Purified plasmid DNA, synthetic ssDNA or any cDNA/DNA sample expressing the target gene can be used to generate the standard curve. This method is used in experiments requiring the absolute quantitation of sample (Arya et al., 2005; Schmittgen and Livak, 2008).

1.5.1.3.2. Relative Quantification/ Comparative C_t/ $2^{-\Delta\Delta Ct}$ Method

In the comparative C_t method, quantification is carried out by comparing the C_t value of the sample of interest to the C_t value of an internal control or some calibrator such as a non-treated sample. Appropriate housekeeping genes (HKGs) are used to normalize the C_t values of both the sample of interest and the internal control. Housekeeping genes commonly used for qPCR include glyceraldehyde-3-phosphate dehydrogenase (GAPDH), β-actin, 28S or 18S ribosomal RNA, β_2-microglobulin, hypoxanthine-guanine, cyclophilin or phophoribosyl transferase (HPRT) (Arya et al., 2005; Derveaux et al., 2010). In order to use the comparative method, it is assumed that PCR reaction efficiency is 1 and that both the sample of interest and internal control have similar PCR efficiency. The amount of target is calculated by the formula $2^{-\Delta\Delta Ct}$ (Livak and Schmittgen, 2001; Schmittgen and Livak, 2008) where

$$\Delta\Delta C_t = \Delta C_{t,sample} - \Delta C_{t,control}$$

$$\Delta C_{t,sample} = C_{t,sample} - C_{t,HKG}$$

$$\Delta C_{t,control} = C_{t,control} - C_{t,HKG}$$

1.5.1.4. Voltage Dependent Anion Channels (VDACs)

Pore-forming VDACs, also known as mitochondrial porins, are found in the mitochondrial outer membrane and brain postsynaptic membranes and are ion channels that facilitate transport of small hydrophilic solutes including ATP, ADP, Pi, Ca^{2+}, K^{+} and Na^{+} from the cytosol to mitochondrial sites of utilization or vice versa. In addition, VDAC along with adenine nucleotide translocase and cyclophilin-D form the mitochondrial permeability transition pore (PTP). Three different isoforms of the VDAC protein: VDAC1, VDAC2 and VDAC3 have been observed in humans. Although the three isoforms are sequentially homologous and are expressed in most tissues, they differ in function and abundance in the human body. For example, VDAC3 has diminished pore-forming ability compared to VDAC1 and VDAC2. VDACs form ion channels between the mitochondrial outer and inner membranes and have been implicated in the regulation of apoptosis and membrane potential, and ATP production. Mitochondrial function is considered to be regulated by the voltage dependent closure/opening of VDACs. Studies show that VDAC forms a single 2.5-3 nm wide pore which shows a slight anion-selectivity in its open state and slight cation- selectivity in its partially closed state. VDACs are open at low voltages (≈ ±10 mV) and closed at higher voltages (over ±30 mV). In addition, VDACs act as coordination sites for multiple ATP using cytosolic enzymes including hexokinase, glucokinase, glycerol kinase and mitochondrial creatine kinase. Multiple studies (Cuadrado-Tejedor et al., 2011; Lovell et al., 2005; Yoo et al., 2001) have shown changes in VDAC proteins in the brain of patients with Alzheimer's disease. Lovell et al. found a significant elevation of VDAC1 levels, no significant

change in VDAC2 levels and a trend towards significant increase of VDAC3 levels in Aβ-treated primary rat cortical neuron cultures (Lovell et al., 2005). Yoo et al. reported a significant decrease in VDAC1 levels in thalamus and frontal and temporal cortex and significant elevation of VDAC2 levels in temporal cortex of AD subjects (Yoo et al., 2001). A recent study by Cuadrado-Tejedor et al. showed an overexpression of VDAC1 in the brain of AD patients (Cuadrado-Tejedor et al., 2011).

1.5.2. Changes in DNA Repair Enzymes of BER Pathway in AD Subjects

Increased oxidative DNA damage seen during the progression of AD could be due to either an increase in formation of oxidized DNA lesions or due to impairments in DNA repair mechanisms or both. Previous studies suggest DNA repair pathways may be diminished in the progression of AD and may contribute to increased accumulation of markers of DNA oxidation (Bohr, 2002; Dianov et al., 2001; Weissman et al., 2007). In this study, we hypothesized that the BER pathway has diminished repair capacity throughout the progression of AD leading to increased oxidative DNA damage seen during AD. To test this hypothesis, custom PCR arrays containing genes for 12 DNA repair enzymes, 2 housekeeping genes (Beta actin (ACTB) and Glyceraldehyde-3-phosphate dehydrogenase (GAPDH)), and negative and positive PCR controls, and qPCR were used to quantify expression levels for DNA repair enzymes relative to the pathogenesis of AD. To confirm PCR results, enzyme activities were assessed using gel shift assays and radiolabeled/fluorescent oligonucleotides and protein levels were quantified using Western blot analysis and antibodies specific for each protein.

For both projects, tissue specimens were analyzed from normal control (NC) subjects and subjects throughout the progression of AD including those with preclinical

AD (PCAD), mild cognitive impairment (MCI), late-onset AD (LAD), and diseased control (DC) including frontotemporal dementia (FTD) and dementia with Lewy bodies (DLB) subjects. Both projects analyzed specimens from a vulnerable brain region (superior and middle temporal gyri (SMTG) and a non-vulnerable region (cerebellum (CER)).

Table 1.1. List of potential genes studied in Project 1

#	Name used in experiment	Gene
1	VDAC1	Voltage dependent anion-selective channel protein 1
2	VDAC2	Voltage dependent anion-selective channel protein 2
3	VDAC3	Voltage dependent anion-selective channel protein 3

CHAPTER TWO: MATERIALS AND METHODS

2.1. Materials

2.1.1. Brain Specimen Sampling

Brain tissue specimens of superior and middle temporal gyri (SMTG) and cerebellum (CER) of NC, MCI, PCAD, LAD and DC subjects were collected from short postmortem interval (PMI) autopsies and stored at -80 ˚C until used for analysis. All subjects were followed longitudinally at the University of Kentucky Alzheimer's Disease Center Clinic (UK-ADC) and had annual neuropsychological testing and physical and neurological exams. Results of neuropsychological testing for NC subjects were in the normal range. MCI subjects were normal upon enrollment into the study cohort but developed MCI during follow up. MCI subjects were diagnosed based on clinical criteria described by Petersen et al. which include: (a) memory complaints (b) objective memory impairment for age and education (c) normal general cognitive function (d) intact activities of daily living and (e) the subject not meeting criteria for dementia (DeCarli, 2003; Maynard et al., 2010; Petersen et al., 2009; Petersen et al., 1999). Histopathologically, MCI subjects showed a significant increase in neuritic plaques in neocortical regions and a significant increase in neurofibrillary tangles in the hippocampus, entorhinal cortex and amygdala, compared to NC subjects (Markesbery et al., 2006). Braak staging scores for MCI subjects were in the range of III-IV. Preclinical AD (PCAD) subjects were diagnosed based on the tentative criteria set by the UK-ADC which includes (a) pronounced AD pathology with Braak scores of III-V and (b) antemortem psychometric tests in the normal range when corrected for age and education (Schmitt et al., 2000). Subjects with Braak scores of VI who met both standard clinical

and histopathological criteria for probable AD were diagnosed with LAD (Bradley et al., 2010; Schmitt et al., 2000).

Samples from subjects with dementia with Lewy bodies (DLB) and frontotemporal dementia (FTD) were analyzed as diseased control specimens. DLB patients showed antemortem diagnostic features including visuospatial problems worse than memory problems, executive dysfunction, sleep disturbance, visual hallucinations, facial masking and decreased dopamine transporter in the absence of systemic or neurologic disorders. Pathologically, DLB was characterized by the presence of ubiquitin and α-synuclein positive Lewy bodies (LB) and α-synuclein positive Lewy neurites (LN) in the limbic and temporal regions of the brain. In addition, some DLB brain specimens may have AD-type pathology including neurofibrillary tangles and diffuse/ neuritic plaques (Ferman and Boeve, 2007; Geldmacher, 2004)

Frontotemporal dementia describes a group of progressive neurodegenerative diseases with diagnostic features including changes in personal and social behavior, akinesia, progressive aphasia, labile blood pressure and a variety of other exclusionary features. Pathological changes include degeneration of frontal and/or anterior temporal lobe and basal ganglia, microvacuolation, swollen cortical neurons, neuron loss and loss of pigmentation in the substantria nigra (Graff-Radford and Woodruff, 2007; Grossman, 2002).

All subjects had neuropathological assessment of multiple sections of neocortex, hippocampus, entorhinal cortex, amygdala, basal ganglia, nucleus basalis of Meynert, midbrain, pons, medulla and cerebellum by the modified Bielschowsky stain, hemotoxylin-eosin stain and Aβ, and α-synuclein immunostains. Braak staging scores

were determined using the Gallyas stain on sections of the hippocampus, entorhinal cortex and amygdala and the Bielschowsky stain on neocortex.

The subject demographics are shown in Table 2.1. Age, and post-mortem intervals are reported as mean ± SEM (Table 2.1) and were compared using ANOVA. Braak staging scores are listed as median [range] values and were compared using the Mann Whitney U test.

Table 2.1. Subject Demographics

	Age (Mean ± SEM)	Braak Score (Median)	PMI (Mean ± SEM)	Sex
NC (N = 15)	86.3 ± 1.4	I	2.8 ± 0.2	4M : 11W
MCI (N = 7)	91.0 ± 1.9*	III*	2.6 ± 0.2	2M : 5W
PCAD (N = 13)	85.7 ± 1.8	IV*	2.8 ± 0.2	3M : 10W
LAD (N = 14)	81.4 ± 1.4	VI*	3.6 ± 0.4	6M : 8W
DC (N = 12)	68.9 ± 4.8*	II*	3.5 ± 0.4	7M : 5W

*** P < 0.05**

2.1.2. Antibodies

Polyclonal rabbit anti-OGG1 was obtained from Novus Biologicals (Littleton, CO, USA). Polyclonal rabbit anti-Ref1, polyclonal rabbit anti-XRCC1, polyclonal rabbit anti-POLB, polyclonal rabbit anti-PARP1, polyclonal rabbit anti-UDG and polyclonal rabbit anti-FEN1 were obtained from Santa Cruz Biotechnology (Santa Cruz, CA, USA).

2.2. Methods

2.2.1 Isolation of Nuclear DNA

For Project 1 (Oxidative DNA damage in genes of proteins modified during AD), two separate methods of DNA isolation were tested to obtain the method with least amount of artifactual oxidation of DNA during isolation. The subject demographics for the study are shown in Table 2.1.

a) Genomic DNA was isolated from brain tissues using a DNeasy Tissue Kit per manufacturer's instructions (Qiagen, Valencia, CA). Briefly, ~ 25 mg brain tissue was lysed by incubating overnight at 56 ^{o}C with proteinase K and lysis buffer. After lysis, AL buffer (proprietary mix containing guanidine hydrochloride) and ethanol were added to the sample mixture and the mixture was pipetted into a DNeasy Mini spin column and centrifuged. The flow-through was discarded. The sample in the DNeasy Mini spin column was washed with wash buffers (proprietary mix containing guanidine hydrochloride and ethanol) and genomic DNA eluted using ddH_2O. Subsequent to elution with ddH_2O, purified DNA was stored at −80 °C.

b) Phenol Extraction Method: Total genomic DNA was isolated from brain tissues using a previously published procedure (Mecocci et al., 1993; Sims and Anderson, 2008; Wang et al., 2005). A glass Dounce homogenizer was used to homogenize brain tissue

specimens in cold isolation buffer (0.3 M sucrose, 10 mM Tris-HCl, 1 mM K_2EDTA, pH 7.4) (10% tissue wet wt/vol). The homogenate was centrifuged at 1,300 x g at 4°C for 3 minutes. The pellet obtained was resuspended in isolation buffer and centrifuged again at 1,300 x g at 4 °C for 3 minutes. The resulting pellet was used for nuclear DNA (nDNA) isolation by the phenol extraction method. The pellet was resuspended in digestion buffer (0.5% sodium dodecyl sulfate, 0.05 M Tris-HCl, 0.1 M Na_2EDTA) with proteinase K (0.5 mg/ml) and incubated overnight in a water bath at 56°C. After overnight incubation, 160 µL of 5 M NaCl per 10 mL solution was added to the mixture. This was followed by extraction with buffer-saturated phenol containing 5.5 mM 8-hydroxyquinoline (to limit artifactual DNA oxidation) three times and three times with chloroform/isoamyl alcohol (24:1). 800 µL of 5 M NaCl per 10 mL was added to the resulting clear extract along with an equal volume of chilled absolute ethanol and left overnight at -20°C to precipitate nDNA. Subsequently, the DNA pellet was centrifuged, washed three times with 60% ethanol and air-dried. The pellet was then dissolved in nuclease-free water. The concentration and purity of DNA samples at 260 and 280 nm was measured using a ND1000 Nanodrop Spectrophotometer (Thermoscientific, Wilmington, DE).

2.2.2. Polymerase Chain Reaction (PCR)

PCR reactions were performed with genomic DNA initially to verify oxidative damage in specific genes with a range of primers designed for each gene (listed in Table 2.2). PCR reactions were also used to validate the primers obtained for RT-PCR (listed in Table 4). A PCR reaction mixture contained 250 ng genomic DNA, 1× Thermoscientific PCR Master Mix and 1 µM primer mix (forward and reverse) in a total volume of 25 µL.

A 1.2% low-melt agarose gel containing ethidium bromide was used to separate the PCR products (Wang et al., 2005).

Table 2.2. Primers for PCR

Gene	DNA bp location	Bp length	Primer sequence	T_m (^oC)	
VDAC1	134-913	780	5’-AATCTGCCAGGGATGTCTTCACCA-3’	60.3	Forward
			5’-CACCAGCATTGACGTTCTTGCCAT-3’	60.3	Reverse
VDAC1	134-505	372	5’-AATCTGCCAGGGATGTCTTCACCA-3’	60.3	Forward
			5’-GCCCAGCAATGTCGAAATCCATGT-3’	60.2	Reverse
VDAC1	438-913	476	5’-AATCAAGACAGGGTACAAGCGGGA-3’	60.2	Forward
			5’-CACCAGCATTGACGTTCTTGCCAT-3’	60.3	Reverse
VDAC2	193-546	354	5’-CAAAGTCTTGCAGTGGCGTGGAAT-3’	60.2	Forward
			5’-CAAGCCAGCCCTCATAACCAAAGA-3’	59.4	Reverse
VDAC2	545-749	205	5’-TGCTGGCTACCAGATGACCTTTGA-3’	60.2	Forward
			5’-ACGAGTGCAGTTGGTACCTGATGT-3’	60.2	Reverse
VDAC2	726-1024	299	5’-ACATCAGGTACCAACTGCACTCGT-3’	60.2	Forward
			5’-CCTGCTGCTGGTCACAATGGAAAT-3’	60.0	Reverse
VDAC2	1024-1404	381	5’-GCTTTTTTCCCCCAAGAAGATGAT-3’	55.9	Forward
			5’-TTGTCATGTTCTGGGATACCAAAA-3’	54.7	Reverse
VDAC2	193-738	546	5’-CAAAGTCTTGCAGTGGCGTGGAAT-3’	60.2	Forward
			5’-TGGTACCTGATGTCCAAGCAAGGT-3’	60.2	Reverse
VDAC2	193-749	557	5’-CAAAGTCTTGCAGTGGCGTGGAAT-3’	60.2	Forward
			5’-ACGAGTGCAGTTGGTACCTGATGT-3’	60.2	Reverse
VDAC2	193-1021	829	5’-CAAAGTCTTGCAGTGGCGTGGAAT-3’	60.2	Forward
			5’-CCTGCTGCTGGTCACAATGGAAAT-3’	60	Reverse

2.2.3. Oxidative DNA Damage

Real time PCR/ quantitative PCR was used to determine the level of oxidative damage in the DNA sequences of various genes. The range of primers designed for each gene, are listed in Table 2.3. Briefly, 250 ng of total genomic DNA was incubated with 8 units of formamidopyrimidine glycosylase (fpg) and 100 μg/ml of BSA at 37°C for 12 h. The fpg enzyme was inactivated after 12 h by incubation at 60°C for 10 min. Real time/ quantitative PCR was carried out with an aliquot of the reaction mixture on an ABI 7000 Sequence Detection System using TaqMan 2x PCR Master Mix (Applied Biosystems, Carlsbad, CA) and SYBR Green for detection. The RT-PCR reaction mixture contained 1× TaqMan PCR Master Mix, 4 μM primer mix (forward and reverse), SYBR Green, ROX reference dye and template genomic DNA. The absolute concentrations of intact DNA in the template were calculated using a standard curve derived from 5-fold serial dilutions of genomic DNA from NC subjects. The data presented show the average of triplicates from RT-PCR. Oxidative damage was calculated as

$$\% \text{ Oxidative damage} = \frac{(\text{intact DNA in nontreated aliquot} - \text{intact DNA in fpg treated aliquot})}{\text{intact DNA in nontreated aliquot}}$$

RT-PCR reaction mixtures without template DNA served as negative controls in order to monitor nonspecific amplification. PCR products were verified by melting curves (Du et al., 2009).

Table 2.3. Primers for RT-PCR

Table 2.3.1. VDAC1 primers

Gene	DNA bp location	bp length	Primer sequence	T_m (^oC)	
VDAC1A	438-613	176	5’-AATCAAGACAGGGTACAAGCGGGA-3’	60.2	Forward
			5’-CAACTGCAAAGTTGCTCTGGGTCA-3’	60.0	Reverse
VDAC1B	482-689	208	5’-ACATGGATTTCGACATTGCTGGGC-3’	60.2	Forward
			5’-TTCTGGTAAATGGAGCCGCCAAAC-3’	59.9	Reverse
VDAC1C	666-913	248	5’-GTTTGGCGGCTCCATTTACCAGAA-3’	59.9	Forward
			5’-CACCAGCATTGACGTTCTTGCCAT-3’	60.3	Reverse
VDAC1D	695-896	202	5’-ACAAGAAGTTGGAGACCGCTGTCA-3’	60.4	Forward
			5’-TTGCCATCCAGAAGAGCTGACAGT-3’	60.4	Reverse
VDAC1E	722-913	192	5’-TTGCCTGGACAGCAGGAAACAGTA-3’	60.5	Forward
			5’-CACCAGCATTGACGTTCTTGCCAT-3’	60.3	Reverse
VDAC1G	914-1173	260	5’-GCCACAAGCTTGGTCTAGGACTGG-3’	61.6	Forward
			5’-AAGTTCTCCCCGAGTCTACCACTG-3’	59.8	Reverse
VDAC1H	1174-1411	238	5’-GAGAACTTGGTGGCCCCTTTGAGA-3’	61.0	Forward
			5’-GGGGTGGGAACAGGTCATGAAGAT-3’	60.8	Reverse
VDAC1I	1398-1594	196	5’-CCTGTTCCCACCCCAGTTCATCAT-3’	61.0	Forward
			5’-GCTGGAGCTCCTGGAAGCTATTTC-3’	59.6	Reverse

Table 2.3.2. VDAC2 primers

Gene	DNA bp location	bp length	Primer sequence	T_m (^oC)	
VDAC2A	24-213	190	5'-GCGAAGTGAAGGAGACACCGTTCC -3'	61.7	Forward
			5'-CCACGCCACTGCAAGACTTTGTTT -3'	60.6	Reverse
VDAC2B	167-354	188	5'-TGGGTTGGTGAAACTGGATGTGAA -3'	58.9	Forward
			5'-TTGCGATTTCTGTTCCCAGAGTGT -3'	58.8	Reverse
VDAC2C	331-538	208	5'-ACACTCTGGGAACAGAAATCGCAA -3'	58.8	Forward
			5'-CCCTCATAACCAAAGACAGCTGAACC	59.4	Reverse
VDAC2D	522-738	217	5'-GTCTTTGGTTATGAGGGCTGGCTT -3'	59.4	Forward
			5'-TGGTACCTGATGTCCAAGCAAGGT -3'	60.2	Reverse
VDAC2E	726-956	231	5'-ACATCAGGTACCAACTGCACTCGT -3'	60.2	Forward
			5'-TCAGCTGGATTAAGCCTCCAACTC -3'	58.7	Reverse
VDAC2G	948-1152	205	5'-TCCAGCTGAAAGAAACCTTTGGGA -3'	58.7	Forward
			5'-GCAGGACTGCAGCATTGGTAACTA -3'	59.3	Reverse
VDAC2H	1126-1310	185	5'-ATCTAGTTACCAATGCTGCAGTCC -3'	56.8	Forward
			5'-CCACTGATCCATCTCATTCAATGGT -3'	56.9	Reverse

Table 2.3.3: VDAC3 primers

Gene	DNA bp location	bp length	Primer sequence	T_m (^oC)	
VDAC3A	248-447	200	5’-AGGGAAAGCATCAGGCAACCTAGA-3’	60.1	Forward
			5’-AGGAGGCCTTCAATTTCCCACTCT-3’	60.2	Reverse
VDAC3B	367-651	285	5’-TGGCTGAAGGGTTGAAACTGACTC-3’	59.2	Forward
			5’-GTTCTCATGTGTGTGCAGATGGAA-3’	57.5	Reverse
VDAC3C	540-735	196	5’-TGGCTTGCTGGCTATCAGATGAGT-3’	60.3	Forward
			5’-TCCCAGCTGTCCAAGCAAGGTTTA-3’	60.6	Reverse
VDAC3D	627-865	239	5’-TTCCAGCTGCACACACATGTGAAC-3’	60.2	Forward
			5’-ATTTGACTCCTGGTCGAAGGGTCT-3’	59.7	Reverse
VDAC3E	718-932	215	5’-TTGCTTGGACAGCTGGGAGTAACA-3’	60.5	Forward
			5’-AAATCCCAAGCCAACCTTGTGACC-3’	60.1	Reverse

2.2.4. Oxoguanine Incorporation into IGF2 Gene Sequence

PCR reactions were performed with genomic DNA with primers designed specifically for IGF2. PCR reaction mixtures contained 100 ng genomic DNA, 10mM dATP, 10mM dCTP, 10mM dTTP, 10mM (deoxyguanine/8-oxoguanine in varying ratios), 10X PCR reaction buffer, Taq polymerase, 25 mM $MgCl_2$ and 10 μM primer mix (forward and reverse) in a total volume of 25 μL. A 1.2% low-melt agarose gel containing ethidium bromide was used to separate the PCR products (Wang et al., 2005). The PCR product band was excised from the agarose gel and purified DNA was obtained using a gel extraction kit and a DNA clean-up and concentration kit per manufacturer's instructions (Zymo Research, Irvine, CA).

2.2.5. In vitro Transcription

IGF2 DNA with 8-OHG was transcribed to RNA *in vitro* using a Megascript kit per manufacturer's instructions (Life Technologies, Grand Island, NY). Briefly, 100-500 ng of template DNA was incubated with dNTPs (2 μl each of ATP, CTP, GTP and UTP), 2 μl enzyme mix, 2 μl of 10X reaction buffer and water at 37 °C for 16 hours. The reaction mixture was then incubated at 37 °C for 15 minutes with 1 μl DNase to remove template DNA. The RNA transcript was purified using the phenol:chloroform extraction and isopropanol precipitation. RNA transcript was diluted by addition of 115 μl of water and 15 μl ammonium acetate solution and extracted with an equal volume of phenol and then with an equal volume of chloroform. RNA was then precipitated with an equal volume of isopropanol overnight. The pellet removed after centrifugation was resuspended in nuclease-free water and sample was stored at −20°C.

2.2.6. In vitro Translation

IGF2 protein was synthesized *in vitro* using a Retic Lysate IVT kit per manufacturer's instructions (Life Technologies, Grand Island, NY). Briefly, 100-750 ng in vitro transcribed RNA was incubated in a reaction mixture containing 20X translation mix (-Met), 50 µl L-Met, 17 µl retic lysate and nuclease-free water at 30 °C for 90 minutes. The mixture was then incubated with 2.5 µl of 1 mg/ml RNase at 30 °C for 10 minutes. Subsequently, the reaction mixture was placed on ice for 5 minutes to quench all reactions and stored at −20 °C.

2.2.7. IGF2 Activity Assay

IGF2 activity assays were as previously described (Gicquel et al., 2004; Spicer et al., 1994). Briefly, IGF2 was radioiodinated in a 20 µl reaction mixture containing 0.3M PBS, 1mCi Na-^{125}I and 1.6 µg chloramine-T at 25 °C for 30 s. 6 µg of sodium metabisulfite was added to quench the reaction. Iodinated IGF2 specimens were incubated with 150 µl plasma samples in a reaction mixture containing 25 mM Hepes (ph 7.4), 0.1% BSA and 0.1% Triton X-100 overnight at 4 °C. IGF2 binding complex pellets were separated by precipitation with 4% gammaglobulin and 18% w/v PEG 6K, and subsequent centrifugation. The pellet was counted in a scintillation counter. Blanks containing only iodinated IGF2 and no plasma were run for each sample set.

2.2.8. RNA Isolation and cDNA Synthesis

a) RNA isolation: Total RNA was isolated from tissue specimens using an RNeasy Tissue Kit per manufacturer's instructions (Qiagen, Valencia, CA). Briefly, ~ 20 mg of brain tissue was homogenized in RLT buffer (proprietary mix containing guanidine thiocyanate and β-mercaptoethanol). Ethanol (one volume) was added to the

homogenized sample and the reaction mixture was transferred to an RNeasy Mini spin column. The spin column was subsequently washed with multiple washing buffers and total RNA eluted using RNAse-free H_2O. Following elution with RNAse free H_2O, purified RNA was stored at −80 °C or used directly for cDNA synthesis.

b) cDNA synthesis: RNA samples were converted into cDNA using the RT^2 First Strand Kit per manufacturer's instructions (SABiosciences, Frederick, MD). Briefly, 75-100 ng of RNA were incubated with genomic DNA elimination buffer at 42°C for 5 minutes in order to eliminate genomic DNA contamination. The reaction mixture was then mixed with a reverse transcription cocktail provided in the kit and incubated at 42 °C for exactly 15 minutes. The reverse transcription reaction was quenched by heating the mixture at 95°C for 5 minutes. The sample was diluted with RNAse free H_2O and stored at −20°C overnight.

2.2.9. Quantitative Polymerase Chain Reaction with custom PCR arrays

Quantitative PCR was carried out on an ABI 7000 Sequence Detection System using 2x SABiosciences RT^2 qPCR Master Mix. The qPCR reaction mixture contained 2x SABiosciences RT^2 qPCR Master Mix, and 250 ng of cDNA. 25 µl of the sample experimental cocktail was added to each well of 96-well Custom PCR arrays and placed in the real-time thermal cycler. The thermal cycler was run according to the real-time thermal cycler program recommended by the manufacturer (SABiosciences, Frederick, MD). The Custom PCR arrays contained primers for genes coding for DNA repair enzymes and housekeeping genes (ACTB & GAPDH) and positive and negative PCR controls (Table 2.4). The absolute concentrations of intact DNA in the template were

calculated using the web-based PCR Array Data Analysis Software provided by the manufacturer (SABiosciences).

Table 2.4. Custom PCR array layout

	1	2	3	4	5	6	7	8	9	10	11	12
A	PARP1	MRE1	PARP1	MRE1	PARP	MRE11	PARP	MRE1	PARP1	MRE11	PARP1	MRE11
	1	1A	17	1A	1	A	1	1A	1	A	17	A
B	APEX1	RAD5	APEX1	RAD5	APEX	RAD50	APEX	RAD5	APEX1	RAD50	APEX1	RAD50
	2	0	18	0	1	10	1	0	2	10	18	26
C	OGG1	ATM	OGG1	ATM	OGG1	ATM	OGG1	ATM	OGG1	ATM	OGG1	ATM
	3	11	19	27	3	11	19	27	3	11	19	27
D	POLB	EXO1	POLB	EXO1	POLB	EXO1	POLB	EXO1	POLB	EXO1	POLB	EXO1
	4	12	20	28	4	12	20	28	4	12	20	28
E	UNG	ACTB	UNG	ACTB	UNG	ACTB	UNG	ACTB	UNG	ACTB	UNG	ACTB
	5	13	21	29	5	13	21	29	5	13	21	29
F	XRCC1	GAPD	XRCC1	GAPD	XRCC	GAPD	XRCC	GAPD	XRCC1	GAPDH	XRCC1	GAPD
	6	H	22	H	1	H	1	H	6	14	22	H
G	XPA	HGD	XPA	HGD	XPA	HGDC	XPA	HGD	XPA	HGDC	XPA	HGDC
	7	C	23	C	7	15	23	C	7	15	23	31
H	FEN1	PPC	FEN1	PPC	FEN1	PPC	FEN1	PPC	FEN1	PPC	FEN1	PPC
	8	16	24	32	8	16	24	32	8	16	24	32

PPC: Positive PCR Control; HGDC: Human Genomic DNA Contamination

2.2.10. Protein Isolation and Quantification

Tissue samples were homogenized on ice with a Dounce homogenizer in a buffer containing 10 mM 2-[4-(2-hydroxyethyl)-1-piperazinyl]-ethanesulfonic acid (HEPES), 137 mM NaCl, 4.6 mM KCl, 0.6 mM $MgSO_4$, 0.7 µg/ml pepstatin A, 0.5 µg/ml leupeptin, 0.5 µg/ml aprotinin and 40 µg/ml PMSF). The resulting homogenate was centrifuged at 100,000 x g for 1 hour at 4 °C. Protein concentration of the supernatant was measured using the Pierce BCA protein assay (Sigma, St. Louis, MO).

2.2.11. Western Blot Analysis

20 µg of protein of each sample was separated on Criterion 4-15% Tris-HCL electrophoresis gradient gels followed by transfer to nitrocellulose transfer membranes. The membranes were then incubated in blocking buffer (5 % milk in 0.5% Tween-20/Tris-buffered saline (TTBS)) for 1 hour. Specific rabbit polyclonal anti-human primary antibodies against OGG1 (Novus Biologicals, Littleton, CO, USA), UNG, APE1, POLB, PARP1, XRCC1 & FEN1 (Santa Cruz Biotechnology Inc., Santa Cruz, CA, USA) (1:1000 dilution) were added and the membranes were placed on an orbital shaker overnight at 4°C. Subsequently, the membranes were washed with TTBS three times followed by incubation with 1:1000 dilution of horseradish peroxidase-labeled goat anti-rabbit secondary antibody (Jackson Immunoreasearch Laboratories Inc., West Grove, PA, USA) for 2 hours. The membranes were again washed with TTBS three times and the bands developed using enhanced chemiluminescence according to the manufacturer's instructions (Amersham Pharmacia Biotech, Piscataway, NJ, USA). Band intenisties were quantified using Scion Image Analysis (NIH). Results are expressed as mean ± SEM % control immunostaining.

2.2.12. Enzyme Activity Assays

2.2.12.1. Oligonucleotides

Oligonucleotides used in this study containing 8-oxodG, deoxy-uracil or tetrahydrofuran (THF) (Midland Certified Reagent Company, Midland, TX) and their complementary strand sequences are listed in Table 2.5. The lesion-containing oligonucleotides were 5′-^{32}P-labeled by incubation with [γ-^{32}P] ATP (PerkinElmer, Boston, MA, USA) and T4 polynucleotide kinase. G25 desalting columns (GE Healthcare Corp., Piscataway, NJ, USA) were used to remove the unincorporated free [γ-^{32}P] ATP from the reaction mixtures. The ^{32}P-labeled oligonucleotides were annealed to their complementary strands in annealing buffer (100 mM KCL, 10 mM Tris-HCl, pH 7.8 and 1mM EDTA) by heating the samples at 90°C for 5 min. A double-stranded DNA substrate containing a double flap region used for the FEN1 activity assay was prepared by annealing three oligodeoxynucleotides (Table 2.5) (Biosearch Technologies Inc. Novato, CA, USA) in a reaction buffer containing 50 mM Tris (pH 8), 100 mM KCl and 5mM MgCl2 by heating to 95 C for 5 minutes and subsequent cooling to room temperature.

2.2.12.2. OGG1 Activity Assay

OGG1 activity assays were carried out as previously described (Croteau and Bohr, 1997; Shao et al., 2008). Briefly, 20 µg of protein were incubated at 37°C for 1 h in a 20 µl reaction mixture containing 40 mM Hepes-KOH (pH 7.6), 5 mM EDTA, 2 mM DTT, 75 mM KCl, 10% glycerol and 88.7 fmol ^{32}P-labeled duplex oligonucleotide (Table 2.5). Reactions were subsequently quenched by addition of 20 µl of loading buffer containing 90% formamide, 0.002% bromophenol blue, and 0.002% xylene green and heated at

95°C for 5 min. After cooling to room temperature, the reaction mixture was separated on a 20% denaturing polyacrylamide gel containing 7 M urea prerun at 18 W for 30 min. Samples were separated by electrophoresis for 90 min at 16 W using 1X Tris borate EDTA (TBE) (pH 8.0) as a running buffer. A reaction mixture consisting of 20 μg protein, heat-inactivated by boiling at 95°C for 5 min before initiating the activity assay was used as blank for the assay.

Samples were analyzed with NC, MCI, PCAD and LAD samples on the same gel to allow comparison. Radiolabeled bands were visualized as previously described (Croteau and Bohr, 1997; Souza-Pinto et al., 1999) and band intensities of the cleaved product and parent oligonucleotide bands were quantified using Scion Image Analysis (NIH). Activities were calculated as the amount of radioactivity in the incised product band relative to the total radioactivity in the lane (incised product + intact duplex oligonucleotide). Results are expressed as mean ± SEM % control protein activity.

2.2.12.3. UNG Activity Assay

UNG activity assays were as previously described (Maynard et al., 2010; Weissman et al., 2007). Briefly, 20 μl reaction mixtures containing 70 mM HEPES–KOH (pH 7.4), 5 mM EDTA, 1 mM DTT, 75 mM NaCl, 10% glycerol, 50 fmol ^{32}P-labeled duplex oligonucleotide (Table 2.5) and 10 μg of protein were incubated for 1 h at 37°C. Reactions were subsequently quenched by addition of formamide dye and converted to a single-strand break product by addition of 50 mM NaOH and incubation at 75°C for 15 minutes. Samples were resolved and analyzed as described for the measurement of OGG1 activity.

2.2.12.4. APE1 Activity Assay

APE1 activity assays were carried out as previously described (Maynard et al., 2010; Weissman et al., 2007). Briefly, 5 μg of protein was incubated at 37°C for 1 h in a 10 μl reaction mixture containing 20 μg of protein was incubated at 37°C for 1 h in a 20 μl reaction mixture containing 25 mM HEPES–KOH (pH 7.4), 25 mM KCl, 0.1 mg/ml BSA, 5 mM $MgCl_2$, 10% glycerol, 0.05% Triton X-100 and 1.0 pmol ^{32}P-labeled duplex oligonucleotide (Table 2.5). Reactions were terminated and samples resolved and evaluated as described for the measurement of OGG1 activity.

2.2.12.5. POLB Activity Assay

POLB activity assays were as previously described (Maynard et al., 2010; Weissman et al., 2007). Samples were diluted in 10mM Tris-HCl (pH 7.4) containing 100 mM KCl. 20 μl reaction mixtures containing 50 mM Tris-HCl (pH 7.4), 50 mM KCl, 1 mM DTT, 75 mM $MgCl_2$, 5% glycerol, 5 μM dCTP (Roche Applied Sciences, Indianapolis, IN, USA), 4 μCi α^{32}P-dCTP (GE Healthcare Corp., Piscataway, NJ, USA), 1 pmol duplex gap oligonucleotide (Table 2.5) and 5 μg of protein were incubated for 1 h at 37°C. Reactions were terminated and samples resolved and evaluated as described for the measurement of OGG1 activity.

2.2.12.6. FEN1 Activity Assay

FEN1 activity assays were as previously described (Dorjsuren et al., 2011). Briefly, a 40 μl reaction mixture containing 50 mM Tris-HCl pH 8.0, 10 mM $MgCl_2$, 1 mM DTT, 0.01% Tween-20, 5 μg of protein and 1 pmol labeled oligonucleotide (Table 2.5) were pipetted into a 96-well plate and data collected using a FLx800 fluorescence microplate

reader (Biotek, Winooski, VT, USA) equipped with standard optics (excitation filter 525 nm and emission filter 598 nm).

2.2.12.7. PARP1 Activity Assay

PARP1 activity assays were carried out as previously described (Adamczyk et al., 2005; Strosznajder et al., 2000a, b). Briefly 100 μg of protein was incubated in 100 μl reaction mixture containing 200 uM [^{14}C]NAD ($2x10^5$ d.p.m), 100 mM Tris-HCl (pH 8.0), 10 mM $MgCl_2$,1 mM DTT and 50 uM p-amidinophenylmethanesulfonyl fluoride (APMSF) for 5 minutes at 37°C. Reactions were terminated by addition of 800 μl of 25% ice-cold trichloroacetic acid (TCA). After collection of the precipitate on Whatman GF/B filters, it was washed five times with ice-cold 5% TCA, dried and ^{14}C radioactivity was measured using a Packard 2500 TR scintillation counter (Thermo Fisher Scientific, Waltham, MA, USA).

2.2.13. Statistical Analysis

The % oxidative damage values from the fpg reaction and RT-PCR studies are reported as mean ± SD. Data obtained for gene expression fold change, protein levels and protein activities were tested for normality using the Wilks-Shapiro test. Statistical comparisons were carried out using the Mann-Whitney U-test for non-parametrically distributed data with values reported as the median [range]. For normally distributed data, statistical comparisons were carried out using ANOVA with Dunnett's test for individual comparisons and the values reported as mean ± SEM. $P < 0.05$ was considered significant.

Table 2.5. Names and sequences of oligonucleotides used in protein activity assays

Assay	**Sequence**
8-Oxoguanine incison	5′-GAA CGA CTG T(**oxoG**)A CTT GAC TGC TAC TGA T-3′ 3′-CTT GCT GAC A C T GAA CTG ACG ATG ACT A-5′
Uracil incision	5′-ATA TAC CGC GG(**U**) CGG CCG ATC AAG CTT ATT-3′ 3′-TAT ATG GCG CC G GCC GGC TAG TTC GAA TAA-5′
AP-site incision	5′-GAA CGA CTG T(**abasic**)A CTT GAC TGC TAC TGA T-3′ 3′-CTT GCT GAC A C T GAA CTG ACG ATG ACT A-5′
POLB gap-filling	5′-CTGCAGCTGATGCGC(**spacerC3**)GTACGGATCCCCGGGTAC-3′ 3′-GAC GTC GAC TAC GCG GCA TGC CTA GGG GCC CAT G-5′
FEN1 incision	Quencher 5′-CACGTTGACTACCGCTCAATCCTGACGAACACATC-BHQ-2 Flap 5′-TAMRA-GATGTCAAGCAGTCCTAACTTTGAGGCAGAGTCCGC Template 5′-GCGGACTCTGCCTCAAGACGGTAGTCAACGTG-3′

CHAPTER THREE: RESULTS

3.1. Oxidative DNA Damage in Genes of Proteins Modified during AD

Percent oxidative DNA damage was calculated in the SMTG (a vulnerable brain region) and cerebellum (a non-vulnerable brain region) of fourteen age-matched NC, five MCI, thirteen PCAD, thirteen LAD and nine DC subjects. The subject demographics are shown in Table 3.1. No significant differences were observed in PMI for any of the subjects studied. Although, there were no significant differences in ages of MCI (91.6 ± 2.7 years), PCAD (85.7 ± 1.8 years) and LAD (81.2 ± 1.6 years) subjects compared to NC subjects (85.9 $\pm$ 1.4 years), DC subjects which have an earlier disease age of onset (70.4 $\pm$ 5.9 years) were significantly younger than NC subjects. Median Braak staging scores were significantly ($P < 0.05$) higher for PCAD (IV), MCI (III), LAD subjects (VI) and DC subjects (II) compared to NC subjects (I).

Two different DNA isolation methods, phenol-chloroform extraction and extraction using Qiagen DNeasy Tissue Kit, were compared to determine the method with minimal artifactual oxidation. Data obtained showed DNA isolated using the DNeasy kit demonstrated 10-20% more artifactual oxidation compared to phenol-chloroform extraction method. Based on these results, phenol extraction method was used for DNA isolation in this project. Initially, samples were subjected to the Fpg reaction and oxidative damage as evidenced by fpg cleavage was analyzed using traditional PCR and a range of primers and visualized using agarose gel electrophoresis. The gels showed smaller molecular mass bands for fpg treated samples compared to the non-treated samples but did not provide quantitative data. Hence qPCR was used to quantitatively determine the % oxidative damage in this study. Primers were designed for PCR and

qPCR to encompass the coding sequence of each gene and are listed in Table 2.2 and 2.3 respectively. The fluorescent dye SYBR Green was used for detection in the qPCR reactions. The absence/presence of non-specific amplification in a qPCR reaction was verified using melt curves. Amplicons highlighted in red in Tables 3.2-3.4 showed a significant increase ($P < 0.05$) or a trend towards a significant increase ($0.05 < P < 0.1$) in oxidative damage in MCI/PCAD/LAD/DC subjects compared to NC subjects. Results of this study were non-normally distributed (Wilks-Shapiro test) and are reported as Median [Range] % of NC values. Oxidative damage data for VADC1I in SMTG and VDAC2D in cerebellum displayed a normal distribution and are reported as mean (± SEM) % of NC. All comparisons are based on the average of triplicate experiments. As the data are non-normally distributed, box and whisker plots were used to describe the results. An example of a typical box and whisker plot is shown in Figure 3.1. The median value is represented by the line within the box. The boundaries of the box indicate the 25^{th} (lower boundary, near zero) and 75^{th} percentile (upper boundary) and the whiskers denote the 10^{th} (whisker below the box) and the 90^{th} percentile (bar above the box). The dots (●) above and below the whiskers represent extreme data points or outliers.

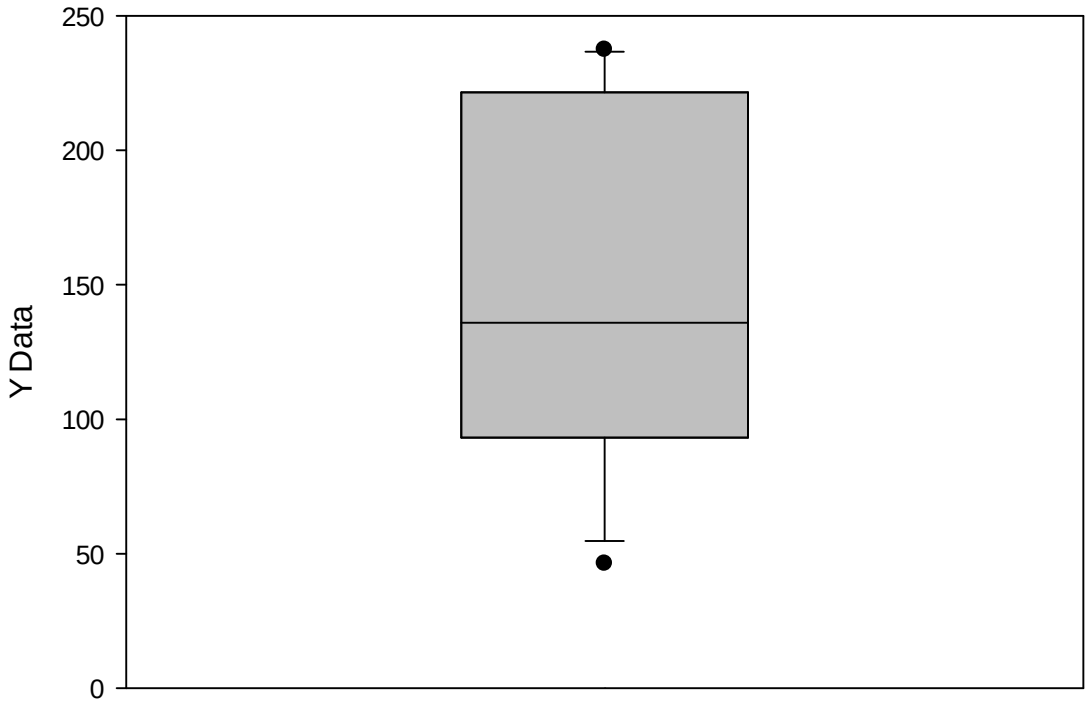

Figure 3.1. Example of a box and whisker plot

3.1.1. VDAC1

Eight sets of VDAC1 primers (Table 2.3.1) were used to examine the % oxidative damage in the coding sequence of VDAC1 and significant differences in oxidative damage were observed for 5 amplicons. The results for quantification of oxidative damage for all 8 amplicons are described in the following section. For the VDAC1A amplicon (bp 438-613), no significant differences in % oxidative damage were observed in the SMTG of MCI (184.24 [6.78-244.05]), LAD (71.06 [0-320.84] %) or DC (8.87 [0-304.49] %) subjects compared to NC subjects (19.14 [0-366.74] %). Median levels of % oxidative damage were significantly higher in the SMTG of PCAD subjects (288.36 [0-355.38] %) compared to NC subjects for VDAC1A (Figure 3.2A). In the cerebellum, % oxidative damage was not significantly altered in MCI (0 [0-219.58] %), PCAD (0 [0-301.71] %), LAD (72.49 [25.44-281.03] %) or DC (0 [0-298.98] %) subjects compared to NC subjects (102.83 [0-216.08] %) (Figure 3.2B) for VDAC1A. In the SMTG, there was a significant increase in median levels of % oxidative damage in LAD (231.53 [0-524.96] %) and DC (228.7 [62.32-371.39] %) subjects and a trend towards significant increase in PCAD subjects (217.49 [0-351.31] %) compared to NC subjects (0 [0-380.29] %) for the VDAC1B amplicon (bp 482-689). No significant changes in the median levels of % oxidative damage were observed in the SMTG of MCI subjects (214.86 [60.49-357.45] %) compared to NC subjects for VDAC1B (Figure 3.3A). In the cerebellum, median levels of % oxidative damage were significantly elevated in DC subjects (0 [0-298.98] %) compared to NC subjects (111.87 [0-223.75] %) for VDAC1B. In contrast, there were no significant differences in MCI (0 [0-219.58] %), PCAD (7.5 [0-286.51] %), LAD (126.63 [0-337.72] %) for VDAC1B (Figure 3.3B).

Analysis of the VDAC1C amplicon (bp 666-913) showed no significant differences in % oxidative damage in the SMTG of MCI (326.07 [0-439.58] %) but a significant increase in PCAD (276.22 [94.08-482.44] %), LAD (311.02 [0-494.12] %) and DC (263.46 [0-528.53] %) subjects compared to NC subjects (69.2 [0-467.70] %) (Figure 3.4A). We observed no significant changes in median levels of % oxidative damage in the cerebellum of MCI (107.56 [0-283] %), PCAD (137.55 [0-369.19] %), LAD (70.04 [0-362.01] %) or DC (13.83 [0-261.65 %) subjects compared to NC subjects (26.84 [0-327.84] %) (Figure 3.4B). Median levels of % oxidative damage showed no significant differences in the SMTG of MCI (121.81 [0.01-186.61] %), PCAD (149.04 [0-185.66] %), LAD (53.43 [2.88-143.89] %) or DC (148.09 [0-187.9] %) subjects compared to NC subjects (126.55 [0-168.46] %) (Figure 3.5A) for the VDAC1D amplicon (bp 695-896). Similarly, there were no significant differences seen in % oxidative damage for VDAC1D in the cerebellum of MCI (0 [0-263.16] %), PCAD (0 [0-248.47] %), LAD (93.88 [0-229.52] %) or DC (48.55 [0-210.79 %) subjects compared NC subjects (104.87 [0-240.47] %) (Figure 3.5B).

Median levels of % oxidative damage were significantly higher in the SMTG of PCAD (251.5 [0-294.42] %), LAD (192.57 [0-277.07] %) and DC (212.27 [0-301.77] %) subjects compared to NC subjects (148.07 [0-160.26] %) for the VDAC1E amplicon (bp 722-913). There was a trend towards a significant increase in oxidative damage in SMTG of MCI (175.67 [123.8-269.36] %) compared to NC subjects (Figure 3.6A). No significant differences in % oxidative damage were observed for the VDAC1E amplicon in the cerebellum of MCI (223.13 [0-322.19] %), PCAD (78.16 [0-278.49] %), LAD (113.23 [0-309.12] %) or DC (143.9 [0-297.43] %) subjects compared to NC subjects

(69.59 [0-306.2] %) (Figure 3.6B). In the SMTG, there was a significant increase in median levels of % oxidative damage in LAD (157.87 [0-165.69] %) but no significant changes in MCI (121.37 [0-140] %), PCAD (139.66 [39.67-162.11] %) or DC (141.42 [18.73-167.65] %) subjects compared to NC subjects (121.92 [0-160.26] %) for the VDAC1G amplicon (bp 914-1173) (Figure 3.7A). There were no significant differences observed in % oxidative damage for VDAC1G in the cerebellum of MCI (167.37 [0-295.77] %), PCAD (54.69 [0-230.39] %), LAD (101.2 [0-284.02] %) or DC (159.48 [0-266.9] %) subjects compared to NC subjects (25.78 [0-285.38] %) (Figure 3.7B).

Analysis of the VDAC1H amplicon (bp 1174-1411) showed no significant differences in % oxidative damage in the SMTG of MCI (85.34 [0-110.68] %), PCAD (87.82 [0-146.28] %), LAD (126.09 [0-153.39] %) or DC (122.2 [0-149.48] %) subjects compared to NC subjects (105.75 [10.83-141.4] %) (Figure 3.8A). Median levels of % oxidative damage were not significantly different in the cerebellum of MCI (171.58 [69.69-429.3] %), PCAD (0 [0-292.21] %), LAD (106.23 [0-312.94] %) or DC (195.92 [0-383.87] %) subjects compared to NC subjects (67.66 [0-335.75] %) (Figure 3.8B). In the SMTG, there were no significant differences in average % oxidative damage in MCI (80.27 ± 15.75 %), PCAD (78.22 ± 12.88 %), LAD (102.75 ± 14.74 %) and DC (113.17 ± 9.11 %) subjects compared to NC subjects (100 ± 8.05 %) for the VDAC1I amplicon (bp 1398-1594) (Figure 3.9A). No significant changes in median levels of % oxidative damage were observed for VDAC1I in the cerebellum of MCI (131.28 [0-190.85] %), PCAD (58.5 [0-337.85] %), LAD (45.85 [0-424.78] %) or DC (174.37 [0-350.29] %) subjects compared to NC subjects (75.46 [0-308.38] %) (Figure 3.9B).

Table 3.1. Subject demographics for the oxidative damage study

	Age (Mean ± SEM)	Braak Score (Median)	PMI (Mean ± SEM)	Sex
NC (N = 14)	85.9 ± 1.4	I	2.8 ± 0.2	4M : 10W
MCI (N = 5)	91.6 ± 2.7	III*	2.6 ± 0.2	2M : 3W
PCAD (N = 13)	85.7 ± 1.8	IV*	2.8 ± 0.2	3M : 10W
LAD (N = 13)	81.2 ± 1.6	VI*	3.6 ± 0.4	6M : 7W
DC (N = 9)	70.4 ± 5.9	II*	3.2 ± 0.3	5M : 4W

*** P < 0.05**

NC: Normal Control; MCI: Mild Cognitive Impairment; PCAD: Preclinical Alzheimer's Disease; LAD: Late-stage Alzheimer's Disease; SEM: Standard Error of Mean; PMI: Postmortem Interval; M: Men; W: Women

Table 3.2. Percent oxidative DNA damage for VDAC1 amplicons (Significant differences are shown in bold)

Amplicon	NC		MCI		PCAD		LAD		DC	
	SMTG	CER	SMTG	CER	SMTG	CER	SMTG	CER	SMTG	CER
VDAC1A	19.14 [0-366.74]	102.83 [0-216.08]	184.24 [6.78-325.69]	0 [0-244.05]	***288.36 [0-355.38]**	0 [0-301.71	71.062 [0-320.84]	72.49 [25.44-281.03]	8.87 [0-304.49]	4.96 [0-249.67]
VDAC1B	0 [0-380.29]	111.87 [0-223.75]	214.86 [60.49-357.45]	0 [0-219.58]	****217.4 94 [0-351.31]***	7.5 [0-286.51]	***231.53 [0-524.96]**	126.63 [0-337.72]	***228.7 [62.32-371.39]**	***0 [0-298.98]**
VDAC1C	69.20 [0-467.70]	26.84 [0-327.84]	326.07 [0-439.58]	107.56 [0-283]	***276.22 [94.08-482.44]**	137.55 [0-369.19]	***311.02 [0-494.12]**	70.04 [0-362.01]	***263.46 [0-528.53]**	13.83 [0-261.65]
VDAC1D	126.55 [0-168.46]	104.87 [0-240.47]	121.81 [0.01-186.61]	0 [0-263.16]	149.04 [0-185.66]	0 [0-248.47]	53.43 [2.88-143.89]	93.88 [0-229.52]	148.09 [0-187.9]	48.55 [0-210.79]
VDAC1E	148.07 [0-224.85]	69.59 [0-306.2]	****175.67 [123.8-269.36]***	223.13 [0-322.19]	***251.5 [0-294.42]**	78.16 [0-278.49]	***192.57 [0-277.07]**	113.23 [0-309.12	***212.27 [0-301.77]**	143.9 [0-297.43]
VDAC1G	121.92 [0-160.26]	25.78 [0-285.38]	121.37 [0-140]	167.37 [0-295.77]	139.66 [39.67-162.11]	54.68 [0-230.39]	***157.87 [0-165.59]**	101.2 [0-284.02]	141.42 [18.73-167.65]	159.48 [0-266.9]
VDAC1H	105.75 [10.83-141.4]	67.66 [0-335.75]	85.34 [0-110.68]	171.58 [69.69-429.3]	87.82 [0-146.28]	0 [0-292.21]	126.09 [0-153.39]	106.23 [0-312.94]	122.2 [0-149.48]	195.92 [0-383.87]
VDAC1I	100 (± 8.05)	75.46 [0-308.38]	80.27 (± 15.75)	131.28 [0-190.85]	78.22 (± 12.88)	58.5 [0-337.85]	102.75 (± 14.74)	45.85 [0-424.78]	113.17 (± 9.11)	174.37 [0-350.29]

*** P < 0.05**
**** 0.05 < P < 0.1**

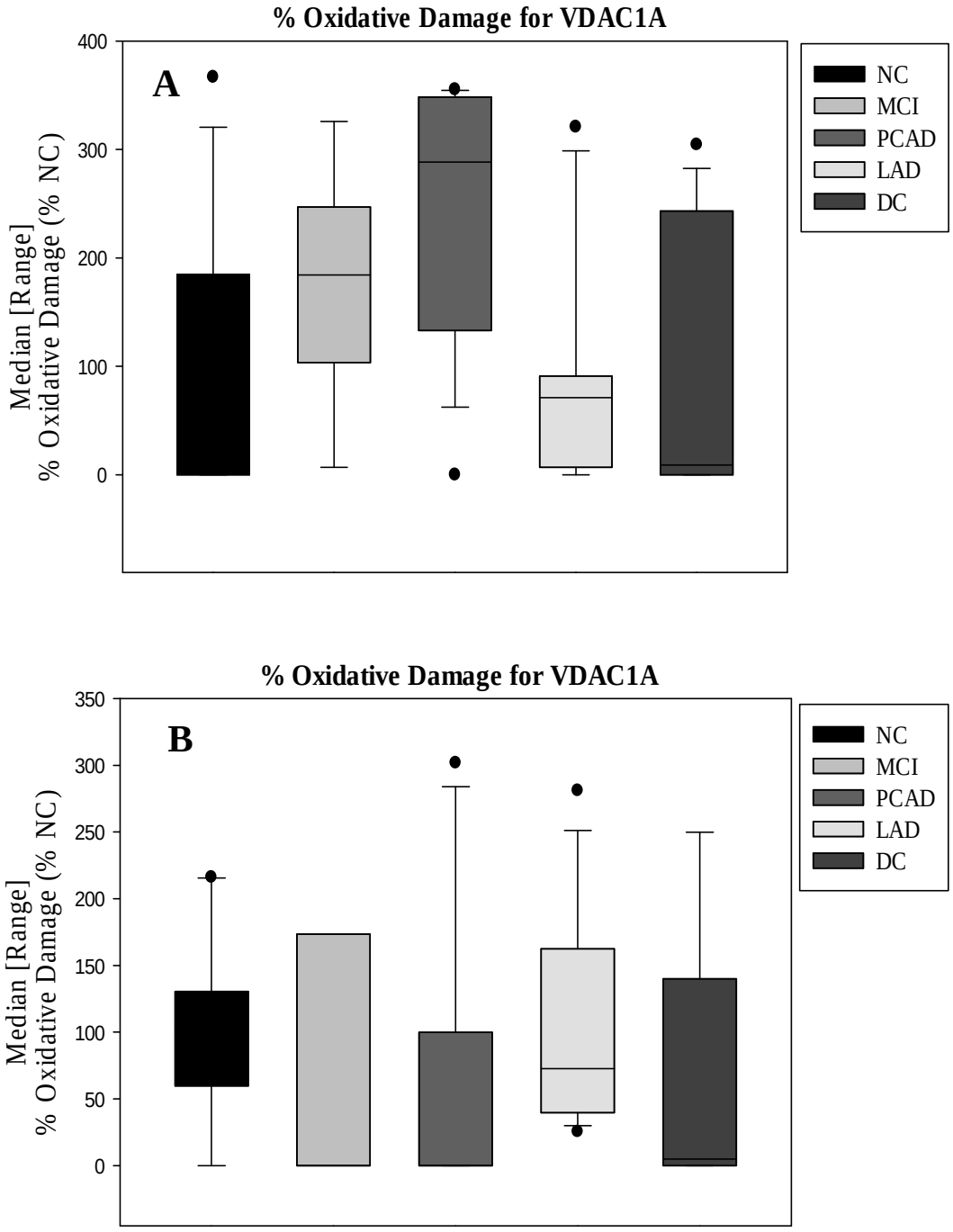

Figure 3.2. Oxidative damage in amplicons for VDAC1A in A) SMTG B) Cerebellum

(***** P < 0.05; ****** 0.05 < P < 0.1)

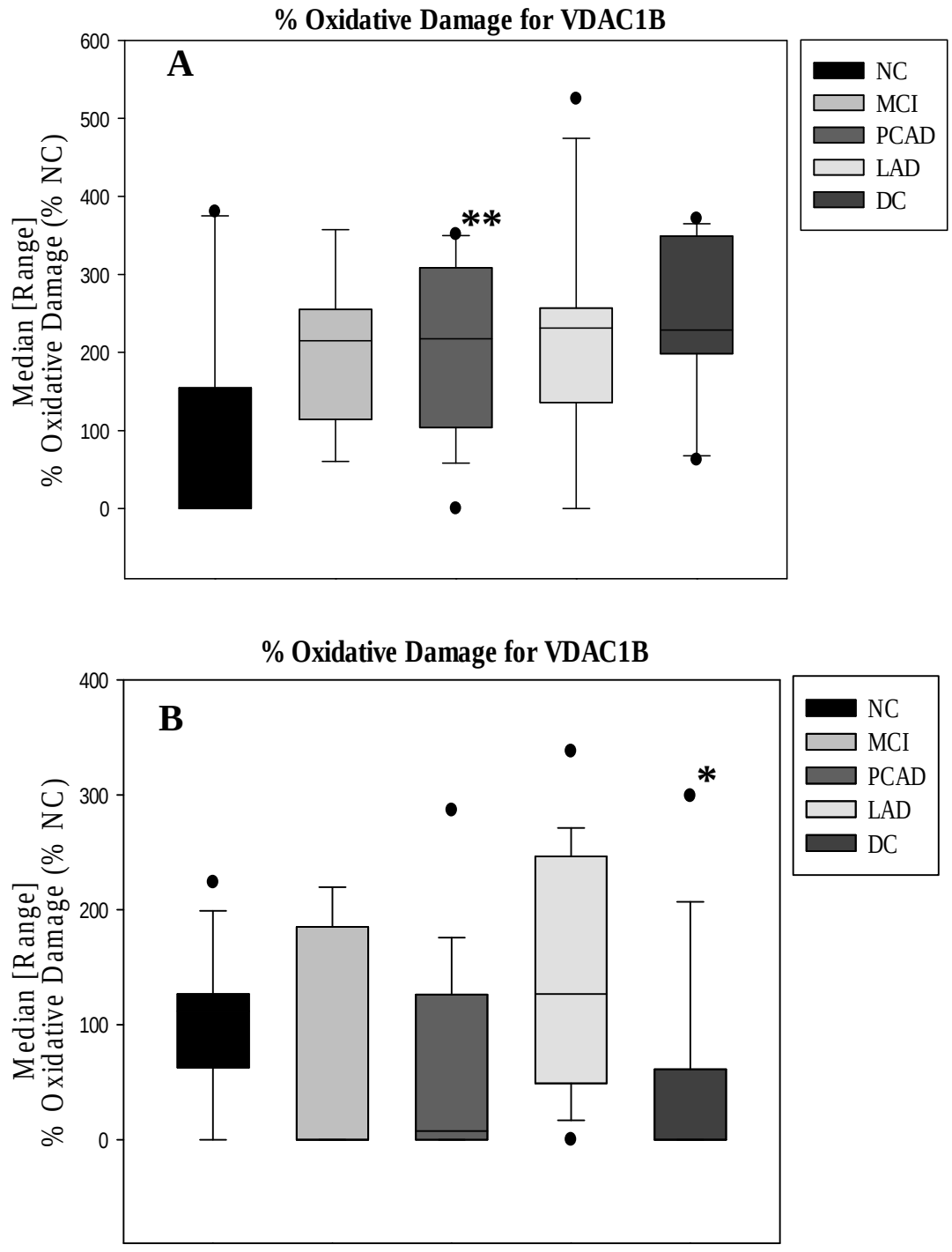

Figure 3.3. Oxidative damage in amplicons for VDAC1B in A) SMTG B) Cerebellum

(* $P < 0.05$; ** $0.05 < P < 0.1$)

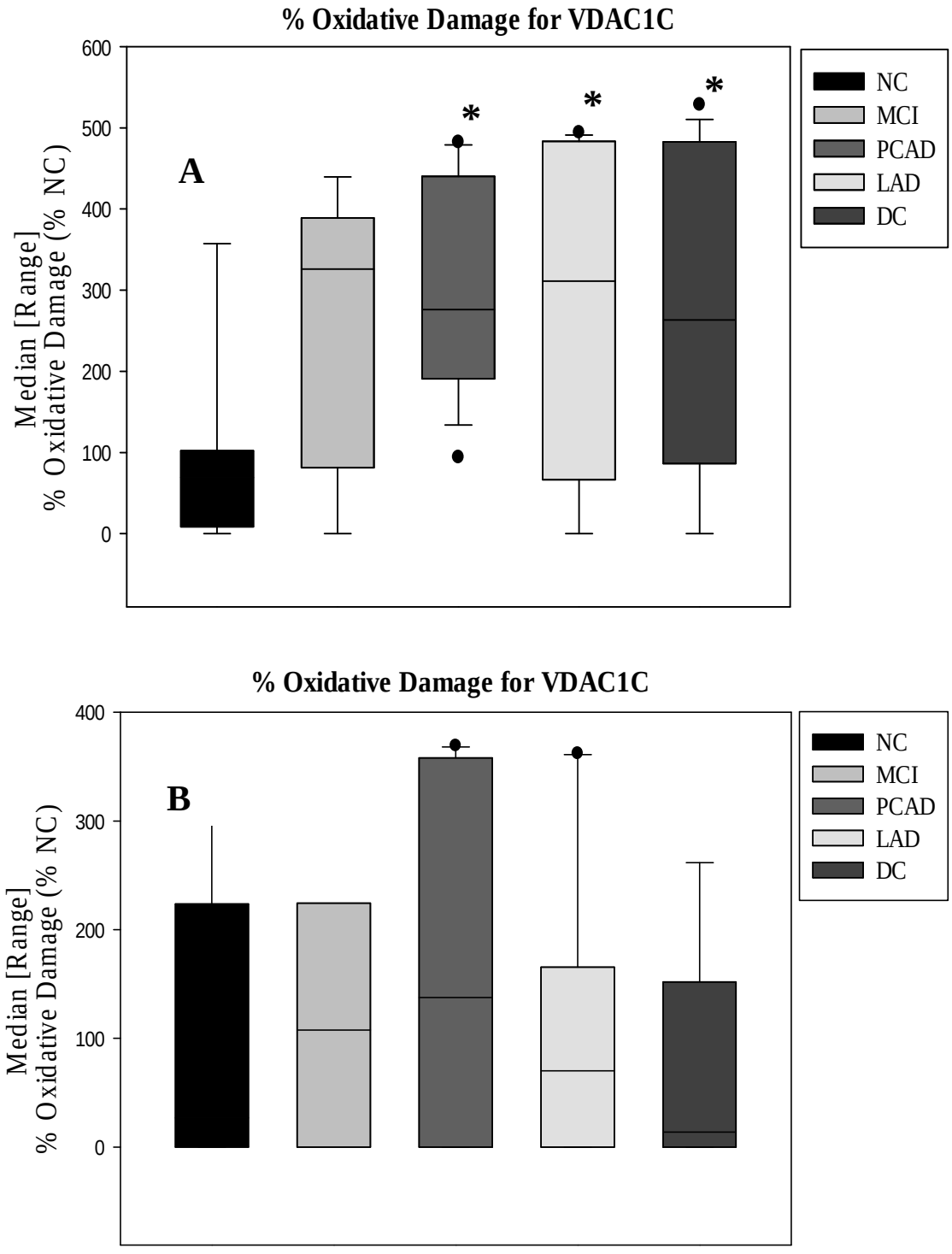

Figure 3.4. Oxidative damage in amplicons for VDAC1C in A) SMTG B) Cerebellum

(* $P < 0.05$; ** $0.05 < P < 0.1$)

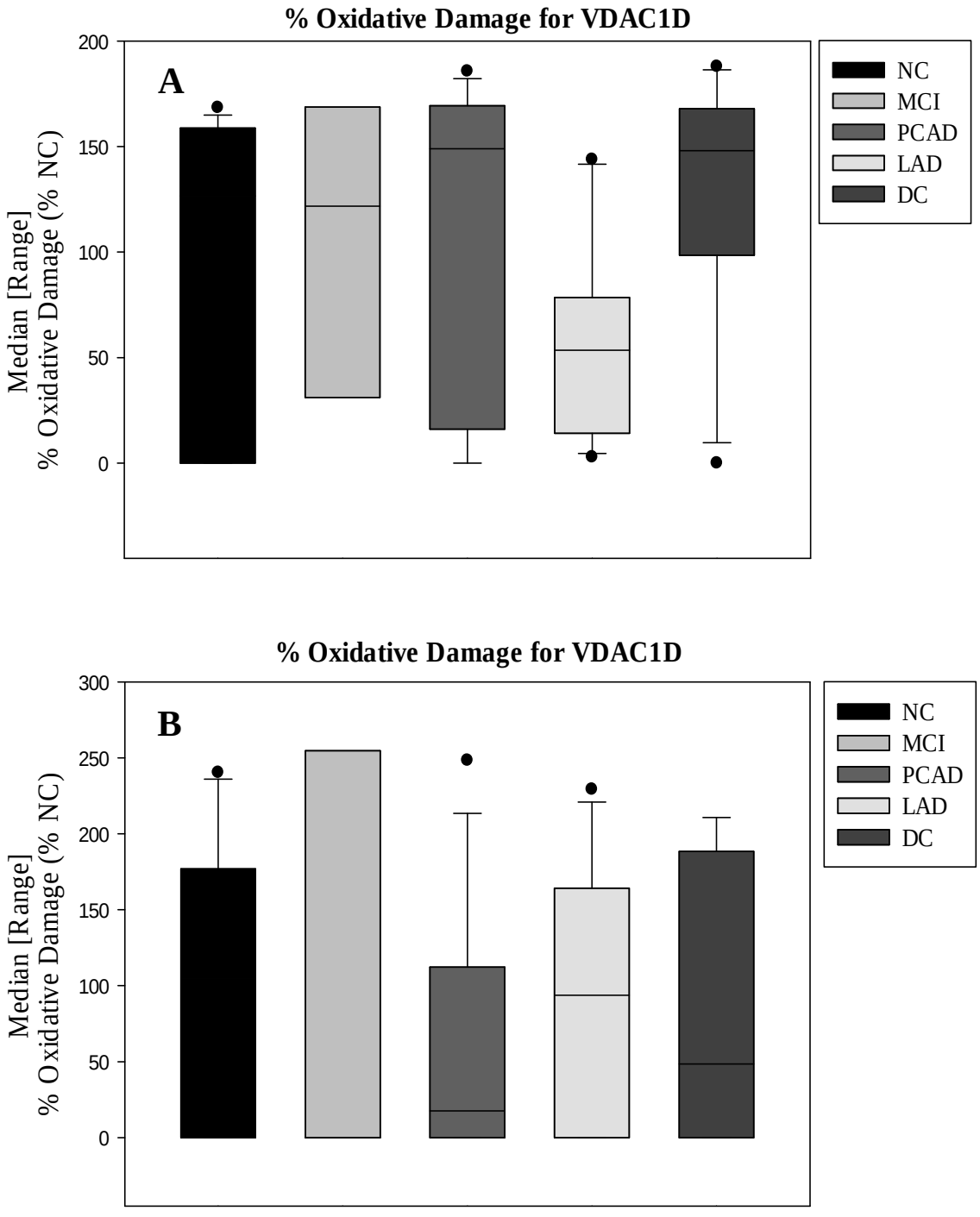

Figure 3.5. Oxidative damage in amplicons for VDAC1D in A) SMTG B) Cerebellum

(***** P < 0.05; ****** 0.05 < P < 0.1)

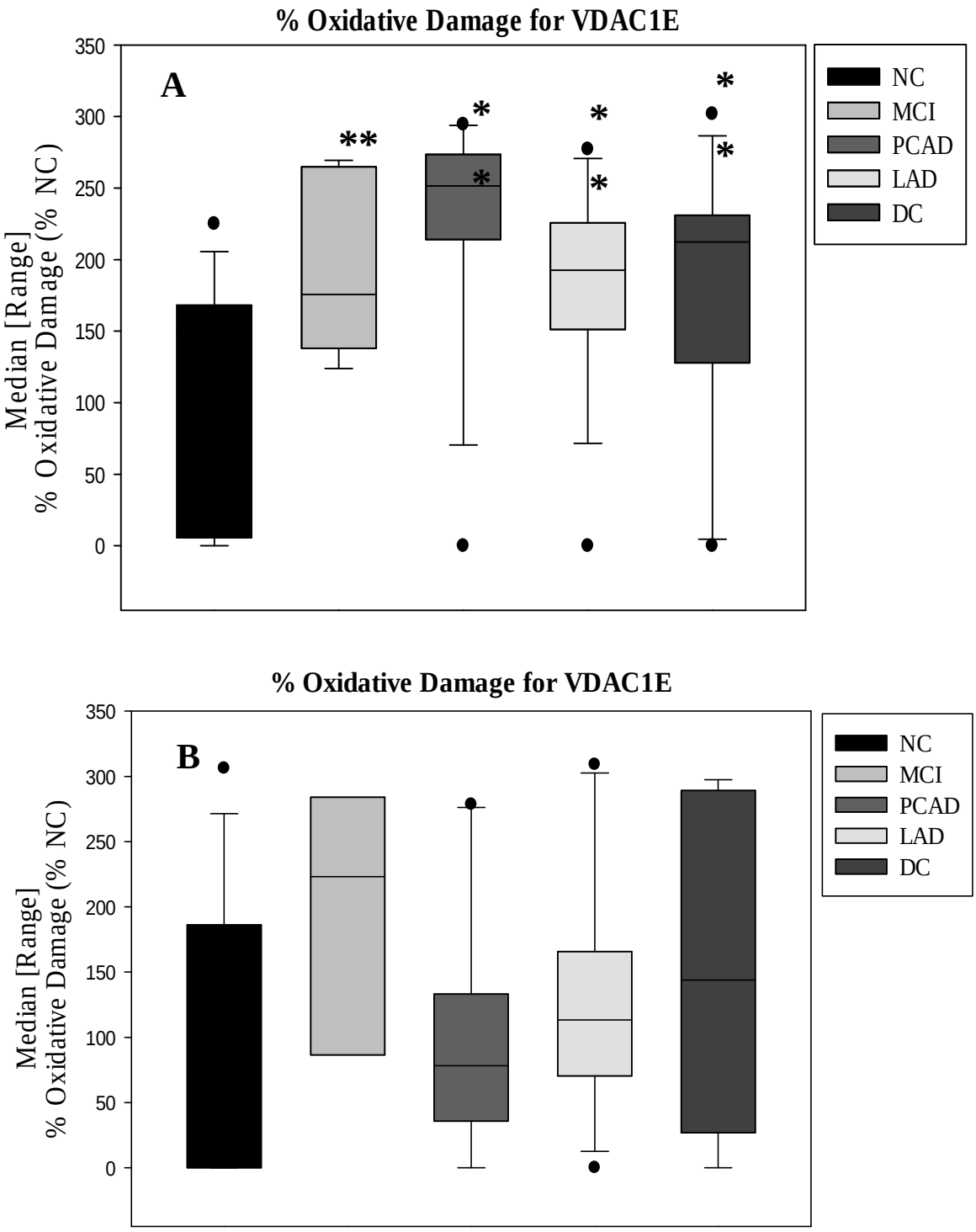

Figure 3.6. Oxidative damage in amplicons for VDAC1E in A) SMTG B) Cerebellum

(* $P < 0.05$; ** $0.05 < P < 0.1$)

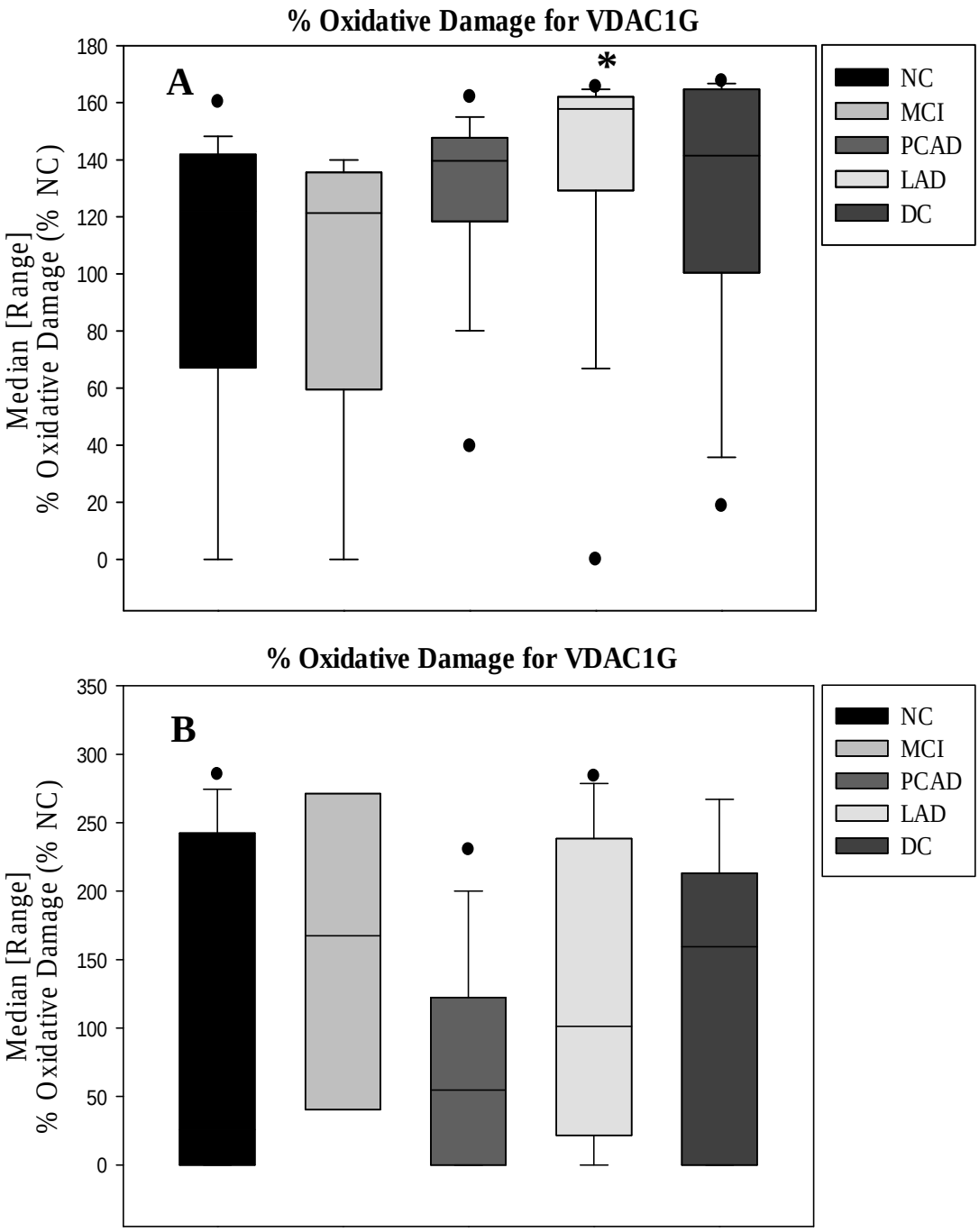

Figure 3.7. Oxidative damage in amplicons for VDAC1G in A) SMTG B) Cerebellum

(***** P < 0.05; ****** 0.05 < P < 0.1)

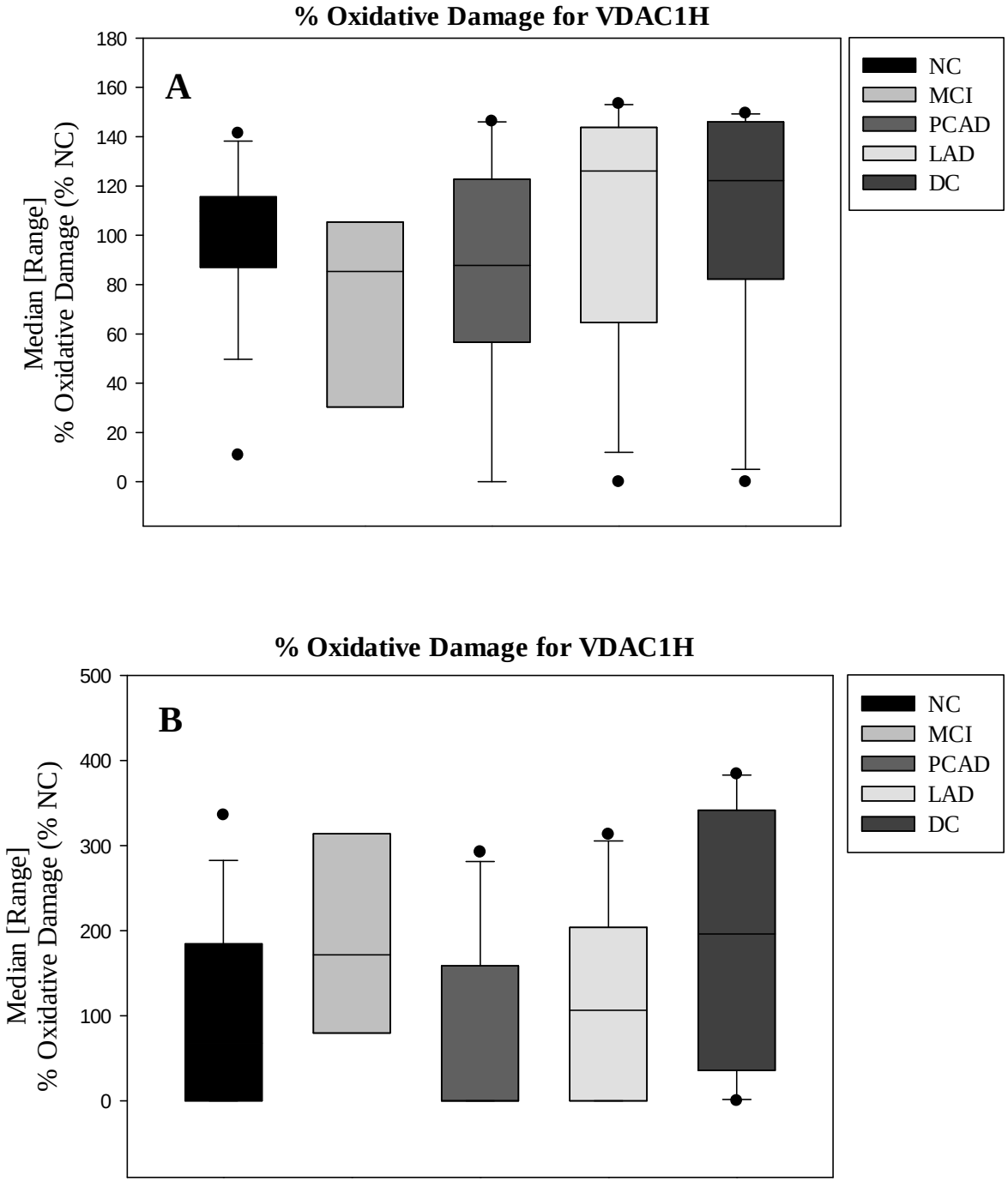

Figure 3.8. Oxidative damage in amplicons for VDAC1H in A) SMTG B) Cerebellum

(***** P < 0.05; ****** 0.05 < P < 0.1)

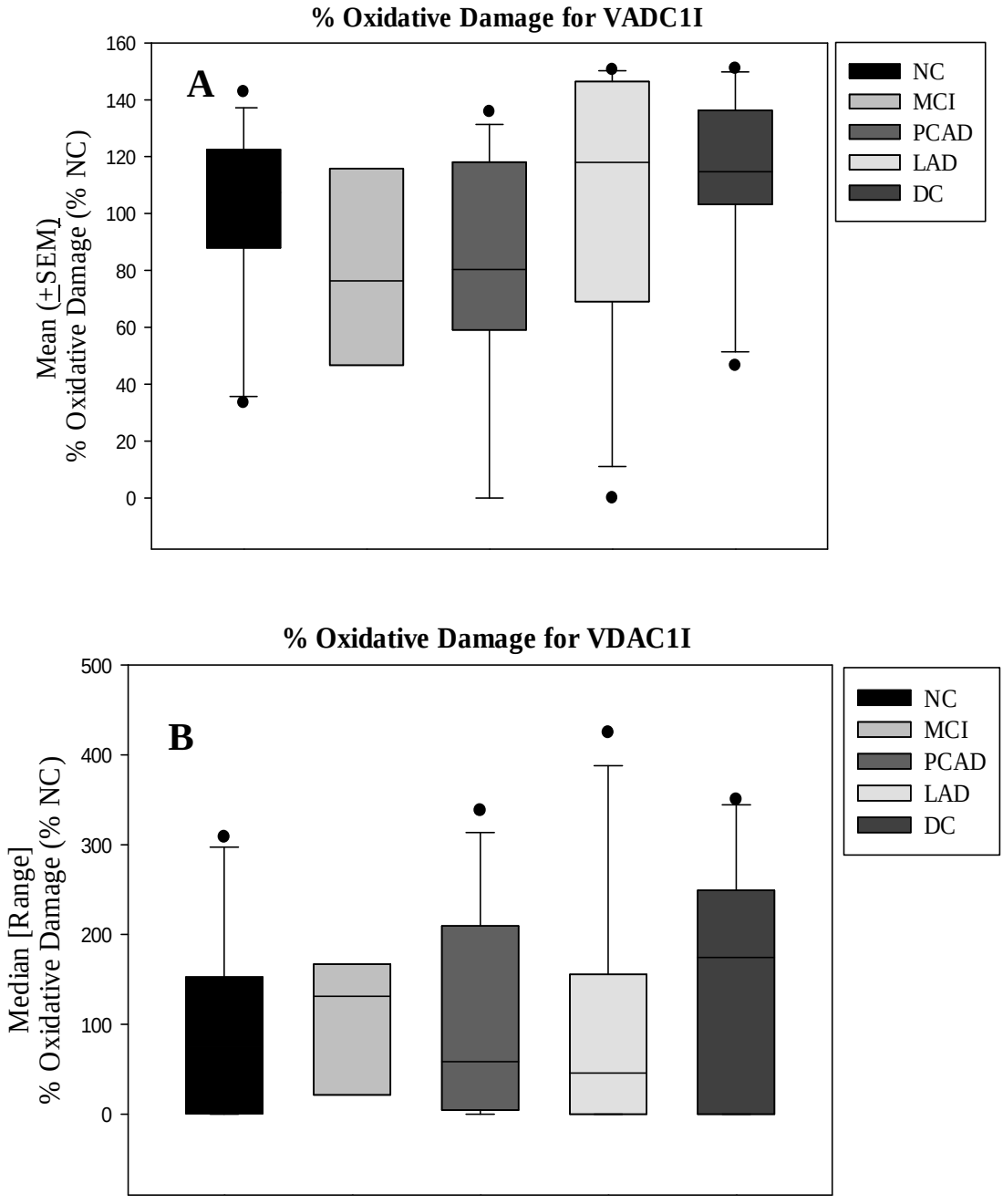

Figure 3.9. Oxidative damage in amplicons for VDAC1I in A) SMTG B) Cerebellum

(***** P < 0.05; ****** 0.05 < P < 0.1)

3.1.2. VDAC2

Seven sets of VDAC2 primers (Table 2.3.2) were used to examine levels of oxidative damage in the coding sequence of VDAC2. The results of oxidative damage calculated for all the amplicons are discussed in detail in this section. All the amplicons had a GC content ratio of 44-50% except for the VDAC2A amplicon (bp 24-213) which had a > 50% GC content ratio. Melt curve analysis of qPCR reactions with primers for the VDAC2A amplicon showed multiple curves indicating high levels of non-specific binding. Therefore, the data obtained for VDAC2A could not be used to determine % oxidative damage. For the VDAC2B amplicon (bp 167-354), no significant differences in % oxidative damage were observed in the SMTG of MCI (43.71 [0-195.88] %), PCAD (10.75 [0-457.89] %), LAD (0 [0-202.83] %) or DC (59.88 [0-378.58] %) subjects compared to NC subjects (21.45 [0-421.84] %) (Figure 3.10A). Similarly, median levels of % oxidative damage were not significantly different in the cerebellum of MCI (0 [0-144.87] %), PCAD (14.42 [0-219.49 %), LAD (229.59 [0-378.58] %) or DC (0 [0-224.49] %) subjects compared to NC subjects (31.77 [0-368.24] %) for VDAC2B (Figure 3.10B). For VDAC2C (bp 331-538), % oxidative damage was not significantly altered in the SMTG of MCI (44.98 [1-251.56] %), PCAD (0 [0-250.21] %), LAD (0 [0-338.84] %) or DC (0 [0-216.49] %) subjects compared to NC subjects (62.79 [0-414.16] %) (Figure 3.11A). In the cerebellum, analysis of VDAC2C showed no significant differences in median levels of % oxidative damage in MCI (0 [0-404.84] %), PCAD (0 [0-370.89] %), LAD (292.5 [0-625.31] %) or DC (3.04 [0-517.63] %) subjects compared to NC subjects (1.03 [0-484.2] %) (Figure 3.11B).

No significant differences in median levels of % oxidative damage were observed in the SMTG of MCI (0 [0-872.98] %), PCAD (0 [0-1053.69] %), LAD (0 [0-667.96] %) or DC (82.35 [0-1249.86] %) subjects compared to NC subjects (0 [0-778.04] %) (Figure 3.12A) for the VDAC2D amplicon (bp 522-738). In the cerebellum, mean levels of % oxidative damage were not significantly altered in MCI (127.09 (±39.75) %), PCAD (114.82 (±22.44) %), LAD (84.44 (±19.12) %) or DC (88.73 (±25.56) %) subjects compared to NC subjects (100 (±21.2) %) for VDAC2D (Figure 3.12B). Analysis of the VDAC2E amplicon (bp 726-956), showed no significant differences in % oxidative damage in the SMTG of MCI (0 [0-573.73] %), PCAD (0 [0-1120.85] %), LAD (0 [0-676.49] %) or DC (0 [0-830.88 %) subjects compared to NC subjects (0 [0-1176.67 %) (Figure 3.13A). In cerebellum, oxidative damage in VDAC2E was not significant different in MCI (39.67 [0-146.82] %), PCAD (97.59 [0-200.54] %), LAD (94.65 [0-190.47] %) or DC (126.19 [0-181.23] %) subjects compared to NC subjects (116.4 [0-182.12] %) (Figure 3.13B).

Median levels of % oxidative damage were not significantly different in the SMTG of MCI (0 [0-93.25] %), PCAD (182.34 [0-383.78] %) or LAD (19.98 [0-257.61] %) subjects compared to NC subjects (42.47 [0-313.84] %) (Figure 3.14A) for VDAC2G (bp 948-1152). No significant differences in % oxidative damage were observed for VDAC2G in the cerebellum of MCI (0 [0-276.84] %), PCAD (1.61 [0-198.04] %), LAD (174.93 [0-351.57] %) or DC (140.05 [0-236.69] %) subjects compared to NC subjects (5.48 [0-312.73] %) (Figure 3.14B). Quantification of oxidative damage in VDAC2H amplicon (bp 1126-1310), showed no significant differences in the SMTG of MCI (0 [0-5291.24] %), PCAD (0 [0-4418.17] %), LAD (0 [0-3746.8] %) or DC (0 [0-4425.36] %)

subjects compared to NC subjects (0 [0-1140.54] %) (Figure 3.15A). In the cerebellum, median levels of % oxidative damage were not significantly different in MCI (116.75 [119.11-275.63] %), PCAD (167.86 [0-265.88] %), LAD (46.86 [0-267.57] %) or DC (131.67 [0-248.92] %) subjects compared to NC subjects (85.44 [0-278.89] %) for VDAC2H (Figure 3.15B).

Table 3.3. Percent oxidative DNA damage for VDAC2 amplicons (There were no significant differences observed for any of the subjects studied)

Amplicon	NC		MCI		PCAD		LAD		DC	
	SMTG	**CER**	**SMTG**	**CER**	**SMTG**	**CER**	**SMTG**	**CER**	**SMTG**	**CER**
VDAC2B	21.45 [0-421.84	31.77 [0-368.24]	43.71 [0-195.88]	0 [0-144.87]	10.75 [0-457.89]	14.42 [0-219.49]	0 [0-202.83]	229.59 [0-407.21]	59.88 [0-378.58]	0 [0-224.49]
VDAC2C	62.79 [0-414.16]	1.03 [0-484.2]	44.98 [1-251.56]	0 [0-404.84]	0[0-250.21]	0 [0-370.89]	0 [0-338.84]	292.5 [0-625.31]	0 [0-216.49]	3.04 [0-517.63]
VDAC2D	0 [0-778.04]	100 (± 21.2)	0 [0-872.98]	127.09 (± 39.75)	0 [0-1053.69]	114.82 (± 22.44)	0 [0-667.96]	84.44 (± 19.12)	82.35 [0-1249.86]	88.73 (± 25.56)
VDAC2E	0 [0-1176.67]	116.4 [0-182.12]	0 [0-573.73]	39.67 [0-146.82]	0 [0-1120.85]	97.59 [0-200.54]	0 [0-676.49]	94.65 [0-190.47]	0 [0-830.88]	126.19 [0-181.23]
VDAC2G	42.47 [0-313.84]	5.48 [0-312.73]	0 [0-93.25]	0 [0-276.84]	182.34 [0-383.78]	1.61 [0-198.04]	19.98 [0-257.61]	174.93 [0-351.57]		140.05 [0-236.69]
VDAC2H	0 [0-1140.54]	85.44 [0-278.89]	0 [0-5291.24]	116.75 [19.11-275.63]	0 [0-4418.17]	167.86 [0-265.88]	0 [0-3746.8]	46.86 [0-267.57]	0 [0-4425.36]	131.67 [0-248.92]

*** P < 0.05**
**** 0.05 < P < 0.1**

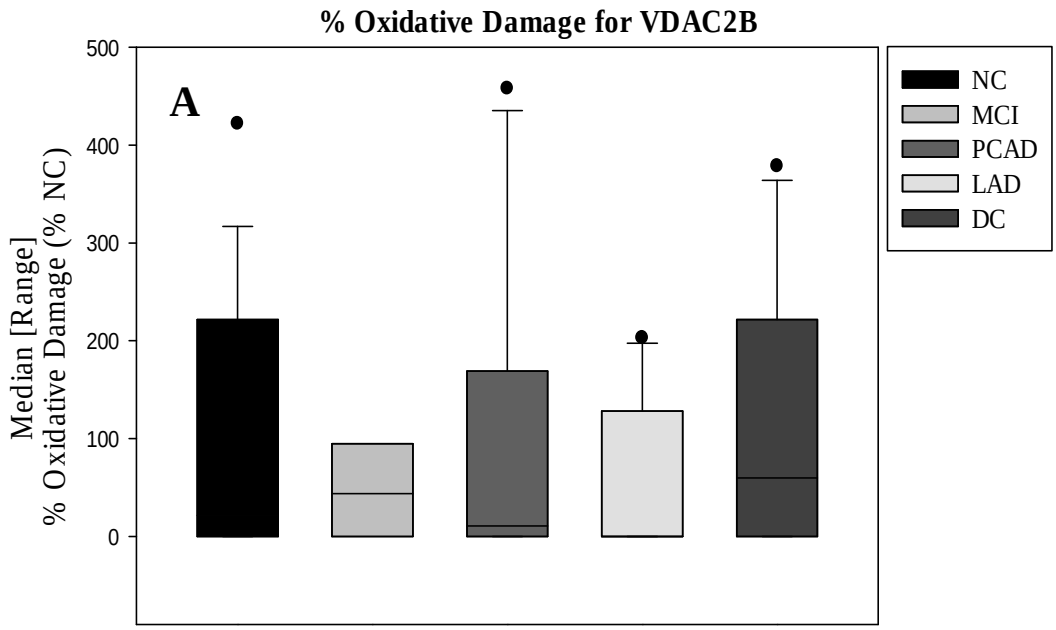

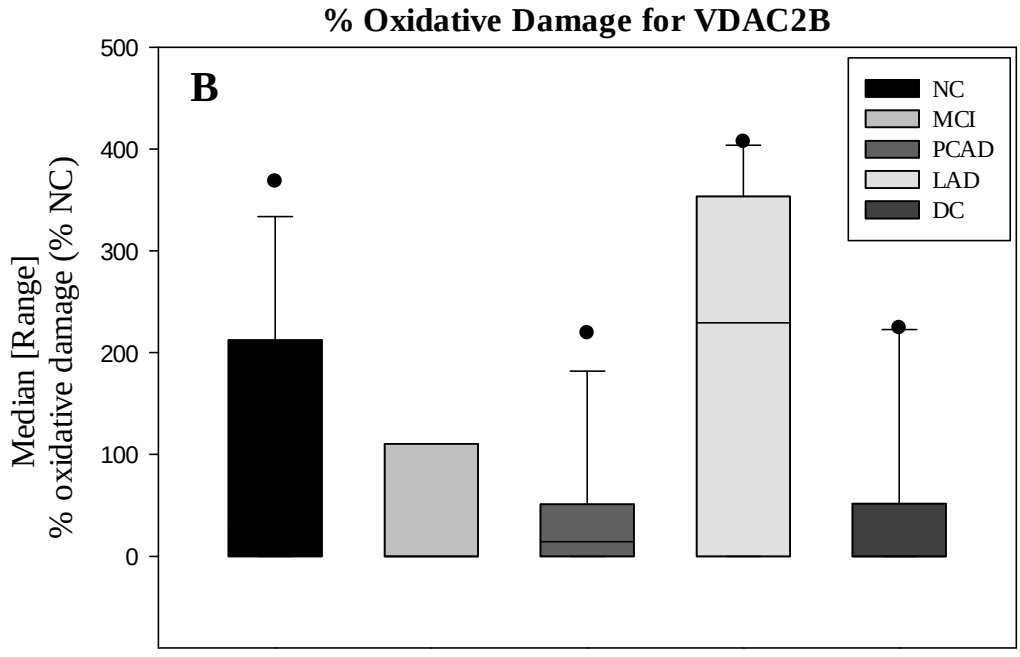

Figure 3.10. Oxidative damage in amplicons for VDAC2B in A) SMTG B) Cerebellum

(***** P < 0.05; ****** 0.05 < P < 0.1)

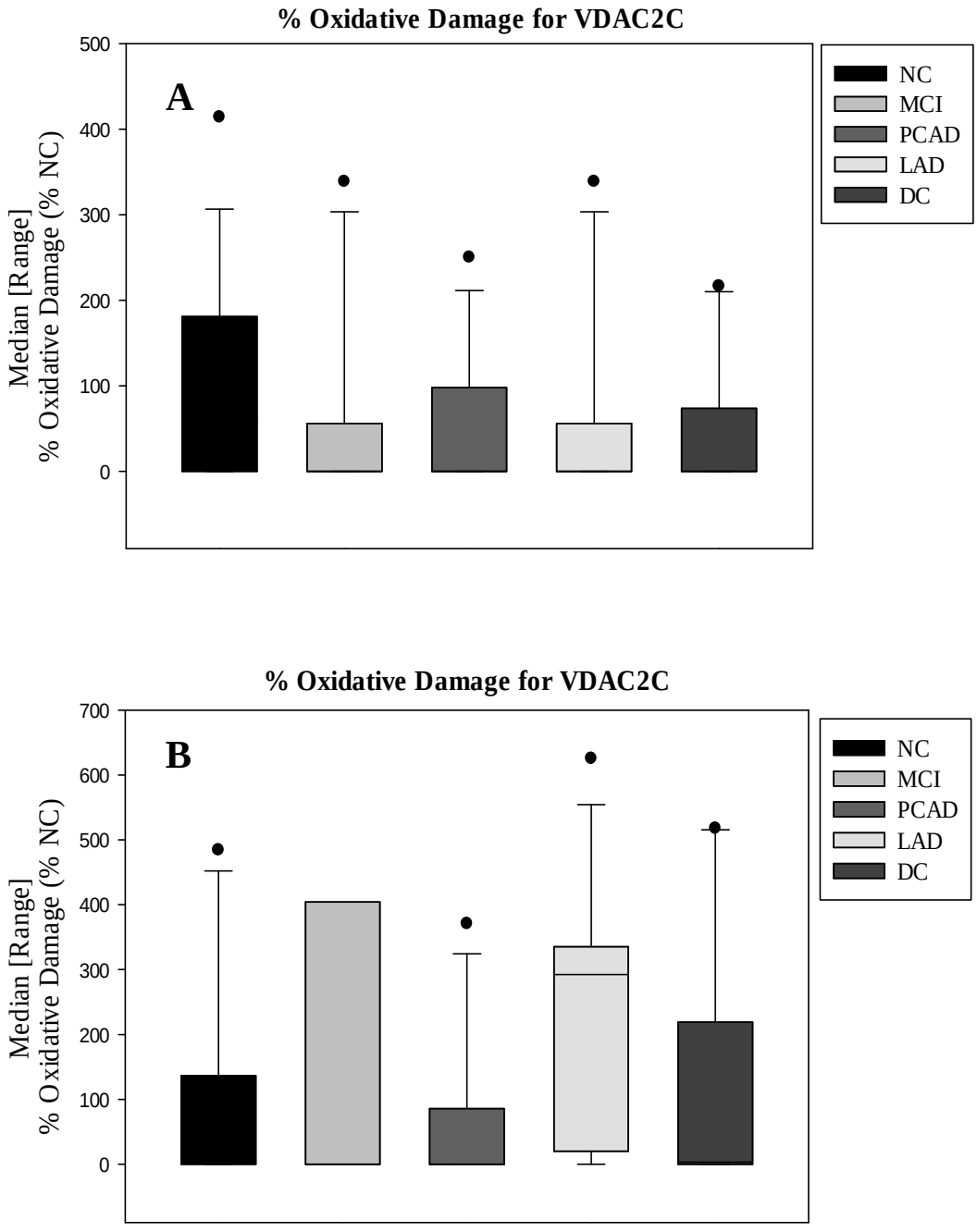

Figure 3.11. Oxidative damage in amplicons for VDAC2C in A) SMTG B) Cerebellum

(***** P < 0.05; ****** 0.05 < P < 0.1)

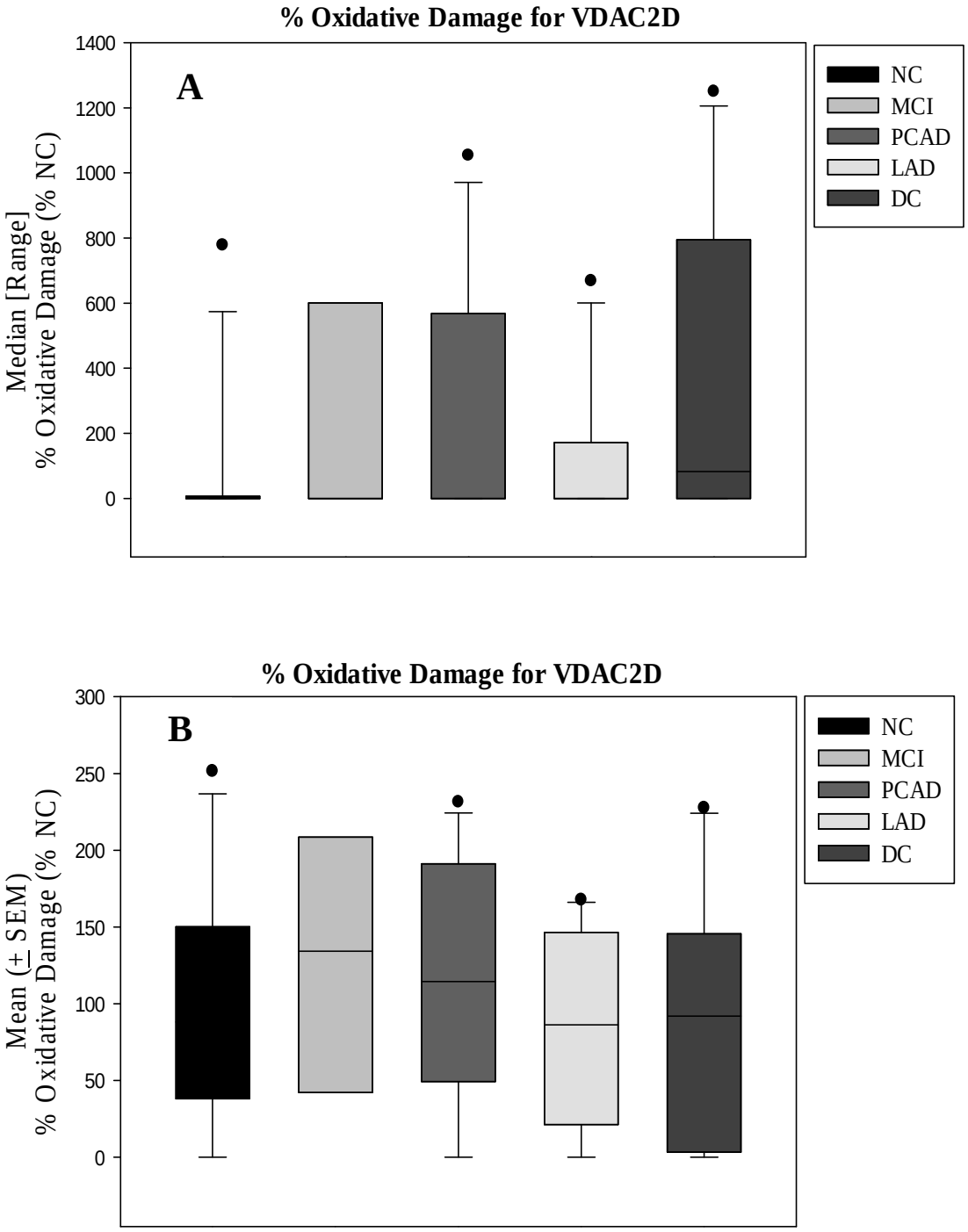

Figure 3.12. Oxidative damage in amplicons for VDAC2D in A) SMTG B) Cerebellum

(***** P < 0.05; ****** 0.05 < P < 0.1)

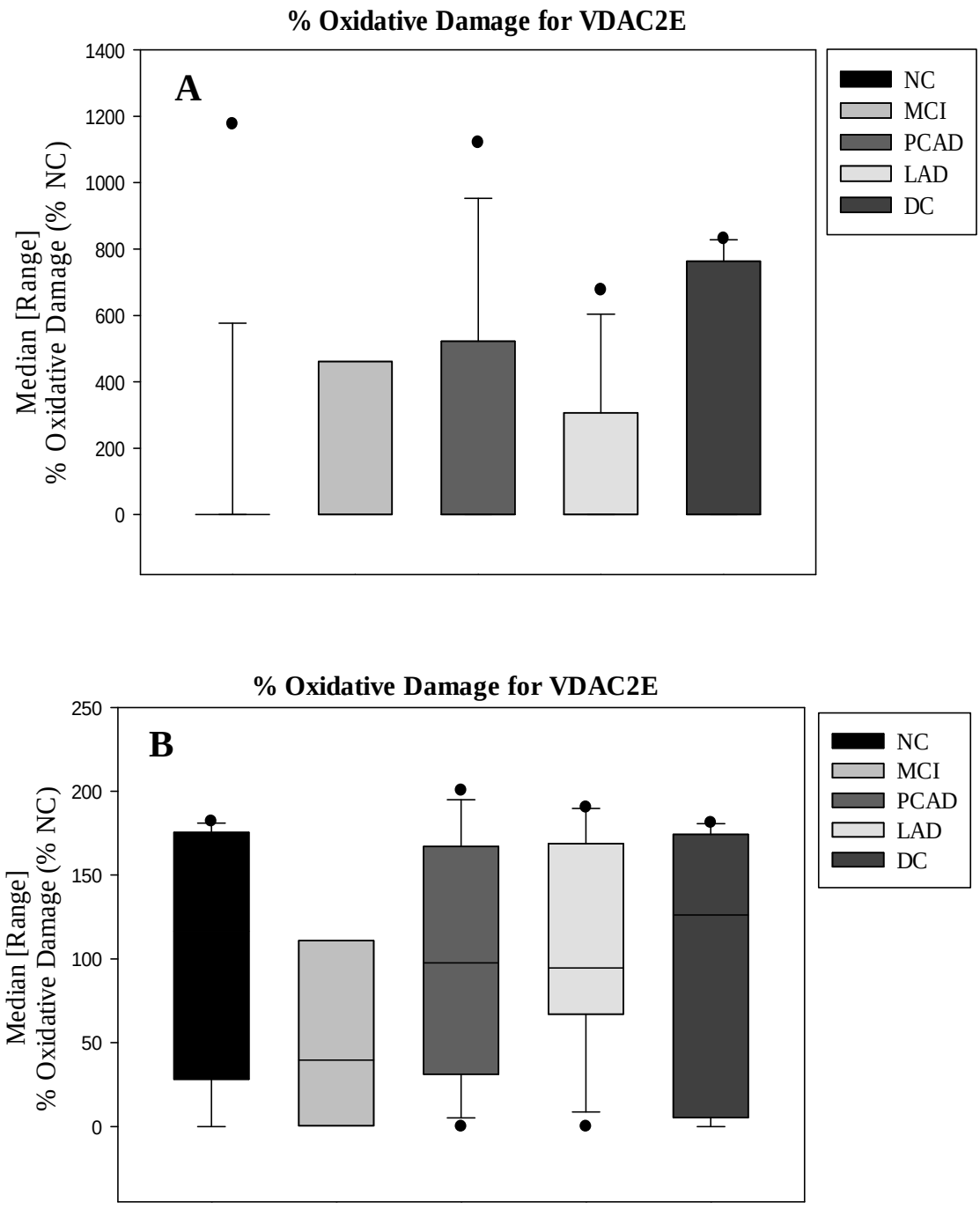

Figure 3.13. Oxidative damage in amplicons for VDAC2E in A) SMTG B) Cerebellum

(***** P < 0.05; ****** 0.05 < P < 0.1)

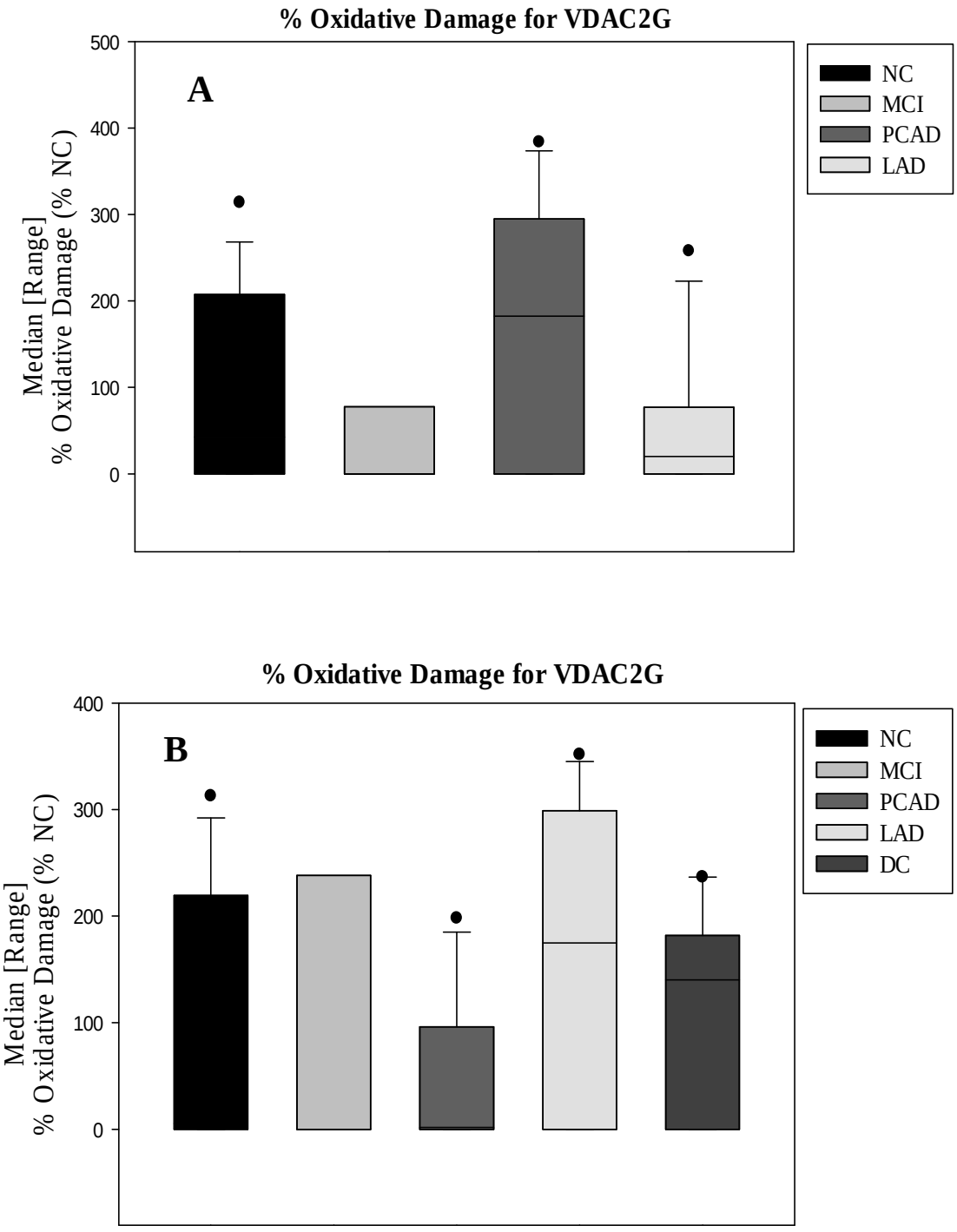

Figure 3.14. Oxidative damage in amplicons for VDAC2G in A) SMTG B) Cerebellum

(***** P < 0.05; ****** 0.05 < P < 0.1)

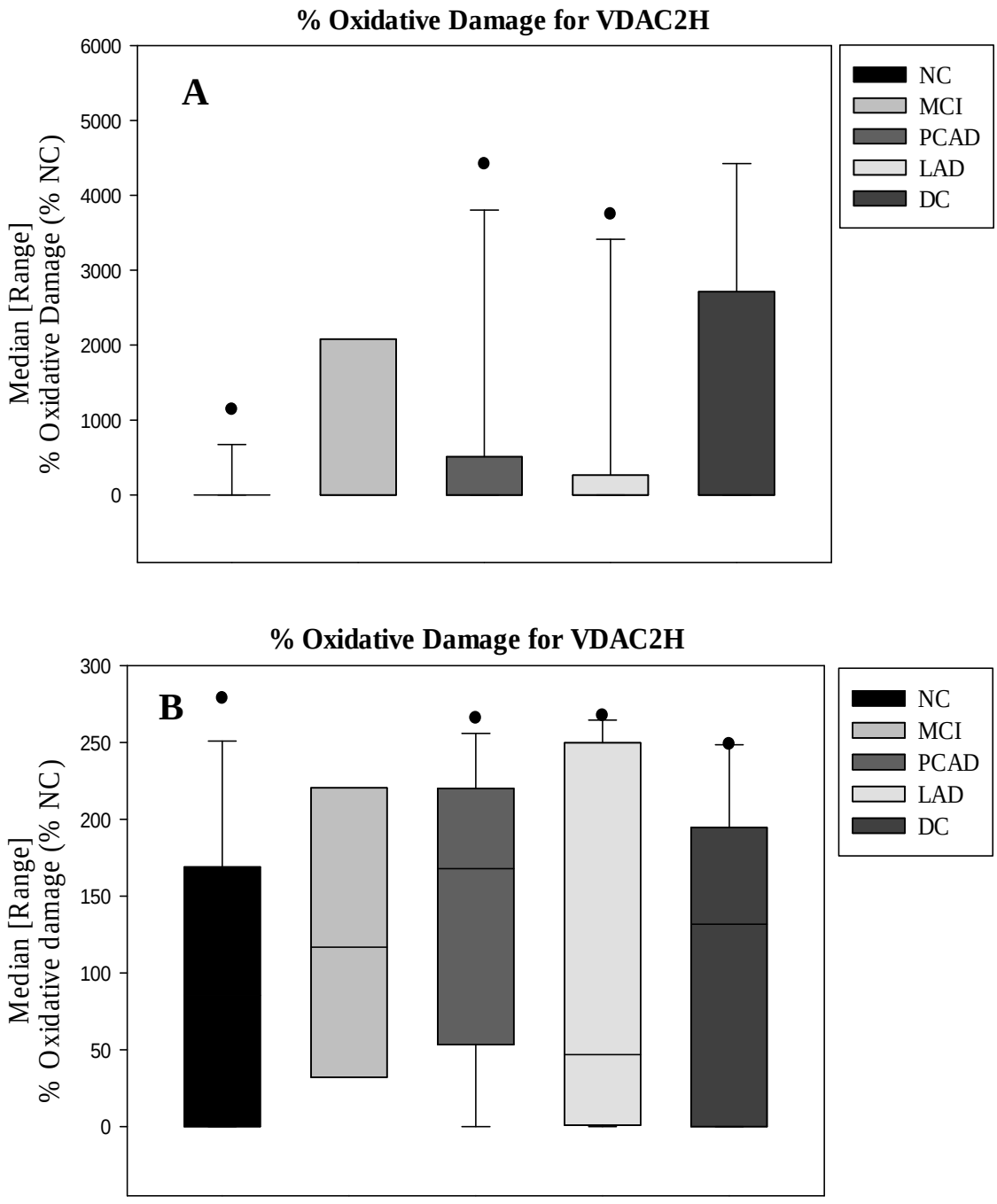

Figure 3.15. Oxidative damage in amplicons for VDAC2H in A) SMTG B) Cerebellum

(***** P < 0.05; ****** 0.05 < P < 0.1)

3.1.3. VDAC3

For quantification of oxidative damage to VDAC3, 5 primer sets encompassing the coding sequence were used in the study (Table 2.3.3). The results for oxidative damage observed for all the amplicons are described in detail in this section. In case of the VDAC3A amplicon (bp 248-447) melt curve analysis of qPCR reactions showed multiple curves and hence the data obtained for VDAC3A could not be used to determine % oxidative damage. For the VDAC3B amplicon (bp 367-651), no significant differences in % oxidative damage were observed in the SMTG of MCI (0 [0-258.07] %), PCAD (36.49 [0-301.24] %), LAD (9.7 [0-238.82] %) or DC (0 [0-291.6] %) subjects compared to NC subjects (59.85 [0-286.62] %) (Figure 3.16A). Similarly, median levels of % oxidative damage were not significantly altered in the cerebellum of MCI (0 [0-181.16] %), PCAD (71.48 [0-152.14] %), LAD (91.72 [0-209.81] %) or DC (49.33 [0-197.9] %) subjects compared to NC subjects (113.97 [0-201.24] %) in case of VDAC3B (Figure 3.16B).

In SMTG, there were no significant differences in median levels of % oxidative damage in MCI (84.24 [0-187.08] %), PCAD (20.59 [0-254.05] %), LAD (86.78 [0-213.66] %) or DC (63.34 [0-182.46] %) subjects compared to NC subjects (72.99 [0-308.28] %) (Figure 3.17A) for the VDAC3C amplicon (bp 540-735). In the cerebellum, median levels of % oxidative damage were not significantly changed in MCI (66.32 [0-399.31] %), PCAD (30.49 [0-287.94] %), LAD (82.21 [0-378.46] %) or DC (182.86 [0-327.51] %) subjects compared to NC subjects (34.43 [0-338.25] %) for VDAC3C (Figure 3.17B). For the VDAC3D amplicon (bp 627-865), % oxidative damage was not significantly altered in the SMTG of MCI (15.4 [0-130.09] %), PCAD (8.18 [0-183.27] %), LAD (131.5 [0-253.12] %) or DC (48.35 [0-181.7] %) subjects compared to NC

subjects (56.27 [0-291.79] %) (Figure 3.18A). No significant changes in median levels of % oxidative damage were observed in the cerebellum of MCI (91.4 [0-304.81] %), PCAD (111.01 [0-305.05] %), LAD (89.29 [0-238.13] %) or DC (19.65 [0-294.59] %) subjects compared to NC subjects (60.96 [0-298.08] %) for VDAC3D (Figure 3.18B). In contrast, there was a significant increase in median levels of % oxidative damage in LAD subjects (249.8 [0-413.33] %) compared to NC subjects (49.04 [0-288.34] %) in the SMTG for the VDAC3E amplicon (bp 718-932). There were no significant differences in % oxidative damage in the SMTG of MCI (121.48 [0-336.77] %), PCAD (228.88 [0-447.4] %) or DC (220.95 [0-414.53] %) subjects compared to NC subjects for VDAC3E (Figure 3.19A). Median levels of % oxidative damage were not significantly changed in the cerebellum of MCI (70.27 [0-353.98] %), PCAD (29.4 [0-321.21] %), LAD (5.15 [0-256.01] %) or DC (145.49 [31.65-288.02] %) subjects compared to NC subjects (83.92 [0-290.73] %) for VDAC3E (Figure 3.19B).

Table 3.4. Percent oxidative DNA damage for VDAC3 amplicons (Significant differences are shown in bold)

Amplicon	NC		MCI		PCAD		LAD		DC	
	SMTG	**CER**	**SMTG**	**CER**	**SMTG**	**CER**	**SMTG**	**CER**	**SMTG**	**CER**
VDAC3B	59.85 [0-286.62]	113.97 [0-201.24]	0 [0-258.07]	0 [0-181.16]	36.49 [0-301.24]	71.48 [0-152.14]	9.7 [0-238.82]	91.72 [0-209.81]	0 [0-291.6]	49.33 [0-197.9]
VDAC3C	72.99 [0-308.28]	34.43 [0-338.25]	84.24 [0-187.08]	66.32 [0-399.31]	20.59 [0-254.05]	30.49 [0-287.94]	86.78 [0-213.66]	82.21 [0-378.46]	63.34 [0-182.46]	182.86 [0-327.51]
VDAC3D	56.27 [0-291.79]	60.96 [0-298.08]	15.4 [0-130.09]	91.4 [0-304.81]	8.18 [0-183.27]	111.01 [0-305.05]	131.5 [0-253.12]	89.29 [0-238.13]	48.35 [0-181.7]	19.65 [0-294.59]
VDAC3E	49.04 [0-288.34]	83.92 [0-290.73]	121.48 [0-336.77]	70.27 [0-353.98]	228.88 [0-447.4]	29.4 [0-321.21]	***249.8 [0-413.33]**	5.15 [0-256.01]	220.95 [0-414.53]	145.49 [31.65-288.02]

*** P < 0.05**

**** 0.05 < P < 0.1**

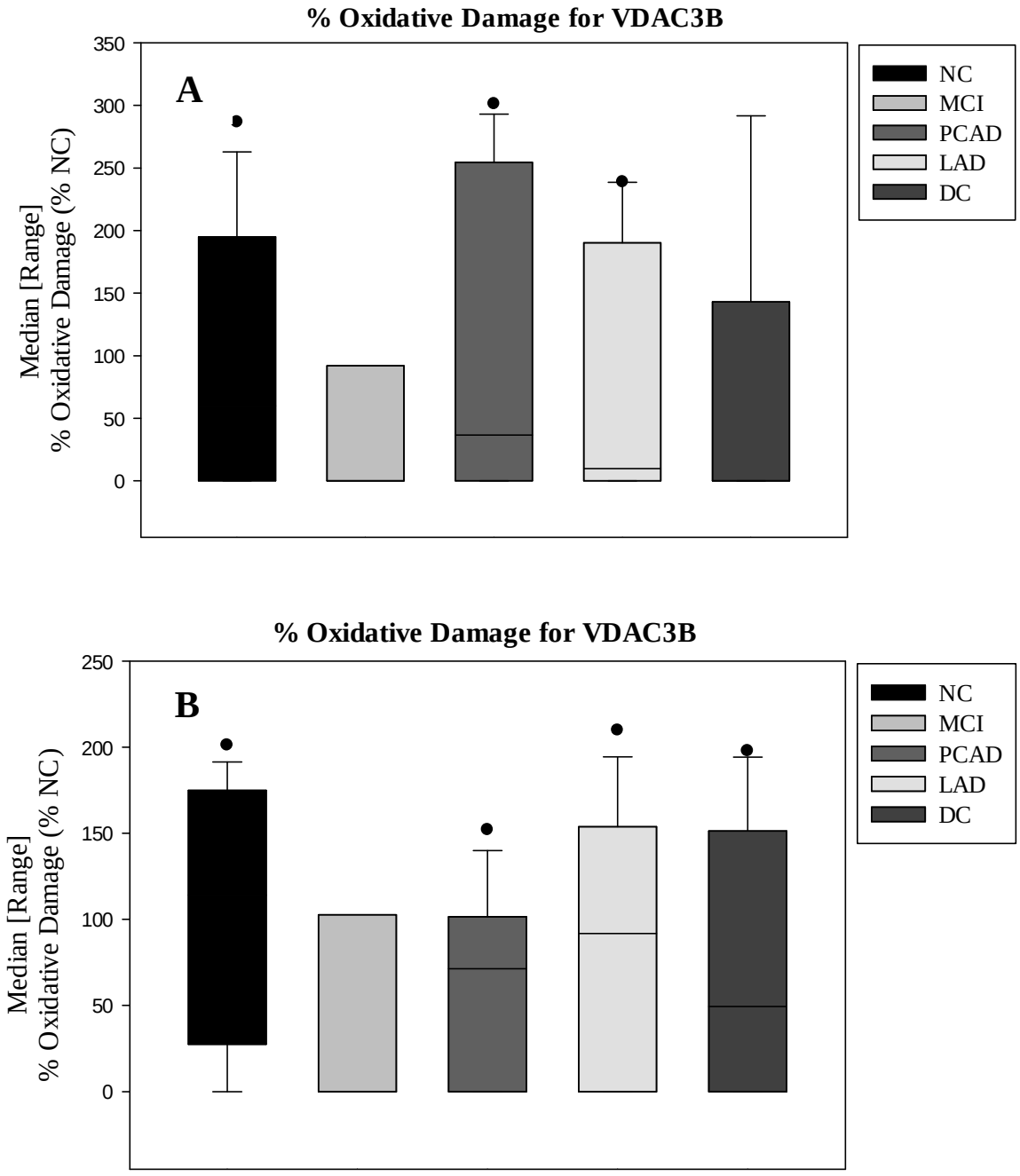

Figure 3.16. Oxidative damage in amplicons for VDAC3B in A) SMTG B) Cerebellum

(***** P < 0.05; ****** 0.05 < P < 0.1)

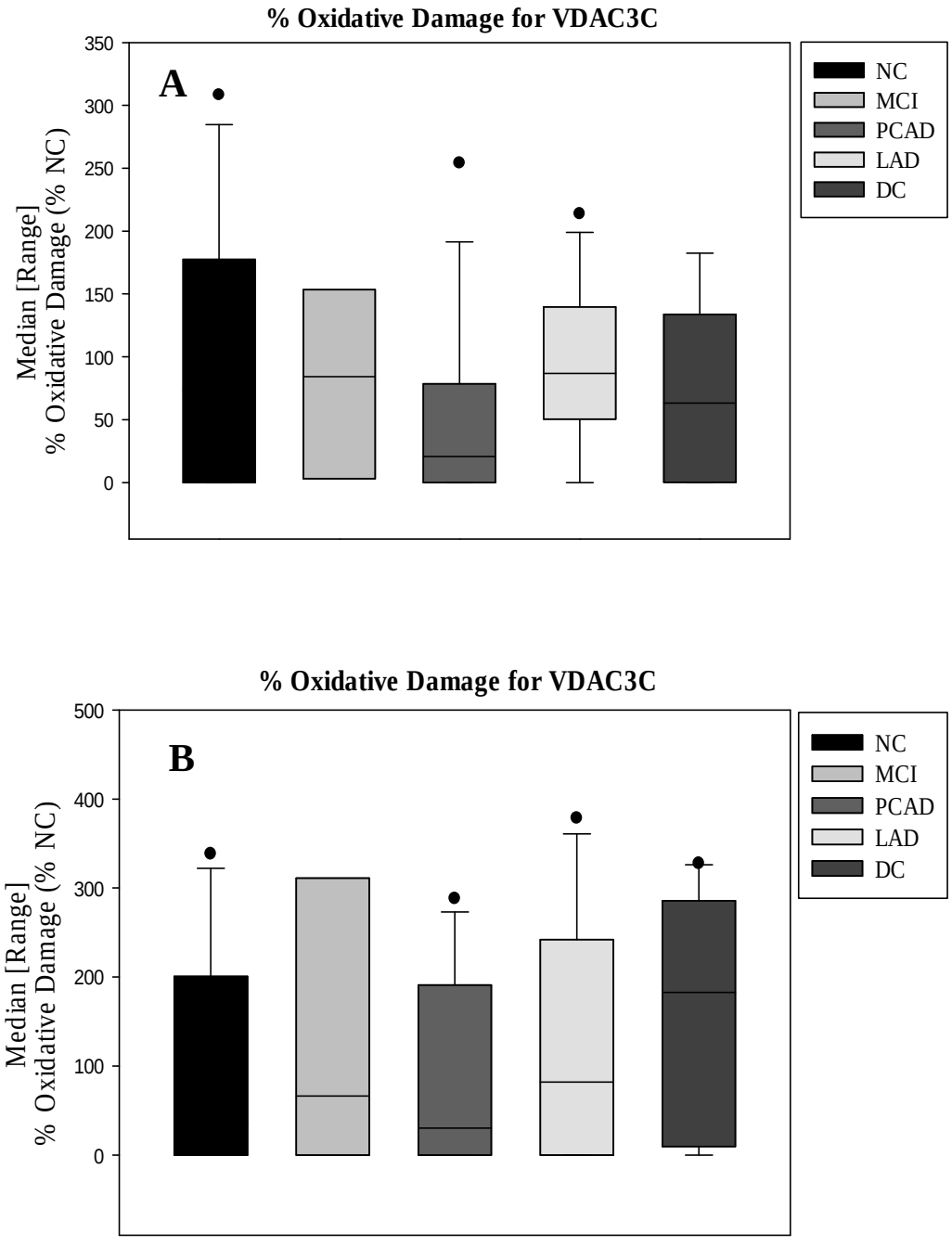

Figure 3.17. Oxidative damage in amplicons for VDAC3C in A) SMTG B) Cerebellum

(***** P < 0.05; ****** 0.05 < P < 0.1)

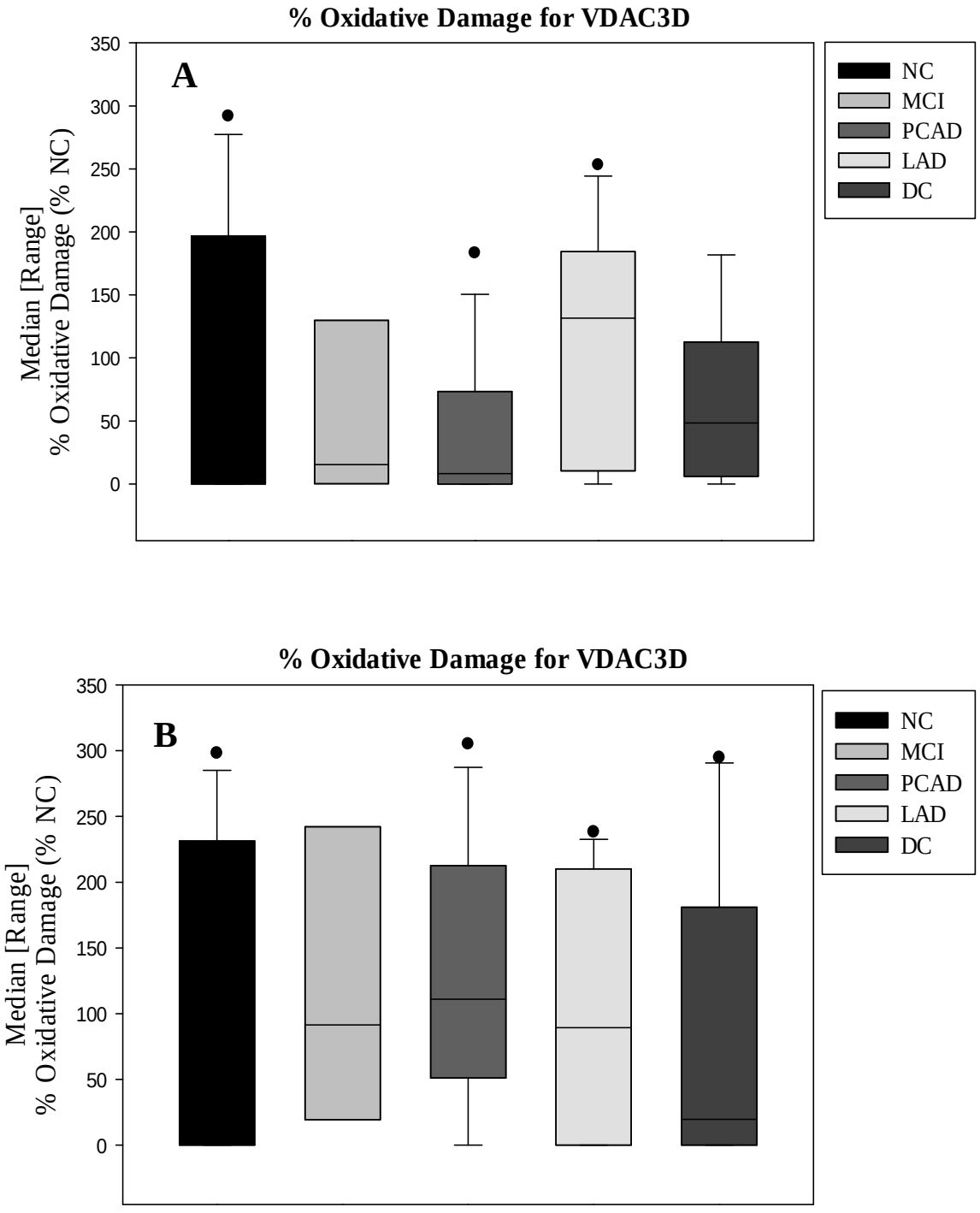

Figure 3.18. Oxidative damage in amplicons for VDAC3D in A) SMTG B) Cerebellum

(***** P < 0.05; ****** 0.05 < P < 0.1)

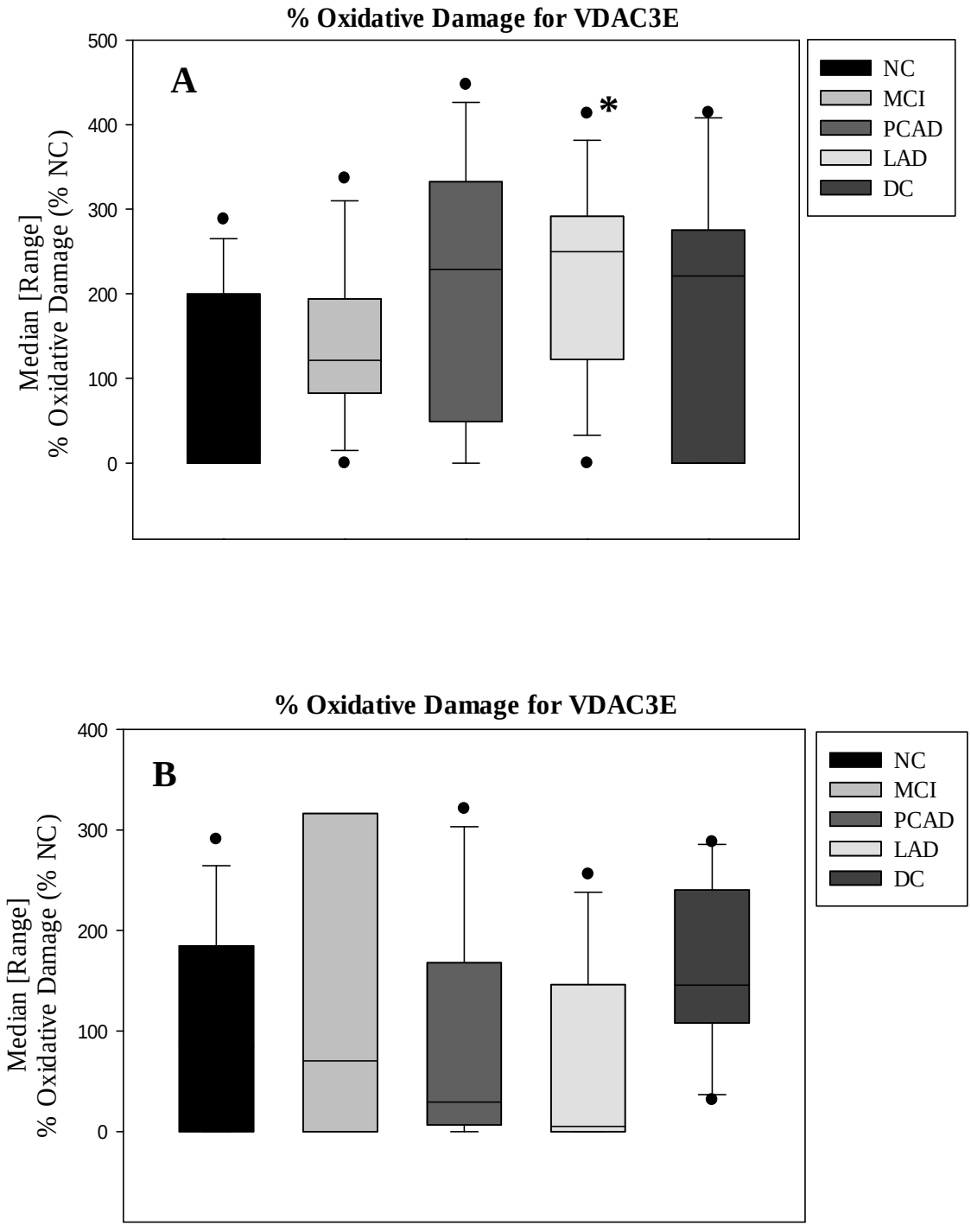

Figure 3.19. Oxidative damage in amplicons for VDAC3E in A) SMTG B) Cerebellum

(***** P < 0.05; ****** 0.05 < P < 0.1)

3.1.4. IGF2

A progressively increasing percentage of 8-oxoguanine was incorporated into IGF2 gene sequence via PCR. DNA obtained was first transcribed to RNA *in vitro* and the RNA was translated to protein *in vitro* using cell free systems. No product was obtained for the sample incorporated with 100% 8-oxoguanine. Protein samples from the cell free expression system were subjected to Western blot analysis and probed for IGF2 using a specific antibody and IGF2 enzyme activities were calculated to determine if the presence of oxidized guanines in DNA can lead to changes in protein levels or protein activity. The IGF2 enzyme activity was measured as the binding of radiolabeled IGF2 with IGF2 receptors present in human plasma. Samples with 0% 8-oxoguanine (100% guanine) were used as positive control (PC) for the reaction. Mean ± SEM IGF2 protein levels (% PC) and protein activity levels (% PC) are shown in Table 3.5. IGF2 protein levels were significantly increased for 10% (161.47 ± 7.59), 25% (149.32 ± 10.63), 35% (149.46 ± 9.25) and 50% (146.27 ± 10.19) 8-oxoguanine incorporated samples compared to PC samples (100 ± 12.07). There was a trend towards significance for IGF2 protein levels in samples with 75% 8-xoguanine (139.27 ± 16.32) compared to PC samples. For protein activity levels, significant decreases were seen in samples with 10% (23.89 ± 2.48), 35% (15.36 ± 4.54), 50% (56.95 ± 10.02) and 75% (35.6 ± 9.76) incorporation of 8-oxoguanine compared to PC samples (100 ± 4.65). No significant differences were observed for samples with 25% 8-oxoguanine incorporated samples (40.78 ± 26.27) compared to PC samples.

Table 3.5. Protein levels and Enzyme activity levels of 8-oxoguanine incorporated IGF2 [% PC] (Significant differences are shown in bold)

#	% Oxo guanine	IGF2 protein levels Mean ± SEM (% PC)	IGF2 activity Mean ± SEM (% PC)
1	0 (PC)	100 ± 12.07	100 ± 4.65
2	10	**161.47 ± 7.59***	**23.89 ± 2.48***
3	25	**149.32 ± 10.63***	40.78 ± 26.27
4	35	**149.46 ± 9.25***	**15.36 ± 4.54***
5	50	**146.27 ± 10.19***	**56.95 ± 10.02***
6	75	***139.27 ± 16.32****	**35.6 ± 9.76***

PC = Positive Control

***** $P < 0.05$

****** $0.05 < P < 0.1$

3.2. Changes in DNA Repair Enzymes of BER Pathway in AD Subjects

Changes in DNA repair enzymes involved in multiple pathways including OGG1, UNG, APE1, POLB, FEN1, PARP1, XRCC1, EXO1, RAD50, XPA, MRE11A and ATM were determined in the SMTG (a vulnerable brain region) and cerebellum (a non-vulnerable brain region) of fifteen age-matched NC, six MCI, thirteen PCAD, fourteen LAD and twelve DC subjects. Subject demographic data are shown in Table 2.1. There were no significant differences in PMI between MCI/PCAD/LAD/DC subjects compared to age-matched NC subjects. No significant differences were observed in age of MCI (91.0 ± 2.2 years), PCAD (85.7 ± 1.8 years) or LAD (81.4 ± 1.4 years) subjects compared to age-matched NC subjects (86.3 ± 1.4 years) athough DC (68.9 ± 4.8 years) subjects were significantly younger than NC subjects. Braak staging scores are reported as median values and were significantly higher ($P < 0.05$) for MCI (III), PCAD (IV) LAD (VI) and DC subjects (II) compared to age-matched NC subjects (I). The data for this study were tested for normality using the Wilks-Shapiro test. Non-normally distributed is reported as Median [Range] and normally distributed data is described as mean (± SEM). The results for this study are summarized in Table 3.9.

3.2.1. Gene Expression

Gene expression of 12 genes involved in multiple DNA repair pathways including OGG1, UNG, APE1, POLB, FEN1, PARP1, XRCC1, EXO1, RAD50, XPA, MRE11A and ATM was analyzed using the DNA repair pathway RT^2 custom PCR array (SABiosciences) (Table 2.4) and quantitative reverse transcription PCR in the SMTG and the cerebellum from PCAD, MCI, LAD, DC and age-matched NC subjects. The housekeeping genes, β-actin and glyceraldehyde 3-phosphate dehydrogenase (GAPDH)

were used for normalization. Results are expressed in terms of fold change in gene expression in MCI/PCAD/LAD/DC subjects compared to age-matched NC subjects. Fold change is defined as the ratio of $2^{-\Delta Ct}$ values for samples from varied disease stages (MCI, PCAD, LAD) to the average $2^{-\Delta Ct}$ value of NC samples. Positive and negative controls were run on each plate to verify genomic integrity and PCR efficiency. The data were found to be non-normally distributed as determined by the Wilks-Shapiro test for normality. Table 3.6 shows the fold change values obtained for expression of specific genes in specimens of SMTG and cerebellum as median [range] for NC, MCI, PCAD, LAD and DC subjects.

A statistically significant increase ($P < 0.05$) was observed in fold change for OGG1 in SMTG of PCAD (1.6 [1.34-4.14]) and LAD (2.06 [0.79-3.85]) subjects compared to NC subjects (1.21 [0.19-1.49]) whereas SMTG samples from MCI (1.33 [0.55-1.55]) and DC (1.14 [0.13-3.17]) subjects showed no significant changes in OGG1 gene expression compared to NC subjects. OGG1 gene expression levels in cerebellum showed no significant differences in MCI (1.11 [0.7-1.56]), PCAD (1.12 [0.75-1.96]), LAD (1.12 [0.67-3.68]) or DC (1.28 [0.55-2.09]) subjects compared to NC subjects (0.98 [0.27-2.15]). Levels of UNG expression were significantly increased in the SMTG of PCAD (1.72 [0.56-5.4]), LAD (1.59 [0.29-4.09]) and DC (2.48 [0.59-7.76]) subjects but showed no change in SMTG of MCI subjects (1.29 [0.85-4.65]) compared to NC subjects (0.89 [0.45-1.79]). UNG gene expression levels in cerebellum were not significantly changed for any of the subject groups studied including MCI (0.96 [0.41-2.25]), PCAD (1.07 [0.49-2.2]), LAD (0.99 [0.43-4.89]) and DC (1.05 [0.5-2.6]) subjects compared to NC subjects (0.99 [0.35-1.87]).

No significant differences in the median levels of fold change in gene expression of APE1 were observed in the SMTG of MCI (0.91 [0.46-3.4]), PCAD (0.97 [0.4-1.63])), LAD (1.19 [0.66-2.71]) and DC (0.73 [0.02-1.7]) subjects compared to NC subjects (1.02 [0.14-1.4]). In cerebellum, median fold change in APE1 expression levels were comparable for all the disease states studied including MCI (1.02 [0.47-1.12]), PCAD (0.85 [0.48-2.12]), LAD (1.07 [0.76-2.06]) and DC (1.14 [0.76-1.89]) subjects compared to NC subjects (0.95 [0.66-1.9]). Fold change in POLB expression levels were not significantly different in SMTG of MCI (1.23 [0.92-2.46]) and DC (1.02 [0.1-2.25]) subjects but showed a statistically significant increase in PCAD (1.35 [1.05-2.22]) and LAD (1.32 [0.84-3.27]) subjects compared to NC subjects (1.04 [0.38-1.34]). Comparison of fold change in POLB expression levels across the disease spectrum in the cerebellum showed no significant changes in MCI (1.3 [0.64-3.3]), PCAD (1.28 [0.24-3.51]) and LAD (1.2 [0.4-4.81]) compared to NC subjects (1.15 [0.1-1.3]). In contrast, there was a significant increase in fold change of POLB expression in the cerebellum of DC (1.73 [0.47-3.14]) subjects compared to NC subjects.

In the SMTG, there were no significant changes in median levels of fold change in FEN1 expression levels in MCI (0.89 [0.38-1.39]), PCAD (1.05 [0.32-3.53]), LAD (1.1 [0.21-2.51]) or DC (1.24 [0.11-2.18]) subjects compared to NC subjects (0.86 [0.41-2.44]). Median levels of fold change in FEN1 expression levels were also significantly unchanged in the cerebellum of MCI (0.98 [0.75-1.45]), PCAD (1.17 [0.69-1.84]), LAD (1.29 [0.74-3.14]) and DC (1.33 [0.49-2.27]) subjects compared to NC subjects (1.04 [0.49-1.32]). For PARP1 expression, there were no significant differences in the SMTG of MCI (0.94 [0.68-1.26]), PCAD (0.99 [0.29-2.01]) or DC (0.98 [0.02-2.82]) subjects

although there was a significant increase in fold change in LAD subjects (1.54 [0.67-3.05]) compared to NC subjects (0.83 [0.41-2.44]). No significant differences in fold change in PARP1 expression levels were observed in the cerebellum of MCI (1.0 [0.64-1.55]), PCAD (1.32 [0.35-5.11]), LAD (1.02 [0.53-4.15]) and DC (1.1 [0.5-2.86]) subjects compared to NC subjects (0.73 [0.47-3.27]).

In SMTG, median fold change in XRCC1 expression levels were comparable throughout the progression of AD including MCI (1.05 [0.75-2.09]), PCAD (1.12 [0.47-7.08]) and LAD (1.41 [0.57-4.05]) subjects and also in DC (1.25 [0.61-6.19]) subjects compared to NC subjects (0.92 [0.35-1.59]). There was no significant difference observed in fold change in XRCC1 expression in the cerebellum of MCI (0.87 [0.51-1.31]), PCAD (1.13 [0.53-1.76]), LAD (0.86 [0.7-8.39]) and DC (0.89 [0.51-2.0]) subjects compared to NC subjects (0.8 [0.32-3.15]). No significant changes in the median levels of fold change in EXO1 expression levels were observed in the SMTG of MCI (0.44 [0.11-2.19]), PCAD (0.33 [0.11-1.97]), LAD (0.55 [0.22-2.41]) and DC (0.66 [0.22-12.69]) subjects compared to NC subjects (0.44 [0.11-7.0]). In the cerebellum, median levels of fold change in EXO1 expression levels were not significantly different in MCI (0.61 [0.4-1.13]), PCAD (0.48 [0.16-4.44]), LAD (0.36 [0.16-13.39]) and DC (0.48 [0.08-18.55]) subjects compared to NC subjects (0.32 [0.16-7.1]).

Fold change in RAD50 expression levels were not significantly different in SMTG of MCI (0.9 [0.41-1.69]), PCAD (0.9 [0.23-2.82]) or DC (0.79 [0.11-4.36]) subjects but showed a statistically significant increase in LAD subjects (1.35 [0.3-3.61]) compared to NC subjects (0.83 [0.08-3.68]). In contrast, no significant differences in fold change in RAD50 expression levels were observed in the cerebellum of MCI (1.0 [0.78-1.71]),

PCAD (0.78 [0.15-2.55]), LAD (1.08 [0.24-4.97]) or DC (0.93 [0.36-5.33]) subjects compared to NC subjects (0.82 [0.42-2.73]). In SMTG, median fold change in XPA expression levels were comparable throughout the progression of AD including MCI (0.99 [0.47-1.71]), PCAD (0.82 [0.6-9.6]) and LAD (1.04 [0.46-2.87]) and also in DC (1.06 [0.58-3.29]) subjects compared to NC subjects (0.82 [0.35-2.62]). Median levels of fold change in XPA expression levels were not significantly altered in the cerebellum of MCI (1.0 [0.15-1.92]), PCAD (1.15 [0.58-3.28]), LAD (1.07 [0.47-6.12]) and DC (0.9 [0.48-1.96]) subjects compared to NC subjects (0.88 [0.35-2.33]).

No significant changes in median levels of fold change in MRE11A were observed in the SMTG of MCI (1.27 [0.32-2.81]), PCAD (0.77 [0.27-2.81]), LAD (0.93 [0.45-5.12]) or DC (1.09 [0.13-5.25]) subjects compared to NC subjects (0.91 [0.27-2.94]). In the cerebellum, median levels of fold change in MRE11A expression levels were not significantly changed in MCI (1.36 [0.82-2.23]), PCAD (1.38 [0.5-2.3]), LAD (1.2 [0.11-3.57]) or DC (1.59 [0.22-6.07]) subjects compared to NC subjects (0.88 [0.3-1.94]). In case of the fold change in ATM expression levels, there were no significant differences in the SMTG of MCI (0.71 [0.46-2.13]), PCAD (0.72 [0.16-2.64]), LAD (1.13 [0.44-4.81]) and DC (0.63 [0.09-3.77]) subjects compared to NC subjects (0.79 [0.14-2.61]). There were no significant differences observed in fold change in ATM expression levels in the cerebellum of MCI (1.08 [0.83-1.91]), PCAD (1.11 [0.53-5.27]), LAD (1.27 [0.52-10.24]) or DC (1.12 [0.44-2.74]) subjects compared to NC subjects (1.0 [0.21-1.93]).

Table 3.6. Fold change in expression of DNA repair genes as determined by DNA Damage Repair PCR Custom PCR array (Bold numbers indicate significant difference)

Gene	NC Median (Range)		MCI Median (Range)		PCAD Median (Range)		LAD Median (Range)		DC Median (Range)	
	SMTG	**Cer**	**SMTG**	**Cer**	**SMTG**	**Cer**	**SMTG**	**Cer**	**SMTG**	**Cer**
OGG1	1.21 [0.19-1.49]	0.98 [0.27-2.15]	1.33 [.55-1.55]	1.11 [0.7-1.56]	***1.6 [1.34-4.14]**	1.12 [0.75-1.96]	***2.06 [0.79-3.85]**	1.12 [0.67-3.68]	1.14 [0.13-3.17]	1.28 [0.55-2.09]
UNG	0.89 [0.45-1.79]	0.99 [0.35-1.87]	1.29 [0.85-4.65]	0.96 [0.41-2.25]	***1.72 [0.56-5.4]**	1.07 [0.49-2.2]	***1.59 [0.29-4.09]**	0.99 [0.43-4.89]	***2.48 [0.59-7.76]**	1.05 [0.5-2.6]
APE1	1.02 [0.14-1.4]	0.95 [0.66-1.9]	0.91 [0.46-3.4]	1.02 [0.47-1.12]	0.97 [0.4-1.63]	0.85 [0.48-2.12]	1.19 [0.66-2.71]	1.07 [0.76-2.06]	0.73 [0.02-1.7]	1.14 [0.76-1.89]
POLB	1.04 [0.38-1.34]	1.15 [0.1-1.3]	1.23 [0.92-2.46]	1.3 [0.64-3.3]	***1.35 [1.05-2.22]**	1.28 [0.24-3.51]	***1.32 [0.84-3.27]**	1.2 [0.4-4.81]	1.02 [0.1-2.25]	***1.73 [0.47-3.14]**
FEN1	0.86 [0.41-2.44]	1.04 [0.49-1.32]	0.89 [0.38-1.39]	0.98 [0.75-1.45]	1.05 [0.32-3.53]	1.17 [0.69-1.84]	1.1 [0.21-2.51]	1.29 [0.74-3.14]	1.24 [0.11-2.18]	1.33 [0.49-2.27]
PARP1	0.83 [0.17-3.03]	0.73 [0.47-3.27]	0.94 [0.68-1.26]	1.0 [0.64-1.55]	0.99 [0.29-2.01]	1.32 [0.35-5.11]	***1.54 [0.67-3.05]**	1.02 [0.53-4.15]	0.98 [0.02-2.82]	1.1 [0.5-2.86]
XRCC1	0.92 [0.35-1.59]	0.8 [0.32-3.15]	1.05 [0.75-2.09]	0.87 [0.51-1.31]	1.12 [0.47-7.08]	1.13 [0.53-1.76]	1.41 [0.57-4.05]	0.86 [0.7-8.39]	1.25 [0.61-6.19]	0.89 [0.51-2.0]

Table 3.6. Contd. Fold change in expression of DNA repair genes as determined by DNA Damage Repair PCR Custom PCR array (Bold numbers indicate significant difference)

Gene	**NC Median (Range)**		**MCI Median (Range)**		**PCAD Median (Range)**		**LAD Median (Range)**		**DC Median (Range)**	
	SMTG	**Cer**	**SMTG**	**Cer**	**SMTG**	**Cer**	**SMTG**	**Cer**	**SMTG**	**Cer**
EXO1	0.44 [0.11-7.0]	0.32 [0.16-7.1]	0.44 [0.11-2.19]	0.61 [0.4-1.13]	0.33 [0.11-1.97]	0.48 [0.16-4.44]	0.55 [0.22-2.41]	0.36 [0.16-13.39]	0.66 [0.22-12.69]	0.48 [0.08-18.55]
RAD50	0.83 [0.08-3.68]	0.82 [0.42-2.73]	0.9 [0.41-1.69]	1.0 [0.78-1.71]	0.9 [0.23-2.82]	0.78 [0.15-2.55]	***1.35 [0.3-3.61]**	1.08 [0.24-4.97]	0.79 [0.11-4.36]	0.93 [0.36-5.33]
XPA	0.82 [0.35-2.62]	0.88 [0.35-2.33]	0.99 [0.47-1.71]	1.0 [0.15-1.92]	0.82 [0.6-9.6]	1.15 [0.58-3.28]	1.04 [0.46-2.87]	1.07 [0.47-6.12]	1.06 [0.58-3.29]	0.9 [0.48-1.96]
MRE11A	0.91 [0.27-2.94]	0.88 [0.3-1.94]	1.27 [0.32-2.81]	1.36 [0.82-2.23]	0.77 [0.27-2.81]	1.38 [0.5-2.3]	0.93 [0.45-5.12]	1.2 [0.11-3.57]	1.09 [0.13-5.25]	1.59 [0.22-6.07]
ATM	0.79 [0.14-2.61]	1.0 [0.21-1.93]	0.71 [0.46-2.13]	1.08 [0.83-1.91]	0.72 [0.16-2.64]	1.11 [0.53-5.27]	1.13 [0.44-4.81]	1.27 [0.52-10.24]	0.63 [0.09-3.77]	1.12 [0.44-2.74]

*** P < 0.05**

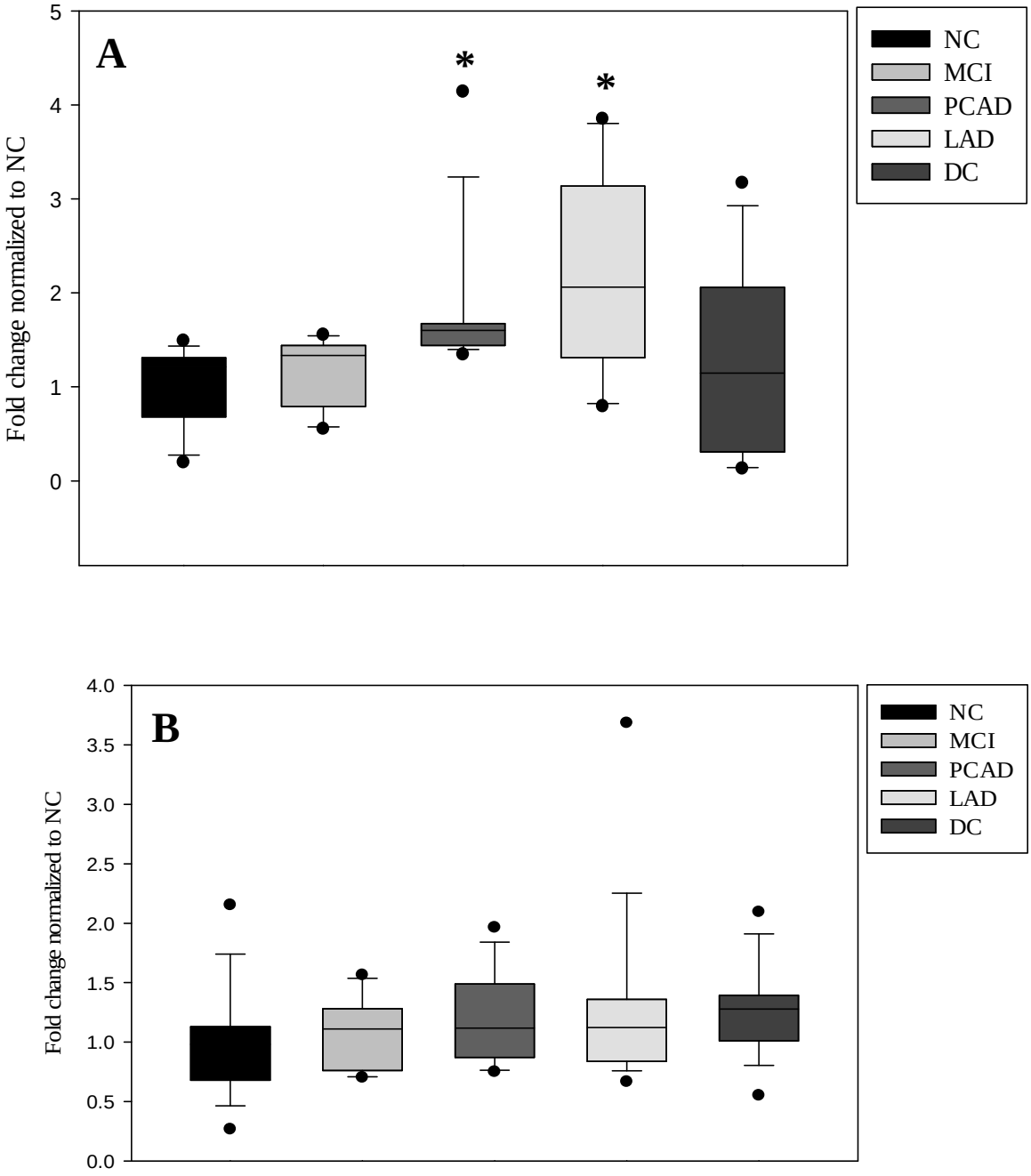

Figure 3.20. Fold change in gene expression for OGG1 in A) SMTG B) Cerebellum

(* $P < 0.05$)

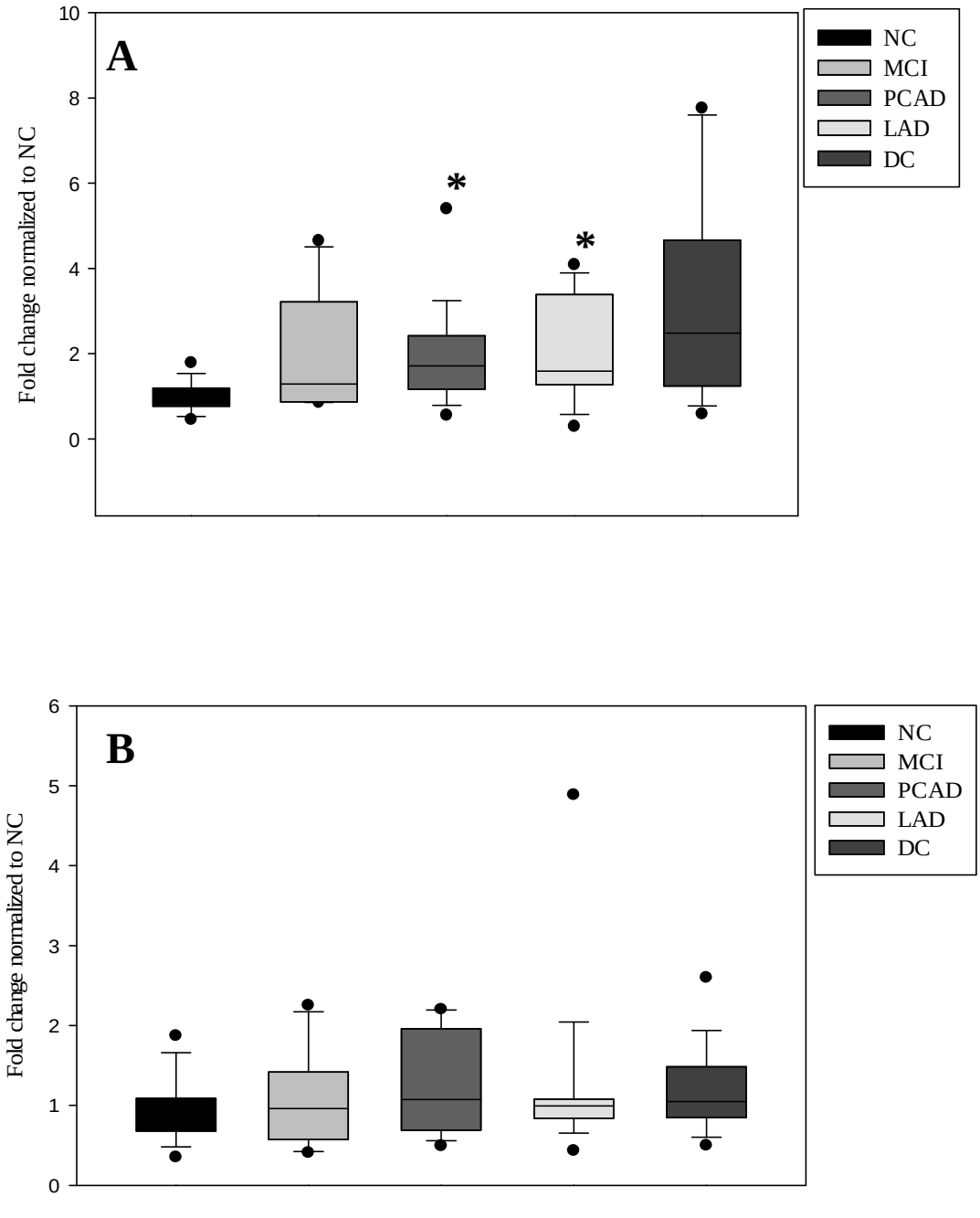

Figure 3.21. Fold change in gene expression for UNG in A) SMTG B) Cerebellum

(* $P < 0.05$)

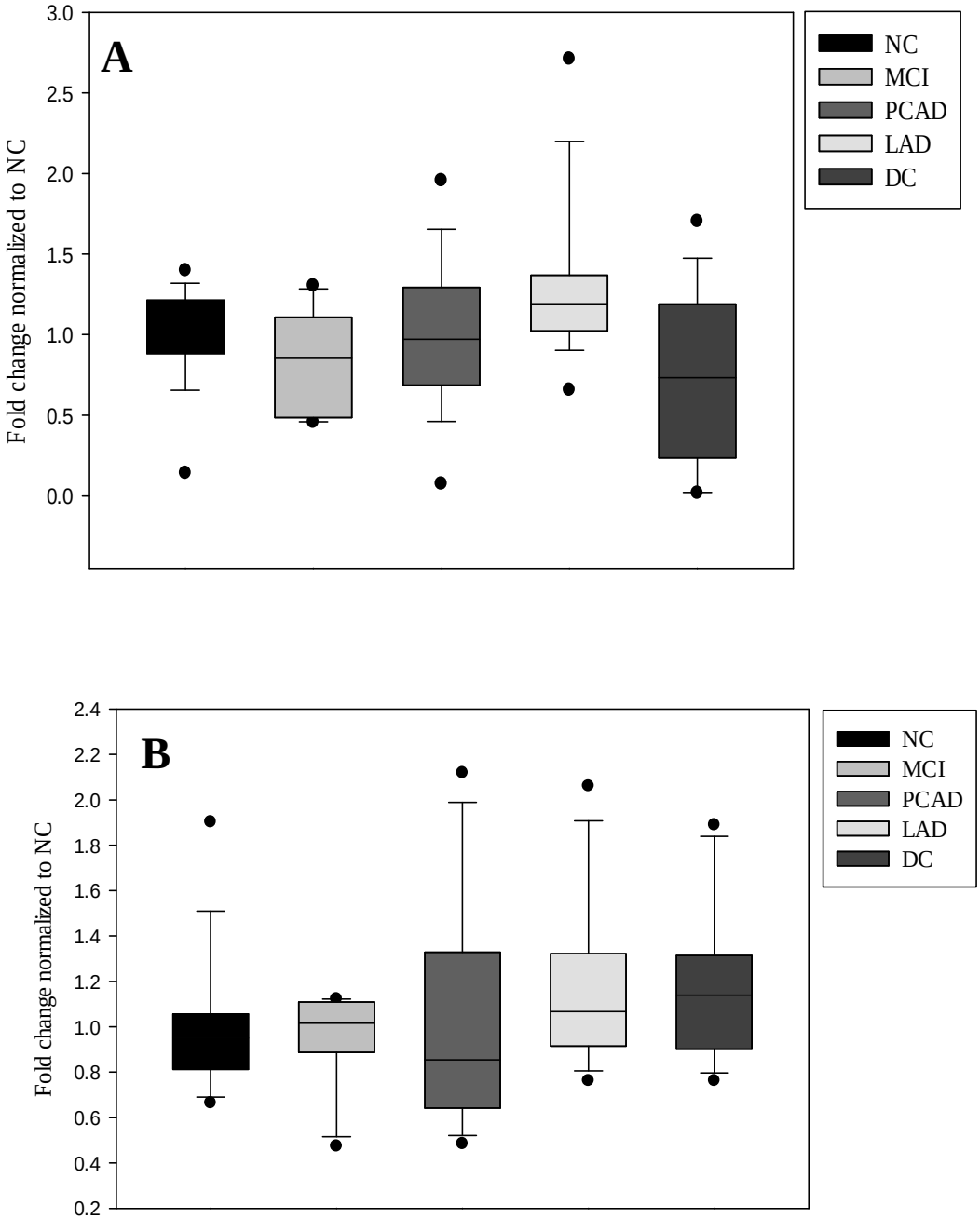

Figure 3.22. Fold change in gene expression (SMTG) for APE1 in A) SMTG B) Cerebellum

(***** P < 0.05)

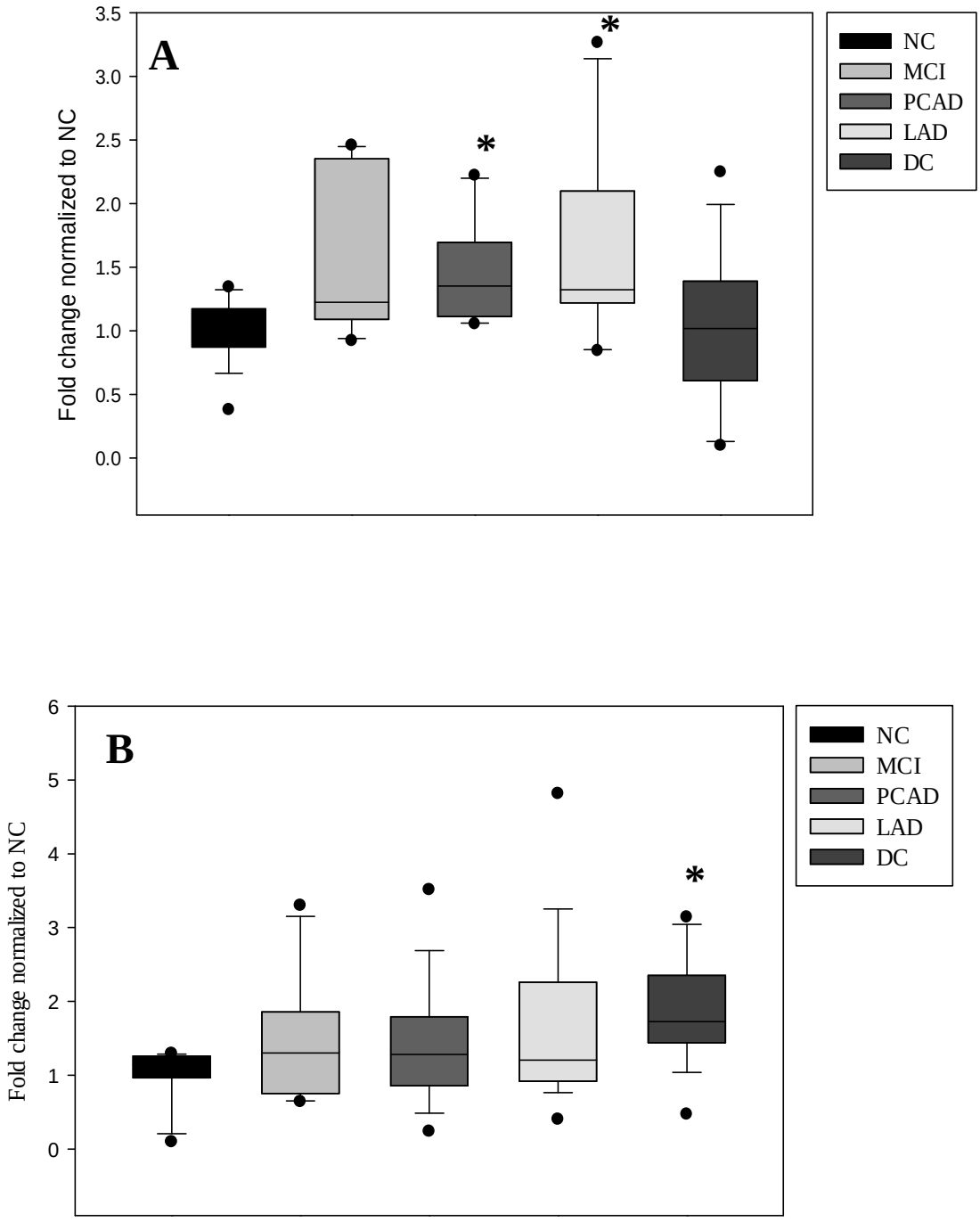

Figure 3.23. Fold change in gene expression for POLB in A) SMTG B) Cerebellum

(* P < 0.05)

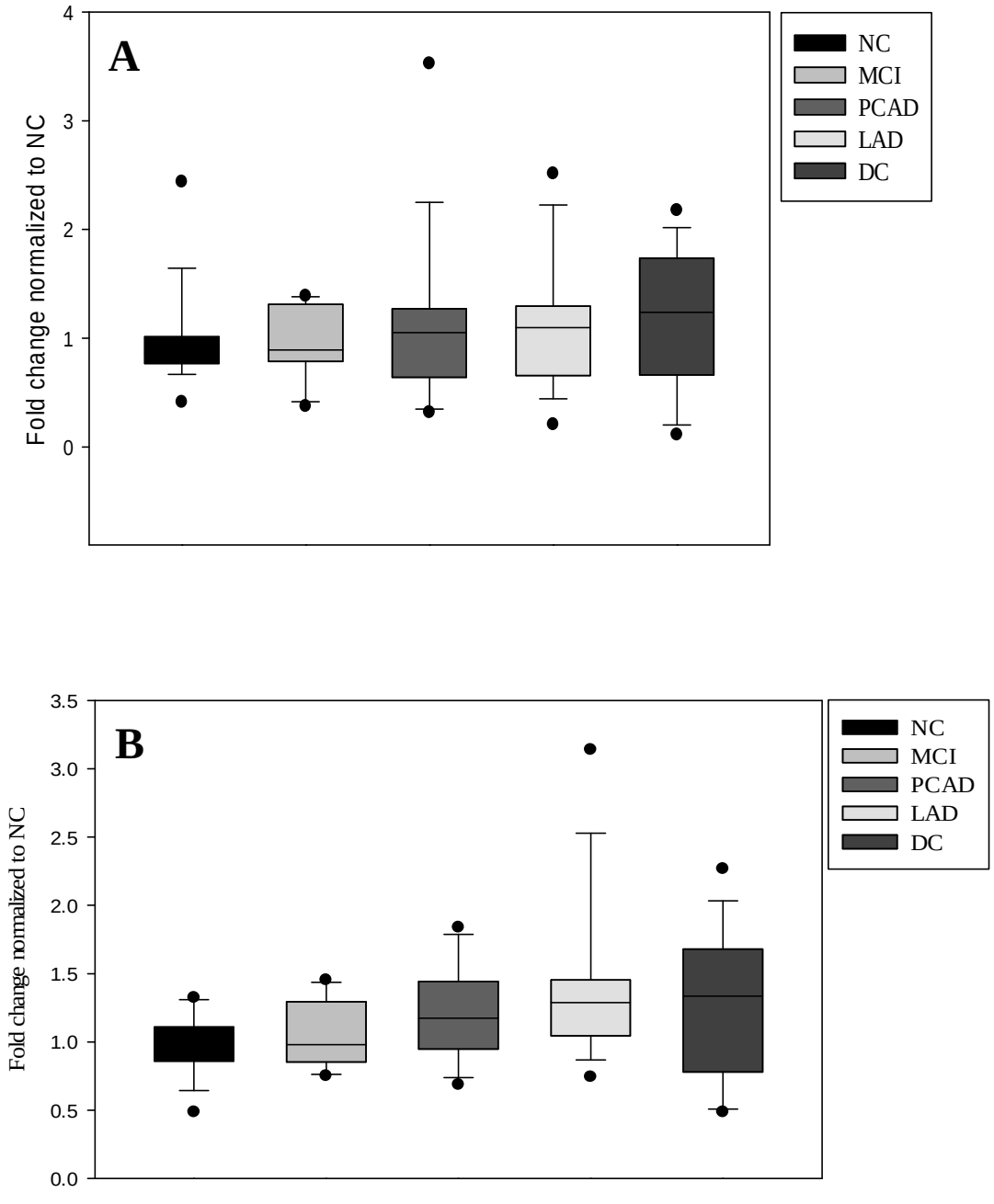

Figure 3.24. Fold change in gene expression for FEN1 in A) SMTG B) Cerebellum

(***** P < 0.05)

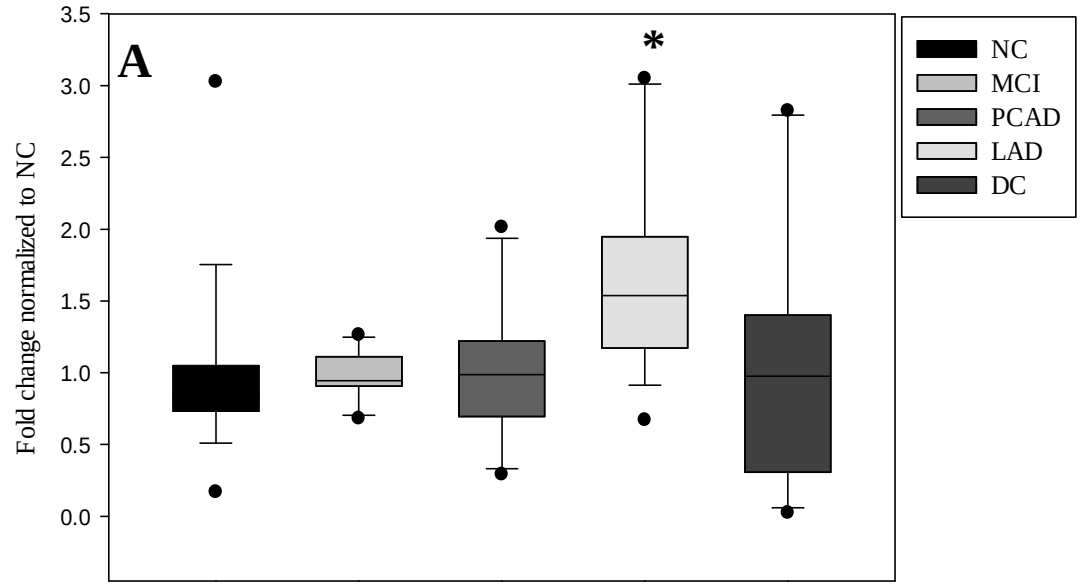

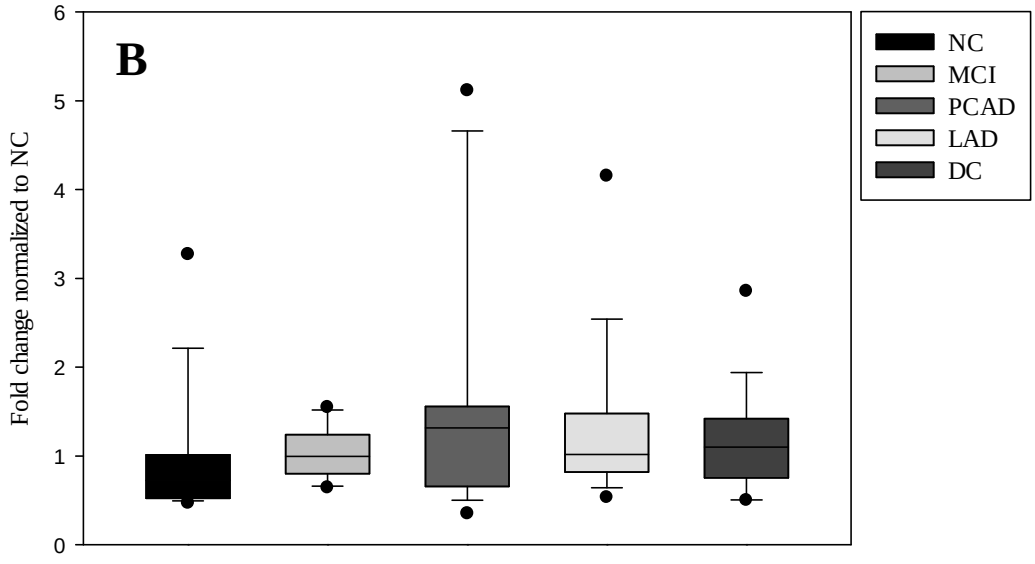

Figure 3.25. Fold change in gene expression for PARP1 in A) SMTG B) Cerebellum

(* $P < 0.05$)

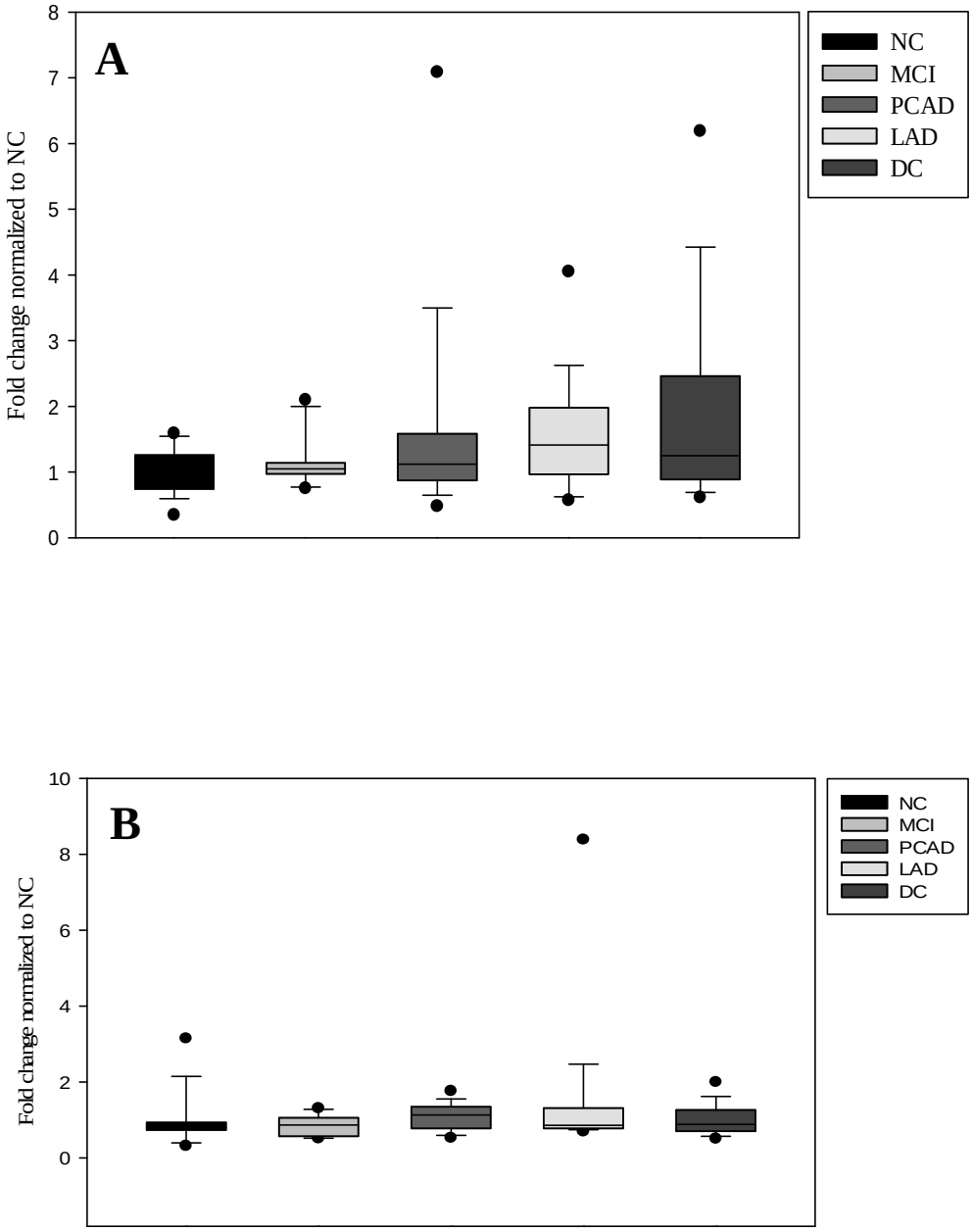

Figure 3.26. Fold change in gene expression for XRCC1 in A) SMTG B) Cerebellum

(***** $P < 0.05$)

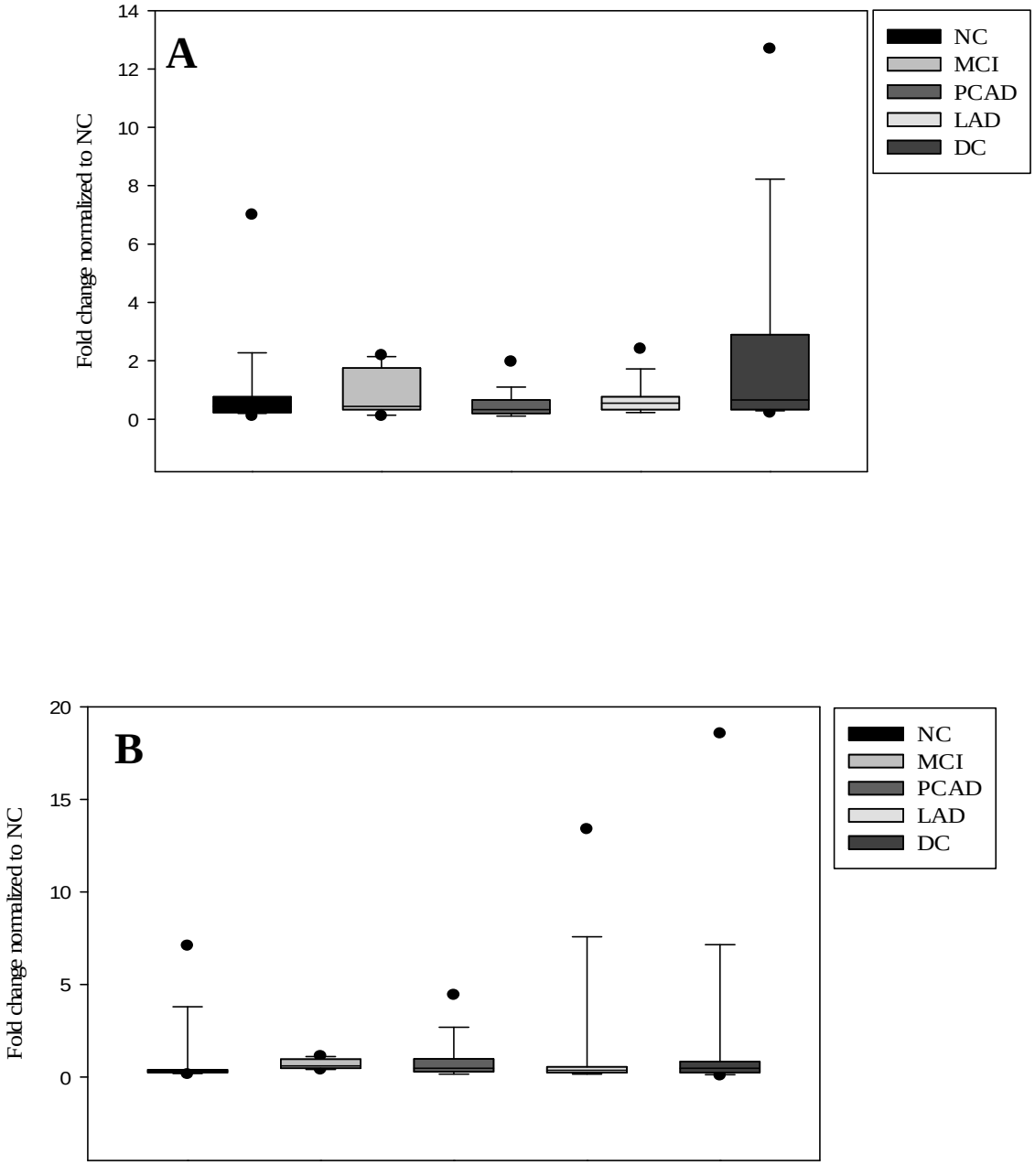

Figure 3.27. Fold change in gene expression for EXO1 in A) SMTG B) Cerebellum

(***** P < 0.05)

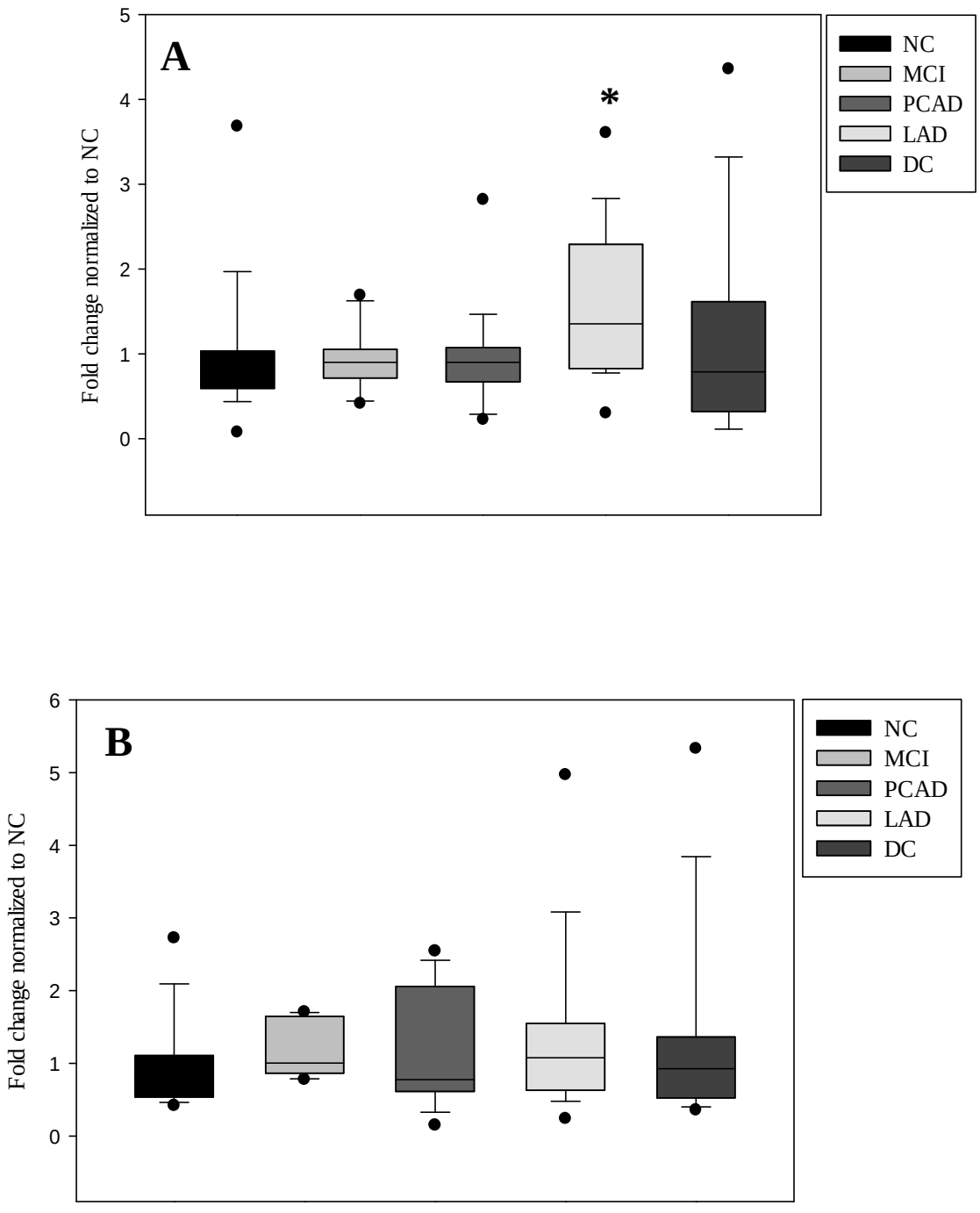

Figure 3.28. Fold change in gene expression for RAD50 in A) SMTG B) Cerebellum (* $P < 0.05$)

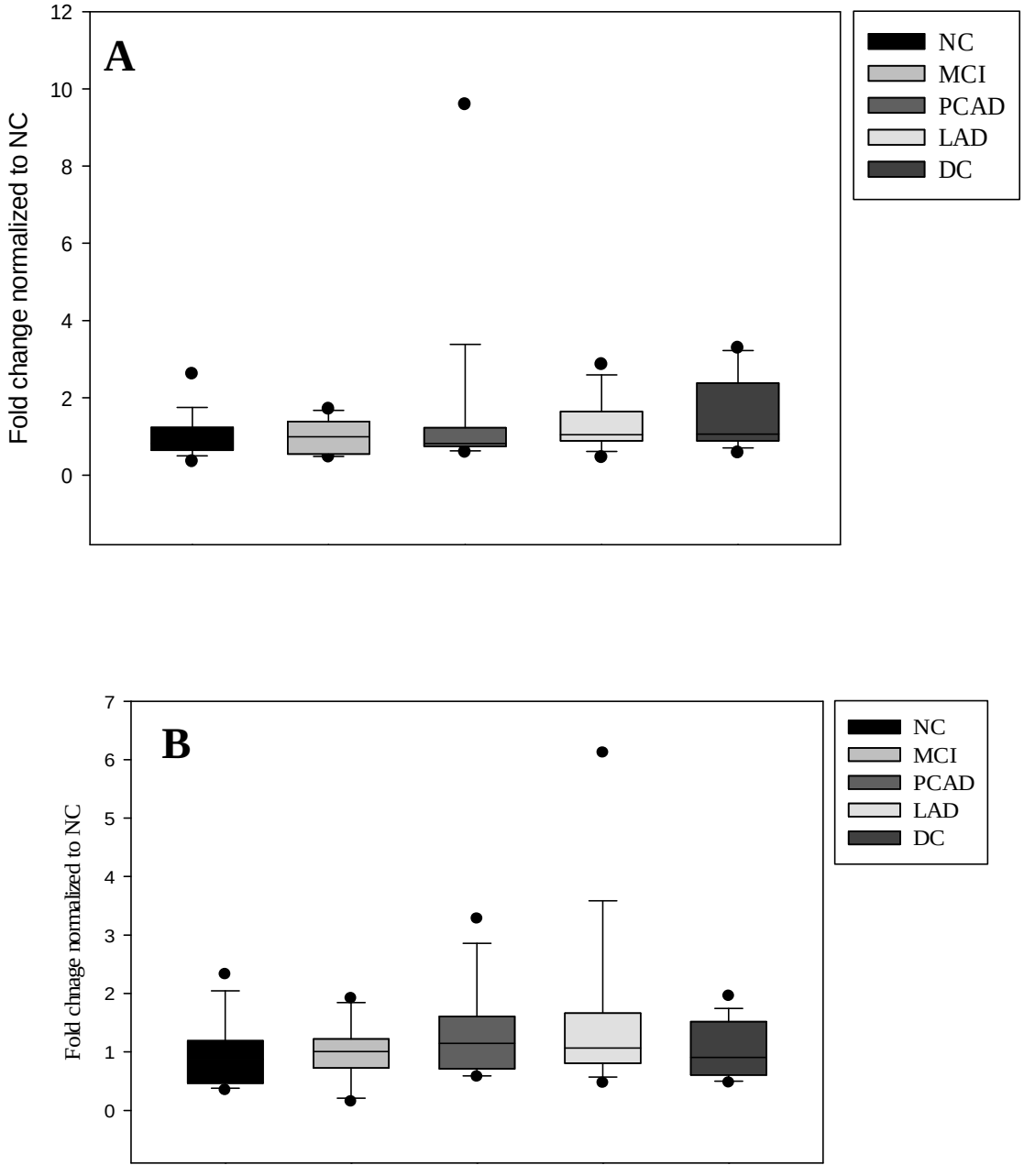

Figure 3.29. Fold change in gene expression for XPA in A) SMTG B) Cerebellum

(***** P < 0.05)

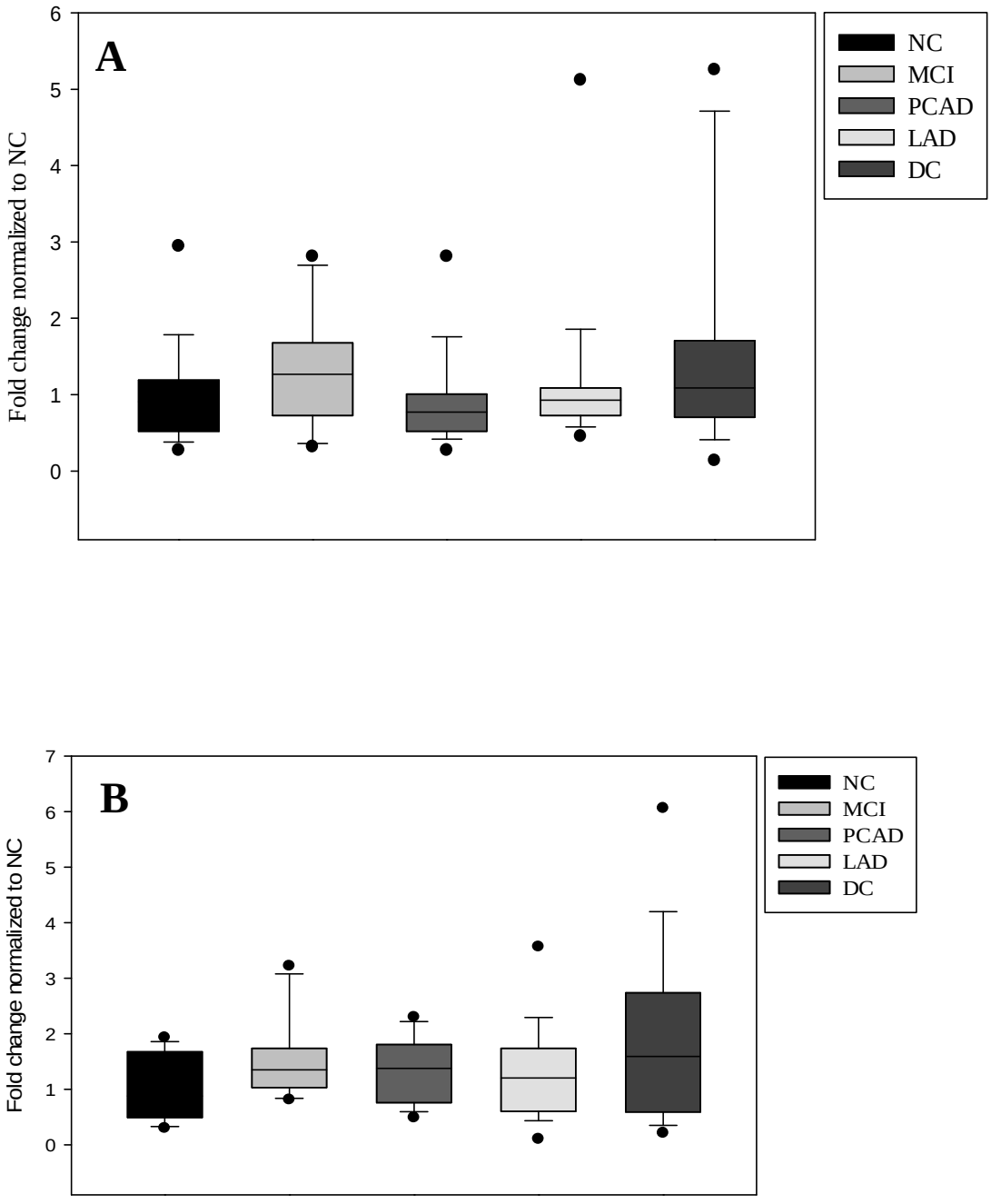

Figure 3.30. Fold change in gene expression for MRE11A in A) SMTG B) Cerebellum

(***** P < 0.05)

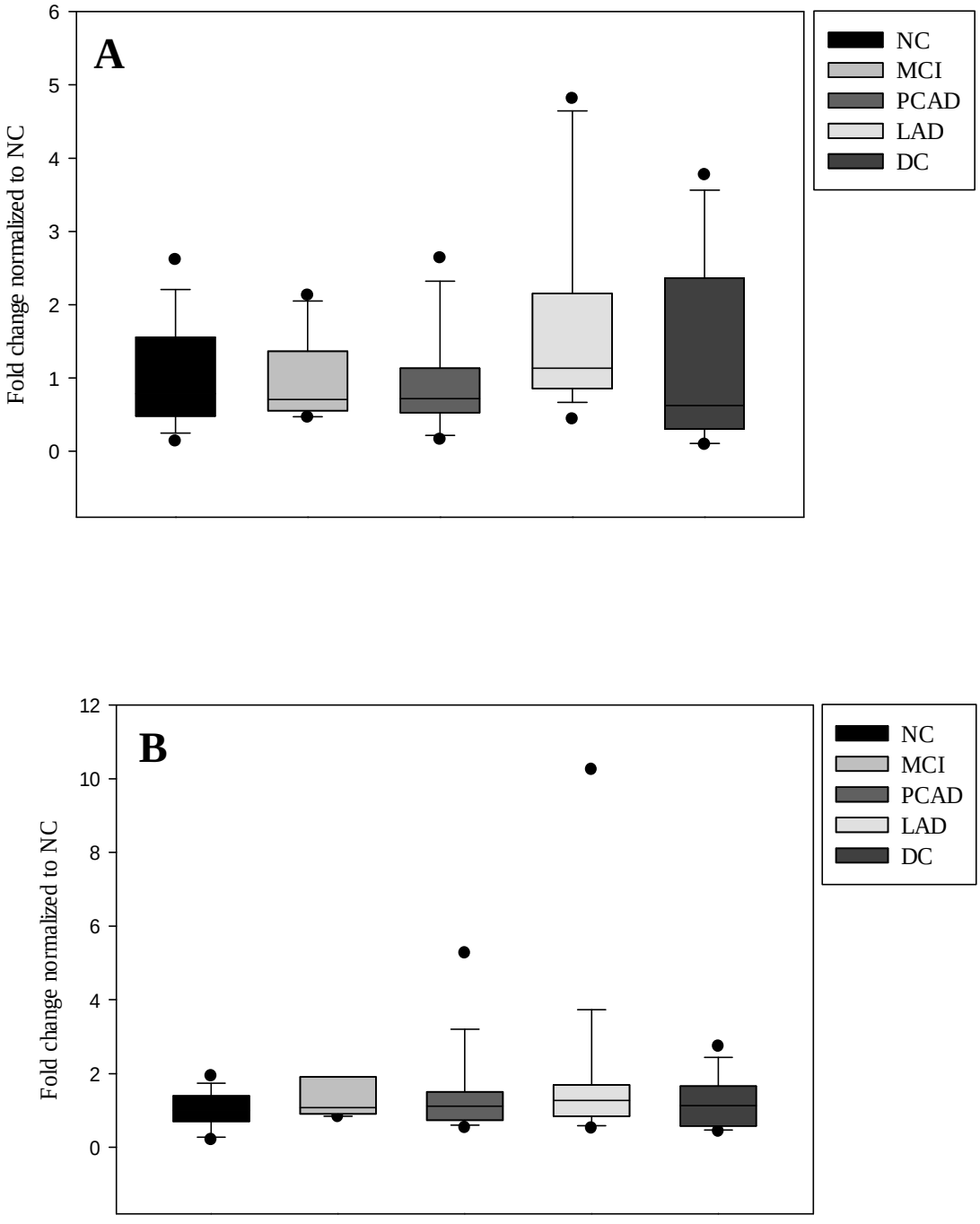

Figure 3.31. Fold change in gene expression for ATM in A) SMTG B) Cerebellum

(***** P < 0.05)

3.2.2. Protein levels

To determine if changes in gene expression correspond to changes in protein level, 20 µg protein specimens from samples used for the gene expression studies were subjected to Western blot analysis and separately probed for proteins involved in the BER pathway including OGG1, UNG, APE1, POLB, FEN1, PARP1 and XRCC1, using specific antibodies. A representative image of Western blots for the seven proteins in SMTG is shown in Figure 3.32. Median [Range] or Mean ± SEM OGG1, UNG APE1, POLB, FEN1, PARP1 and XRCC1 protein levels (% NC) are shown in Table 3.7. OGG1 protein levels were not significantly different in SMTG of MCI (76.16 [33.31-108.11] % NC) or LAD (92.57 [52.26-164.13] % NC) subjects but showed a statistically significant increase in PCAD subjects (107.02 [75.96-178.47] % NC) and a significant decrease in DC subjects (50.98 [4.1-79.45] % NC) compared to NC subjects (99.24 [65.31-194.71] % NC) (Figure 3.33A). In contrast, no significant differences in OGG1 protein levels were observed in the cerebellum of MCI (106.18 (±13.33) % NC), PCAD (104.97 (±6.79) % NC), LAD (90.82 (±6.92) % NC) or DC (104.83 (±9.68) % NC) subjects compared to NC (100 (±6.61) % NC) subjects (Figure 3.33B). In SMTG, median UNG protein levels were comparable throughout the progression of AD including MCI (88.98 [67.89-215.66] % NC), PCAD (99.07 [63.93-148.97] % NC) and LAD (97.47 [57.39-153.74] % NC) subjects compared to age-matched NC (94.72 [79.76-142.91] % NC) subjects and DC (87.19 [67.26-174.25] % NC) subjects (Figure 3.34A). UNG levels were significantly higher in the cerebellum of LAD subjects (124.3 [75.73-241.98] % NC) but showed no significant differences in MCI (113.27 [41.28-172.23] % NC), PCAD (110.52 [80.09-

253.3] % NC) or DC (115.52 [75.38-214.37] % NC) subjects compared to NC subjects (97.37 [82.17-123.99] % NC) (Figure 3.34B).

A statistically significant decrease in APE1 protein was observed in SMTG of MCI (86.73 [78.63-98.61] % NC) and DC (71.17 [52.98-86.89] % NC) subjects. In contrast, no significant differences were observed in PCAD (110.02 [85.76-156.87] % NC) or LAD (96.14 [67.39-117.9] % NC) subjects compared to NC subjects (101.04 [87.4-111.47] % NC) (Figure 3.35A). APE1 levels were not significantly different in the cerebellum for any of the subject groups studied including MCI (124.03 [80.21-160.84] % NC), PCAD (112.84 [62.81-263.69] % NC), LAD (109.53 [13.07-289.69] % NC) or DC (105.14 [21.29-139.31] % NC) subjects compared to NC subjects (93.69 [37.47-156.38] % NC) (Figure 3.35B). In the SMTG, there was a significant decrease in mean levels of POLB protein in MCI subjects (76.09 (±5.39) % NC) compared to NC subjects (100 (±3.42) % NC). No significant changes in mean POLB protein levels were observed in the SMTG of PCAD (100.28 (±8.11) % NC), LAD (123.4 (±11.79) % NC) or DC (85.89 (±16.59) % NC) subjects compared to NC subjects (100 (±3.42) % NC) (Figure 3.36A). In the cerebellum, median POLB protein levels were not significantly altered in MCI (101.33 [52.09-166.54] % NC), PCAD (109.93 [52.9-246.08] % NC), LAD (110.61 [62.34-310.57] % NC) or DC (90.5 [37.25-196.69] % NC) subjects compared to NC subjects (99.14 [59.7-183.28] % NC) (Figure 3.36B).

Mean FEN1 protein levels were significantly higher in the SMTG of PCAD (146.42 (±9.15) % NC) and LAD (132.21 (±10.24) % NC) subjects and showed no change in SMTG of MCI subjects (90.93 (±6.0) % NC) compared to NC subjects (98.59 (±4.3) % NC). In contrast, a significant decrease in FEN1 protein levels was observed in the

SMTG of DC subjects (63.98 (±5.63) % NC) compared to NC subjects (Figure 3.37A). Median FEN1 protein levels were not significantly altered in the cerebellum of MCI (98 [39.09-161.83] % NC), PCAD (120.23 [54.86-141.24] % NC) or LAD (154.97 [23.18-195.74] % NC) subjects but were significantly elevated in DC subjects (132.6 [116.37-329.44] % NC) compared to NC subjects (99.14 [59.7-183.28] % NC) (Figure 3.37B). Median PARP1 protein levels were significantly decreased in SMTG of PCAD (33.1 [17.53-121.42] % NC) and LAD (42.33 [13.66-193.82] % NC) subjects but was not altered in MCI (45.39 [22.59-135.98] % NC) or DC (61.14 [14.26-253.39] % NC) subjects compared to NC subjects (102.92 [23.32-238.01] % NC) (Figure 3.38A). In the cerebellum, mean PARP1 protein levels were significantly decreased in LAD (48.43 (±6.35) % NC) and DC (43.85 (±7.73) % NC) subjects but showed no change in MCI (78.75 (±6.57) % NC) or PCAD (108.41 (±9.22) % NC) subjects compared to NC subjects (98.2 (±9.74) % NC) (Figure 3.38B). A statistically significant increase in XRCC1 protein levels was observed in SMTG of MCI (126.8 [117.33-146.41] % NC) and PCAD (126.64 [96.93-138.54] % NC) subjects but no significant changes were observed in SMTG of LAD (109.54 [77.87-135.92] % NC) or DC (99.6 [87.87-132.5] % NC) subjects compared to age-matched NC subjects (99.89 [85.7-113.16] % NC) (Figure 3.39A). Median levels of XRCC1 protein throughout the progression of AD including MCI (101.54 (±7.29) % NC), PCAD (99.76 (±8.77) % NC) and LAD (102.22 (±11.41) % NC) subjects were comparable to those in age-matched NC subjects (100 (±3.42) % NC) in the cerebellum. However, XRCC1 protein levels in the cerebellum of DC subjects (144.73 (±24.55) % NC) were significantly increased compared to NC subjects (Figure 3.39B).

Table 3.7: Protein levels of DNA repair genes [% NC] **(**Bold numbers indicate significant difference)

Gene	NC		MCI		PCAD		LAD		DC	
	SMTG	**CER**	**SMTG**	**CER**	**SMTG**	**CER**	**SMTG**	**CER**	**SMTG**	**CER**
OGG1	99.24 [65.31-194.71]	100 (±6.61)	76.16 [33.31-108.11]	106.18 (±13.33)	***107.02 [75.96-178.47]**	104.97 (±6.79)	92.57 [52.26-164.13]	90.82 (±6.92)	***50.98 [4.1-79.45]**	104.83 (±9.68)
UNG	94.72 [79.76-142.91]	97.37 [82.17-123.99]	88.98 [67.89-215.66]	113.27 [41.28-172.23]	99.07 [63.93-148.97]	110.52 [80.09-253.3]	97.47 [57.39-153.74]	***124.3 [75.73-241.98]**	87.19 [67.26-174.25]	115.52 [75.38-214.37]
APE1	101.04 [87.4-111.47]	93.69 [37.47-156.38]	***86.73 [78.63-98.61]**	124.03 [80.21-160.84]	110.02 [85.76-156.87]	112.84 [62.81-263.69]	96.14 [67.39-117.9]	109.53 [13.07-289.69]	***71.17 [52.98-86.89]**	105.14 [21.29-139.31]
POLB	100 (±3.42)	101.41 [66.8-131.99]	***76.09 (±5.39)**	101.33 [52.09-166.54]	100.28 (±8.11)	109.93 [52.9-246.08]	***123.4 (±11.79)**	110.61 [62.34-310.57]	85.89 (±16.59)	90.5 [37.25-196.69]
FEN1	98.59 (±4.3)	99.14 [59.7-183.28]	90.93 (±6.0)	98 [39.09-161.83]	***146.42 (±9.15)**	120.23 [54.86-141.24]	***132.21 (±10.24)**	154.97 [23.18-195.74]	***63.98 (±5.63)**	***132.6 [116.37-329.44]**
PARP1	102.92 [23.32-238.01]	98.2 (±9.74)	45.39 [22.59-135.98]	78.75 (± 6.57)	***33.1 [17.53-121.42]**	108.41 (±9.22)	***42.33 [13.66-193.82]**	***48.43 (± 6.35)**	61.14 [14.26-253.39]	***43.85 (±7.73)**
XRCC1	99.89 [85.7-113.16]	100 (±3.42)	***126.8 [117.33-146.41]**	101.54 (±7.29)	***126.64 [96.93-138.54]**	99.76 (±8.77)	109.54 [77.87-135.92]	102.22 (±11.41)	99.6 [87.87-132.5]	***144.73 (±24.55)**

*** P < 0.05**

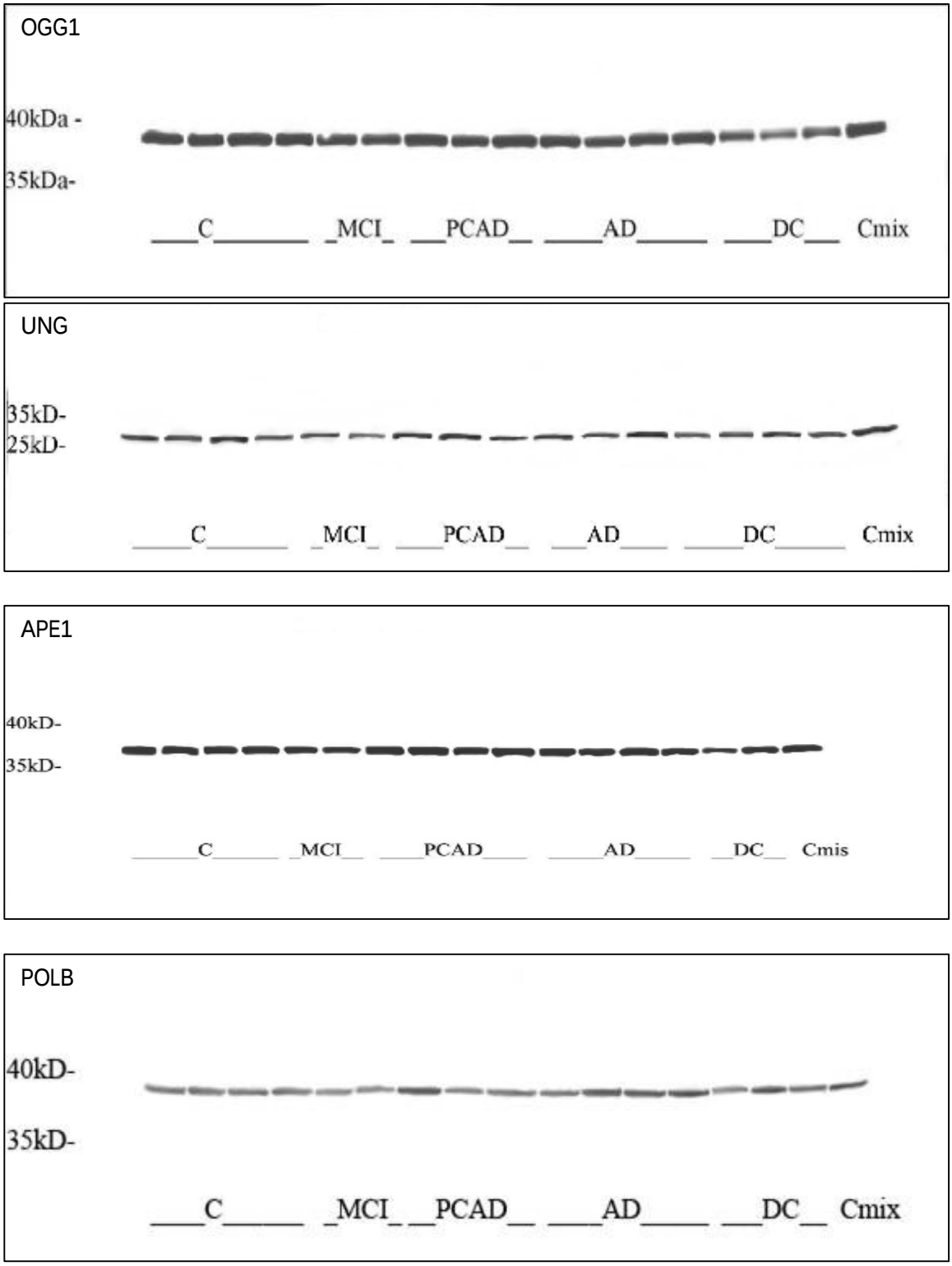

Figure 3.32A. Representative images of Western blots for OGG1, UNG, APE1 and POLB

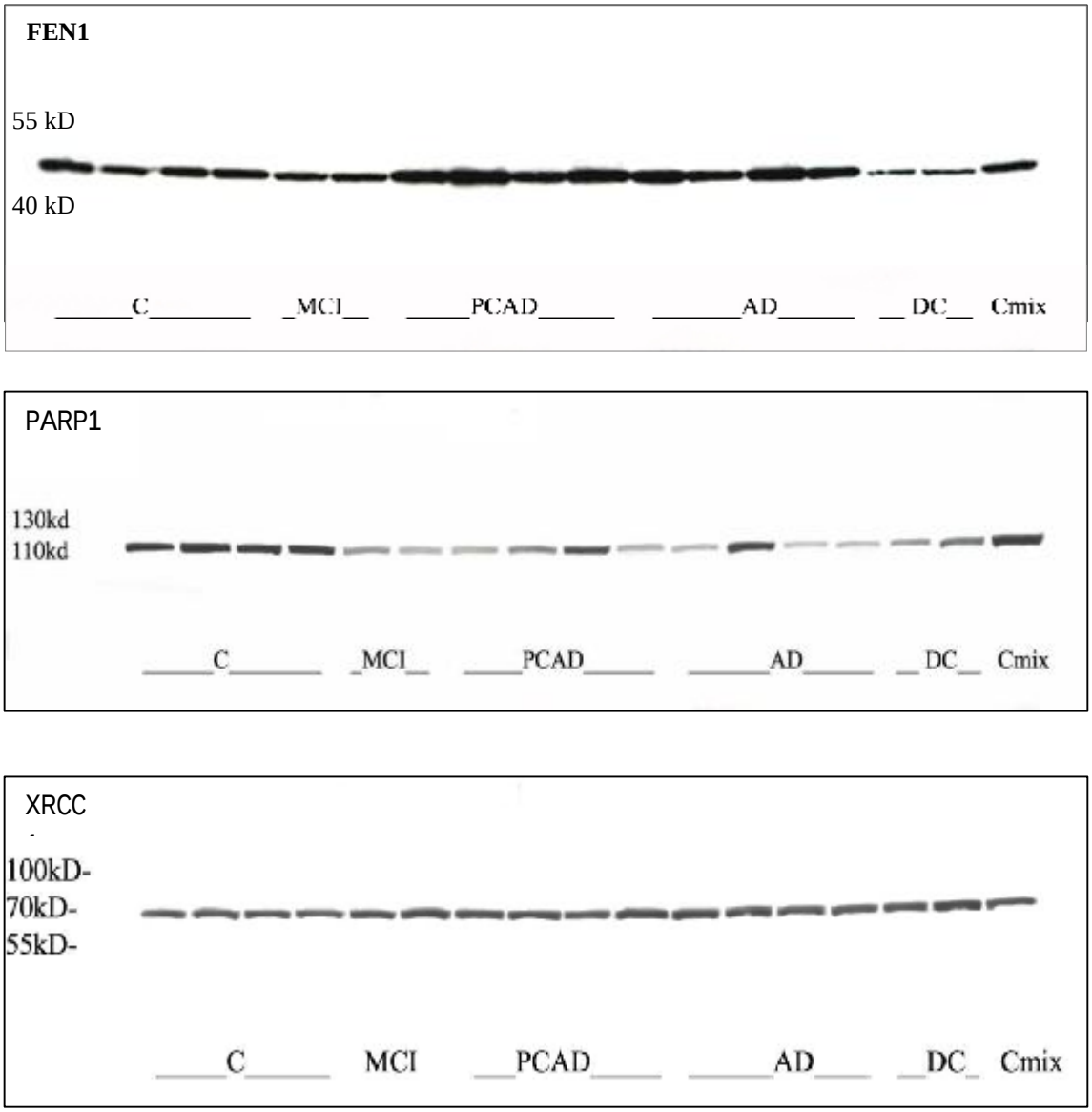

Figure 3.32B. Representative images of Western blots for FEN1, PARP1 and XRCC1

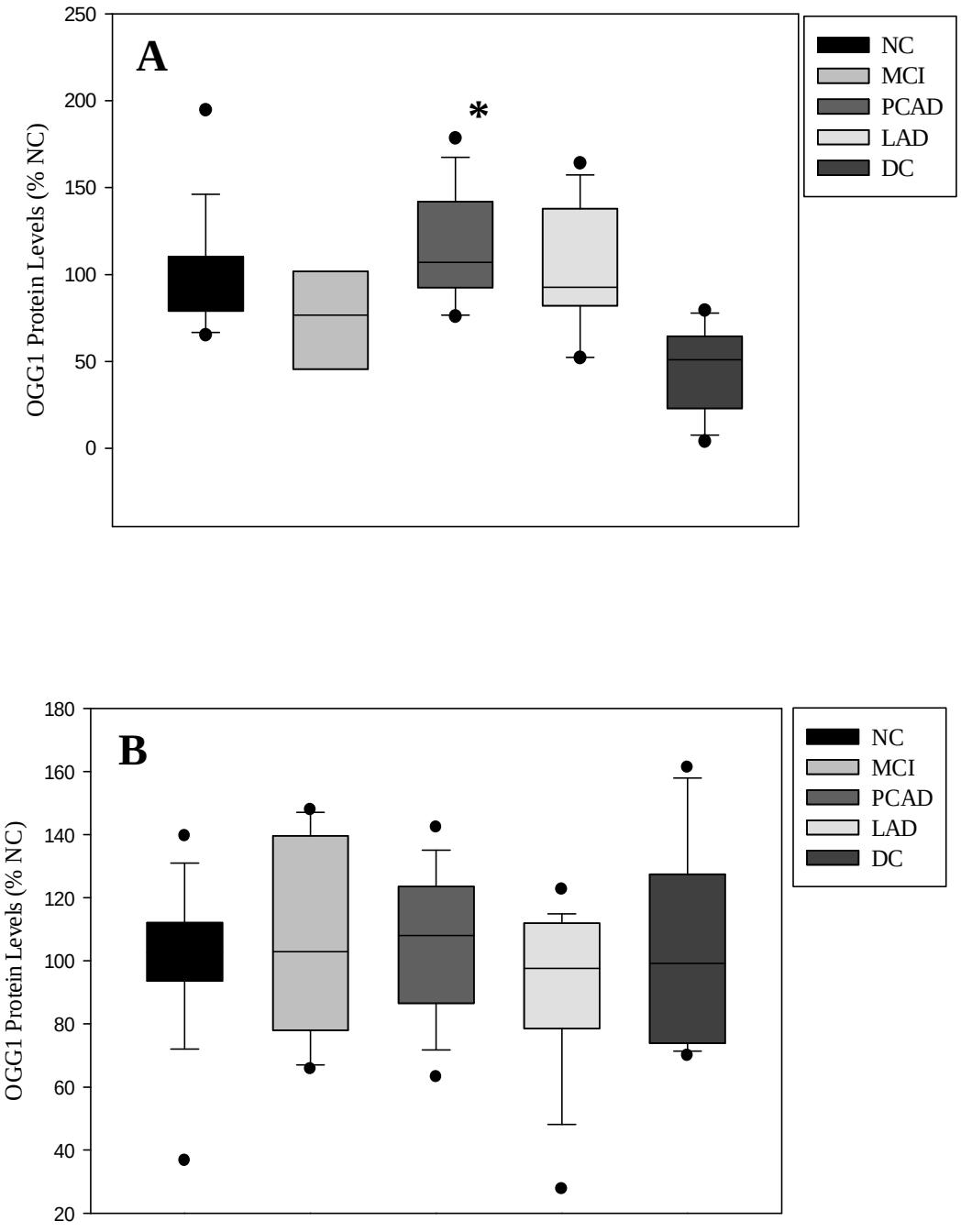

Figure 3.33. Protein Levels of OGG1 (% NC) in A) SMTG and B) Cerebellum

(* $P < 0.05$)

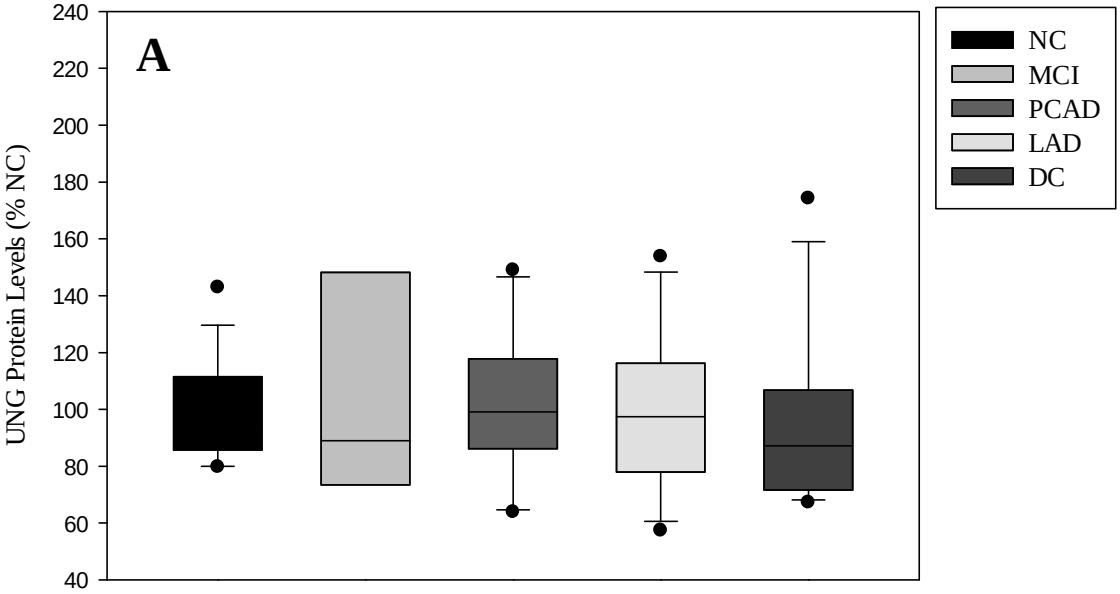

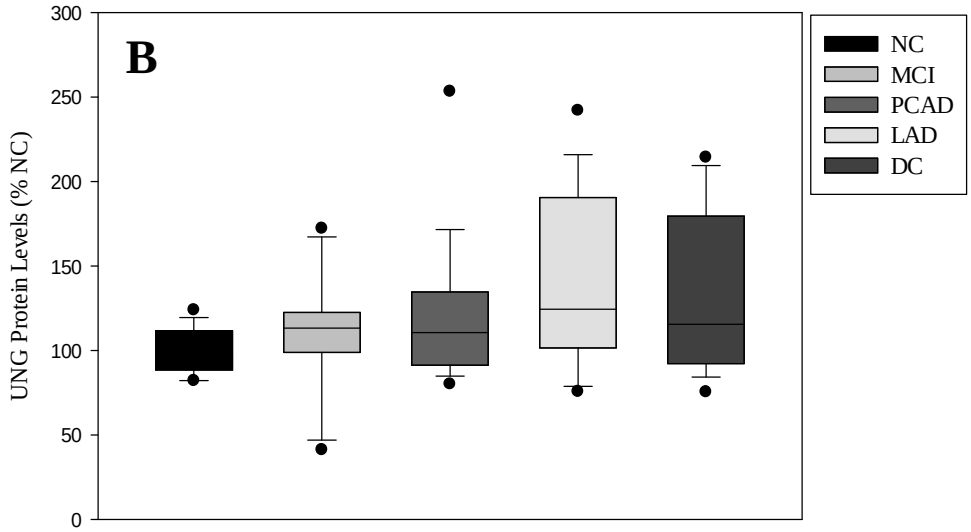

Figure 3.34. Protein Levels of UNG (% NC) in A) SMTG and B) Cerebellum

(***** P < 0.05)

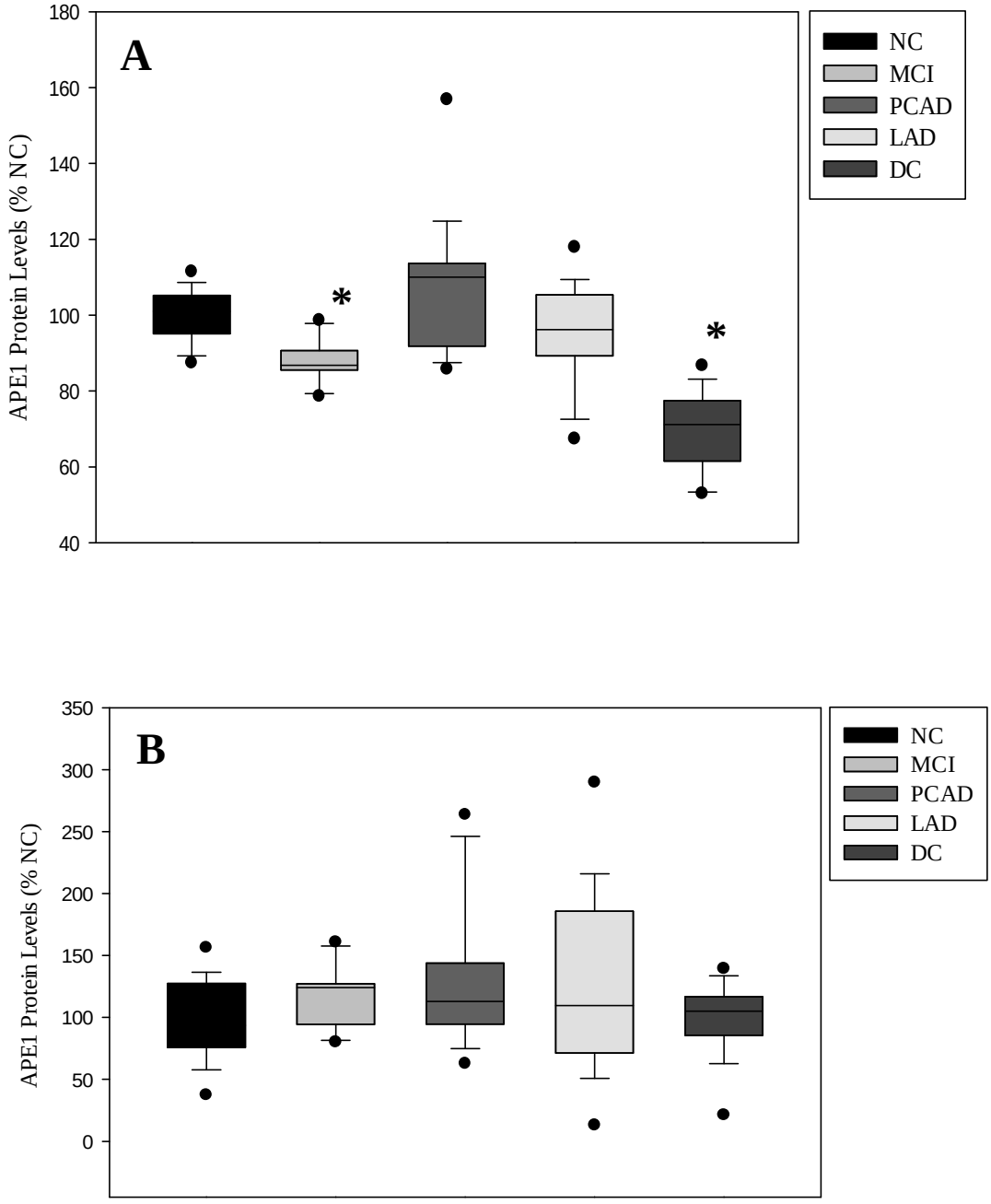

Figure 3.35. Protein Levels of APE1 (% NC) in A) SMTG and B) Cerebellum

(* $P < 0.05$)

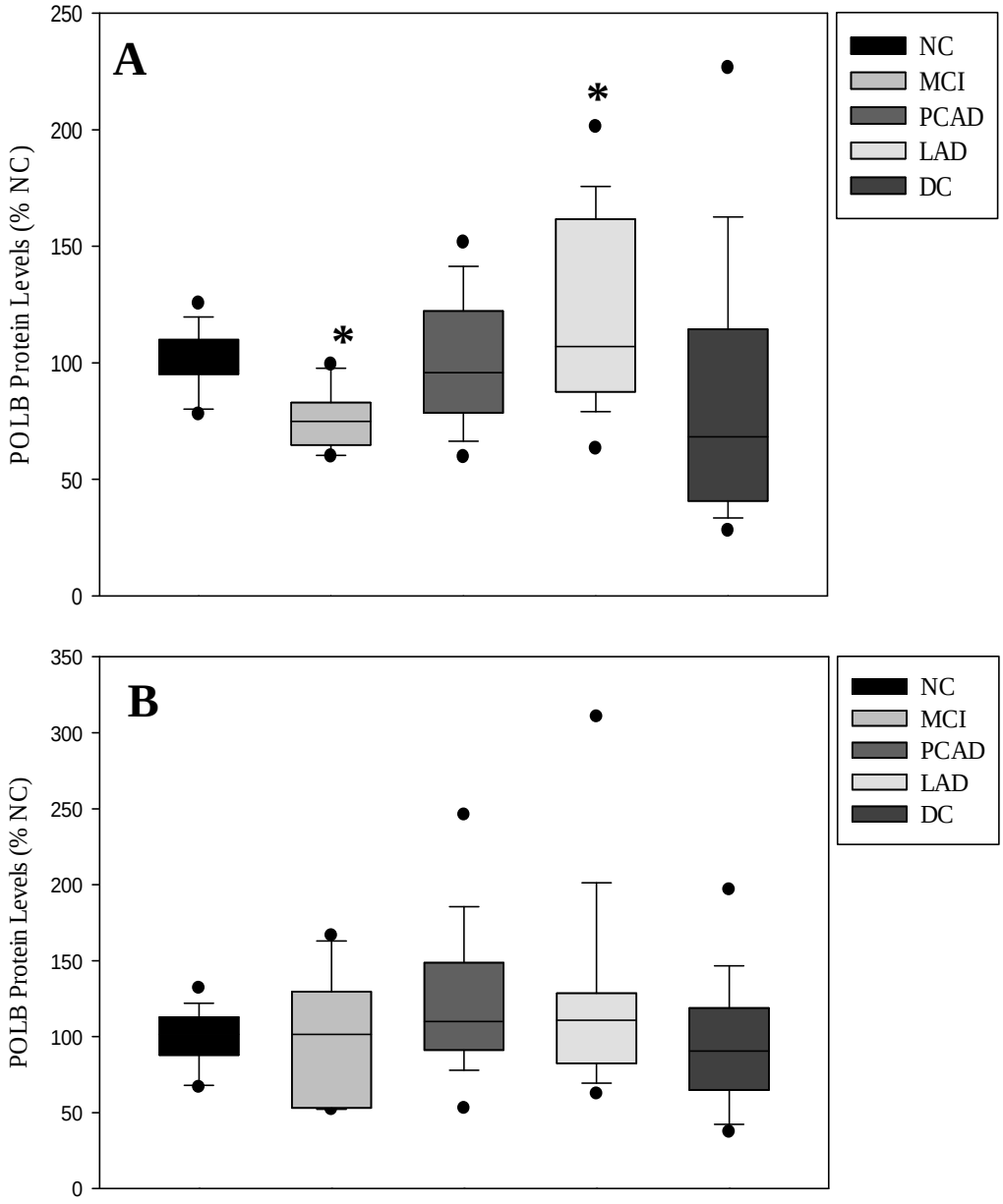

Figure 3.36. Protein Levels of POLB (% NC) in A) SMTG and B) Cerebellum

(* $P < 0.05$)

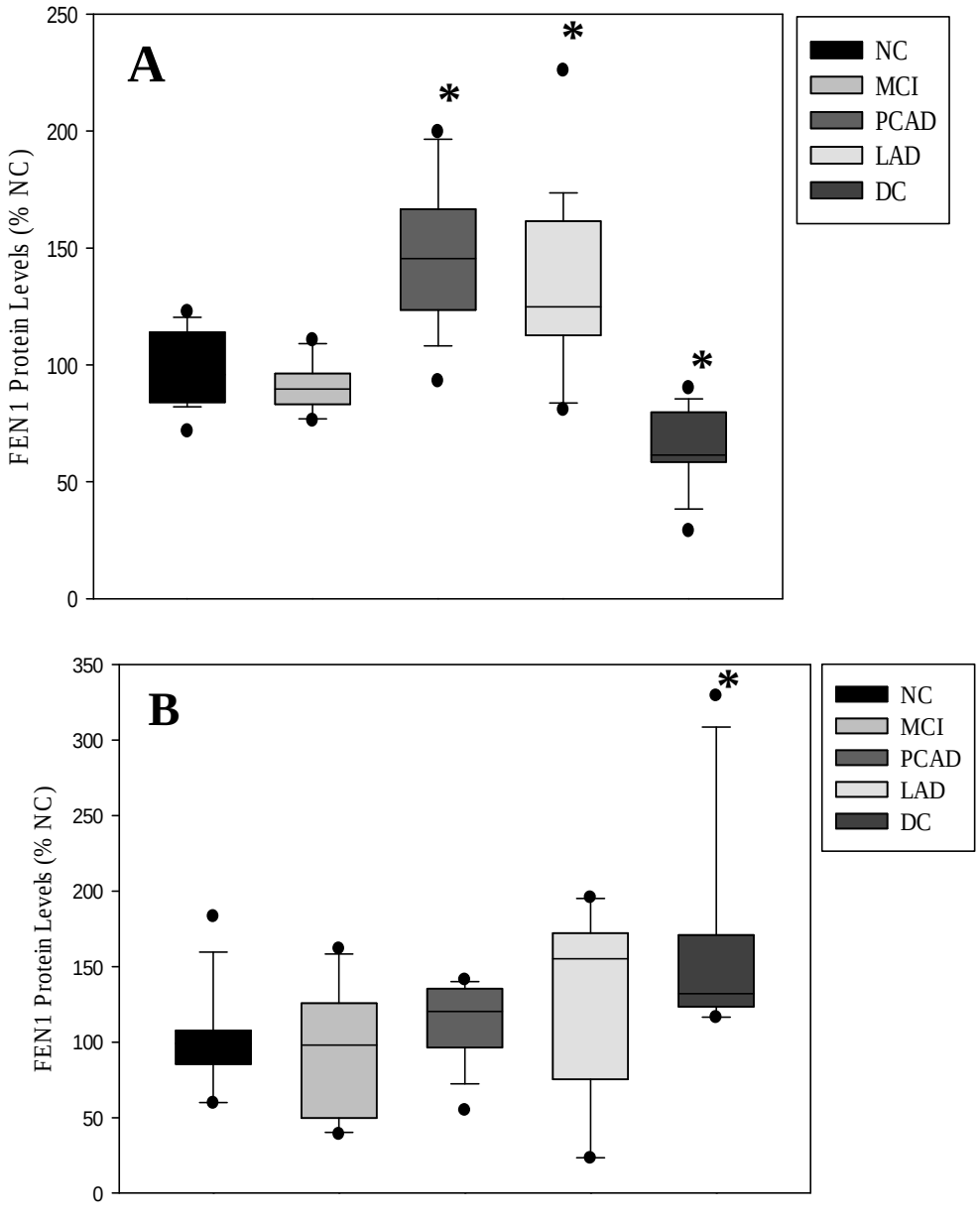

Figure 3.37. Protein Levels of FEN11 (% NC) in A) SMTG and B) Cerebellum

(* $P < 0.05$)

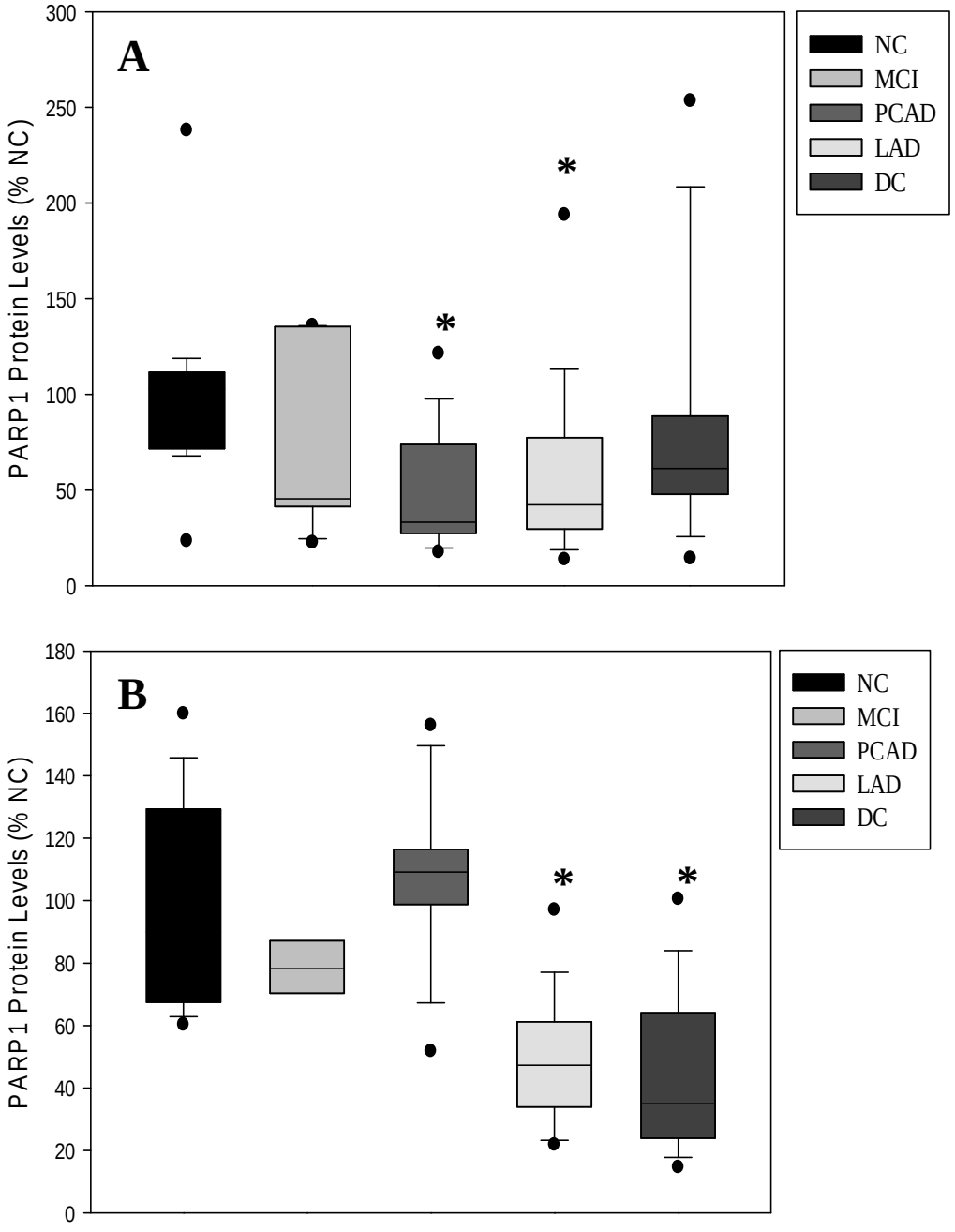

Figure 3.38. Protein Levels of PARP1 (% NC) in A) SMTG and B) Cerebellum

(* $P < 0.05$)

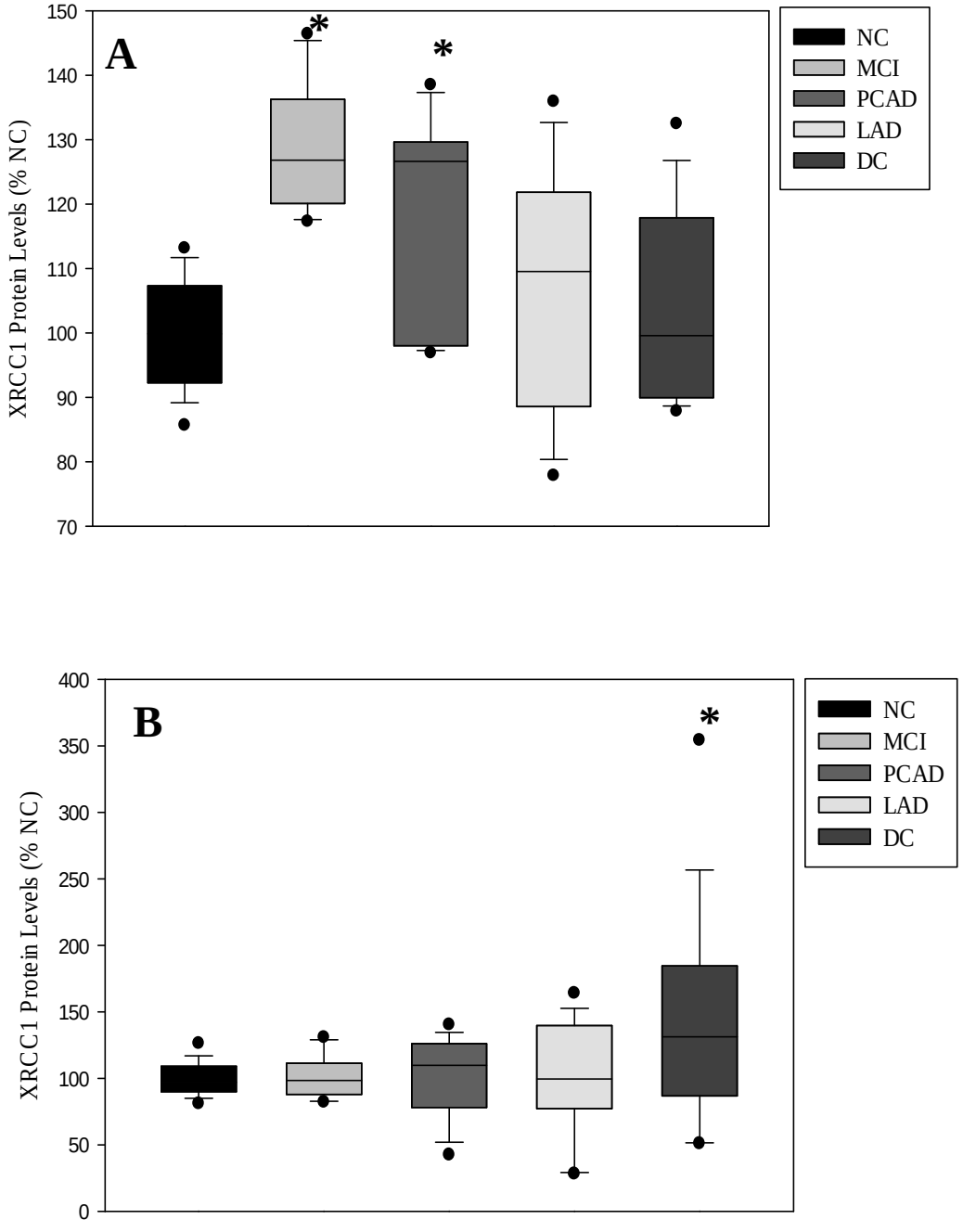

Figure 3.39. Protein Levels of XRCC1 (% NC) in A) SMTG and B) Cerebellum

(* $P < 0.05$)

3.2.3 Enzyme activity levels

Enzyme activities for OGG1, UNG, APE1, POLB, FEN1 and PARP1 were calculated to determine if changes in protein levels led to a corresponding enhancement/loss in protein activity. OGG1, UNG and APE1 activity was measured by examining their ability to cleave radiolabeled duplex DNA oligos (Table 2.5) containing a single 8-oxodG, deoxy-uracil or tetrahydrofuran lesion by electrophoresis on a 20% denaturing gel. The band intensities of the intact oligonucleotide and the incision product of each sample were quantified and incision activities of each assay were calculated as the percentage of the amount of radioactivity in the incised product band relative to the total radioactivity in the lane (incised product + intact duplex oligonucleotide). Activity of POLB was measured as the incorporation of a radiolabeled single nucleotide (α^{32}P-dCTP) into a 34-mer oligonucleotide containing a single gap followed by electrophoresis on a 20% denaturing gel. A dsDNA substrate containing flap strands prepared from three oligonucleotides (Table 2.5) labeled with a 6-TAMRA (fluorophore donor) at the 5' end and BHQ-2 (fluorophore quencher) at the 3' end was used in the FEN1 activity assay. Enzymatic cleavage of the flap strand by FEN1 leads to the release of a 6-TAMRA labeled short single stranded product and consequently an increase in fluorescence. [adenine-^{14}C]NAD was used as the substrate to determine PARP1 activity by measurement of radioactive ^{14}C incorporation into a TCA-insoluble material (protein-bound [^{14}C](ADP-ribose)$_n$). Enzyme activity levels for OGG1, UNG, APE1, POLB, FEN1 and PARP1 are shown in Table 3.8 and are reported as median [range] or mean (±SEM) % NC activity. Representative images for activity assays of OGG1, UNG, APE1 and POLB in SMTG are shown in Figure 3.40. No activity was observed in

representative protein samples heat-inactivated by boiling at 95°C before initiating the activity assays (blank).

OGG1 incision activity was not significantly different in the SMTG of MCI (123.89 [95.89-144.47] % NC), PCAD (99.65 [91.62-106.35] % NC), LAD (99.81 [87.92-101.73] % NC) or DC (99.07 [94.81-103.05] % NC) subjects compared to NC subjects (100 [87.15-111.92] % NC) (Figure 3.41A). Comparison of OGG1 activity across the disease spectrum in the cerebellum showed no significant changes in MCI (93.35 (±2.5) % NC), PCAD (97.81 (±2.51) % NC), LAD (101.56 (±2.1) % NC) or DC (96.99 (±1.7) % NC) subjects compared to NC subjects (99.19 (±1.48) % NC) (Figure 3.41B). UNG activity levels on the other hand were significantly higher in the SMTG of MCI (133.72 (±4.64) % NC), PCAD (149.67 (±4.42) % NC) and LAD (134.61 (±8.7) % NC) subjects compared to NC subjects (100 (±4.82) % NC). Mean levels of UNG activity were not significantly changed in SMTG of DC subjects (122.71 (±11.19) % NC) compared to NC subjects (Figure 3.42A). No significant differences were observed in UNG activity in CER of any of the diseased subjects studied including MCI (110.91 (±10.05) % NC), PCAD (120.94 (±7.44) % NC), LAD (106.81 (±6.5) % NC) and DC (91.58 (±11.7) % NC) subjects compared to NC subjects (100 (±6.05) % NC) (Figure 3.42B).

Levels of APE1 activity were not significantly changed in samples from SMTG of MCI (107.3 (±6.53) % NC), LAD (111.29 (±5.65) % NC) and DC (109.48 (±6.46) % NC) subjects but were significantly elevated in samples from PCAD subjects (116.42 (±5.99) % NC) compared to those from NC subjects (100 (±3.64) % NC) (Figure 3.43A). In contrast, APE1 activity levels were significantly reduced in the cerebellum of PCAD (77.38 [12.12-98.74] % NC) and LAD (61.09 [20.75-125.45] % NC) subjects compared

to age-matched NC subjects (99.95 [61.3-145.03] % NC). Median APE1 activity levels showed no significant changes in cerebellum of MCI subjects (128.4 [88.87-139.37] % NC) or DC (47.01 [16.38-144.87] % NC) subjects compared to NC subjects (Figure 3.43B). A statistically significant increase in POLB enzyme activity was observed in SMTG of MCI (113.25 [106.21-124.93] % NC) and PCAD (114.55 [86.81-146.31] % NC) subjects compared to NC subjects (101.82 [79.54-121.2] % NC). No significant changes in POLB enzyme activity levels were observed in SMTG of LAD (105.73 [94.47-140.29] % NC) or DC (100.66 [91.22-116.09] % NC) subjects compared to NC subjects (Figure 3.44A). Mean POLB enzyme activity levels were not significantly altered in the cerebellum of MCI (106.85 (±3.98) % NC), LAD (105.03 (±3.2) % NC) or DC subjects (106.55 (±4.59) % NC) but were significantly elevated in PCAD (115.56 (±3.48) % NC) subjects compared to NC subjects (98.69 (±2.66) % NC) (Figure 3.44B).

Mean levels of FEN1 activity were significantly decreased in SMTG of PCAD (88.5 (±2.47) % NC), LAD (81.79 (±4.41) % NC) and DC (57.49 (±7.13) % NC) subjects but showed no change in MCI subjects (92.77 (±3.31) % NC) compared to NC subjects (100 (±2.7) % NC) (Figure 3.45A). Comparison of FEN1 activity across the disease spectrum in the cerebellum showed no significant changes in MCI (108.64 (±13.39) % NC), PCAD (105.92 (±14.06) % NC) or LAD (71.96 (±9.4) % NC) subjects compared to NC subjects (100 (±7.86) % NC). A statistically significant decrease in FEN1 enzyme activity was observed in cerebellum of DC subjects (65.26 (±6.1) % NC) compared to NC subjects (Figure 3.45B). In SMTG, median PARP1 enzyme activity levels were not significantly different in MCI (65.84 [16.38-235.67] % NC), PCAD (100.82 [4.93-295.05] % NC) or DC (63.21 [36.74-502.77] % NC) subjects but were significantly elevated in LAD

subjects (229.08 [92.35-498.61] % NC) compared to NC subjects (56.19 [5.56-379.45] % NC) (Figure 3.46A). Median PARP1 activity levels were not significantly altered in the cerebellum of MCI subjects (147.89 [130.41-188.95] % NC) but were significantly higher in PCAD (213.1 [44.17-252.59] % NC), LAD (170.43 [63.84-338.08] % NC) and DC (295.34 [82.95-410.47] % NC) subjects compared to NC subjects (72.74 [19.26-243.66] % NC) (Figure 3.46B).

Figure 3.40A. Representative images of activity assays for OGG1 and UNG

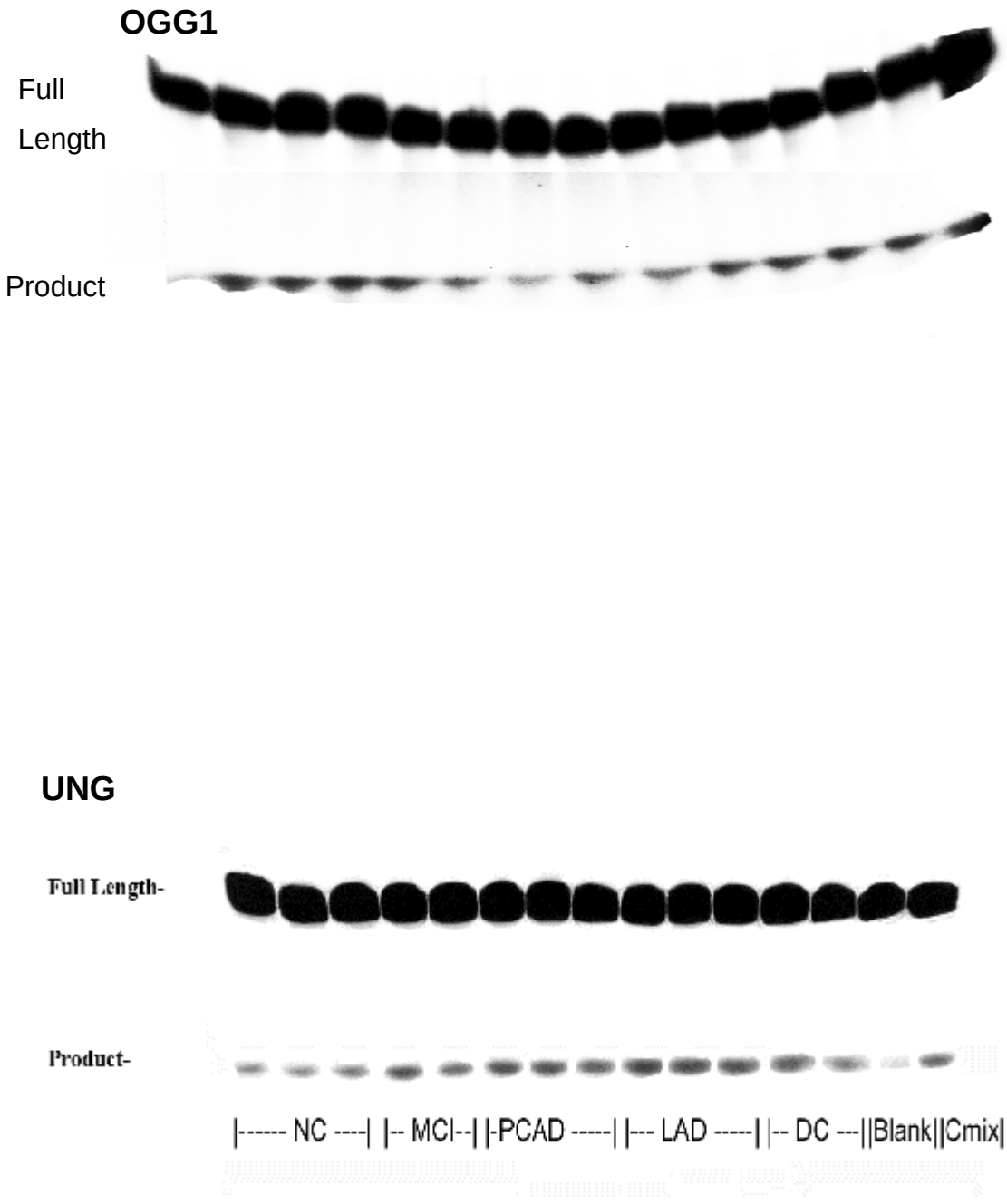

Figure 3.40B. Representative images of activity assays for APE1 and POLB

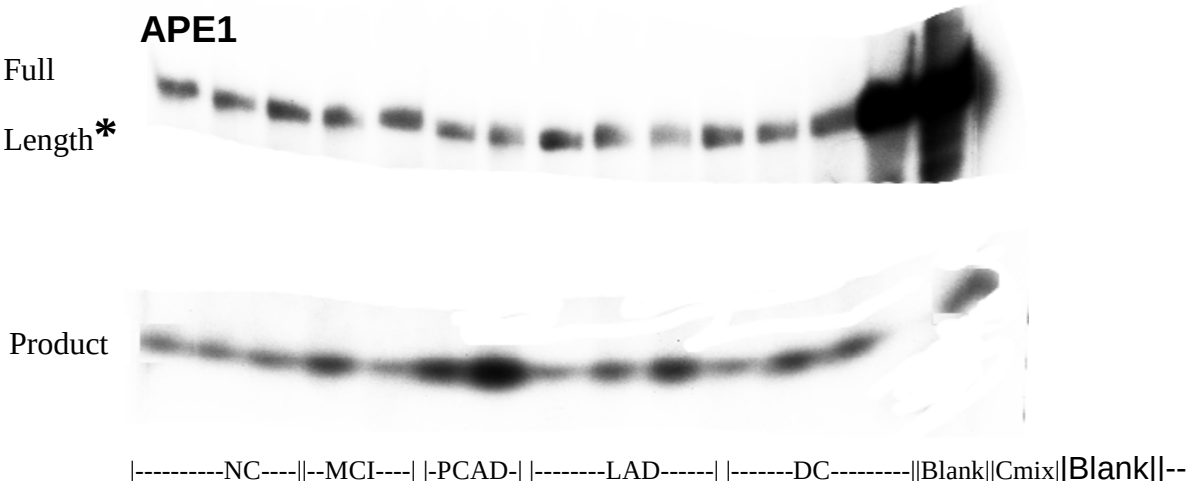

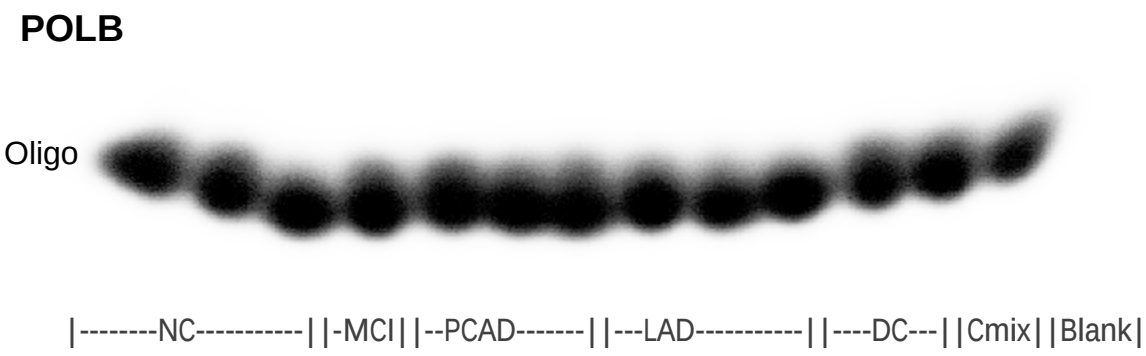

Table 3.8: Enzyme activity Levels of DNA repair genes [% NC] **(**Bold numbers indicate significant difference)

Gene	NC		MCI		PCAD		LAD		DC	
	SMTG	**CER**	**SMTG**	**CER**	**SMTG**	**CER**	**SMTG**	**CER**	**SMTG**	**CER**
OGG1	100 [87.15-111.92]	99.19 (±1.48)	123.89 [95.89-144.47]	93.35 (±2.5)	99.65 [91.62-106.35]	97.81 (±2.51)	99.81 [87.92-101.73]	101.56 (±2.1)	99.07 [94.81-103.05]	96.99 (±1.7)
UNG	100 (±4.82)	100 (±6.05)	***133.72 (±4.64)**	110.91 (± 10.05)	***149.67 (±4.42)**	120.94 (±7.44)	***134.61 (±8.7)**	106.81 (±6.5)	122.71 (±11.19)	91.58 (±11.70)
APE1	100 (±3.64)	99.95 [61.3-145.03]	107.3 (±6.53)	128.4 [88.87-139.37]	***116.42 (±5.99)**	***77.38 [12.12-98.74]**	111.29 (±5.65)	***61.09 [20.75-125.45]**	109.48 (±6.46)	47.01 [16.38-144.87]
POLB	101.82 [79.54-121.2]	98.69 (±2.66)	***113.25 [106.21-124.93]**	106.85 (±3.98)	***114.55 [86.81-146.31]**	***115.56 (±3.48)**	105.73 [94.47-140.29]	105.03 (±3.2)	100.66 [91.22-116.09]	106.55 (±4.59)
FEN1	100 (±2.70)	100 (±7.86)	92.77 (±3.31)	108.64 (±13.39)	***88.50 (±2.47)**	105.92 (±14.06)	***81.79 (±4.41)**	71.96 (±9.40)	***57.49 (±7.13)**	***65.26 (±6.10)**
PARP1	56.19 [5.56-379.45]	72.74 [19.26-243.66]	65.84 [16.38-235.67]	147.89 [130.41-188.95]	100.82 [4.93-295.05]	***213.10 [44.17-252.59]**	***229.08 [92.35-498.61]**	***170.43 [63.84-338.08]**	63.21 [36.74-502.77]	***295.34 [82.95-410.47]**

*** P < 0.05**

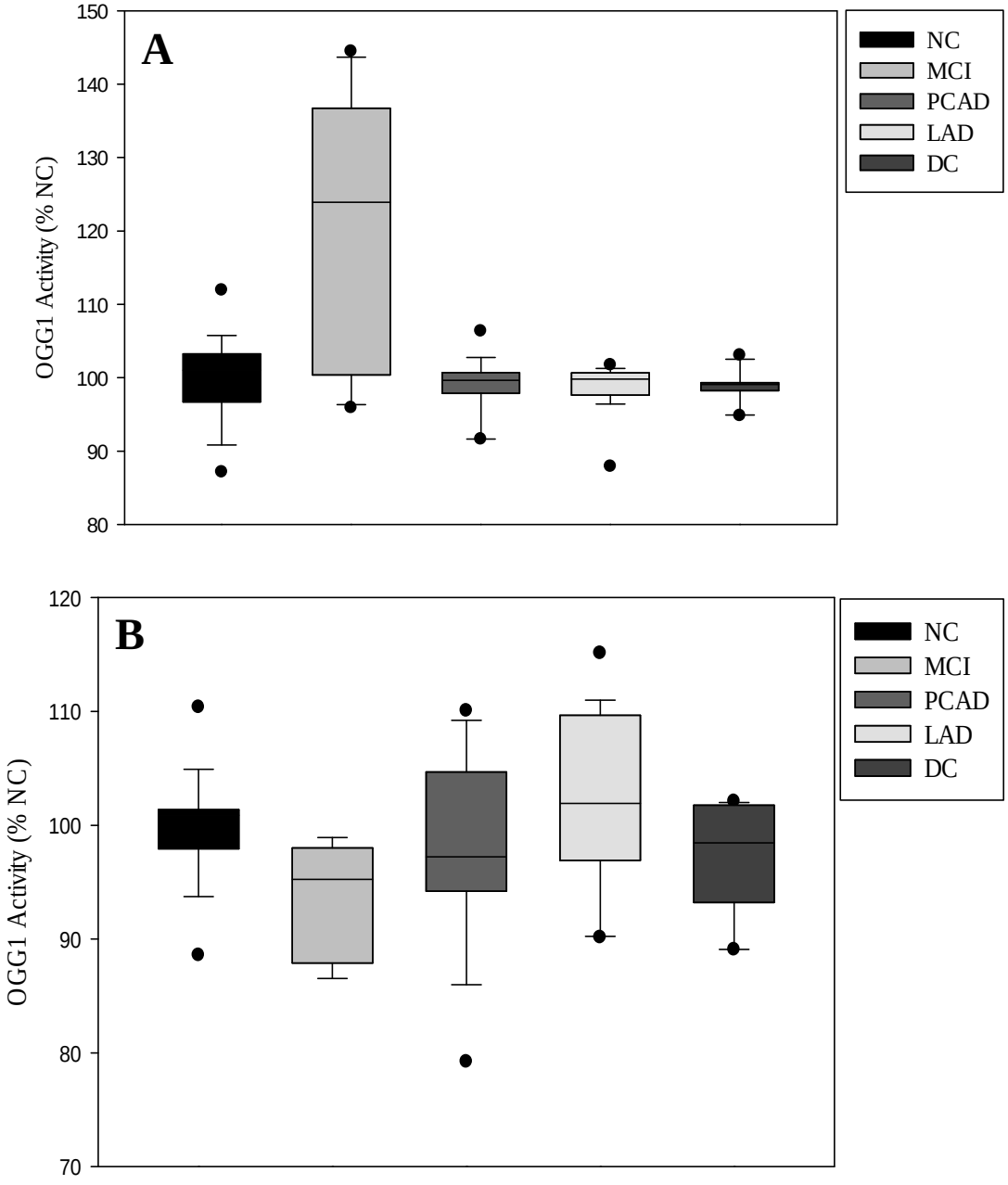

Figure 3.41. Protein Activity Levels of OGG1 (% NC) in A) SMTG and B) Cerebellum (* $P < 0.05$)

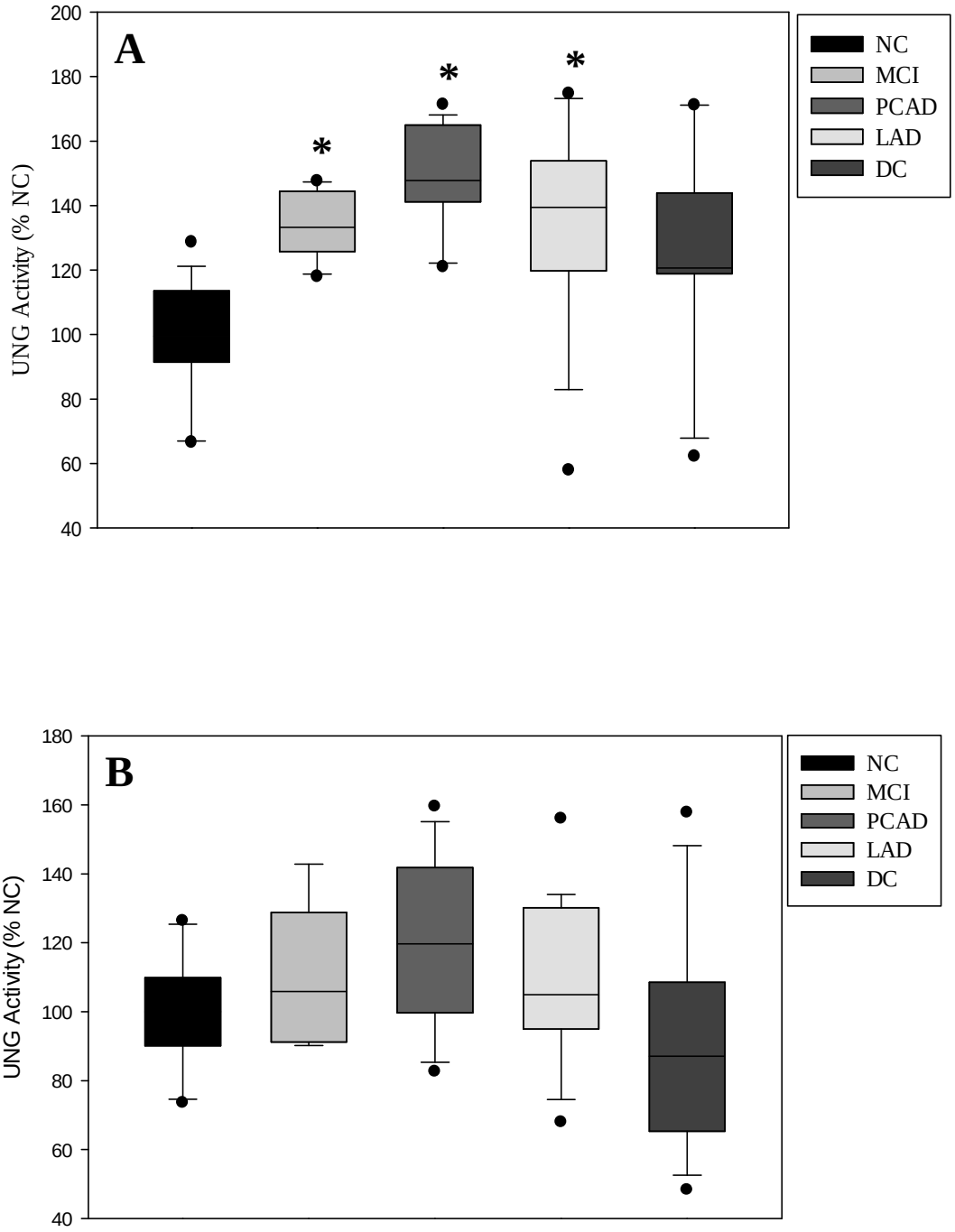

Figure 3.42. Protein Activity Levels of UNG (% NC) in A) SMTG and B) Cerebellum

(* $P < 0.05$)

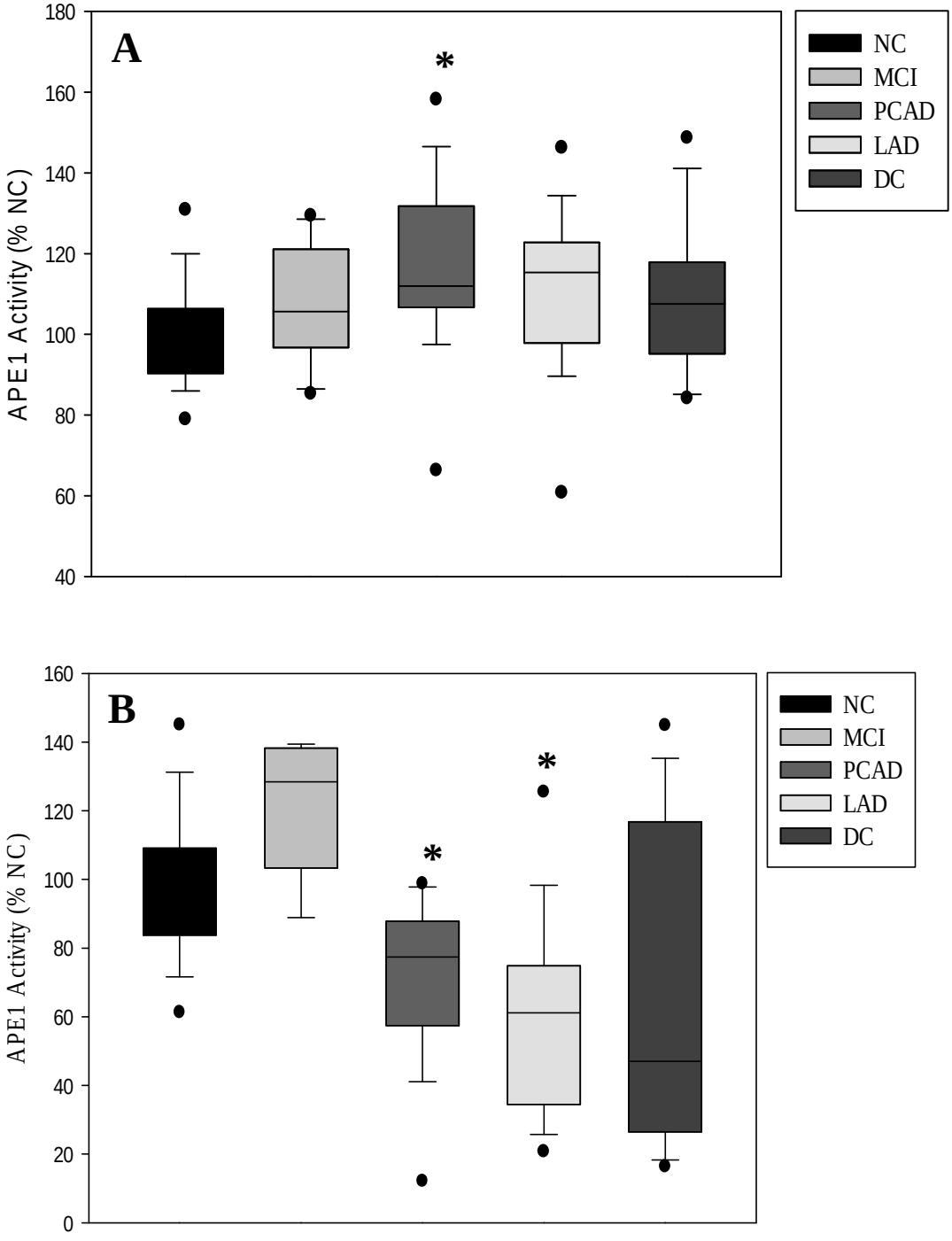

Figure 3.43. Protein Activity Levels of APE1 (% NC) in A) SMTG and B) Cerebellum (* P < 0.05)

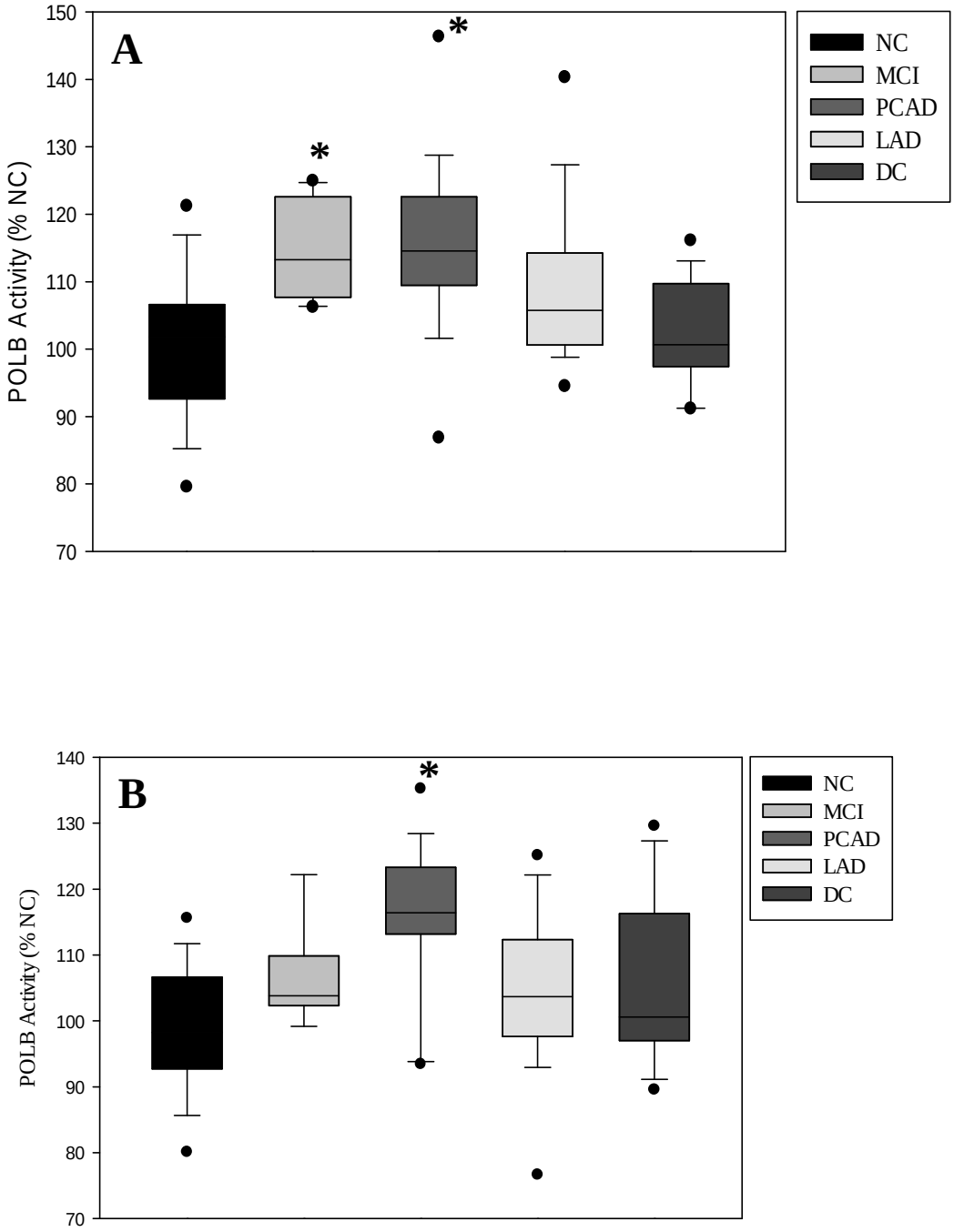

Figure 3.44. Protein Activity Levels of POLB (% NC) in A) SMTG and B) Cerebellum (* $P < 0.05$)

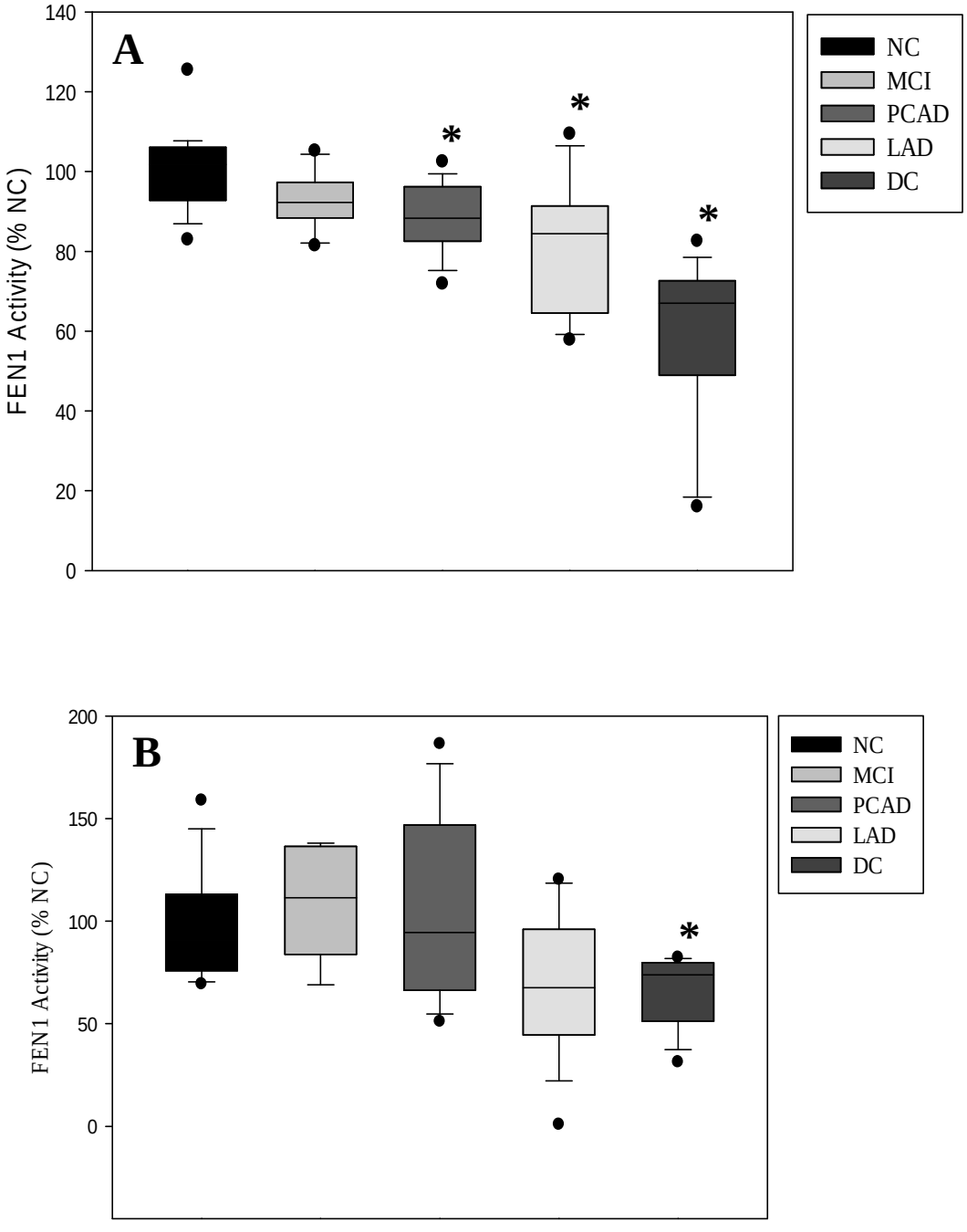

Figure 3.45. Protein Activity Levels of FEN1 (% NC) in A) SMTG and B) Cerebellum (* $P < 0.05$)

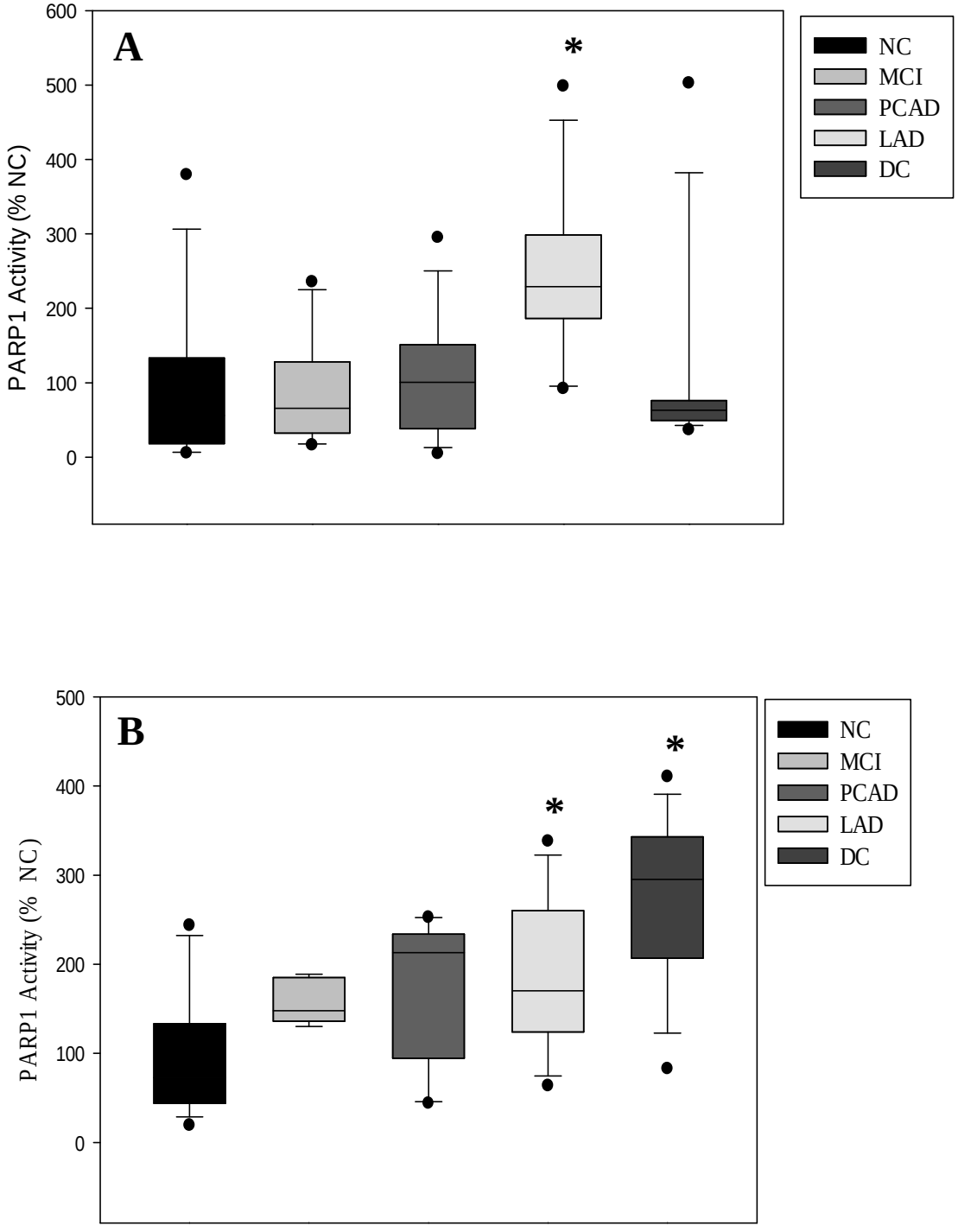

Figure 3.46. Protein Activity Levels of PARP1 (% NC) in A) SMTG and B) Cerebellum

(* $P < 0.05$)

Table 3.9. Summary of results for BER pathway

Gene			OGG1	UNG	APE1	POLB	PARP 1	FEN 1	XRCC 1
MCI	SMTG	Gene expression	–	–	–	–	–	–	–
		Protein level	–	–	↓	↓	–	–	↑
		Enzyme activity	–	↑	–	↑	–	–	
	CER	Gene expression	–	–	–	–	–	–	–
		Protein level	–	–	–	–	–	–	–
		Enzyme activity	–	–	–	–	–	–	
PCAD	SMTG	Gene expression	↑	↑	–	↑	–	–	–
		Protein level	↑	–	–	–	↓	↑	↑
		Enzyme activity	–	↑	↑	↑	–	↓	–
	CER	Gene expression	–	–	–	–	–	–	–
		Protein level	–	↑	–	–	–	–	–
		Enzyme activity	–	–	↓	↑	↑	–	
LAD	SMTG	Gene expression	↑	↑	–	↑	↑	–	–
		Protein level	–	–	–	↑	↓	↑	–
		Enzyme activity	–	↑	↑	–	↑	↓	
	CER	Gene expression	–	–	–	–	–	–	–
		Protein level	–	–	–	–	↓	–	–
		Enzyme activity	–	–	↓	–	↑	–	
DC	SMTG	Gene expression	–	↑	–	–	–	–	–
		Protein level	↓	–	↓	–	–	↓	–
		Enzyme activity	–	–	–	–	–	↓	
	CER	Gene expression	–	–	–	↑	–	–	–
		Protein level	–	–	–	–	↓	↑	↑
		Enzyme activity	–	–	–	–	↑	↓	

Chapter 4: Discussion

Oxidative stress is considered one of the many contributing factors to the pathogenesis of AD. Reactive oxygen species (ROS), a major contributor to oxidative stress, are continuously produced in the human body by both endogenous (byproducts of cellular metabolism) and exogeneous (smoking, pollution, radiation) methods. ROS-mediated oxidative damage is extremely critical in non-dividing postmitotic cells like neurons, as the damaged cells cannot be replaced by new ones. Oxidative damage to the nucleic acid framework (nDNA, mtDNA and RNA) in such cells can lead to neuronal dysfunction and loss associated with aging and neurodegenerative processes like AD (Beal, 2005; Lu et al., 2004; Moreira et al., 2008; Nunomura et al., 1999). Multiple studies have shown an increase in biomarkers of oxidative DNA damage including 8-hydroxyguanine (the predominant marker of oxidative DNA damage), 8-hydroxyadenine, 8-hydroxycytosine, thymine glycol, fapy-adenine, fapy-guanine and 5-hydroxyuracil in brain tissues, leukocytes and ventricular CSF of AD subjects. Some of these changes were observed even in the earliest clinically detectable phase of AD (MCI) (Gabbita et al., 1998; Keller et al., 2005; Lovell and Markesbery, 2001; Lyras et al., 1997; Markesbery and Carney, 1999; Mecocci et al., 1994; Mecocci et al., 2002; Migliore et al., 2005; Wang et al., 2005). The reason for increased oxidative damage in the progression of AD is at present unclear but could possibly be due to an increase in production of ROS and subsequent increased oxidative stress on DNA or decreased efficiency of DNA repair mechanisms or a combination of the two.

This dissertation is unique in that both DNA oxidative damage in specific genes affected during AD and changes in enzymes of the main DNA repair pathway that (BER)

were studied in a single well-characterized cohort of subjects throughout the progression of AD. This study utilized DNA, RNA and protein isolated from bulk tissue, so the results obtained reflect a comprehensive quantity of oxidative damage, gene expression, protein levels and enzyme activity from both neurons and glia. Previous studies (Nunomura et al., 1999; Smith et al., 2000a; Smith et al., 2000b) have indicated that although AD brains often display increased astrocytosis, 8-hydroxyguanine immunoreactivity was negligible in glial cells but significantly increased in neuronal cytoplasm. This suggests that DNA oxidative damage and changes in the BER enzymes measured in this study are largely a neuronal manifestation rather than a glial one.

4. 1. Oxidative DNA Damage in Genes of Proteins Modified during AD

DNA is vital to cellular function, therefore DNA oxidative damage could possibly be one of the most important factors in the neuronal degeneration observed in AD subjects. This study is the first to determine oxidative damage in the coding sequence of genes of proteins affected during AD in subjects throughout the progression of AD. Oxidative DNA damage was quantified using fpg mediated glycosylase activity and qPCR for the three isoforms of voltage-dependent anion channel protein (VDAC)- VDAC1, VDAC2 and VDAC3. VDACs, also known as mitochondrial porins, are the most abundant proteins in the mitochondrial outer membrane and principally function as voltage-dependent pores in the mitochondrial membrane for transfer of substrates (pyruvate, malate ATP, hemes, NADH, succinate and phosphate) used in oxidative phosphorylation and electron transport chain pathways. The three isoforms, VDAC1, VDAC2 and VDAC3, show an essentially conserved sequence but differ in abundance, size, function and activity. VDAC1 is the most abundant isoform of the VDAC family followed by

VDAC2 and then VDAC3. The VDAC isoforms were chosen for analysis because previous studies show differential expression of protein levels for the three proteins in AD. Yoo et al. (Yoo et al., 2001) reported a significant decrease in VDAC1 levels in the frontal cortex and thalamus and a significant increase in VDAC2 protein levels in temporal cortex in AD subjects compared to age-matched control subjects. Yoo et al. did not report any changes in VDAC3 protein levels as it was not detected in the analyzed samples (Yoo et al., 2001). Lovell et al. showed a statistically significant elevation in VDAC1 protein levels, a trend towards significant increase in VDAC3 levels and no change in VDAC2 levels in primary neuron cultures treated with Aβ (Lovell et al., 2005). Based on these observations, we hypothesized there may be oxidative damage in the coding sequences of VDAC1 and VDAC3 but not in that of VDAC2.

Comparison of oxidative damage in DNA isolated using the phenol-chloroform extraction and extraction using a Qiagen DNeasy Tissue Kit showed 10-20% more artifactual oxidation in DNA from the Qiagen DNeasy Tissue Kit. Thus the phenol-chloroform extraction method was used to extract all DNA samples used in this project. In the phenol-chloroform extraction method, 8-hydroxyquinoline was used as an antioxidant additive to phenol to prevent artifactual oxidation. Furthermore, oxidation by trace metals was prevented by chelation with EDTA during DNA isolation. The study utilized tissue samples from brain specimens with short PMI (Table 2.1) to further reduce the chances of artifactual oxidation. Levels of oxidative DNA damage were quantified using the fpg enzyme, primers designed to encompass each gene's coding sequence and qPCR. The data obtained for this study were analyzed using the standard curve analysis method for qPCR derived from 5 to 7-fold serial dilutions of genomic DNA from NC

subjects. To prevent artifactual oxidation by freeze-thawing, new DNA samples were isolated from tissue for each qPCR reaction. Primers for qPCR were designed to have ~50% GC ratio, 24 bp length, T_m of ~60 (±2) °C and an amplicon size of 175-285 for maximum efficiency. The fluorescent dye SYBR Green which intercalates with dsDNA was used to measure amount of product in the qPCR reaction.

Among the 8 amplicons studied for VDAC1, 3 amplicons including VDAC1D, VDAC1H and VDAC1I showed no statistically significant changes in either the SMTG or cerebellum. In contrast, VDAC1B, VDAC1C, VDAC1E and VDAC1G showed statistically significant increases in % oxidative damage in SMTG of LAD subjects. Levels of % oxidative damage were also significantly elevated in the SMTG of PCAD subjects for VDAC1A, VDAC1C and VDAC1E. A trend towards a significant increase was observed for VDAC1B in SMTG of PCAD subjects and for VDAC1E in SMTG of MCI subjects. The cerebellum, where minimal AD pathology is observed, showed no significant changes at any stage of disease progression suggesting a brain region dependent differential distribution of oxidative DNA damage during the progression of AD. There was significant oxidative damage in the VDAC1B, VDAC1C and VDAC1E amplicons in the SMTG of DC subjects and in cerebellum of DC subjects for the VDAC1B amplicon. This suggests oxidative damage in these two regions is probably not AD-specific but is a shared characteristic of multiple neurodegenerative diseases. The lack of detection of oxidative damage for any VDAC2 amplicon suggests VDAC2 is minimally affected during the progression of AD or other neurodegenerative diseases including FTD and DLB. VDAC3 is the smallest gene among the three and shows oxidative damage only in one amplicon, VDAC3E, in the SMTG of LAD subjects.

These data are supportive of our initial hypothesis. Lovell et al. showed a significant increase in VDAC1 protein levels in Aβ-treated cultures and only a trend towards a significant increase in VDAC3 protein levels and we hypothesized that maximum oxidative damage would be seen in VDAC1 followed by some oxidation in VDAC3. Overall, our studies also suggest oxidative DNA damage in enzymes affected during AD occurs early in AD pathogenesis with more damage in areas with extensive AD pathology. A common characteristic of the regions with more oxidative damage is the presence of groups of multiple guanines. Prat et al. suggested that oxidation of one guanine reduces the ionization potential of sequential guanines present thus promoting increased oxidation (Prat et al., 1998).

At present, it is still unclear what effect genomic oxidation has on subsequent transcription and translation processes. Previous studies show oxidative DNA damage leads to mismatched base pairs (Cysewski and Olinski, 1999), strand breaks (Cullis et al., 1996; Devasagayam et al., 1991) and protein crosslinking (Hickerson et al., 1999; Kurbanyan et al., 2003; Nguyen et al., 2000) in nuclear and mitochondrial DNA. For VDACs, an increase in oxidative damage seems to correlate with increased translation and thus increased protein levels though the impact of this oxidative DNA damage on the functionality of VDAC proteins is as yet unknown. To begin to try and understand the effects of DNA oxidation on translated proteins, we chose to study IGF2, a small protein with a 202 bp coding sequence. Varying ratios of 8-oxoguanine/guanine (10/90, 25/75, 35/65, 50/50, 75/25 and 0/100) were incorporated in the IGF2 coding sequence via PCR reactions and resulting DNA transcribed and translated using a cell-free system. Protein levels generated were quantified using Western blot analysis and showed a significant

increase in IGF2 in all the samples with 8-oxoguanine incorporation, although there was no clear concentration-based trend observed. This is similar to the data observed for VDAC oxidative damage and protein levels (Lovell et al., 2005). A previous study by Hailer-Morrison et al. showed an increase in binding affinity of the p50 subunit of the transcription factor NF-κB on substitution of guanine by 8-oxogunanine at sites critical for protein binding (Hailer-Morrison et al., 2003). Protein activity of IGF2 on the other hand showed significant decreases in 8-oxoguanine incorporated samples compared to the positive control sample. Again there was no concentration based trend observed for enzyme activity with increasing amounts of 8-oxoguanine. A decrease in protein activity could be due to the production of non-functional protein due to presence of oxidation in the gene sequence and hence subsequent mistakes during transcription and translation.

4.2. Changes in DNA Repair Enzymes of BER Pathway in AD Subjects

An increase in oxidative base lesions could be due to inactivity/alterations of the DNA repair enzymes or an increase in oxidative stress on DNA or a combination of both factors (Dianov et al., 2001; Lovell et al., 2000; Wang et al., 2005; Weissman et al., 2007). It is postulated that in age-related neurodegenerative diseases like AD, the DNA repair system loses its capacity for repair resulting in accumulated oxidative DNA damage (Lovell et al., 2000; Markesbery and Lovell, 2006; Moreira et al., 2008; Weissman et al., 2007). In the brain, the BER pathway is the major pathway for repair of small base modifications in DNA caused by oxidation, alkylation or deamination. The BER pathway can primarily be broken down to five key steps: (1) recognition and elimination of damaged base (2) excision of abasic site (3) removal of 5□-abasic terminal fragment (4) gap filling with correct base and (5) ligation of the DNA strand. Based on

the size of the excised nucleotide, the BER pathway is further divided into two sub-pathways: short-patch BER (single nucleotide excision) and long-patch BER (2-8 nucleotides excision). Multiple enzymes including appropriate DNA glycosylases (OGG1, UNG etc.), endonucleases (APE1, FEN1), phosphatases, kinases, polymerases (POLB, POLδ, POLε), PARP1, XRCC1, ligases (LIG1, LIG3) and auxillary factors (e.g. p53, p21, PCNA, RPA) are required for the effective implementation of DNA repair via the BER pathway (Fan and Wilson, 2005; Izumi et al., 2003; Kim and Wilson, 2012; Parsons and Dianov, 2013). Multiple studies have reported alteration in enzymes of the BER pathway in AD subjects although research has been more focused on the enzymes in the early phase of BER specifically OGG1, UNG and APE1 (Coppede and Migliore, 2009; Davydov et al., 2003; Iida et al., 2002; Love et al., 1999; Lovell et al., 2000; Tan et al., 1998; Weissman et al., 2007). This study is unique in the fact that changes in the seven major enzymes of the BER pathway were studied in a single well-characterized cohort of subjects throughout the progression of AD. In order to determine if the DNA repair enzymes of the BER pathway were inactive or altered, custom PCR arrays and quantitative reverse transcription polymerase chain reaction (qPCR), Western blot analysis and enzyme activity assays were used to quantify changes in BER enzymes (OGG1, UNG, APE1, POLB, FEN1, PARP1 and XRCC1).

Substrate-specific DNA glycosylases initiate the BER pathway by recognizing and subsequently removing the impaired base. One of the major lesions of DNA oxidative damage is the oxidation product of guanine, 8-hydroxyguanine which is primarily removed by OGG1 in both nDNA (α-OGG1) and mtDNA (β-OGG1). OGG1 is the one of the best characterized BER proteins but the regulation of OGG1 expression and function,

and consequently its role in multiple diseases including cancer and AD is still being investigated. Studies have suggested association of transcriptional regulation of the OGG1 gene with expression of p53 and Zn depletion (Habib et al., 2008; Sharif et al., 2012; Song et al., 2009; Youn et al., 2007). Our data showed no significant changes in OGG1 gene expression, protein levels or nuclear OGG1 incision activity in the SMTG of MCI subjects compared to NC. In contrast, Shao et al. showed a significant increase in protein levels but a significant decrease in OGG1 activity in the SMTG of MCI subjects compared to NC subjects (Shao et al., 2008; Weissman et al., 2007). In the current study, we saw a statistically significant increase in fold change in gene expression of OGG1, a corresponding statistically significant increase in OGG1 protein levels but no significant changes in OGG1 incision activity in SMTG of PCAD subjects compared to NC subjects, suggesting regulation of OGG1 transcription and translation as a result of injury (oxidative damage) but functional inactivation of the protein. Shao et al. (Shao et al., 2008) suggested that a decrease in OGG1 activity could be due to HNE (4-hydroxynonenal, a by-product of lipid peroxidation) mediated aldehydic modification of OGG1. There was a significant increase in gene expression in SMTG of LAD subjects compared to NC subjects, but no corresponding change in protein level or incision activity of OGG1. The contrast in gene expression levels, protein and activity levels in the current study could be due to formation of modified protein more susceptible to proteolytic degradation after translation from oxidatively damaged genes in a ROS rich environment present in LAD subjects' brain (Tanaka et al., 2007). In contrast, Lovell et al. and others showed decreased OGG1 activity and protein levels in SMTG of LAD subjects compared to NC subjects (Iida et al., 2002; Lovell et al., 2000; Weissman et al.,

2007). No significant differences were observed in gene expression or protein activity in SMTG of DC subjects but there was a significant decrease observed in protein levels compared to NC subjects. Comparison of OGG1 gene expression, protein levels or enzyme activity levels in the cerebellum showed no significant differences for any of the subject groups studied which concurs with previous studies (Iida et al., 2002; Lovell et al., 2000; Weissman et al., 2007).

UNG, another DNA glycosylase highly specific for removal of uracil lesions in nuclear and mitochondrial DNA was also investigated in this study. Uracil can be introduced into genomic DNA by deamination of cytosine to 5'- hydroxyuracil by ROS. A significant decrease in UNG protein levels and activities in AD subjects compared to NC subjects in multiple brain regions was reported by Weissman et al. (Weissman et al., 2007). Our results show a significant increase ($P < 0.05$) in gene expression but no corresponding change in protein levels of UNG in SMTG of MCI subjects compared to NC subjects. UNG activities were significantly higher in the SMTG of MCI subjects compared to NC subjects. There was a significant increase in gene expression but no corresponding change in protein levels of UNG in SMTG of PCAD and LAD subjects compared to NC subjects which could be attributed to modifications in the protein sequence leading to abnormal structure during the translation process due to the presence of oxidized bases in the protein coding sequence. Our study of UNG activity levels show a significant increase in SMTG of PCAD and LAD subjects compared to NC subjects. Previous studies show UNG activities can be enhanced by APE1 (Parikh et al., 1998) which was also elevated in SMTG of PCAD and LAD subjects. For DC subjects, levels of UNG gene expression were significantly elevated in SMTG although there were no

corresponding changes in protein levels or activities compared to NC subjects. This suggests alterations in UNG expression may not be AD-specific but may be a general event associated with neurodegeneration and can be seen in other forms of dementia including FTD and DLB. In the cerebellum, UNG gene expression levels and activity levels showed no significant difference for any of the subject groups studied. UNG protein levels on the other hand showed a significant increase in PCAD subjects in the cerebellum but no changes for the other subject groups.

DNA glycosylases remove damaged bases in a DNA strand generating an apurinic/apyrmidinic (AP) site also called a single strand break (SSB) site. APE1 cleaves the AP site generated in the second step of the BER pathway creating a gap which is filled by DNA polymerases. It has been postulated that this excision of the AP site is the rate determining step of the pathway and that 95% of the excision can be attributed to APE1 (Chen et al., 1991). APE1 also plays a critical role in conservation of gene expression efficiency by regulating DNA binding capacity of multiple transcription factors including p53, NF-κB and AP1 and acting as a transcriptional repressor of its own gene and other genes including the PTH (parathyroid hormone) gene (Fritz, 2000; Izumi et al., 1996). Fritz et al. suggests regulation of APE1 activities by posttranslational modifications although further study is needed to elucidate the different physiological functions and functional regulation of this highly complex multifunctional enzyme (Fritz, 2000; Fritz and Kaina, 1999). Protein-protein interactions with other enzymes in the BER pathway could also contribute to inhibition/enhancement of APE1 function. Studies have shown interactions between APE1 and multiple DNA glycosylases including OGG1 and UNG. A significant increase in activity of both OGG1 and UNG was observed in the

presence of APE1 (Aliyev et al., 2005a; Aliyev et al., 2005b; Aliyev and Aliyev, 2005; Hill et al., 2001; Parikh et al., 1998). Masuda et al. suggested that APE1 underwent product inhibition and showed an increase in APE1 activity in presence of POLB (Masuda et al., 1998). Similarly XRCC1, a scaffold protein involved in the BER pathway, has been shown to stimulate APE1 activity by protein-protein interactions (Sak et al., 2005; Vidal et al., 2001). Although multiple studies have shown physical interaction of APE1 with POLB, FEN1 and p53, the effect of these interactions on APE1 functional regulation needs further investigation (Bennett et al., 1997; Dianova et al., 2001; Gaiddon et al., 1999; Ranalli et al., 2002). It also remains unclear if the redox functions of APE1 affect its endonuclease activity.

Multiple studies have shown an increase in APE1 nuclear immunostaining in the cerebral cortex and hippocampus of AD subjects compared to NC subjects (Edwards et al., 1998a; Edwards et al., 1998b; Marcon et al., 2009). In this study, we found no significant changes in APE1 gene expression or protein levels in SMTG of PCAD or LAD subjects compared to NC subjects. APE1 enzyme activities interestingly were elevated in SMTG of both PCAD and LAD subjects compared to NC subjects. This increased APE1 activity could be due to posttranslational modifications, protein-protein interactions with other enzymes in the pathway or other as yet undiscovered regulatory mechanisms. Previous studies have also suggested interactions between APE1 and OGG1 and UNG that affect enzymatic activity (Aliyev et al., 2005b; Aliyev and Aliyev, 2005; Tengiz et al., 2005). Surprisingly, our data also showed significant reduction in APE1 activity levels in the cerebellum of PCAD and LAD subjects compared to those from NC subjects although no corresponding changes had been observed in gene expression or

APE1 protein levels indicating that changes in APE enzymatic activity could be brain region specific. The decrease in APE1 activity could be due to posttranslational modifications of APE1 such as phosphorylation, acetylation, ubiquitylation, poly(ADP-ribosyl)ation or HNE mediated aldehydic modification as observed for OGG1 (Fritz and Kaina, 1999; Shao et al., 2008). This difference in activity levels in the SMTG (increase) and cerebellum (decrease) could also be due to differential protein-protein interactions with other BER proteins including glycosylases (OGG1, UNG), POLB, FEN1, PARP1 and XRCC1. We found no significant changes in APE1 expression in MCI subjects but there was a statistically significant decrease in APE1 protein levels (but no corresponding change in APE1 activity) in SMTG of MCI and DC subjects compared to NC subjects. This increase in enzymatic activity could be due to the multifactorial reasons discussed previously. The changes seen in DC subjects suggest changes in APE1 are not AD specific but could possibly be present in other forms of dementia also.

The fourth enzyme investigated in this study was POLB. POLB is the primary polymerase for gap filling in both the short-patch and long-patch version of BER (Podlutsky et al., 2001a; Podlutsky et al., 2001b). The vital role played by POLB in fetal growth and development can be deduced by the fact that POLB deficient mice show embryonic lethality (Gu et al., 1994). Although multiple studies have suggested posttranslational modifications including acetylation, methylation, ubiquitylation and phosphorylation play a vital role in regulation of POLB activity and coordination of BER, the functional impact of most of these modifications still needs to be elucidated (El-Andaloussi et al., 2007; El-Andaloussi et al., 2006; Hasan et al., 2002; Parsons et al., 2011; Parsons et al., 2008). Parsons et al. suggested that availability of active BER

enzymes including POLB is directly dependent on the number of DNA lesions present in the cell. They suggested that excess POLB is sequentially ubiquitylated by the ubiquitin ligases Mule and CHIP and then degraded via the proteasome pathway. In case of an increase in amount of DNA lesions, higher amount of active POLB can be obtained by inhibition of Mule activity by the protein ARF (Alternative Reading Frame) and/or deubiquitylation of POLB by ubiquitin-specific proteases (USPs) (Chen et al., 2005; Gallagher et al., 2006; Lee et al., 2005; Parsons et al., 2011; Parsons et al., 2008; Parsons et al., 2009). Mule also regulates the activity of p53 which in turn interacts with multiple BER proteins.

Previous studies have also shown that protein-protein interactions between POLB and other proteins including APE1, PCNA, FEN1, PARP1, XRCC1, WRN, HMGB1, p53, LIG1, LIG3, RPA, Rad9/Rad1/Hus1 (9-1-1 complex) and APC could help in the regulation of POLB activity and selection between SP-BER and LP-BER (Goellner et al., 2012; Yamtich and Sweasy, 2010). APE1 has been shown to stimulate POLB 5□-dRP lyase activity (Bennett et al., 1997) while APC (Adenomatous polyposis coli) inhibits POLB lyase activity (Balusu et al., 2007; Jaiswal et al., 2006; Narayan et al., 2005). Enhanced BER activity observed in the presence of p53 could be due to the interactions of POLB, p53 and APE1 as p53 seems to stabilize the POLB–AP–DNA complex in presence of APE1 (Zhou et al., 2001). XRCC1, LIG1 and APC inhibit POLB strand displacement synthesis thus promoting SP-BER (Balusu et al., 2007; Jaiswal et al., 2006; Kubota et al., 1996; Narayan et al., 2005; Prasad et al., 1996). Though it has been proposed that strand displacement synthesis by POLB is stimulated by FEN1, studies suggest that the impact of the interactions between the two enzymes is more intricate and

may depend on a number of factors including enzyme concentration and nature and amount of substrate. (Balakrishnan et al., 2009; Pascucci et al., 2002; Pascucci et al., 1999; Prasad et al., 2000). POLB strand displacement synthesis is also enhanced by PARP1, the 9-1-1 complex and WRN (Werner syndrome, RecQ helicase) (Harrigan et al., 2003; Prasad et al., 2001; Toueille et al., 2004). POLB has also been shown to interact with multiple other proteins like HMGB1 (high mobility group box 1) and OGG1 but the functional impact of these interactions is not yet fully understood (Braithwaite et al., 2010; Prasad et al., 2007).

Weissman et al. reported a decrease in POLB protein and activity levels in the inferior parietal lobule (IPL) and cerebellum of AD subjects (Weissman et al., 2007). Copani et al. showed a decrease in POLB expression in midtemporal cortex of AD subjects (Copani et al., 2006). Our data is in contrast to both these studies. There were no changes in POLB expression levels in SMTG of MCI subjects but there was a significant decrease in protein levels and surprisingly an increase in POLB enzymatic activity. In this study, we found that there was a statistically significant increase in gene expression in SMTG of PCAD subjects, no corresponding changes in POLB protein levels and interestingly a significant increase in POLB activity. POLB activity levels were also elevated in the cerebellum of PCAD subjects although POLB expression and protein levels were unchanged. It has been proposed that a fraction of POLB produced by the cells is stored in the cytoplasm in its mono-ubiquitylated form and is activated by deubiquitylation when required which in turn depends on the number of DNA lesions and the activity of the enzymes in the early phase of BER (Goellner et al., 2012; Parsons et al., 2011; Woodhouse et al., 2008). This storage mechanism, effects of post translational

modifications, and protein-protein interactions with other BER proteins could account for the discrepancy between gene expression, protein levels and levels of enzymatic activity that we observed. There were no changes in POLB gene expression, protein levels or enzyme activity in the cerebellum of MCI subjects. In the SMTG, there was a significant increase in POLB expression levels, a corresponding increase in protein levels but no analogous changes in enzyme activity in LAD subjects. No changes in POLB gene expression, protein levels or enzyme activity were observed in the cerebellum of LAD subjects. In case of DC subjects, gene expression, protein levels and POLB activity levels were unaltered in the SMTG. Although POLB expression levels were significantly higher in the cerebellum of DC subjects there were no corresponding changes in protein expression and enzymatic activity. In the SMTG, alterations in POLB enzyme levels seem to be an AD-specific event. The changes in POLB in the cerebellum seem to be a more generalized event in neurodegeneration rather than being specific to AD. These results again seem to point to a brain region-specific response to oxidative damage and alteration of BER enzymes.

FEN1 is the major endonuclease involved in LP-BER and cleaves the 5□-flap structure produced by strand-displacement synthesis. FEN1 activity on flap containing substrates has been shown to be stimulated by multiple proteins including POLB, PARP1, LIG1, PCNA, WRN, BLM, HMGB1, Rad9/Rad1/Hus1 complex and even APE1. The interaction of APE1, PARP1 and POLB with FEN1 seems to be a vital factor in stimulation of LP-BER (Brosh et al., 2001; Dianova et al., 2001; Friedrich-Heineken et al., 2005; Prasad et al., 2000; Prasad et al., 2001; Prasad et al., 2007; Ranalli et al., 2002; Sharma et al., 2004; Tom et al., 2000; Wu et al., 1996). FEN1 is regulated not just by

protein-protein interactions but also by posttranslational modifications. Phosphorylation of FEN1 by cyclin-dependent kinase1 (Cdk-1)-Cyclin A decreases FEN1 activity and inhibits interaction of FEN1 with PCNA (Henneke et al., 2003). p300 acetylates FEN1 which also leads to reduced FEN1 activity (Hasan et al., 2001). We saw no significant changes in FEN1 expression, protein levels or activity levels in SMTG or cerebellum of MCI subjects. Although there were no changes in gene expression, protein levels were significantly elevated and FEN1 activity levels were significantly decreased in SMTG of PCAD subjects. Surprisingly, the same trend of no change in gene expression, an increase in protein level and a decrease in enzyme activity was observed in the SMTG of LAD subjects and the cerebellum of DC subjects. Translational and posttranslational regulation by protein-protein interactions and posttranslational modifications could account for this trend in FEN1 protein and activity levels. In the cerebellum, no changes in gene expression, protein levels and FEN1 activity were seen in PCAD and LAD subjects. In SMTG of DC subjects, we saw no significant changes in gene expression but observed a decrease in protein level and a corresponding decrease in enzyme activity. Thus, changes in FEN1 seem to be a part of the neurodegenerative process rather than just being AD specific. Different brain regions also seem to have differential distribution of FEN1 alterations.

Although the complete functionality of PARP1 still needs to be elucidated, it has been proposed that PARP1 plays an extremely critical role in BER as recruiter for other BER proteins to the damaged site and for recognition of the single stranded break (SSB) site. Besides BER, PARP1 is also involved in other cellular processes including transcriptional regulation, cell differentiation, chromatin modification, necrosis and

apoptosis. It has been proposed that PARP1 activity is also regulated by multiple posttranslational modifications including phosphorylation, poly(ADPribosylation), ubiquitylation, sumoylation and acetylation (Strosznajder et al., 2012). The idea that PARP1 is a recruiter protein for the latter half of BER is perpetuated by the interaction of PARP1 with multiple proteins of BER pathway including POLB, FEN1, XRCC1 and LIG3 probably by poly(ADP-ribosyl)ation of these proteins by PARP1. XRCC1 was reported to decrease PARP1 activity (El-Khamisy et al., 2003). Though it is known that PARP1 interacts with multiple other proteins, the functional impact of these interactions on PARP1 activity remains unclear. PARP1 activity has been reported to increase up to 500 fold upon binding to damaged DNA (Adamczyk et al., 2005; Strosznajder et al., 2012). Grube et al. and Muiras et al. found a positive correlation between PARP1 activity and longevity with maximum activity being observed in cells from centenarians though there was no change in PARP1 protein levels (Burkle et al., 1992; Grube and Burkle, 1992; Muiras et al., 1998). Previous studies have reported an increase in PARP1 activity and accumulation of its reaction product, PAR (poly(ADP-ribose)) in frontal and temporal lobes, skin fibroblasts and lymphoblasts in AD patients (Cecchi et al., 2002; Love et al., 1999). PARP1 polymorphisms are also being associated as a risk factor for AD (Infante et al., 2007; Liu et al., 2010).

Our data showed no significant differences in PARP1 expression, protein levels or protein activity in the SMTG or cerebellum of MCI subjects. Although there were no significant changes in gene expression and enzymatic activity in SMTG of PCAD subjects, there was a significant decrease in protein levels. Surprisingly, in the cerebellum of PCAD subjects, there was an increase in protein activity but no analogous changes in

gene expression and protein levels. In the SMTG of LAD subjects, there was a significant increase in gene expression and a significant decrease in protein levels which could be in response to increased pathologic changes. There was a significant increase in enzyme activity in SMTG of LAD subjects which is consistent with the study by Adamczyk et al. that reported increased PARP1 activity on binding to damaged DNA (Adamczyk et al., 2005; Strosznajder et al., 2012). No significant differences in fold change in PARP1 expression levels were observed in the cerebellum of LAD subject but like in the SMTG, protein levels were significantly decreased and activity levels were significantly elevated. The same pattern of no change in gene expression, lower protein levels and higher enzymatic activity was seen in the cerebellum of DC subjects indicating that PARP1 alterations are present in the seemingly non-vulnerable cerebellar region and that these changes are a part of neurodegenration rather than just AD. No changes in gene expression, protein levels and activity were observed in SMTG of DC subjects.

It is proposed that XRCC1 acts as a scaffold protein in the BER pathway as XRCC1 reacts with multiple enzymes of BER but has no apparent enzyme activity. Protein-protein interactions have been reported between XRCC1 and almost all the major enzymes involved in BER indicating the vital role this protein plays in genomic stability. XRCC1 interacts with and affects the activity of DNA glycosylases, APE1, POLB, PARP1, PCNA, LIG1 and LIG3 (El-Khamisy et al., 2003; Kubota et al., 1996; Sak et al., 2005; Strom et al., 2011; Thompson and West, 2000; Vidal et al., 2001) though the effect of these proteins on XRCC1 activity is still not known. Fisher et al. reported down regulation of XRCC1 accumulation at site of DNA damage by the PAR degradation enzyme, poly(ADP-ribose) glycohydrolase (PARG) thus affecting the scaffold action of

XRCC1 (Fisher et al., 2007). We were unable to measure XRCC1 activity as XRCC1 has as yet no known enzymatic function. In SMTG of MCI subjects although no changes in gene expression were observed, there was a significant increase in protein levels. The same trend was observed in SMTG of PCAD subjects and cerebellum of DC subjects. There were no changes in gene expression and protein levels seen in the SMTG of LAD and DC subjects, cerebellum of MCI, PCAD and LAD subjects. Increases in XRCC1 mRNA and protein levels after damage to DNA were reported by Yacoub et al. via activation of the XRCC1 promoter by the transcription factor EGF-2 (Yacoub et al., 2003). It has been proposed that like the other enzymes in BER, XRCC1 is also regulated by posttranslational modifications including ubiquitylation, phosphorylation and PARP1-mediated poly(ADP-ribosyl)ation (El-Khamisy et al., 2003; Parsons et al., 2008; Strom et al., 2011; Whitehouse et al., 2001). XRCC1 deficiency has been shown to decrease BER repair capacity indicating that overall BER functionality may depend to some extent on available active XRCC1 (Brem and Hall, 2005; Iftner et al., 2002; Vidal et al., 2001).

Overall, our findings suggest gene expression of DNA repair pathway enzymes is significantly affected in patients with AD and some of these changes can be seen even in the initial stages of AD (MCI and PCAD). Significant alterations in BER enzymes in the cerebellum, a brain region typically considered as an internal control in AD indicates that oxidative damage and consequently the repair response could be a global event in AD. A few previous studies have also shown disease related changes in the cerebellum. Braak et al. and Yamaguchi et al. showed diffuse amyloid plaques in the cerebellar cortex of AD subjects (Braak et al., 1989; Yamaguchi et al., 1989). A significant decrease in volume of the molecular and granular layers of AD subjects was observed by Wegiel et al. (Wegiel

et al., 1999). Thomann et al. (Thomann et al., 2008) showed a decrease in volume of the posterior cerebellar regions in AD subjects. This study also suggests that changes in BER enzymes could be an event common to neurodegeneration rather than an AD-associated event. The increase in gene expression seen with these proteins could be a compensatory response as the disease progresses. Protein-protein interactions between the various BER proteins and between BER proteins and other proteins like p300, p53 and HMGB1, and posttranslational modifications including ubiquitylation, phosphorylation and PARP1-mediated poly(ADP-ribosyl)ation could account for the alterations in protein levels and enzymatic activity. The changes observed in this study will hopefully provide a platform for further studies investigating the function, regulation and interactions of the enzymes of the complex BER pathway and thus offer further understanding of the ramifications of oxidative stress during the progression of Alzheimer's disease.

Chapter 5: Conclusions

Demographics show that decreasing fertility rates and increased life expectancy have led to an aging world population. Approximately 800 million people were aged 65 and older in 2010 and this number is estimated to grow to 2 billion people by 2050 (22% of world's population) (2010; Bloom et al., 2010; UNPD, 2011). Therefore there is an increasing need for awareness, diagnosis and treatment of age-related diseases including cardiovascular diseases, dementia and Alzheimer's disease. Batsch et al. estimated that in 2010, there were 36 million people suffering from dementia worldwide with a global cost of $604 billion (Batsch, 2012). Approximately 5 million of these AD patients live in the US with the number of AD patients expected to triple to 13.8 million by the year 2050 in the US alone (Thies and Bleiler, 2011, 2013). The cost of AD is an estimated $203 billion in 2013 projected to increase to $1.2 trillion in 2050. This number does not take into account the financial, emotional and physical toll the disease puts on the 15.4 million caregivers who provided an estimated 17.4 billion hours of unpaid care in 2012.

In spite of the increasing threat of financial and health crises that can be created by AD, early detection and treatment of the disease is still in its infancy. Most current drug therapeutics available to patients at present are symptomatic rather than curative/preventive. Although MCI patients are easily diagnosed by a skilled physician, detection of PCAD patients ante-mortem is still challenging. Early detection of AD would help patients be better prepared and possibly in the future have a better chance of treatment. As the exact etiology of AD is still unknown and seems to be multifactorial, it has been difficult for researchers to provide efficient stratagems for treatment. Studies have suggested oxidative stress plays a major role in AD pathogenesis and could thus be

a target for therapeutic strategies (Cooke et al., 2003; Lovell and Markesbery, 2007a; Markesbery, 1997b; Markesbery and Carney, 1999). Recent studies have shown an increase in markers of oxidative damage of biomolecules including proteins, lipids and nucleic acids in AD subjects (Gabbita et al., 1998; Keller et al., 2005; Milne et al., 2005; Williams et al., 2006). DNA oxidative damage is extremely critical in post-mitotic cells like neurons as it could lead to genomic instability, loss of fidelity during transcription and translation, and ultimately cell death. While previous studies have shown an increase in oxidative DNA damage in AD subjects (Gabbita et al., 1998; Lovell and Markesbery, 2001; Wang et al., 2008), it is not yet clear if genomic oxidation is a global, random phenomenon or is it targeted to specific areas of the genome. Accumulation of oxidative DNA damage in AD brains could be due to two factors: an increase in ROS production or breakdown of the repair mechanisms especially the BER pathway (main repair pathway for oxidative damage in brain). The purpose of this study was twofold: (A) to determine if genomic oxidation was targeted to representative genes that show protein alterations during the progression of AD and (B) to determine if increased oxidative DNA damage was a result of a decrease in any of the seven major enzymes of the BER pathway during AD progression, in a single well-characterized cohort of samples.

We hypothesized that oxidative DNA damage is not a random global event but is targeted to specific areas of coding sequences of proteins that ultimately show alterations in AD. To study this, we focused our analyses on the three isoforms of the mitochondrial porin protein, VDAC. VDAC was the ideal candidate for this study as the three forms differ in abundance, size and activity, and are altered differentially in the AD brain. Lovell et al. (Lovell et al., 2005) reported a significant increase in levels of VDAC1, a

trend towards significant increase in VDAC3 and no changes in VDAC2 in Aβ-treated primary neuronal cultures. Based on our hypothesis, we should see the maximum increase/decrease in oxidative damage in VDAC1, some change in VDAC3 and no oxidative damage in VDAC2 coding sequences. Our results support the hypothesis. We saw an increase in oxidative damage in four areas of the VDAC1 coding sequence and one area of the VDAC3 coding sequence in the SMTG of subjects with AD. No oxidative damage was observed in the VDAC2 coding sequence in the SMTG of MCI, PCAD, LAD and DC subjects. Study of the oxidative damage in the 3 VDAC isoforms in tissue specimens from diseased control (FTD and DLB) subjects suggests that oxidative damage in VDAC is a global event associated with neurodegeneration rather than just being AD-specific. We did not see changes in the cerebellum for any of the three isoforms indicating a region-specific attack by ROS on VDAC. It would be interesting to see if this model is replicated for other proteins that show altered levels/activity during AD. As VDAC has no known enzymatic function, we could not measure its activity. It would have been instructive to see if increased genomic oxidation leads to changes in the functionality of the proteins. We observed that when we introduced 8-oxoguanine into a gene sequence (IGF2), there were significant changes in protein levels and activity which would indicate that genomic oxidation leads to changes in transcription and translation. This experiment was unique as the effect of oxidative stress on transcription and translation was studied for the first time using a cell free system.

This oxidative damage seen can be as a result of a breakdown in the DNA repair mechanisms in the brain. The second part of this study focused on investigating if alterations occur in gene expression, protein levels and protein activity levels in the 7

major enzymes involved in the BER pathway in an AD brain. The enzymes studied included OGG1 (major DNA glycosylase for removal of 8-oxoguanine), UNG (uracil DNA glycosylase), APE1 (accounts for 95% endonuclease activity), POLB (major DNA polymerase), FEN1 (major endonuclease in long patch BER), PARP1 (poly(ADP)ribosylation and binding to SSbs) and XRCC1 (scaffold protein). Studies show that null mutation in APE1, POLB, FEN1, PARP1 and XRCC1 are embryonically lethal in mice indicating the vital role these enzymes play in cellular viability and development (Sobol et al., 1996; Tebbs et al., 1999; Woodhouse and Dianov, 2008; Wu et al., 1996; Xanthoudakis and Curran, 1992). The understanding of the BER pathway is further complicated by the fact that these enzymes are regulated by multiple protein-protein interactions and posttranslational modifications. The functional impact of these interactions on some of the BER enzymes is still unknown. Some BER proteins like APE1 and PARP1 are also involved in other cellular pathways making it difficult to fully understand how they are regulated. The study of BER enzymes in AD has mainly focused on OGG1 with relatively few studies of APE1, UNG and POLB. Surprisingly all seven enzymes have not yet been studied in a well-characterized cohort in brain tissue specimens from the SMTG and cerebellum of MCI, PCAD, LAD and DC subjects. We did not see a direct correlation between gene expression, protein levels and protein activity for most of the enzymes which is understandable considering the complexity of the BER pathway and the multitude of interactions each protein undergoes. We saw no changes in gene expression for any of the proteins in SMTG of MCI subjects. Protein levels, on the other hand, were altered for APE1, POLB and XRCC1, and protein activity levels were significantly increased for UNG and POLB in SMTG of MCI subjects. A

significant increase in gene expression was observed for OGG1, UNG and POLB in SMTG of PCAD subjects. Change in protein levels was seen for OGG1, FEN1, PARP1 and XRCC1 and change in protein activity levels were observed for UNG, APE1, POLB and FEN1 in SMTG of PCAD subjects. In SMTG of LAD subjects, changes were seen in OGG1, UNG, POLB and PARP1 expression. Protein levels were altered for POLB, FEN1 and PARP1 and protein activity levels for UNG, FEN1 and PARP1 in SMTG of LAD subjects. Changes were also observed in UNG gene expression; OGG1, APE1 and FEN1 protein levels; and FEN1 protein activity levels in SMTG of DC subjects indicating that alterations in BER enzyme especially the glycosylases and endonucleases could be an event associated with neurodegeneration. The results of the BER pathway analysis are discussed in more detail in Chapters 3 & 4. As some of these enzymes are also involved in other pathways, the alterations could also be due to interactions other than during BER. For example, we saw an increase in PARP1 activity in LAD subjects which implies an increase in BER activity but extensive PARP1 activation can also lead to neuronal death. Thus, the biological significance of all these changes in AD pathogenesis still needs to be elucidated. Some of the effects of protein-protein interactions and posttranslational modifications observed with BER enzymes might be better understood through gene expression, protein level and activity studies in appropriate mouse models. Because APE1, POLB, PARP1, XRCC1 and FEN1 deficient mice show embryonic lethality, the effect of the deficiency of these enzymes can be studied using lentivirus mediated knockdown in mice. We hope the current study will contribute to the understanding of BER enzymes in AD. Expectantly, understanding the changes in BER enzymes will open the platform for identification of novel therapeutic

strategies in AD. Inhibitors to some of the enzymes including APE1 and PARP1 are already either in use to treat cancer patients or are in clinical trials. Recently, PARP1 inhibitors that assuage ischemic brain injury have also been introduced. Thus, as these enzymes are already therapeutic targets for other diseases, hopefully it would be less challenging to go from basic research to develop clinical trials as compared to completely unexplored targets. Most studies of the BER pathway in AD have focused on the glycolysases, especially OGG1. Very few studies are available that evaluate changes in XRCC1 which may be a critical lynchpin of BER. XRCC1 acts as a scaffold protein and also interacts with almost every protein in the BER pathway. Although the effect of interactions between XRCC1 and other BER proteins is unclear there is a strong effect on enzymatic activity at least for some enzymes (APE1, PARP1). This study showed that XRCC1 protein levels were significantly lower in the disease groups, which could be one of the major reasons for decreased BER repair capacity in AD seen by multiple studies. Although more studies are needed to completely understand the role of XRCC1 in BER it is possible that activation of XRCC1 could possibly lead to an increase in repair of DNA oxidative damage making this an interesting novel target for therapeutic strategies.

The cerebellum is usually treated as an internal control in the AD brain as it has less AD-associated pathology. Although our studies didn't show changes in oxidative damage in the VDAC isoforms, we saw significant changes in BER enzymes in the cerebellum. Some of the changes were in marked contrast to the changes observed in the SMTG indicating a region specific response. For example, while there was no difference in PARP1 activity in the SMTG of PCAD and DC subjects, there was a significant elevation observed in the cerebellum of these subjects. So the data from this study suggest that not

only is BER pathway affected during the process of neurodegeneration in general, the BER enzymes show a brain-region specific response even in the absence of substantial disease pathology.

References

2010. World Population Prospects: The 2008 Revision, Highlights. Population and Development Review 36, 854-855.

Adamczyk, A., Jesko, H., Strosznajder, R.P., 2005. Alzheimer's disease related peptides affected cholinergic receptor mediated poly(ADP-ribose) polymerase activity in the hippocampus. Folia Neuropathol 43, 139-142.

Aliyev, A., Chen, S.G., Seyidova, D., Smith, M.A., Perry, G., de la Torre, J., Aliev, G., 2005a. Mitochondria DNA deletions in atherosclerotic hypoperfused brain microvessels as a primary target for the development of Alzheimer's disease. J Neurol Sci 229-230, 285-292.

Aliyev, F., Habeb, M., Babalik, E., Karadag, B., 2005b. Thrombolysis with streptokinase during cardiopulmonary resuscitation: a single center experience and review of the literature. J Thromb Thrombolysis 20, 169-173.

Aliyev, N.A., Aliyev, Z.N., 2005. Application of glycine in acute alcohol hallucinosis. Hum Psychopharmacol 20, 591-594.

Apel, K., Hirt, H., 2004. Reactive oxygen species: metabolism, oxidative stress, and signal transduction. Annu Rev Plant Biol 55, 373-399.

Arya, M., Shergill, I.S., Williamson, M., Gommersall, L., Arya, N., Patel, H.R., 2005. Basic principles of real-time quantitative PCR. Expert Rev Mol Diagn 5, 209-219.

Balakrishnan, L., Brandt, P.D., Lindsey-Boltz, L.A., Sancar, A., Bambara, R.A., 2009. Long patch base excision repair proceeds via coordinated stimulation of the multienzyme DNA repair complex. Journal of Biological Chemistry 284, 15158-15172.

Balusu, R., Jaiswal, A.S., Armas, M.L., Kundu, C.N., Bloom, L.B., Narayan, S., 2007. Structure/function analysis of the interaction of adenomatous polyposis coli with DNA polymerase beta and its implications for base excision repair. Biochemistry 46, 13961-13974.

Batsch, N.L., Mittelman, M.S., 2012. World Alzheimer Report 2012, Overcoming the stigma of dementia. Alzheimer’s Disease International, London.

Beal, M.F., 2005. Mitochondria take center stage in aging and neurodegeneration. Ann Neurol 58, 495-505.

Bennett, R.A., Wilson, D.M., 3rd, Wong, D., Demple, B., 1997. Interaction of human apurinic endonuclease and DNA polymerase beta in the base excision repair pathway. Proc Natl Acad Sci U S A 94, 7166-7169.

Bhattacharya, P.K., Barton, J.K., 2001. Influence of intervening mismatches on long-range guanine oxidation in DNA duplexes. Journal of the American Chemical Society 123, 8649-8656.

Bloom, D.E., Canning, D., Fink, G., 2010. Implications of population ageing for economic growth. Oxford Review of Economic Policy 26, 583-612.

Bohr, V.A., 2002. Repair of oxidative DNA damage in nuclear and mitochondrial DNA, and some changes with aging in mammalian cells. Free Radic Biol Med 32, 804-812.

Bowling, A.C., Schulz, J.B., Brown, R.H., Jr., Beal, M.F., 1993. Superoxide dismutase activity, oxidative damage, and mitochondrial energy metabolism in familial and sporadic amyotrophic lateral sclerosis. J Neurochem 61, 2322-2325.

Braak, H., Braak, E., 1991. Neuropathological stageing of Alzheimer-related changes. Acta Neuropathol 82, 239-259.

Braak, H., Braak, E., 1997. Frequency of stages of Alzheimer-related lesions in different age categories. Neurobiol Aging 18, 351-357.

Braak, H., Braak, E., Bohl, J., Lang, W., 1989. Alzheimer's disease: amyloid plaques in the cerebellum. Journal of the neurological sciences 93, 277-287.

Bradley, M.A., Markesbery, W.R., Lovell, M.A., 2010. Increased levels of 4-hydroxynonenal and acrolein in the brain in preclinical Alzheimer disease. Free Radical Biology and Medicine 48, 1570-1576.

Braithwaite, E.K., Kedar, P.S., Stumpo, D.J., Bertocci, B., Freedman, J.H., Samson, L.D., Wilson, S.H., 2010. DNA polymerases beta and lambda mediate overlapping and independent roles in base excision repair in mouse embryonic fibroblasts. PLoS One 5, e12229.

Brem, R., Hall, J., 2005. XRCC1 is required for DNA single-strand break repair in human cells. Nucleic Acids Res 33, 2512-2520.

Brookmeyer, R., Corrada, M.M., Curriero, F.C., Kawas, C., 2002. Survival following a diagnosis of Alzheimer disease. Arch Neurol 59, 1764-1767.

Brosh, R.M., Jr., von Kobbe, C., Sommers, J.A., Karmakar, P., Opresko, P.L., Piotrowski, J., Dianova, I., Dianov, G.L., Bohr, V.A., 2001. Werner syndrome protein interacts with human flap endonuclease 1 and stimulates its cleavage activity. Embo Journal 20, 5791-5801.

Bruce-Keller, A.J., Begley, J.G., Fu, W., Butterfield, D.A., Bredesen, D.E., Hutchins, J.B., Hensley, K., Mattson, M.P., 1998a. Bcl-2 protects isolated plasma and mitochondrial membranes against lipid peroxidation induced by hydrogen peroxide and amyloid beta-peptide. J Neurochem 70, 31-39.

Bruce-Keller, A.J., Li, Y.J., Lovell, M.A., Kraemer, P.J., Gary, D.S., Brown, R.R., Markesbery, W.R., Mattson, M.P., 1998b. 4-Hydroxynonenal, a product of lipid peroxidation, damages cholinergic neurons and impairs visuospatial memory in rats. J Neuropathol Exp Neurol 57, 257-267.

Burkle, A., Grube, K., Kupper, J.H., 1992. Poly(ADP-ribosyl)ation: its role in inducible DNA amplification, and its correlation with the longevity of mammalian species. Exp Clin Immunogenet 9, 230-240.

Burns, A., Iliffe, S., 2009. Alzheimer's disease. BMJ 338, b158.

Bustin, S.A., Benes, V., Nolan, T., Pfaffl, M.W., 2005. Quantitative real-time RT-PCR--a perspective. J Mol Endocrinol 34, 597-601.

Candeias, L.P., Steenken, S., 1989. Structure and Acid-Base Properties of One-Electron-Oxidized Deoxyguanosine, Guanosine, and 1-Methylguanosine. Journal of the American Chemical Society 111, 1094-1099.

Cecchi, C., Fiorillo, C., Sorbi, S., Latorraca, S., Nacmias, B., Bagnoli, S., Nassi, P., Liguri, G., 2002. Oxidative stress and reduced antioxidant defenses in peripheral cells from familial Alzheimer's patients. Free Radic Biol Med 33, 1372-1379.

Chapman, J.R., Taylor, M.R., Boulton, S.J., 2012. Playing the end game: DNA double-strand break repair pathway choice. Mol Cell 47, 497-510.

Chen, D., Kon, N., Li, M., Zhang, W., Qin, J., Gu, W., 2005. ARF-BP1/Mule is a critical mediator of the ARF tumor suppressor. Cell 121, 1071-1083.

Chen, D.S., Herman, T., Demple, B., 1991. Two distinct human DNA diesterases that hydrolyze 3'-blocking deoxyribose fragments from oxidized DNA. Nucleic Acids Res 19, 5907-5914.

Cheng, K.C., Cahill, D.S., Kasai, H., Nishimura, S., Loeb, L.A., 1992. 8-Hydroxyguanine, an Abundant Form of Oxidative DNA Damage, Causes G -> T and a -> C Substitutions. Journal of Biological Chemistry 267, 166-172.

Cooke, M.S., Evans, M.D., Dizdaroglu, M., Lunec, J., 2003. Oxidative DNA damage: mechanisms, mutation, and disease. FASEB J 17, 1195-1214.

Copani, A., Hoozemans, J.J., Caraci, F., Calafiore, M., Van Haastert, E.S., Veerhuis, R., Rozemuller, A.J., Aronica, E., Sortino, M.A., Nicoletti, F., 2006. DNA polymerase-beta is expressed early in neurons of Alzheimer's disease brain and is loaded into DNA replication forks in neurons challenged with beta-amyloid. Journal of Neuroscience 26, 10949-10957.

Coppede, F., Migliore, L., 2009. DNA damage and repair in Alzheimer's disease. Curr Alzheimer Res 6, 36-47.

Croteau, D.L., Bohr, V.A., 1997. Repair of oxidative damage to nuclear and mitochondrial DNA in mammalian cells. Journal of Biological Chemistry 272, 25409-25412.

Cuadrado-Tejedor, M., Vilarino, M., Cabodevilla, F., Del Rio, J., Frechilla, D., Perez-Mediavilla, A., 2011. Enhanced expression of the voltage-dependent anion channel 1 (VDAC1) in Alzheimer's disease transgenic mice: an insight into the pathogenic effects of amyloid-beta. J Alzheimers Dis 23, 195-206.

Cullis, P.M., Malone, M.E., Merson-Davies, L.A., 1996. Guanine radical cations are precusors of 7,8-dihydro-8-oxo-2'-deoxyguanosine but are not precusors of immediate strand breaks in DNA. Journal of American Chemical Society 118, 6.

Cysewski, P., Olinski, R., 1999. Theoretical description of the coding potential of diamino-5-formamidopyrimidines. Z Naturforsch C 54, 6.

Davydov, V., Hansen, L.A., Shackelford, D.A., 2003. Is DNA repair compromised in Alzheimer's disease? Neurobiol Aging 24, 953-968.

DeCarli, C., 2003. Mild cognitive impairment: prevalence, prognosis, aetiology, and treatment. Lancet Neurol 2, 15-21.

Derveaux, S., Vandesompele, J., Hellemans, J., 2010. How to do successful gene expression analysis using real-time PCR. Methods 50, 227-230.

Devasagayam, T.P.A., Steeken, S., Maik, S., Obendorf, W., Schulz, W.A., Sies, H., 1991. Formation of 8-hdyroxy(deoxy)guanosine and generation of strand breaks at guanine residues in DNA by singlet oxygen. Journal of American Chemical Society 30, 7.

Dianov, G.L., Souza-Pinto, N., Nyaga, S.G., Thybo, T., Stevnsner, T., Bohr, V.A., 2001. Base excision repair in nuclear and mitochondrial DNA. Prog Nucleic Acid Res Mol Biol 68, 285-297.

Dianova, II, Bohr, V.A., Dianov, G.L., 2001. Interaction of human AP endonuclease 1 with flap endonuclease 1 and proliferating cell nuclear antigen involved in long-patch base excision repair. Biochemistry 40, 12639-12644.

Dogru-Abbasoglu, S., Aykac-Toker, G., Hanagasi, H.A., Gurvit, H., Emre, M., Uysal, M., 2007. The Arg194Trp polymorphism in DNA repair gene XRCC1 and the risk for sporadic late-onset Alzheimer's disease. Neurol Sci 28, 31-34.

Dorjsuren, D., Kim, D., Maloney, D.J., Wilson, D.M., 3rd, Simeonov, A., 2011. Complementary non-radioactive assays for investigation of human flap endonuclease 1 activity. Nucleic Acids Res 39, e11.

Du, Y., Wooten, M.C., Gearing, M., Wooten, M.W., 2009. Age-associated oxidative damage to the p62 promoter: implications for Alzheimer disease. Free Radic Biol Med 46, 492-501.

Dubois, B., Feldman, H.H., Jacova, C., Dekosky, S.T., Barberger-Gateau, P., Cummings, J., Delacourte, A., Galasko, D., Gauthier, S., Jicha, G., Meguro, K., O'Brien, J., Pasquier, F., Robert, P., Rossor, M., Salloway, S., Stern, Y., Visser, P.J., Scheltens, P., 2007. Research criteria for the diagnosis of Alzheimer's disease: revising the NINCDS-ADRDA criteria. Lancet Neurol 6, 734-746.

Edwards, M., Kent, T.A., Rea, H.C., Wei, J., Quast, M., Izumi, T., Mitra, S., Perez-Polo, J.R., 1998a. APE/Ref-1 responses to ischemia in rat brain. Neuroreport 9, 4015-4018.

Edwards, M., Rassin, D.K., Izumi, T., Mitra, S., Perez-Polo, J.R., 1998b. APE/Ref-1 responses to oxidative stress in aged rats. J Neurosci Res 54, 635-638.

El-Andaloussi, N., Valovka, T., Toueille, M., Hassa, P.O., Gehrig, P., Covic, M., Hubscher, U., Hottiger, M.O., 2007. Methylation of DNA polymerase beta by protein arginine methyltransferase 1 regulates its binding to proliferating cell nuclear antigen. FASEB J 21, 26-34.

El-Andaloussi, N., Valovka, T., Toueille, M., Steinacher, R., Focke, F., Gehrig, P., Covic, M., Hassa, P.O., Schar, P., Hubscher, U., Hottiger, M.O., 2006. Arginine methylation regulates DNA polymerase beta. Mol Cell 22, 51-62.

El-Khamisy, S.F., Masutani, M., Suzuki, H., Caldecott, K.W., 2003. A requirement for PARP-1 for the assembly or stability of XRCC1 nuclear foci at sites of oxidative DNA damage. Nucleic Acids Res 31, 5526-5533.

Espy, M.J., Uhl, J.R., Sloan, L.M., Buckwalter, S.P., Jones, M.F., Vetter, E.A., Yao, J.D., Wengenack, N.L., Rosenblatt, J.E., Cockerill, F.R., 3rd, Smith, T.F., 2006. Real-time PCR in clinical microbiology: applications for routine laboratory testing. Clin Microbiol Rev 19, 165-256.

Evans, D.A., Funkenstein, H.H., Albert, M.S., Scherr, P.A., Cook, N.R., Chown, M.J., Hebert, L.E., Hennekens, C.H., Taylor, J.O., 1989. Prevalence of Alzheimer's disease in a community population of older persons. Higher than previously reported. JAMA 262, 2551-2556.

Fagan, A.M., Csernansky, C.A., Morris, J.C., Holtzman, D.M., 2005. The search for antecedent biomarkers of Alzheimer's disease. J Alzheimers Dis 8, 347-358.

Fan, J., Wilson, D.M., 3rd, 2005. Protein-protein interactions and posttranslational modifications in mammalian base excision repair. Free Radic Biol Med 38, 1121-1138.

Farrer, L.A., Cupples, L.A., Haines, J.L., Hyman, B., Kukull, W.A., Mayeux, R., Myers, R.H., Pericak-Vance, M.A., Risch, N., van Duijn, C.M., 1997. Effects of age, sex, and ethnicity on the association between apolipoprotein E genotype and Alzheimer disease. A meta-analysis. APOE and Alzheimer Disease Meta Analysis Consortium. JAMA 278, 1349-1356.

Ferman, T.J., Boeve, B.F., 2007. Dementia with Lewy bodies. Neurol Clin 25, 741-760, vii.

Fisher, A.E., Hochegger, H., Takeda, S., Caldecott, K.W., 2007. Poly(ADP-ribose) polymerase 1 accelerates single-strand break repair in concert with poly(ADP-ribose) glycohydrolase. Mol Cell Biol 27, 5597-5605.

Friedrich-Heineken, E., Toueille, M., Tannler, B., Burki, C., Ferrari, E., Hottiger, M.O., Hubscher, U., 2005. The two DNA clamps Rad9/Rad1/Hus1 complex and proliferating

cell nuclear antigen differentially regulate flap endonuclease 1 activity. J Mol Biol 353, 980-989.

Fritz, G., 2000. Human APE/Ref-1 protein. Int J Biochem Cell Biol 32, 925-929.

Fritz, G., Kaina, B., 1999. Phosphorylation of the DNA repair protein APE/REF-1 by CKII affects redox regulation of AP-1. Oncogene 18, 1033-1040.

Gabbita, S.P., Lovell, M.A., Markesbery, W.R., 1998. Increased nuclear DNA oxidation in the brain in Alzheimer's disease. J Neurochem 71, 2034-2040.

Gaiddon, C., Moorthy, N.C., Prives, C., 1999. Ref-1 regulates the transactivation and pro-apoptotic functions of p53 in vivo. Embo Journal 18, 5609-5621.

Gallagher, S.J., Kefford, R.F., Rizos, H., 2006. The ARF tumour suppressor. Int J Biochem Cell Biol 38, 1637-1641.

Garrett, R., Grisham, C.M., 2010. Biochemistry, 4th ed. Brooks/Cole, Cengage Learning, Belmont, CA.

Geddes, J.W., Tekirian, T.L., Soultanian, N.S., Ashford, J.W., Davis, D.G., Markesbery, W.R., 1997. Comparison of neuropathologic criteria for the diagnosis of Alzheimer's disease. Neurobiol Aging 18, S99-105.

Geldmacher, D.S., 2004. Dementia with Lewy bodies: diagnosis and clinical approach. Cleve Clin J Med 71, 789-790, 792-784, 797-788 passim.

Gicquel, C., Weiss, J., Amiel, J., Gaston, V., Le Bouc, Y., Scott, C.D., 2004. Epigenetic abnormalities of the mannose-6-phosphate/IGF2 receptor gene are uncommon in human overgrowth syndromes. J Med Genet 41, e4.

Goellner, E.M., Svilar, D., Almeida, K.H., Sobol, R.W., 2012. Targeting DNA polymerase ss for therapeutic intervention. Curr Mol Pharmacol 5, 68-87.

Graff-Radford, N.R., Woodruff, B.K., 2007. Frontotemporal dementia. Semin Neurol 27, 48-57.

Grossman, M., 2002. Frontotemporal dementia: A review. Journal of the International Neuropsychological Society 8, 566-583.

Grube, K., Burkle, A., 1992. Poly(ADP-ribose) polymerase activity in mononuclear leukocytes of 13 mammalian species correlates with species-specific life span. Proc Natl Acad Sci U S A 89, 11759-11763.

Grundke-Iqbal, I., Iqbal, K., Tung, Y.C., Quinlan, M., Wisniewski, H.M., Binder, L.I., 1986. Abnormal phosphorylation of the microtubule-associated protein tau (tau) in Alzheimer cytoskeletal pathology. Proc Natl Acad Sci U S A 83, 4913-4917.

Gu, H., Marth, J.D., Orban, P.C., Mossmann, H., Rajewsky, K., 1994. Deletion of a DNA polymerase beta gene segment in T cells using cell type-specific gene targeting. Science 265, 103-106.

Gustafson, D., Rothenberg, E., Blennow, K., Steen, B., Skoog, I., 2003. An 18-year follow-up of overweight and risk of Alzheimer disease. Arch Intern Med 163, 1524-1528.

Habib, S.L., Riley, D.J., Mahimainathan, L., Bhandari, B., Choudhury, G.G., Abboud, H.E., 2008. Tuberin regulates the DNA repair enzyme OGG1. Am J Physiol Renal Physiol 294, F281-290.

Hailer-Morrison, M.K., Kotler, J.M., Martin, B.D., Sugden, K.D., 2003. Oxidized guanine lesions as modulators of gene transcription. Altered p50 binding affinity and repair shielding by 7,8-dihydro-8-oxo-2'deoxyguanosine lesions in the NF-kappaB promoter element. Biochemistry 42, 10.

Harman, D., 1956. Aging: a theory based on free radical and radiation chemistry. J Gerontol 11, 298-300.

Harrigan, J.A., Opresko, P.L., von Kobbe, C., Kedar, P.S., Prasad, R., Wilson, S.H., Bohr, V.A., 2003. The Werner syndrome protein stimulates DNA polymerase beta strand displacement synthesis via its helicase activity. Journal of Biological Chemistry 278, 22686-22695.

Hasan, S., El-Andaloussi, N., Hardeland, U., Hassa, P.O., Burki, C., Imhof, R., Schar, P., Hottiger, M.O., 2002. Acetylation regulates the DNA end-trimming activity of DNA polymerase beta. Mol Cell 10, 1213-1222.

Hasan, S., Stucki, M., Hassa, P.O., Imhof, R., Gehrig, P., Hunziker, P., Hubscher, U., Hottiger, M.O., 2001. Regulation of human flap endonuclease-1 activity by acetylation through the transcriptional coactivator p300. Mol Cell 7, 1221-1231.

Hebert, L.E., Weuve, J., Scherr, P.A., Evans, D.A., 2013. Alzheimer disease in the United States (2010-2050) estimated using the 2010 census. Neurology.

Hegde, M.L., Hazra, T.K., Mitra, S., 2008. Early steps in the DNA base excision/single-strand interruption repair pathway in mammalian cells. Cell Res 18, 27-47.

Henchcliffe, C., Dodel, R., Beal, M.F., 2011. Biomarkers of Parkinson's disease and Dementia with Lewy bodies. Prog Neurobiol 95, 601-613.

Henderson, A.S., 1986. The epidemiology of Alzheimer's disease. Br Med Bull 42, 3-10.

Henneke, G., Koundrioukoff, S., Hubscher, U., 2003. Phosphorylation of human Fen1 by cyclin-dependent kinase modulates its role in replication fork regulation. Oncogene 22, 4301-4313.

Hensley, K., Hall, N., Subramaniam, R., Cole, P., Harris, M., Aksenov, M., Aksenova, M., Gabbita, S.P., Wu, J.F., Carney, J.M., et al., 1995. Brain regional correspondence between Alzheimer's disease histopathology and biomarkers of protein oxidation. J Neurochem 65, 2146-2156.

Hickerson, R.P., Chepanoske, C.L., Williams, S.D., David, S.S., Burrows, C.J., 1999. Mechansims-based DNA-protein cross-linking of MutY via oxidation of 8-oxoguanosine. Journal of American Chemical Society 121, 2.

Higuchi, R., Fockler, C., Dollinger, G., Watson, R., 1993. Kinetic PCR analysis: real-time monitoring of DNA amplification reactions. Biotechnology (N Y) 11, 1026-1030.

Hill, J.W., Hazra, T.K., Izumi, T., Mitra, S., 2001. Stimulation of human 8-oxoguanine-DNA glycosylase by AP-endonuclease: potential coordination of the initial steps in base excision repair. Nucleic Acids Res 29, 430-438.

Hippius, H., Neundorfer, G., 2003. The discovery of Alzheimer's disease. Dialogues Clin Neurosci 5, 101-108.

Hollingworth, P., Harold, D., Jones, L., Owen, M.J., Williams, J., 2011. Alzheimer's disease genetics: current knowledge and future challenges. Int J Geriatr Psychiatry 26, 793-802.

Hsieh, P., Yamane, K., 2008. DNA mismatch repair: molecular mechanism, cancer, and ageing. Mech Ageing Dev 129, 391-407.

Hutton, M., Lendon, C.L., Rizzu, P., Baker, M., Froelich, S., Houlden, H., Pickering-Brown, S., Chakraverty, S., Isaacs, A., Grover, A., Hackett, J., Adamson, J., Lincoln, S., Dickson, D., Davies, P., Petersen, R.C., Stevens, M., de Graaff, E., Wauters, E., van Baren, J., Hillebrand, M., Joosse, M., Kwon, J.M., Nowotny, P., Che, L.K., Norton, J., Morris, J.C., Reed, L.A., Trojanowski, J., Basun, H., Lannfelt, L., Neystat, M., Fahn, S., Dark, F., Tannenberg, T., Dodd, P.R., Hayward, N., Kwok, J.B., Schofield, P.R.,

Andreadis, A., Snowden, J., Craufurd, D., Neary, D., Owen, F., Oostra, B.A., Hardy, J., Goate, A., van Swieten, J., Mann, D., Lynch, T., Heutink, P., 1998. Association of missense and 5'-splice-site mutations in tau with the inherited dementia FTDP-17. Nature 393, 702-705.

Iftner, T., Elbel, M., Schopp, B., Hiller, T., Loizou, J.I., Caldecott, K.W., Stubenrauch, F., 2002. Interference of papillomavirus E6 protein with single-strand break repair by interaction with XRCC1. Embo Journal 21, 4741-4748.

Iida, T., Furuta, A., Nishioka, K., Nakabeppu, Y., Iwaki, T., 2002. Expression of 8-oxoguanine DNA glycosylase is reduced and associated with neurofibrillary tangles in Alzheimer's disease brain. Acta Neuropathol 103, 20-25.

Infante, J., Llorca, J., Mateo, I., Rodriguez-Rodriguez, E., Sanchez-Quintana, C., Sanchez-Juan, P., Fernandez-Viadero, C., Pena, N., Berciano, J., Combarros, O., 2007. Interaction between poly(ADP-ribose) polymerase 1 and interleukin 1A genes is associated with Alzheimer's disease risk. Dement Geriatr Cogn Disord 23, 215-218.

Izumi, T., Henner, W.D., Mitra, S., 1996. Negative regulation of the major human AP-endonuclease, a multifunctional protein. Biochemistry 35, 14679-14683.

Izumi, T., Wiederhold, L.R., Roy, G., Roy, R., Jaiswal, A., Bhakat, K.K., Mitra, S., Hazra, T.K., 2003. Mammalian DNA base excision repair proteins: their interactions and role in repair of oxidative DNA damage. Toxicology 193, 43-65.

Jacobsen, E., Beach, T., Shen, Y., Li, R., Chang, Y., 2004. Deficiency of the Mre11 DNA repair complex in Alzheimer's disease brains. Brain Res Mol Brain Res 128, 1-7.

Jaiswal, A.S., Balusu, R., Armas, M.L., Kundu, C.N., Narayan, S., 2006. Mechanism of adenomatous polyposis coli (APC)-mediated blockage of long-patch base excision repair. Biochemistry 45, 15903-15914.

Jenner, P., 2003. Oxidative stress in Parkinson's disease. Ann Neurol 53 Suppl 3, S26-36; discussion S36-28.

Jicha, G.A., Markesbery, W.R., 2010. Omega-3 fatty acids: potential role in the management of early Alzheimer's disease. Clin Interv Aging 5, 45-61.

Kainz, P., 2000. The PCR plateau phase - towards an understanding of its limitations. Biochim Biophys Acta 1494, 23-27.

Kawas, C., Gray, S., Brookmeyer, R., Fozard, J., Zonderman, A., 2000. Age-specific incidence rates of Alzheimer's disease: the Baltimore Longitudinal Study of Aging. Neurology 54, 2072-2077.

Keith-Rokosh, J., Ang, L.C., 2008. Progressive supranuclear palsy: a review of co-existing neurodegeneration. Can J Neurol Sci 35, 602-608.

Keller, J.N., Schmitt, F.A., Scheff, S.W., Ding, Q., Chen, Q., Butterfield, D.A., Markesbery, W.R., 2005. Evidence of increased oxidative damage in subjects with mild cognitive impairment. Neurology 64, 1152-1156.

Khachaturian, Z.S., Radebaugh, T.S., 1996. Alzheimer's Disease: Cause(s), Diagnosis, Treatment, and Care CRC Press, Boca Raton, FL

Kim, Y.J., Wilson, D.M., 3rd, 2012. Overview of base excision repair biochemistry. Curr Mol Pharmacol 5, 3-13.

Kruman, II, Schwartz, E., Kruman, Y., Cutler, R.G., Zhu, X., Greig, N.H., Mattson, M.P., 2004. Suppression of uracil-DNA glycosylase induces neuronal apoptosis. Journal of Biological Chemistry 279, 43952-43960.

Kubota, Y., Nash, R.A., Klungland, A., Schar, P., Barnes, D.E., Lindahl, T., 1996. Reconstitution of DNA base excision-repair with purified human proteins: interaction between DNA polymerase beta and the XRCC1 protein. Embo Journal 15, 6662-6670.

Kurbanyan, K., Nguyen, K.L., To, P., Rivas, E.V., Lueras, A.M., Kosinski, C., Steryo, M., Gonzalez, A., Mah, D.A., Stemp, E.D., 2003. DNA-protein cross-linking via guanine oxidation: dependence upon protein and photosensitizer. Biochemistry 42, 10269-10281.

Lambon Ralph, M.A., Graham, K.S., Patterson, K., Hodges, J.R., 1999. Is a picture worth a thousand words? Evidence from concept definitions by patients with semantic dementia. Brain and Language 70, 309-335.

Lange, K.L., Bondi, M.W., Salmon, D.P., Galasko, D., Delis, D.C., Thomas, R.G., Thal, L.J., 2002. Decline in verbal memory during preclinical Alzheimer's disease: examination of the effect of APOE genotype. J Int Neuropsychol Soc 8, 943-955.

Lee, C., Smith, B.A., Bandyopadhyay, K., Gjerset, R.A., 2005. DNA damage disrupts the p14ARF-B23(nucleophosmin) interaction and triggers a transient subnuclear redistribution of p14ARF. Cancer Res 65, 9834-9842.

Lehninger, A.L., Nelson, D.L., Cox, M.M., 2005. Lehninger principles of biochemistry, 4th ed. W.H. Freeman, New York.

Liu, H.P., Lin, W.Y., Wu, B.T., Liu, S.H., Wang, W.F., Tsai, C.H., Lee, C.C., Tsai, F.J., 2010. Evaluation of the poly(ADP-ribose) polymerase-1 gene variants in Alzheimer's disease. J Clin Lab Anal 24, 182-186.

Livak, K.J., Schmittgen, T.D., 2001. Analysis of relative gene expression data using real-time quantitative PCR and the 2(-Delta Delta C(T)) Method. Methods 25, 402-408.

Loft, S., Hogh Danielsen, P., Mikkelsen, L., Risom, L., Forchhammer, L., Moller, P., 2008. Biomarkers of oxidative damage to DNA and repair. Biochem Soc Trans 36, 1071-1076.

Love, S., Barber, R., Wilcock, G.K., 1999. Increased poly(ADP-ribosyl)ation of nuclear proteins in Alzheimer's disease. Brain 122 (Pt 2), 247-253.

Lovell, M.A., Ehmann, W.D., Markesbery, W.R., 1993. Laser microprobe analysis of brain aluminum in Alzheimer's disease. Annals of neurology 33, 36-42.

Lovell, M.A., Gabbita, S.P., Markesbery, W.R., 1999. Increased DNA oxidation and decreased levels of repair products in Alzheimer's disease ventricular CSF. J Neurochem 72, 771-776.

Lovell, M.A., Markesbery, W.R., 2001. Ratio of 8-hydroxyguanine in intact DNA to free 8-hydroxyguanine is increased in Alzheimer disease ventricular cerebrospinal fluid. Arch Neurol 58, 392-396.

Lovell, M.A., Markesbery, W.R., 2007a. Oxidative damage in mild cognitive impairment and early Alzheimer's disease. J Neurosci Res 85, 3036-3040.

Lovell, M.A., Markesbery, W.R., 2007b. Oxidative DNA damage in mild cognitive impairment and late-stage Alzheimer's disease. Nucleic Acids Res 35, 7497-7504.

Lovell, M.A., Robertson, J.D., Teesdale, W.J., Campbell, J.L., Markesbery, W.R., 1998. Copper, iron and zinc in Alzheimer's disease senile plaques. Journal of the neurological sciences 158, 47-52.

Lovell, M.A., Xie, C., Markesbery, W.R., 2000. Decreased base excision repair and increased helicase activity in Alzheimer's disease brain. Brain Res 855, 116-123.

Lovell, M.A., Xiong, S.L., Markesbery, W.R., Lynn, B.C., 2005. Quantitative proteomic analysis of mitochondria from primary neuron cultures treated with amyloid beta peptide. Neurochem Res 30, 113-122.

Lu, T., Pan, Y., Kao, S.Y., Li, C., Kohane, I., Chan, J., Yankner, B.A., 2004. Gene regulation and DNA damage in the ageing human brain. Nature 429, 883-891.

Lyras, L., Cairns, N.J., Jenner, A., Jenner, P., Halliwell, B., 1997. An assessment of oxidative damage to proteins, lipids, and DNA in brain from patients with Alzheimer's disease. J Neurochem 68, 2061-2069.

Lyras, L., Perry, R.H., Perry, E.K., Ince, P.G., Jenner, A., Jenner, P., Halliwell, B., 1998. Oxidative damage to proteins, lipids, and DNA in cortical brain regions from patients with dementia with Lewy bodies. J Neurochem 71, 302-312.

Mackay, I.M., Arden, K.E., Nitsche, A., 2002. Real-time PCR in virology. Nucleic Acids Res 30, 1292-1305.

Mahapatra, R.K., Edwards, M.J., Schott, J.M., Bhatia, K.P., 2004. Corticobasal degeneration. Lancet Neurol 3, 736-743.

Mann, D.M., Jones, D., Prinja, D., Purkiss, M.S., 1990. The prevalence of amyloid (A4) protein deposits within the cerebral and cerebellar cortex in Down's syndrome and Alzheimer's disease. Acta Neuropathol 80, 318-327.

Mao, G.G., Pan, X.Y., Zhu, B.B., Zhang, Y.B., Yuan, F.H., Huang, J., Lovell, M.A., Lee, M.P., Markesbery, W.R., Li, G.M., Gu, L.Y., 2007. Identification and characterization of OGG1 mutations in patients with Alzheimer's disease. Nucleic Acids Res 35, 2759-2766.

Marcon, G., Tell, G., Perrone, L., Garbelli, R., Quadrifoglio, F., Tagliavini, F., Giaccone, G., 2009. APE1/Ref-1 in Alzheimer's disease: an immunohistochemical study. Neurosci Lett 466, 124-127.

Markesbery, W.R., 1997a. Neuropathological criteria for the diagnosis of Alzheimer's disease. Neurobiol Aging 18, S13-19.

Markesbery, W.R., 1997b. Oxidative stress hypothesis in Alzheimer's disease. Free Radic Biol Med 23, 134-147.

Markesbery, W.R., Carney, J.M., 1999. Oxidative alterations in Alzheimer's disease. Brain Pathol 9, 133-146.

Markesbery, W.R., Lovell, M.A., 2006. DNA oxidation in Alzheimer's disease. Antioxid Redox Signal 8, 2039-2045.

Markesbery, W.R., Schmitt, F.A., Kryscio, R.J., Davis, D.G., Smith, C.D., Wekstein, D.R., 2006. Neuropathologic substrate of mild cognitive impairment. Arch Neurol 63, 38-46.

Masuda, Y., Bennett, R.A., Demple, B., 1998. Dynamics of the interaction of human apurinic endonuclease (Ape1) with its substrate and product. Journal of Biological Chemistry 273, 30352-30359.

Maynard, S., de Souza-Pinto, N.C., Scheibye-Knudsen, M., Bohr, V.A., 2010. Mitochondrial base excision repair assays. Methods 51, 416-425.

McKeith, I.G., Dickson, D.W., Lowe, J., Emre, M., O'Brien, J.T., Feldman, H., Cummings, J., Duda, J.E., Lippa, C., Perry, E.K., Aarsland, D., Arai, H., Ballard, C.G., Boeve, B., Burn, D.J., Costa, D., Del Ser, T., Dubois, B., Galasko, D., Gauthier, S., Goetz, C.G., Gomez-Tortosa, E., Halliday, G., Hansen, L.A., Hardy, J., Iwatsubo, T., Kalaria, R.N., Kaufer, D., Kenny, R.A., Korczyn, A., Kosaka, K., Lee, V.M., Lees, A., Litvan, I., Londos, E., Lopez, O.L., Minoshima, S., Mizuno, Y., Molina, J.A., Mukaetova-Ladinska, E.B., Pasquier, F., Perry, R.H., Schulz, J.B., Trojanowski, J.Q., Yamada, M., Consortium on, D.L.B., 2005. Diagnosis and management of dementia with Lewy bodies: third report of the DLB Consortium. Neurology 65, 1863-1872.

McKhann, G., Drachman, D., Folstein, M., Katzman, R., Price, D., Stadlan, E.M., 1984. Clinical diagnosis of Alzheimer's disease: report of the NINCDS-ADRDA Work Group under the auspices of Department of Health and Human Services Task Force on Alzheimer's Disease. Neurology 34, 939-944.

Mecocci, P., MacGarvey, U., Beal, M.F., 1994. Oxidative damage to mitochondrial DNA is increased in Alzheimer's disease. Ann Neurol 36, 747-751.

Mecocci, P., MacGarvey, U., Kaufman, A.E., Koontz, D., Shoffner, J.M., Wallace, D.C., Beal, M.F., 1993. Oxidative damage to mitochondrial DNA shows marked age-dependent increases in human brain. Ann Neurol 34, 609-616.

Mecocci, P., Polidori, M.C., Cherubini, A., Ingegni, T., Mattioli, P., Catani, M., Rinaldi, P., Cecchetti, R., Stahl, W., Senin, U., Beal, M.F., 2002. Lymphocyte oxidative DNA damage and plasma antioxidants in Alzheimer disease. Arch Neurol 59, 794-798.

Merchant, C., Tang, M.X., Albert, S., Manly, J., Stern, Y., Mayeux, R., 1999. The influence of smoking on the risk of Alzheimer's disease. Neurology 52, 1408-1412.

Migliore, L., Fontana, I., Trippi, F., Colognato, R., Coppede, F., Tognoni, G., Nucciarone, B., Siciliano, G., 2005. Oxidative DNA damage in peripheral leukocytes of mild cognitive impairment and AD patients. Neurobiol Aging 26, 567-573.

Milne, G.L., Musiek, E.S., Morrow, J.D., 2005. F2-isoprostanes as markers of oxidative stress in vivo: an overview. Biomarkers 10 Suppl 1, S10-23.

Mirra, S.S., 1997. The CERAD neuropathology protocol and consensus recommendations for the postmortem diagnosis of Alzheimer's disease: a commentary. Neurobiol Aging 18, S91-94.

Montine, T.J., Markesbery, W.R., Morrow, J.D., Roberts, L.J., 2nd, 1998. Cerebrospinal fluid F2-isoprostane levels are increased in Alzheimer's disease. Ann Neurol 44, 410-413.

Moreira, P.I., Nunomura, A., Nakamura, M., Takeda, A., Shenk, J.C., Aliev, G., Smith, M.A., Perry, G., 2008. Nucleic acid oxidation in Alzheimer disease. Free Radic Biol Med 44, 1493-1505.

Mortimer, J.A., French, L.R., Hutton, J.T., Schuman, L.M., 1985. Head injury as a risk factor for Alzheimer's disease. Neurology 35, 264-267.

Mortimer, J.A., Snowdon, D.A., Markesbery, W.R., 2003. Head circumference, education and risk of dementia: findings from the Nun Study. J Clin Exp Neuropsychol 25, 671-679.

Mortimer, J.A., van Duijn, C.M., Chandra, V., Fratiglioni, L., Graves, A.B., Heyman, A., Jorm, A.F., Kokmen, E., Kondo, K., Rocca, W.A., et al., 1991. Head trauma as a risk factor for Alzheimer's disease: a collaborative re-analysis of case-control studies. EURODEM Risk Factors Research Group. Int J Epidemiol 20 Suppl 2, S28-35.

Muiras, M.L., Muller, M., Schachter, F., Burkle, A., 1998. Increased poly(ADP-ribose) polymerase activity in lymphoblastoid cell lines from centenarians. J Mol Med (Berl) 76, 346-354.

Murphy, M.P., 2009. How mitochondria produce reactive oxygen species. Biochemical Journal 417, 1-13.

Narayan, S., Jaiswal, A.S., Balusu, R., 2005. Tumor suppressor APC blocks DNA polymerase beta-dependent strand displacement synthesis during long patch but not short

patch base excision repair and increases sensitivity to methylmethane sulfonate. Journal of Biological Chemistry 280, 6942-6949.

Neumann, M., Mackenzie, I.R., Cairns, N.J., Boyer, P.J., Markesbery, W.R., Smith, C.D., Taylor, J.P., Kretzschmar, H.A., Kimonis, V.E., Forman, M.S., 2007. TDP-43 in the ubiquitin pathology of frontotemporal dementia with VCP gene mutations. J Neuropathol Exp Neurol 66, 152-157.

Nguyen, K.L., Steryo, M., Kurbanyan, K., Nowitzki, K.M., Butterfield, S.M., Ward, S.R., Stemp, E.D., 2000. DNA-protein cross-linking from oxidation of guanine via the flash-quench technique. Journal of American Chemical Society 112, 10.

NIA-Reagan-Institute, 1997. Consensus recommendations for the postmortem diagnosis of Alzheimer's disease. The National Institute on Aging, and Reagan Institute Working Group on Diagnostic Criteria for the Neuropathological Assessment of Alzheimer's Disease. Neurobiol Aging 18, S1-2.

Nunomura, A., Perry, G., Pappolla, M.A., Wade, R., Hirai, K., Chiba, S., Smith, M.A., 1999. RNA oxidation is a prominent feature of vulnerable neurons in Alzheimer's disease. Journal of Neuroscience 19, 1959-1964.

Ott, A., Slooter, A.J., Hofman, A., van Harskamp, F., Witteman, J.C., Van Broeckhoven, C., van Duijn, C.M., Breteler, M.M., 1998. Smoking and risk of dementia and Alzheimer's disease in a population-based cohort study: the Rotterdam Study. Lancet 351, 1840-1843.

Parikh, S.S., Mol, C.D., Slupphaug, G., Bharati, S., Krokan, H.E., Tainer, J.A., 1998. Base excision repair initiation revealed by crystal structures and binding kinetics of human uracil-DNA glycosylase with DNA. EMBO J 17, 5214-5226.

Parsons, J.L., Dianov, G.L., 2013. Co-ordination of base excision repair and genome stability. DNA Repair (Amst) 12, 326-333.

Parsons, J.L., Dianova, II, Khoronenkova, S.V., Edelmann, M.J., Kessler, B.M., Dianov, G.L., 2011. USP47 is a deubiquitylating enzyme that regulates base excision repair by controlling steady-state levels of DNA polymerase beta. Mol Cell 41, 609-615.

Parsons, J.L., Tait, P.S., Finch, D., Dianova, II, Allinson, S.L., Dianov, G.L., 2008. CHIP-mediated degradation and DNA damage-dependent stabilization regulate base excision repair proteins. Mol Cell 29, 477-487.

Parsons, J.L., Tait, P.S., Finch, D., Dianova, II, Edelmann, M.J., Khoronenkova, S.V., Kessler, B.M., Sharma, R.A., McKenna, W.G., Dianov, G.L., 2009. Ubiquitin ligase ARF-BP1/Mule modulates base excision repair. Embo Journal 28, 3207-3215.

Pascucci, B., Maga, G., Hubscher, U., Bjoras, M., Seeberg, E., Hickson, I.D., Villani, G., Giordano, C., Cellai, L., Dogliotti, E., 2002. Reconstitution of the base excision repair pathway for 7,8-dihydro-8-oxoguanine with purified human proteins. Nucleic Acids Res 30, 2124-2130.

Pascucci, B., Stucki, M., Jonsson, Z.O., Dogliotti, E., Hubscher, U., 1999. Long patch base excision repair with purified human proteins. DNA ligase I as patch size mediator for DNA polymerases delta and epsilon. Journal of Biological Chemistry 274, 33696-33702.

Peake, I., 1989. The polymerase chain reaction. J Clin Pathol 42, 673-676.

Petersen, R.C., Roberts, R.O., Knopman, D.S., Boeve, B.F., Geda, Y.E., Ivnik, R.J., Smith, G.E., Jack, C.R., Jr., 2009. Mild cognitive impairment: ten years later. Arch Neurol 66, 1447-1455.

Petersen, R.C., Smith, G.E., Waring, S.C., Ivnik, R.J., Tangalos, E.G., Kokmen, E., 1999. Mild cognitive impairment: clinical characterization and outcome. Arch Neurol 56, 303-308.

Podlutsky, A.J., Dianova, II, Podust, V.N., Bohr, V.A., Dianov, G.L., 2001a. Human DNA polymerase beta initiates DNA synthesis during long-patch repair of reduced AP sites in DNA. Embo Journal 20, 1477-1482.

Podlutsky, A.J., Dianova, II, Wilson, S.H., Bohr, V.A., Dianov, G.L., 2001b. DNA synthesis and dRPase activities of polymerase beta are both essential for single-nucleotide patch base excision repair in mammalian cell extracts. Biochemistry 40, 809-813.

Poon, H.F., Castegna, A., Farr, S.A., Thongboonkerd, V., Lynn, B.C., Banks, W.A., Morley, J.E., Klein, J.B., Butterfield, D.A., 2004. Quantitative proteomics analysis of specific protein expression and oxidative modification in aged senescence-accelerated-prone 8 mice brain. Neuroscience 126, 915-926.

Prasad, K.N., Cole, W.C., Prasad, K.C., 2002. Risk factors for Alzheimer's disease: role of multiple antioxidants, non-steroidal anti-inflammatory and cholinergic agents alone or in combination in prevention and treatment. J Am Coll Nutr 21, 506-522.

Prasad, R., Dianov, G.L., Bohr, V.A., Wilson, S.H., 2000. FEN1 stimulation of DNA polymerase beta mediates an excision step in mammalian long patch base excision repair. Journal of Biological Chemistry 275, 4460-4466.

Prasad, R., Lavrik, O.I., Kim, S.J., Kedar, P., Yang, X.P., Vande Berg, B.J., Wilson, S.H., 2001. DNA polymerase beta -mediated long patch base excision repair. Poly(ADP-ribose)polymerase-1 stimulates strand displacement DNA synthesis. Journal of Biological Chemistry 276, 32411-32414.

Prasad, R., Liu, Y., Deterding, L.J., Poltoratsky, V.P., Kedar, P.S., Horton, J.K., Kanno, S., Asagoshi, K., Hou, E.W., Khodyreva, S.N., Lavrik, O.I., Tomer, K.B., Yasui, A., Wilson, S.H., 2007. HMGB1 is a cofactor in mammalian base excision repair. Mol Cell 27, 829-841.

Prasad, R., Singhal, R.K., Srivastava, D.K., Molina, J.T., Tomkinson, A.E., Wilson, S.H., 1996. Specific interaction of DNA polymerase beta and DNA ligase I in a multiprotein base excision repair complex from bovine testis. Journal of Biological Chemistry 271, 16000-16007.

Prat, F., Houk, K.N., Foote, C.S., 1998. Effect of guanine stacking on the oxidation of 8-oxoguanine in B-DNA. Journal of the American Chemical Society 120, 845-846.

Ranalli, T.A., Tom, S., Bambara, R.A., 2002. AP endonuclease 1 coordinates flap endonuclease 1 and DNA ligase I activity in long patch base excision repair. Journal of Biological Chemistry 277, 41715-41724.

Rascovsky, K., Hodges, J.R., Knopman, D., Mendez, M.F., Kramer, J.H., Neuhaus, J., van Swieten, J.C., Seelaar, H., Dopper, E.G., Onyike, C.U., Hillis, A.E., Josephs, K.A., Boeve, B.F., Kertesz, A., Seeley, W.W., Rankin, K.P., Johnson, J.K., Gorno-Tempini, M.L., Rosen, H., Prioleau-Latham, C.E., Lee, A., Kipps, C.M., Lillo, P., Piguet, O., Rohrer, J.D., Rossor, M.N., Warren, J.D., Fox, N.C., Galasko, D., Salmon, D.P., Black, S.E., Mesulam, M., Weintraub, S., Dickerson, B.C., Diehl-Schmid, J., Pasquier, F., Deramecourt, V., Lebert, F., Pijnenburg, Y., Chow, T.W., Manes, F., Grafman, J., Cappa,

S.F., Freedman, M., Grossman, M., Miller, B.L., 2011. Sensitivity of revised diagnostic criteria for the behavioural variant of frontotemporal dementia. Brain 134, 2456-2477.

Ratnavalli, E., Brayne, C., Dawson, K., Hodges, J.R., 2002. The prevalence of frontotemporal dementia. Neurology 58, 1615-1621.

Reddy P.V., P.G., Cooke M.S., Sayre L.M. Smith M.A., 2006. DNA Repair and Human Disease: Mechanisms of DNA Damage and Repair in Alzheimer Disease. Springer, Landes Bioscience, New York.

reviewed in Murphy, M.P., LeVine, H., 3rd, 2010. Alzheimer's disease and the amyloid-beta peptide. J Alzheimers Dis 19, 311-323.

Rose, E.A., 1991. Applications of the polymerase chain reaction to genome analysis. FASEB J 5, 46-54.

Rosen, H.J., Gorno-Tempini, M.L., Goldman, W.P., Perry, R.J., Schuff, N., Weiner, M., Feiwell, R., Kramer, J.H., Miller, B.L., 2002. Patterns of brain atrophy in frontotemporal dementia and semantic dementia. Neurology 58, 198-208.

Saiki, R.K., Scharf, S., Faloona, F., Mullis, K.B., Horn, G.T., Erlich, H.A., Arnheim, N., 1985. Enzymatic amplification of beta-globin genomic sequences and restriction site analysis for diagnosis of sickle cell anemia. Science 230, 1350-1354.

Sak, S.C., Harnden, P., Johnston, C.F., Paul, A.B., Kiltie, A.E., 2005. APE1 and XRCC1 protein expression levels predict cancer-specific survival following radical radiotherapy in bladder cancer. Clin Cancer Res 11, 6205-6211.

Saunders, A.M., Strittmatter, W.J., Schmechel, D., George-Hyslop, P.H., Pericak-Vance, M.A., Joo, S.H., Rosi, B.L., Gusella, J.F., Crapper-MacLachlan, D.R., Alberts, M.J., et al., 1993. Association of apolipoprotein E allele epsilon 4 with late-onset familial and sporadic Alzheimer's disease. Neurology 43, 1467-1472.

Scaravilli, T., Tolosa, E., Ferrer, I., 2005. Progressive supranuclear palsy and corticobasal degeneration: lumping versus splitting. Mov Disord 20 Suppl 12, S21-28.

Schmitt, F.A., Davis, D.G., Wekstein, D.R., Smith, C.D., Ashford, J.W., Markesbery, W.R., 2000. "Preclinical" AD revisited: neuropathology of cognitively normal older adults. Neurology 55, 370-376.

Schmittgen, T.D., Livak, K.J., 2008. Analyzing real-time PCR data by the comparative C(T) method. Nat Protoc 3, 1101-1108.

Selkoe, D.J., 2001. Alzheimer's disease: genes, proteins, and therapy. Physiol Rev 81, 741-766.

Shan, X., Chang, Y.M., Lin, C.L.G., 2007. Messenger RNA oxidation is an early event preceding cell death and causes reduced protein expression. Faseb Journal 21, 2753-2764.

Shan, X., Lin, C.L., 2006. Quantification of oxidized RNAs in Alzheimer's disease. Neurobiol Aging 27, 657-662.

Shan, X., Tashiro, H., Lin, C.L.G., 2003. The identification and characterization of oxidized RNAs in Alzheimer's disease. Journal of Neuroscience 23, 4913-4921.

Shao, C., Xiong, S., Li, G.M., Gu, L., Mao, G., Markesbery, W.R., Lovell, M.A., 2008. Altered 8-oxoguanine glycosylase in mild cognitive impairment and late-stage Alzheimer's disease brain. Free Radic Biol Med 45, 813-819.

Sharif, R., Thomas, P., Zalewski, P., Fenech, M., 2012. Zinc deficiency or excess within the physiological range increases genome instability and cytotoxicity, respectively, in human oral keratinocyte cells. Genes Nutr 7, 139-154.

Sharma, S., Sommers, J.A., Wu, L., Bohr, V.A., Hickson, I.D., Brosh, R.M., Jr., 2004. Stimulation of flap endonuclease-1 by the Bloom's syndrome protein. Journal of Biological Chemistry 279, 9847-9856.

Sims, N.R., Anderson, M.F., 2008. Isolation of mitochondria from rat brain using Percoll density gradient centrifugation. Nat Protoc 3, 1228-1239.

Smith, C.D., Carney, J.M., Starke-Reed, P.E., Oliver, C.N., Stadtman, E.R., Floyd, R.A., Markesbery, W.R., 1991. Excess brain protein oxidation and enzyme dysfunction in normal aging and in Alzheimer disease. Proc Natl Acad Sci U S A 88, 10540-10543.

Smith, M.A., Nunomura, A., Zhu, X., Takeda, A., Perry, G., 2000a. Metabolic, metallic, and mitotic sources of oxidative stress in Alzheimer disease. Antioxid Redox Signal 2, 413-420.

Smith, M.A., Richey Harris, P.L., Sayre, L.M., Beckman, J.S., Perry, G., 1997. Widespread peroxynitrite-mediated damage in Alzheimer's disease. Journal of Neuroscience 17, 2653-2657.

Smith, M.A., Rottkamp, C.A., Nunomura, A., Raina, A.K., Perry, G., 2000b. Oxidative stress in Alzheimer's disease. Biochim Biophys Acta 1502, 139-144.

Sobol, R.W., Horton, J.K., Kuhn, R., Gu, H., Singhal, R.K., Prasad, R., Rajewsky, K., Wilson, S.H., 1996. Requirement of mammalian DNA polymerase-beta in base-excision repair. Nature 379, 183-186.

Song, Y., Leonard, S.W., Traber, M.G., Ho, E., 2009. Zinc deficiency affects DNA damage, oxidative stress, antioxidant defenses, and DNA repair in rats. J Nutr 139, 1626-1631.

Soskic, V., Groebe, K., Schrattenholz, A., 2008. Nonenzymatic posttranslational protein modifications in ageing. Exp Gerontol 43, 247-257.

Souza-Pinto, N.C., Croteau, D.L., Hudson, E.K., Hansford, R.G., Bohr, V.A., 1999. Age-associated increase in 8-oxo-deoxyguanosine glycosylase/AP lyase activity in rat mitochondria. Nucleic Acids Res 27, 1935-1942.

Spicer, L.J., Alpizar, E., Vernon, R.K., 1994. Insulin-like growth factor-I receptors in ovarian granulosa cells: effect of follicle size and hormones. Mol Cell Endocrinol 102, 69-76.

Steenken, S., 1989a. Purine-Bases, Nucleosides, and Nucleotides - Aqueous-Solution Redox Chemistry and Transformation Reactions of Their Radical Cations and E- and Oh Adducts. Chemical Reviews 89, 503-520.

Steenken, S., 1989b. Structure, Acid-Base Properties and Transformation Reactions of Purine Radicals. Free Radical Research Communications 6, 117-120.

Steenken, S., Jovanovic, S.V., 1997. How easily oxidizable is DNA? One-electron reduction potentials of adenosine and guanosine radicals in aqueous solution. Journal of the American Chemical Society 119, 617-618.

Strom, C.E., Mortusewicz, O., Finch, D., Parsons, J.L., Lagerqvist, A., Johansson, F., Schultz, N., Erixon, K., Dianov, G.L., Helleday, T., 2011. CK2 phosphorylation of XRCC1 facilitates dissociation from DNA and single-strand break formation during base excision repair. DNA Repair (Amst) 10, 961-969.

Strosznajder, J.B., Czapski, G.A., Adamczyk, A., Strosznajder, R.P., 2012. Poly(ADP-ribose) polymerase-1 in amyloid beta toxicity and Alzheimer's disease. Mol Neurobiol 46, 78-84.

Strosznajder, J.B., Jesko, H., Strosznajder, R.P., 2000a. Age-related alteration of poly(ADP-ribose) polymerase activity in different parts of the brain. Acta Biochim Pol 47, 331-337.

Strosznajder, J.B., Jesko, H., Strosznajder, R.P., 2000b. Effect of amyloid beta peptide on poly(ADP-ribose) polymerase activity in adult and aged rat hippocampus. Acta Biochim Pol 47, 847-854.

Talbot, P.R., Lloyd, J.J., Snowden, J.S., Neary, D., Testa, H.J., 1998. A clinical role for 99mTc-HMPAO SPECT in the investigation of dementia? J Neurol Neurosurg Psychiatry 64, 306-313.

Tan, Z., Sun, N., Schreiber, S.S., 1998. Immunohistochemical localization of redox factor-1 (Ref-1) in Alzheimer's hippocampus. Neuroreport 9, 2749-2752.

Tanaka, M., Chock, P.B., Stadtman, E.R., 2007. Oxidized messenger RNA induces translation errors. Proc Natl Acad Sci U S A 104, 66-71.

Tebbs, R.S., Flannery, M.L., Meneses, J.J., Hartmann, A., Tucker, J.D., Thompson, L.H., Cleaver, J.E., Pedersen, R.A., 1999. Requirement for the Xrcc1 DNA base excision repair gene during early mouse development. Dev Biol 208, 513-529.

Tengiz, I., Aliyev, E., Ercan, E., 2005. An alternative percutaneous interventional approach for post-anastomatic left anterior descending artery stenosis in patients with markedly tortuous LIMA graft. Int J Cardiovasc Imaging 21, 491-494.

Thies, W., Bleiler, L., 2011. 2011 Alzheimer's disease facts and figures. Alzheimers Dement 7, 208-244.

Thies, W., Bleiler, L., 2013. 2013 Alzheimer's disease facts and figures. Alzheimers Dement 9, 208-245.

Thomann, P.A., Schlafer, C., Seidl, U., Santos, V.D., Essig, M., Schroder, J., 2008. The cerebellum in mild cognitive impairment and Alzheimer's disease - a structural MRI study. Journal of psychiatric research 42, 1198-1202.

Thompson, L.H., West, M.G., 2000. XRCC1 keeps DNA from getting stranded. Mutat Res 459, 1-18.

Tom, S., Henricksen, L.A., Bambara, R.A., 2000. Mechanism whereby proliferating cell nuclear antigen stimulates flap endonuclease 1. Journal of Biological Chemistry 275, 10498-10505.

Toueille, M., El-Andaloussi, N., Frouin, I., Freire, R., Funk, D., Shevelev, I., Friedrich-Heineken, E., Villani, G., Hottiger, M.O., Hubscher, U., 2004. The human Rad9/Rad1/Hus1 damage sensor clamp interacts with DNA polymerase beta and increases its DNA substrate utilisation efficiency: implications for DNA repair. Nucleic Acids Res 32, 3316-3324.

UNPD, 2011. World Population Prospects: The 2010 Revision. UN Population Division, New York.

VanGuilder, H.D., Vrana, K.E., Freeman, W.M., 2008. Twenty-five years of quantitative PCR for gene expression analysis. Biotechniques 44, 619-626.

Vidal, A.E., Boiteux, S., Hickson, I.D., Radicella, J.P., 2001. XRCC1 coordinates the initial and late stages of DNA abasic site repair through protein-protein interactions. Embo Journal 20, 6530-6539.

von Kobbe, C., Harrigan, J.A., May, A., Opresko, P.L., Dawut, L., Cheng, W.H., Bohr, V.A., 2003. Central role for the Werner syndrome protein/poly(ADP-ribose) polymerase 1 complex in the poly(ADP-ribosyl)ation pathway after DNA damage. Mol Cell Biol 23, 8601-8613.

Wang, A.L., Lukas, T.J., Yuan, M., Neufeld, A.H., 2008. Increased mitochondrial DNA damage and down-regulation of DNA repair enzymes in aged rodent retinal pigment epithelium and choroid. Mol Vis 14, 644-651.

Wang, J., Xiong, S., Xie, C., Markesbery, W.R., Lovell, M.A., 2005. Increased oxidative damage in nuclear and mitochondrial DNA in Alzheimer's disease. J Neurochem 93, 953-962.

Wegiel, J., Wisniewski, H.M., Dziewiatkowski, J., Badmajew, E., Tarnawski, M., Reisberg, B., Mlodzik, B., De Leon, M.J., Miller, D.C., 1999. Cerebellar atrophy in Alzheimer's disease-clinicopathological correlations. Brain research 818, 41-50.

Weissman, L., Jo, D.G., Sorensen, M.M., de Souza-Pinto, N.C., Markesbery, W.R., Mattson, M.P., Bohr, V.A., 2007. Defective DNA base excision repair in brain from individuals with Alzheimer's disease and amnestic mild cognitive impairment. Nucleic Acids Res 35, 5545-5555.

Whitehouse, C.J., Taylor, R.M., Thistlethwaite, A., Zhang, H., Karimi-Busheri, F., Lasko, D.D., Weinfeld, M., Caldecott, K.W., 2001. XRCC1 stimulates human

polynucleotide kinase activity at damaged DNA termini and accelerates DNA single-strand break repair. Cell 104, 107-117.

Williams, T.I., Lynn, B.C., Markesbery, W.R., Lovell, M.A., 2006. Increased levels of 4-hydroxynonenal and acrolein, neurotoxic markers of lipid peroxidation, in the brain in Mild Cognitive Impairment and early Alzheimer's disease. Neurobiol Aging 27, 1094-1099.

Wiseman, H., Halliwell, B., 1996. Damage to DNA by reactive oxygen and nitrogen species: Role in inflammatory disease and progression to cancer. Biochemical Journal 313, 17-29.

Woodhouse, B.C., Dianov, G.L., 2008. Poly ADP-ribose polymerase-1: an international molecule of mystery. DNA Repair (Amst) 7, 1077-1086.

Woodhouse, B.C., Dianova, II, Parsons, J.L., Dianov, G.L., 2008. Poly(ADP-ribose) polymerase-1 modulates DNA repair capacity and prevents formation of DNA double strand breaks. DNA Repair (Amst) 7, 932-940.

Wu, J., Hecker, J.G., Chiamvimonvat, N., 2009. Antioxidant enzyme gene transfer for ischemic diseases. Adv Drug Deliv Rev 61, 351-363.

Wu, X., Li, J., Li, X., Hsieh, C.L., Burgers, P.M., Lieber, M.R., 1996. Processing of branched DNA intermediates by a complex of human FEN-1 and PCNA. Nucleic Acids Res 24, 2036-2043.

Xanthoudakis, S., Curran, T., 1992. Identification and characterization of Ref-1, a nuclear protein that facilitates AP-1 DNA-binding activity. Embo Journal 11, 653-665.

Xie, Z.C., Tanzi, R.E., 2006. Alzheimer's disease and post-operative cognitive dysfunction. Exp Gerontol 41, 346-359.

Yaari, R., Corey-Bloom, J., 2007. Alzheimer's disease. Semin Neurol 27, 32-41.

Yacoub, A., McKinstry, R., Hinman, D., Chung, T., Dent, P., Hagan, M.P., 2003. Epidermal growth factor and ionizing radiation up-regulate the DNA repair genes XRCC1 and ERCC1 in DU145 and LNCaP prostate carcinoma through MAPK signaling. Radiat Res 159, 439-452.

Yamaguchi, H., Hirai, S., Morimatsu, M., Shoji, M., Nakazato, Y., 1989. Diffuse Type of Senile Plaques in the Cerebellum of Alzheimer-Type Dementia Demonstrated by Beta-Protein Immunostain. Acta Neuropathol 77, 314-319.

Yamtich, J., Sweasy, J.B., 2010. DNA polymerase family X: function, structure, and cellular roles. Biochim Biophys Acta 1804, 1136-1150.

Yoo, B.C., Fountoulakis, M., Cairns, N., Lubec, G., 2001. Changes of voltage-dependent anion-selective channel proteins VDAC1 and VDAC2 brain levels in patients with Alzheimer's disease and Down syndrome. Electrophoresis 22, 172-179.

Youn, C.K., Song, P.I., Kim, M.H., Kim, J.S., Hyun, J.W., Choi, S.J., Yoon, S.P., Chung, M.H., Chang, I.Y., You, H.J., 2007. Human 8-oxoguanine DNA glycosylase suppresses the oxidative stress induced apoptosis through a p53-mediated signaling pathway in human fibroblasts. Mol Cancer Res 5, 1083-1098.

Zaccai, J., McCracken, C., Brayne, C., 2005. A systematic review of prevalence and incidence studies of dementia with Lewy bodies. Age Ageing 34, 561-566.

Zhang, J., Perry, G., Smith, M.A., Robertson, D., Olson, S.J., Graham, D.G., Montine, T.J., 1999. Parkinson's disease is associated with oxidative damage to cytoplasmic DNA and RNA in substantia nigra neurons. American Journal of Pathology 154, 1423-1429.

Zhang, M.Y., Katzman, R., Salmon, D., Jin, H., Cai, G.J., Wang, Z.Y., Qu, G.Y., Grant, I., Yu, E., Levy, P., et al., 1990. The prevalence of dementia and Alzheimer's disease in Shanghai, China: impact of age, gender, and education. Ann Neurol 27, 428-437.

Zheng, L., Jia, J., Finger, L.D., Guo, Z., Zer, C., Shen, B., 2011. Functional regulation of FEN1 nuclease and its link to cancer. Nucleic Acids Res 39, 781-794.

Zhou, C., Huang, Y., Przedborski, S., 2008. Oxidative stress in Parkinson's disease: a mechanism of pathogenic and therapeutic significance. Ann N Y Acad Sci 1147, 93-104.

Zhou, J., Ahn, J., Wilson, S.H., Prives, C., 2001. A role for p53 in base excision repair. Embo Journal 20, 914-923.

VITA

Sony Soman

Education

BS, Chemistry (Hons.), Chemistry, Gargi College, Delhi University, New Delhi, India, May 2000

M.Sc, Chemistry, Indian Institute of Technology -Delhi (IIT-D), New Delhi, India, May 2002

MS, Analytical Chemistry, University of Nebraska-Lincoln, 2008

Ph.D., Bioanalytical Chemistry, University of Kentucky (UK), anticipated Dec 2013

Research Experience

- 2008-present: PhD candidate, Dept. of Chemistry and Sanders-Brown Center on Aging, University of Kentucky.

  Advisor: Dr. Mark Lovell

  My graduate work has focused on multiple aspects of oxidative DNA damage and repair within a single cohort of subjects in multiple brain regions during the progression of Alzheimer's disease (AD). The studies have included quantification and analysis of gene expression, protein levels, and enzyme activities of multiple DNA repair proteins involved in the BER pathway including OGG1, UNG, APE1, POLB, PARP1, XRCC1, and FEN1. A second project focused on the investigation of genomic oxidative damage within the coding sequences of proteins found to be differentially regulated during the progression of AD by real-time PCR analysis.

- 2004-2008: MS, Dept. of Chemistry, University of Nebraska-Lincoln.
  Advisor: Dr. David Hage.

  Projects: (1) Development of new affinity monolithic chromatographic polymer supports for HPLC columns, (2) Development of new techniques to make affinity monolithic polymer microcolumns for HPLC and (3) Characterization of drug-binding between drugs such as lidocaine and verapamil with the protein, human serum albumin using UPLC/RPLC methods.

- 2004: Research Assistant, Dept. of Chemistry, University of Nebraska-Lincoln.
  Advisor: Dr. D.B. Berkowitz

  Project: Development of a convenient, continuous UV assay for cystathionine beta synthase (CBS).

- 2003-2004: Research Associate, Centre for Polymer Science and Engg., IIT-Delhi.
  Advisor: Dr. I.K. Verma

  Projects: Analysis of resin from the Impregnated Filter Paper and development of water based phenolic and acrylic resin.

- 2002-2003: Research Associate, Dept. of Civil Engg., IIT-Delhi.
  Advisor: Dr. Rema Devi

  Project: Chemical/biochemical/bacteriological analysis of river & drain water resources in Delhi.

- 2002: Project associate, Centre for Biomedical Engg., IIT Delhi.
  Advisor: Dr. S.K.Guha

  Project: Effect of excess DMSO and styrene on the DNA of human cells and on

  RISUG (an experimental reversible male contraceptive in its 3rd stage of clinical trial).

- 2001-2002: M.Sc. Project, Dept. of Chemistry, IIT-Delhi.
  Advisor: Dr. M. N. Gupta

Projects: (1) Development of a purification method for effective & economical purification of the enzyme porcine pancreatic alpha-amylase using reversibly soluble insoluble (SIS) polymers and (2) Molecular Imprinting of Eudragit with tartaric acid.

Teaching Experience

- Teaching assistant for Biochemistry, Analytical Chemistry and General Chemistry, Department of Chemistry, University of Kentucky, 2008-2010
- Enrolled in the Preparing Future Faculty program, 2009
- Teaching assistant for General and Organic Chemistry, Department of Chemistry, University of Nebraska- Lincoln, 2004-2008

Publications

1. Optimization of human serum albumin monoliths for chiral separations and high performance affinity chromatography. E. L. Pfaunmiller, M. Hartmann, C. M. Dupper, **S. Soman** and D. S. Hage, *J. Chromatogr. A,* 2012, 1269, 198-207.
2. Increased DNA and RNA oxidation in Preclinical Alzheimer's disease (PCAD) brain. M.A. Lovell, **S. Soman** and M.A. Bradley, **Invited article**, *Mech. Ageing Dev.*, 2011, 132, 443-448.
3. Analysis of lidocaine interactions with serum proteins using high-performance affinity chromatography. **S. Soman**, M.J. Yoo, Y.J. Jang and D. S. Hage, *J. Chromatogr. B Analyt. Technol. Biomed. Life Sci.*, 2010, 878(7-8), 705-708.
4. Synthesis of affinity monoliths and use of affinity HPLC in drug binding studies. **S. Soman**, MS thesis, University of Nebraska-Lincoln 2008.
5. Applications of silica supports in affinity chromatography. J. Schiel, R. Mallik, **S. Soman**, K. Joseph and D.S. Hage, *J. Sep.* Sci., 2006**,** 29, 719-737.
6. New developments in affinity columns (ligands/supports) for chiral separation of drugs. **S. Soman**, E. Papastavros and D. S. Hage. *In process*
7. Affinity monolith microcolumns for studies of drug-protein interactions. **S.Soman**, T. Jiang, and D. S. Hage. *In process*

8. Changes in DNA repair enzymes; OGG1, UNG and APE1 of the BER pathway during the progression of AD. **S. Soman**, S. Xiong-Fister and M. A. Lovell, In preparation: Anticipated submission Sep 22, 2013.
9. Changes in DNA repair enzymes; POLB, PARP1, FEN1 and XRCC1 of the BER pathway during the progression of AD. **S. Soman**, S. Xiong-Fister and M. A. Lovell, In preparation.

Research Presentations

1. Oxidative DNA damage in genes of proteins modified during AD. **S. Soman** and M.A. Lovell, Society of Neuroscience Conference, New Orleans, LA, Oct. 2012
2. Oxidative DNA damage in genes of proteins modified during AD. **S. Soman** and M.A. Lovell, Markesbery Symposium on Aging and Dementia, Lexington, KY, Nov. 2012
3. Nucleic Acid Oxidation in Alzheimer's disease. **S. Soman**, S. Xiong-Fister and M.A. Lovell, Society of Neuroscience Conference, Washington D.C., Nov. 2011
4. Repair of Nucleic Acid Oxidation in Alzheimer's disease. **S. Soman,** S. Xiong-Fister and M.A. Lovell, Markesbery Symposium on Aging and Dementia, 2011
5. Affinity monolith microcolumns for studies of drug-protein interactions. **S. Soman**, T. Jiang, R. Mallik and D. S. Hage, PITTCON Chicago, IL, 2007
6. Affinity monolith microcolumns for studies of drug-protein interactions. **S. Soman**, T. Jiang, R. Mallik and D. S. Hage, Nebraska Science Fair, Lincoln, NE 2007
7. Development of a convenient, continuous UV assay for cystathionine beta synthase (CBS). D. B. Berkowitz, W. Shen, M. K. McGath, and **S. Soman**, 228th National ACS Meeting, Philadelphia, PA 2004

Honors

1. Research Challenge Trust Fund (RCTF) Fellowship, UK, 2010-2012
2. Graduate School Travel Fellowship for Graduate Students, UK 2011, 2012
3. Fast Track Research Award, Department of Chemistry, UK 2010
4. Outstanding Poster award at the Nebraska Science Fair 2007
5. Qualified Council of Scientific and Industrial Research (CSIR)-National Eligibility Test (All India open exam), Dec 2002

6. Qualified Graduate Aptitude Test for Engg. (GATE), All India open exam, Feb 2002